

# **Delineating the Role of Signaling Pathways in Epidermal Stem Cell Regulation**

**By**

**Chovatiya Gopalbhai Lavjibhai**

**(LIFE09201204005)**

**Tata Memorial Centre, Mumbai**

*A thesis submitted to the*

*Board of Studies in Life Sciences*

*In partial fulfillment of requirements*

*For the Degree of*

**DOCTOR OF PHILOSOPHY**

**Of**

**HOMI BHABHA NATIONAL INSTITUTE**



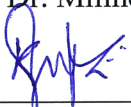
**October 2018**



# Homi Bhabha National Institute<sup>1</sup>

## Recommendations of the Viva Voce Committee

As members of the Viva Voce Committee, we certify that we have read the dissertation prepared by Mr Chovatiya Gopalbhai Lavjibhai entitled “**Delineating the Role of Signaling Pathways in Epidermal Stem Cell Regulation**” and recommend that it may be accepted as fulfilling the thesis requirement for the award of Degree of Doctor of Philosophy.

|  |                    |
|--|--------------------|
| <br>Chairman – Dr. Milind Vaidya              | 24/10/18<br>Date   |
| <br>Guide / Convener – Dr. Sanjeev Waghmare   | 24/10/18<br>Date   |
| <br>External Examiner – Dr. Mrinal Kanti Gosh | 24/10/2018<br>Date |
| <br>Member - Dr. Sanjay Gupta                | 24/10/2018<br>Date |
| <br>Member - Dr. Ashok Varma                | 24/10/2018<br>Date |
| <br>Invitee - Dr. Anjali Shiras             | 24.11.2018<br>Date |

Final approval and acceptance of this thesis is contingent upon the candidate's submission of the final copies of the thesis to HBNI.

I hereby certify that I have read this thesis prepared under my direction and recommend that it may be accepted as fulfilling the thesis requirement.

Date: 24/10/18

Place: Navi-Mumbai

  
Dr. Sanjeev Waghmare  
Guide

<sup>1</sup> This page is to be included only for final submission after successful completion of viva voce.



## **STATEMENT BY AUTHOR**

This dissertation has been submitted in partial fulfillment of requirements for an advanced degree at Homi Bhabha National Institute (HBNI) and is deposited in the Library to be made available to borrowers under rules of the HBNI.

Brief quotations from this dissertation are allowable without special permission, provided that accurate acknowledgement of source is made. Requests for permission for extended quotation from or reproduction of this manuscript in whole or in part may be granted by the Competent Authority of HBNI when in his or her judgment the proposed use of the material is in the interests of scholarship. In all other instances, however, permission must be obtained from the author.

**Chovatiya Gopalbhai Lavjibhai**



## **DECLARATION**

I, hereby declare that the investigation presented in the thesis has been carried out by me. The work is original and has not been submitted earlier as a whole or in part for a degree / diploma at this or any other Institution / University.

**Chovatiya Gopalbhai Lavjibhai**



## **List of Publications arising from the thesis**

### **Journal:**

1. **Secretory phospholipase A2-IIA overexpressing mice exhibit cyclic alopecia mediated through aberrant hair shaft differentiation and impaired wound healing response.** Chovatiya GL, Sarate RM, Sunkara RR, Gawas NP, Kala V, Waghmare SK. *Sci Rep* (2017) 7: 11619
2. **sPLA2 -IIA Overexpression in Mice Epidermis Depletes Hair Follicle Stem Cells and Induces Differentiation Mediated Through Enhanced JNK/c-Jun Activation.** Sarate RM, Chovatiya GL, Ravi V, Khade B, Gupta S, Waghmare SK. *Stem Cells* (2016) 34: 2407-2417
3. **Defining the context-dependent effect of sPLA<sub>2</sub>-IIA induced proliferation on stem cells and cancer cells.** Chovatiya GL, Godbole SR, Sunkara RR, Waghmare SK. (Manuscript under Revision)

### **Conferences:**

1. Chovatiya GL and Waghmare SK. “**Secretory phospholipase A2-IIA overexpression alters epidermal stem cells proliferation dynamics and differentiation associated with asymmetric cell division**” at Gordon Research Conference on Epithelial Differentiation and Keratinization, May 7-12, 2017 Italy (**Poster presentation**).
2. Chovatiya GL and Waghmare SK. “**Effect of secretory phospholipase A2-IIA on epidermal proliferation and differentiation**” at International conference “A



Conference of New Ideas in Cancer-Challenging Dogmas” held at Tata Memorial Centre, 2016, India (**Poster presentation**).

3. Chovatiya GL, Sarate RM and Waghmare SK. “**Effect of Secretory Phospholipase A2-IIA On Epidermal Growth and Differentiation**” at International conference organized on “Tissue Homeostasis and Inflammation”, held at InStem, 2016, India (**Poster presentation**).
  
4. Chovatiya GL Sarate RM and Waghmare SK. “**Synergistic effect of secretory phospholipase A2 IIA controls epidermal homeostasis**” at International conference organized by IACR (34th Annual Convention of Indian Association for Cancer Research), held at Jaipur, 2015, India (**Poster presentation**).
  
5. Chovatiya GL, Khanna P, and Waghmare SK. “**Effect of Lysophospholipids on Proliferative Dynamics of Epidermal Stem Cells**” at XXVII All India Cell Biology Conference (AICBC), held at National Centre for Biological Sciences, 2013, India (**Poster presentation**).

**Chovatiya Gopalbhai Lavjibhai**



**This thesis is dedicated to my beloved  
family and teachers for their endless  
support and constant encouragement**



## **Acknowledgements**

*I would like to express my deepest appreciation in the next lines to a number of people, without whom this thesis would not have been possible. Foremost, I extend my deepest gratitude to my thesis research advisor, Dr Sanjeev Waghmare for his guidance, encouragement, advice and constant support on countless occasions. Thank you for giving me an opportunity and freedom to expose myself to the world of research. Your positive attitude for “get the things done” has indeed intensified my ability and self-confidence.*

*I would like to express my gratitude to Dr. Shubhada Chiplunkar, Director, ACTREC for providing excellent infrastructure, encouragement and endless supports throughout tenure. I am thankful to Dr. Sudeep Gupta, Dy. Director, CRC, ACTREC and Dr. HKV Narayan, Dy. Director, ACTREC for their support and help at different levels. I am also thankful to Dr. Rajiv Sarin (former Director) and Dr. Surekha Zingde (former Dy. Director). I am immensely grateful to Dr. Rita Mulherkar for a generous gift of the K14-sPLA2-TTA transgenic mice.*

*As members of my doctoral committee, I am deeply thankful to Dr. Milind Vaidya, Dr. Sanjay Gupta, Dr. Ashok Varma and Dr. Anjali Shiras for their invaluable input, advice and support in shaping and refining my research work.*

*I would like to acknowledge all the members of Waghmare lab. I am thankful to Rahul, Raghav and Nilesh for their constant support and healthy discussions during last six years. I am also thankful to Saloni, Sayoni, Shushant and Bidita for their cheerful comments and making the lab lively and organized. I specially thank Ganesh for making the things available whenever we required. I also appreciate Nirmala for her support in smooth functioning of the laboratory. I would like to thank all the former members, Prasanna, Monali, Priyanka, Sweta, Puja, Anju, Deepanjali, Shashi, Apeksha, Vidula, and Anisha for their help and contribution for the smooth progress of the project.*

*I am also thankful to scientist and staff of Laboratory Animal Facility, Dr. Arvind Ingle and Dr. Rahul Thorat. I specially thank Mr. Surendra for his ever-present*

support in maintaining the mouse colonies. I would also like to thank Mr. Makarand, Mr. Sada, Mr. Ravi and Mr. Shashi for their help in animal work. I would also like to thank members of the histology department Mr. Chavan, Mr. Sakpal, Mr. Dinesh and Mr. Shridhar for providing extensive help in the histology work. My Very special thanks to members of CIR, Flow cytometry and Imaging facility Mr. Uday Dandekar, Ms. Shamal Vetale, Mrs. Vaishali Kailaje, Mr. Ravi Joshi, Mrs. Rekha Gaur, Mrs. Tanuja Dighe and Mr. Jayraj Kasale. I am thankful to the Director's office (Mrs. Pritha Menon and Mrs. Lata Shelar), Programme office (Mrs. Maya Dolas), Administration, Accounts, Dispatch, Purchase, Stores and Photography department for their constant support throughout the tenure.

I would like to specially acknowledge ACTREC for the fellowship and Indian Council of Medical Research (ICMR), Department of Biotechnology (DBT) and Tata Memorial Centre (TMC) for providing the funds for the research work. I am grateful to DBT, Homi Bhabha National Institute (HBNi) and Sam Mistry for providing financial support to attend the international conference.

Special appreciation also goes out to my batch mates, Pratik, Bhawik, Abha, Prajish, Saujanya, Bhushan, Jacinth and Sameer for their moral support as well as Friday parties, birthday celebrations and creating cheerful environments throughout last six years. I specially thank Pratik and Bhawik for their ever-present unconditional support for scientific and personal work.

I would also like to thank Bhawik, Paresh, Kaushal, Nikhil and Dharmesh for being with me all the time throughout last eight years, where I learnt a lot from their relentless political for spiritual and political debates. I greatly acknowledge their inestimable help and support in my professional and personal growth.

I especially want to extend my deepest gratitude to my mummy and papa for their unconditional love and support, even when I couldn't explain to them what I was doing. They have always given me the latitude to develop my interest in whatever I'm passionate about and have always been happy and proud of my accomplishments. Lastly; I proudly acknowledge support from Yesha. I look forward to our life together!!!

## *Table of Contents*

|   |           |
|---|-----------|
| <b>Synopsis.....</b>  | <b>1</b>  |
| <b>List of Figures.....</b>   | <b>18</b> |
| <b>List of Tables .....</b>   | <b>20</b> |
| <b>Abbreviations .....</b>  | <b>21</b> |
| <b>1. Introduction.....</b>   | <b>24</b> |
| <b>1.1 An introduction to stem cells .....</b>                                      | <b>25</b> |
| <b>1.2 Embryonic stem cells and pluripotency.....</b>                               | <b>25</b> |
| <b>1.3 Tissue stem cells and their potency .....</b>                                | <b>27</b> |
| <b>2. Review of Literature .....</b>  | <b>30</b> |
| <b>2.1 Architecture of skin .....</b>   | <b>31</b> |
| <b>2.2 Epidermal compartments in the human and mouse skin.....</b>                  | <b>32</b> |
| <b>2.3 The Epidermis .....</b>  | <b>32</b> |
| 2.3.1 Development and Stratification of the epidermis .....                         | 33        |
| 2.3.2 The interfollicular epidermis (IFE) and stem cells .....                      | 34        |
| <b>2.4 The hair follicle .....</b>  | <b>36</b> |
| 2.4.1 Hair follicle morphogenesis.....  | 38        |
| 2.4.2 Hair follicle stem cells .....  | 40        |
| 2.4.3 Cyclic regeneration of the hair follicle .....                                | 41        |
| 2.4.4 Proliferation dynamics of the hair follicle stem cells .....                  | 44        |
| <b>2.5 The sebaceous gland (SG) and stem cells.....</b>                             | <b>47</b> |
| <b>2.6 Signaling pathways in hair follicle morphogenesis and HFSCs activation .</b> | <b>49</b> |
| 2.6.1 Growth factors and mitogenic signaling.....                                   | 49        |
| 2.6.2 Wnt/ $\beta$ -catenin signaling and epidermal homeostasis.....                | 50        |
| 2.6.3 BMP signaling and hair follicle stem cells .....                              | 54        |
| 2.6.4 Other signaling pathways in HFSCs regulation.....                             | 56        |

|            |   |           |
|------------|---|-----------|
| 2.6.4.1    | Shh Signaling.....  | 56        |
| 2.6.4.2    | TGF $\beta$ signaling .....   | 57        |
| 2.6.4.3    | Notch signaling .....   | 58        |
| <b>2.7</b> | <b>Wound healing process.....</b>   | <b>60</b> |
| 2.7.1      | Mechanisms involved in wound healing response.....  | 60        |
| 2.7.2      | IFE stem cells in the wound healing process .....   | 61        |
| 2.7.3      | Hair follicle stem cells in the wound healing process.....  | 62        |
| <b>2.8</b> | <b>Development of the alopecia .....</b>  | <b>63</b> |
| 2.8.1      | Types of alopecia .....   | 63        |
| 2.8.2      | Molecular mechanisms involved in alopecia .....   | 64        |
| 2.8.3      | Stem cells and alopecia .....   | 65        |
| 2.8.4      | Mutant mouse models and cyclic alopecia .....   | 66        |
| <b>3.</b>  | <b>Aims and Objectives .....</b>  | <b>68</b> |
| <b>3.1</b> | <b>Rational or statement of the problem .....</b>   | <b>69</b> |
| <b>3.2</b> | <b>Hypothesis.....</b>  | <b>69</b> |
| <b>3.3</b> | <b>Objectives.....</b>  | <b>70</b> |
| <b>3.4</b> | <b>Outline of the study.....</b>  | <b>70</b> |
| <b>3.5</b> | <b>Work done .....</b>  | <b>72</b> |
| <b>4.</b>  | <b>Materials and Methods.....</b>   | <b>73</b> |
| <b>4.1</b> | <b>Mice models .....</b>  | <b>74</b> |
| <b>4.2</b> | <b>Mice genotyping .....</b>  | <b>75</b> |
| 4.2.1      | DNA extraction from tail tissue samples .....   | 75        |
| 4.2.2      | Primer sequences for the genotyping of K14-sPAL <sub>2</sub> -IIA, K14CreER,<br>Dab2flox, Rosa-YFP, H2BGFP and K5tTA..... | 76        |
| 4.2.3      | PCR conditions for the genotyping.....  | 77        |

|             |   |           |
|-------------|---|-----------|
| <b>4.3</b>  | <b>Doxycycline dose for triple transgenic mice for proliferation dynamics</b> ..... | <b>79</b> |
| <b>4.4</b>  | <b>Tissue processing for Histology and paraffin blocks</b> .....                    | <b>79</b> |
| 4.4.1       | Hematoxylin and eosin staining procedure .....                                      | 79        |
| <b>4.5</b>  | <b>Antibody details</b> .....   | <b>80</b> |
| <b>4.6</b>  | <b>Immunohistochemical staining (IHC)</b> .....                                     | <b>81</b> |
| <b>4.7</b>  | <b>Immunofluorescence staining</b> .....  | <b>83</b> |
| <b>4.8</b>  | <b>BrdU label retaining assay</b> .....   | <b>84</b> |
| <b>4.9</b>  | <b>Fluorescence Activated Cell Sorting (FACS)</b> .....                             | <b>84</b> |
| 4.9.1       | Isolation of total epidermal cells.....   | 85        |
| 4.9.2       | Staining procedure for hair follicle stem cells .....                               | 86        |
| <b>4.10</b> | <b>Colony forming efficiency of the hair follicle stem cells</b> .....              | <b>87</b> |
| <b>4.11</b> | <b>Primary keratinocytes culture</b> .....  | <b>87</b> |
| <b>4.12</b> | <b>BrdU cell proliferation assay</b> .....  | <b>91</b> |
| <b>4.13</b> | <b>Western blotting</b> .....   | <b>91</b> |
| 4.13.1      | Protein isolation from keratinocytes and skin.....                                  | 91        |
| 4.13.2      | Protein estimation by modified Lowry's method .....                                 | 92        |
| <b>4.14</b> | <b>RNA extraction and Quantification</b> .....                                      | <b>93</b> |
| <b>4.15</b> | <b>Real time PCR</b> .....  | <b>93</b> |
| <b>4.16</b> | <b>Hair depilation study on the dorsal skin</b> .....                               | <b>94</b> |
| <b>4.17</b> | <b>Topical application of JNK inhibitor on the mice skin</b> .....                  | <b>94</b> |
| <b>4.18</b> | <b>Statistical analysis</b> .....   | <b>94</b> |
| <b>5.</b>   | <b>Objective-I</b> .....  | <b>95</b> |
| <b>5.1</b>  | <b>Introduction</b> .....   | <b>96</b> |
| 5.1.1       | Secretory phospholipases.....   | 96        |
| 5.1.2       | Secretory Phospholipase A <sub>2</sub> Group IIA .....                              | 97        |

|            |   |            |
|------------|---|------------|
| 5.1.3      | Secretory phospholipases in the regulation of skin homeostasis .....  | 98         |
| <b>5.2</b> | <b>Results .....</b>  | <b>101</b> |
| 5.2.1      | Establishment of long-term keratinocytes culture .....  | 101        |
| 5.2.2      | Overexpression of sPLA <sub>2</sub> -IIA reduces colony forming efficiency of primary keratinocytes .....                             | 102        |
| 5.2.3      | Overexpression of sPLA <sub>2</sub> -IIA alters proliferation dynamics of HFSCs....   | 103        |
| 5.2.4      | sPLA <sub>2</sub> -IIA alters EGFR mediates JNK c-Jun signaling .....   | 105        |
| 5.2.5      | Increased c-Jun signaling enhances K14-sPLA <sub>2</sub> -IIA keratinocytes proliferation in vitro .....                              | 107        |
| 5.2.6      | Functional potential of HFSCs in vivo .....   | 109        |
| 5.2.7      | In vivo topical application of JNK inhibitor reverses depilation induced hair growth in K14-sPLA <sub>2</sub> -IIA mice .....         | 110        |
| 5.2.8      | Characterization of K14-sPLA <sub>2</sub> -IIA homozygous mice skin .....   | 111        |
| 5.2.9      | Abnormal organization of epidermal components and stratification of epidermis.....  | 114        |
| 5.2.10     | Drastic depletion of HFSCs in the K14-sPLA <sub>2</sub> -IIA homozygous mice ..   | 115        |
| 5.2.11     | Development of cyclic alopecia in K14-sPLA <sub>2</sub> -IIA homozygous mice..  | 117        |
| 5.2.12     | Mechanism of the development of alopecia .....  | 118        |
| 5.2.13     | sPLA <sub>2</sub> -IIA alters initial wound healing response in vivo .....  | 120        |
| <b>5.3</b> | <b>Graphical representation of abnormalities in the hair follicle cycling and in organization of the epidermal compartments .....</b> | <b>122</b> |
| <b>5.4</b> | <b>Discussion.....</b>  | <b>123</b> |
| <b>6.</b>  | <b>Objective-II.....</b>  | <b>130</b> |
| <b>6.1</b> | <b>Introduction.....</b>  | <b>131</b> |
| 6.1.1      | Disabled-2 (DAB2).....  | 131        |

|            |   |            |
|------------|---|------------|
| 6.1.2      | Role of Dab2 in regulation of Wnt signaling.....  | 132        |
| 6.1.3      | Regulation of TGF- $\beta$ and BMP signaling pathway by Dab2.....                               | 134        |
| 6.1.4      | Regulation of MAPK signaling by Dab2.....   | 135        |
| 6.1.5      | Dab2 and stem cells .....   | 136        |
| 6.1.6      | Dab2 as a tumor suppressor .....  | 137        |
| 6.1.7      | Expression of Dab2 in hair follicle stem cells .....  | 137        |
| <b>6.2</b> | <b>Results .....</b>  | <b>139</b> |
| 6.2.1      | Dab2 is upregulated in quiescent hair follicle stem cells.....                                  | 139        |
| 6.2.2      | Efficiency of K14CreER mediated Dab2 knockout.....  | 140        |
| 6.2.3      | Histology analysis of the hair follicle cycling in Dab2 cKO mice at various postnatal days..... | 141        |
| 6.2.4      | Loss of Dab2 decreases the active $\beta$ -catenin level in hair follicle.....                  | 144        |
| 6.2.5      | Decreased cell proliferation in the Dab2 cKO mice .....   | 145        |
| 6.2.6      | Dab2 deletion does not alter epidermal differentiation.....                                     | 146        |
| 6.2.7      | FACS analysis of hair follicle stem cell population .....                                       | 147        |
| 6.2.8      | Dab2 ablated HFSCs showed reduced colony forming efficiency .....                               | 148        |
| 6.2.9      | BrdU label retaining cells (LRC) assay .....  | 150        |
| <b>6.3</b> | <b>Discussion.....</b>  | <b>152</b> |
| <b>7.</b>  | <b>Summary and Conclusion .....</b>   | <b>155</b> |
| 7.1        | Summary and Conclusion .....  | 156        |
| 7.2        | Future Perspectives.....  | 160        |
| <b>8.</b>  | <b>Bibliography .....</b>   | <b>162</b> |
|            | <b>Publications .....</b>   | <b>180</b> |



# *Synopsis*





## Homi Bhabha National Institute

### Ph.D. PROGRAMME

- 1. Name of the Student:** Mr Chovatiya Gopalbhai Lavjibhai
- 2. Name of the Constituent Institution:** TMC-ACTREC
- 3. Enrolment No.:** LIFE09201204005
- 4. Title of the Thesis:** “Delineating the Role of Signaling Pathways in Epidermal Stem Cell Regulation”
- 5. Board of Studies:** Life Sciences

### SYNOPSIS

#### **1. Introduction:**

The adult tissues contain stem cells reservoir that maintains tissue integrity during homeostasis and injury. The adult tissue stem cells reside in the specific microenvironments known as stem cells niche that provides both the activating and inhibitory cues for the proliferation and quiescence respectively<sup>1</sup>. Further, stem cells divide infrequently throughout the life of an organism to maintain the stem cell pool, which was elegantly shown by the proliferation dynamics of hair follicle stem cells (HFSCs) division that exhibited infrequent cell division and random chromosome segregation<sup>2, 3, 4, 5</sup>. The proliferation of tissue stem cells is tightly regulated by the dynamic interaction between extrinsic signals and intracellular signalling modulators, which maintains a self-renewal capacity<sup>6</sup>. Importantly, these dynamic interactions are governed by complex signalling networks such as Wnt, Bmp, Shh, Notch, EGFR and various growth factors including small metabolites such as lysophosphatidic acid (LPA) and

lysophosphatidylcholine (LPC)<sup>7 8</sup>. Moreover, perturbation in the regulation of these signalling pathways leads to the formation of cancer<sup>9</sup>. Hitherto, how the self-renewal and differentiation of stem cells are being maintained in various tissues with a unique divisional mode is a central issue in stem cell biology?

The skin provides an excellent model system for investigating the stem cell regulation and elucidating the signalling mechanisms, which are regulated by surrounding stem cells-niche factors. Skin is the largest organ of the mammalian body that protects from various external insults. Skin contains pilosebaceous apparatus, which includes hair follicle (HF), sebaceous gland (SG) as well as arrector pili muscle and the pilosebaceous units are connected through the interfollicular epidermis (IFE). The hair follicle cycles through various phases such as growth (anagen), destruction (catagen) and rest (telogen)<sup>10</sup>. The epidermis and hair follicle harbours several distinct stem cells populations that possess an ability to self-renew and produce daughter cells<sup>11, 12</sup>. These daughter cells further produce differentiated cells to fuel constant requirements of the tissue to maintain tissue integrity. The hair follicle growth is initiated by activation of the HFSCs, which resides in the specialised region known as “Bulge”. During the initiation of the Anagen, a cluster of underlying mesenchymal cells termed as dermal papilla (DP) provides signals for the activation of HFSCs<sup>13</sup>. However, how the signalling pathways mediate precise regulation of the HFSCs during its proliferative and quiescent phase is remaining unexplored.

Secretory phospholipase A<sub>2</sub> group IIA (sPLA<sub>2</sub>-IIA) is also known as enhancing factor (EF), which is the mouse homologue of human sPLA<sub>2</sub>-IIA. It is a dual functioning molecule having both the enhancing activity and phospholipase activity<sup>14</sup>. Phospholipase A<sub>2</sub> (sPLA<sub>2</sub>-IIA) catalyses the hydrolysis of the sn-2 position of glycerophospholipids to yield fatty acids and lysophospholipids<sup>15</sup>. sPLA<sub>2</sub>-IIA has been implicated in various forms of cancer such as

intestinal, colorectal and prostate<sup>16</sup>. Importantly, the enhancing factor, sPLA<sub>2</sub>-IIA also shows catalytic independent activity, which enhances binding of EGF in vitro<sup>14</sup>. Recently, Pla2g2a is also reported as  $\beta$ -catenin/TCF target (Wnt target) gene<sup>17</sup>. Mice overexpressing sPLA<sub>2</sub>-IIA caused a reduction in intestinal tumour multiplicity and size<sup>18</sup>, whereas a natural disruption of the secretory group II phospholipase A<sub>2</sub> gene is observed in the mouse strains such as C57BL6 and 129SV<sup>19</sup>, which modifies the numbers of polyps and intestinal tumours induced by the mutation in the APC gene<sup>20</sup>. Overexpression of sPLA<sub>2</sub>-IIA in mice (K14-sPLA<sub>2</sub>-IIA) is susceptible to chemical-induced skin carcinogenesis<sup>21</sup>. Recently, we have reported that the mice overexpressing sPLA<sub>2</sub>-IIA showed a gradual exhaustion of HFSCs<sup>22</sup>. However, the molecular mechanism of sPLA<sub>2</sub>-IIA mediated HFSCs exhaustion is yet to be elucidated.

Wnt signalling is highly conserved and complex signalling pathway that plays a critical role in the embryonic development, self-renewal, proliferation and differentiation of various cell types. Importantly, targeted deletion of  $\beta$ -catenin in the epidermis leads to failure in the placode morphogenesis<sup>23</sup>. On the other hand, ectopic expression of stable  $\beta$ -catenin in epidermis showed precocious hair morphogenesis and multiple hair germ budding<sup>24</sup>. The double knockout of Tcf3 and Tcf4 resulted in the hair loss, suggesting they are involved in the hair follicle development in mice<sup>25</sup>. Recently, it has been shown that Wnt target gene Axin2 marks quiescent HFSCs and constantly expressed during quiescent phase<sup>26</sup>. Further studies of various secretory Wnt inhibitors have highlighted the role of functional Wnt signalling in the HFSCs regulation. The injection of recombinant Dickkopf 1 (rhDKK-1) induces catagen and inhibition of its function by neutralising antibody delayed catagen onset<sup>27</sup>. Importantly, the study from our laboratory showed that the loss of Secreted frizzled-related protein 1 (Sfrp1) affects HFSCs maintenance and enhances tumorigenic potential of CSCs in vivo (Unpublished observation). Another novel intracellular Wnt signalling modulator, Disabled-2

(Dab2), is a member of the disabled gene family and a mammalian structural homolog of the *Drosophila* disabled (Dab). It is a potent tumour suppressor that was initially identified in the ovarian carcinoma<sup>28</sup>, which was subsequently found to be decreased in the breast, prostate and pancreatic carcinoma<sup>29, 30, 31</sup>. Dab2 regulate multiple signalling pathways by controlling clathrin-dependent endocytosis of receptors and by direct association with cytoplasmic signalling components<sup>32</sup>. Dab2 directly binds with Axin and prevents degradation of Axin by LRP5/6 and subsequently stabilise destruction complex, which leads to  $\beta$ -catenin degradation<sup>33</sup>. In addition, Dab2 prevent interaction between axin and PP1, which stabilises Axin and leads to  $\beta$ -catenin degradation<sup>34</sup>. Collectively, it is a crucial linker of receptor endocytosis and intracellular signalling. The Dab2 expression is six to fifteen folds higher in HFSCs as compared to normal cells during quiescence<sup>35, 36</sup>. Therefore, it may have an important role in inhibition of Wnt signalling and activation of BMP signalling during HFSCs quiescence. However, the role of Dab2 in the HFSCs regulation is remaining unexplored.

## **2. Rationale:**

Cell signalling networks of Wnt/Notch/Sonic-hedgehog and others like EGFR pathways etc. regulate stem cell renewal, maintenance, and differentiation. sPLA<sub>2</sub>-IIA is involved in the regulation of signalling pathway such as EGFR and recently reported as a  $\beta$ -catenin /TCF target (Wnt target) gene. However, the mechanism through sPLA<sub>2</sub>-IIA alters HFSCs proliferation and differentiation is remaining unknown. In addition, Wnt signalling modulator, Dab2, acts as a linker between endocytic process and cell signalling that regulate Wnt and Bmp signalling pathway. Recently, it was shown that Dab2 is highly upregulated in the quiescence HFSCs. Hence, understanding the functional role of sPLA<sub>2</sub>-IIA and Dab2 in the regulation of cell signalling pathways may lend insight into the mechanisms of stem cell regulation.

### **3. Aim and Objectives:**

#### **3.1. To decipher the role of group IIA secretory phospholipase A<sub>2</sub>/ enhancing factor in epidermal stem cell regulation**

3.1.1. To determine the role of group IIA secretory phospholipase A<sub>2</sub>/ enhancing factor in regulation of molecular signalling pathways

3.1.2. To determine the functional role of group IIA secretory phospholipase A<sub>2</sub>/ enhancing factor in mouse epidermal keratinocytes

3.1.3. To characterize the K14-sPLA<sub>2</sub>-IIA homozygous mice skin in relation to the hair follicle stem cells loss

#### **3.2. To investigate the role of disabled-2 (Dab2) in epidermal stem cell regulation**

3.2.1. To characterize the effect of Dab2 deletion in hair follicle cycling and stem cells

3.2.2. Functional characterization of hair follicle stem cells in Dab2 knockout mice

### **4. Materials and methods:**

#### **4.1. Ethics statement**

The Institutional Animal Ethics Committee (IAEC) approved all protocols for the animal studies (approval ID: 07/2014 and 27/2013). A Committee formed under the guidelines of Committee for the Purpose of Control & Supervision of Experiments on Animals (CPCSEA), Government of India.

#### **4.2. Transgenic mice and genotyping**

We employed transgenic mice overexpressing sPLA<sub>2</sub>-IIA under Keratin 14 promoter to study its proliferative effect on the epidermal keratinocytes and HFSCs. The K14-sPLA<sub>2</sub>-IIA transgenic mice were a generous gift from Dr Rita Mulherkar<sup>21</sup>. For the proliferation

dynamics, we employed pTRE–H2B–GFP<sup>37</sup> and K5fTA mice<sup>38</sup>. In addition, the Dab2 flox and K14CreER mice were imported from the Jackson Laboratory, USA.

#### **4.3. Fluorescence-activated cell sorting (FACS)**

Skin tissues were incubated in trypsin (0.25%) for overnight digestion to isolate epidermal cells. Isolated cells were stained with the biotin-labelled CD34 antibody (eBioscience) and PE-labelled  $\alpha$ 6-integrin (CD49f) antibody (BD Pharmingen). Streptavidin-APC (BD Pharmingen) was used as a secondary antibody for the biotin-labelled CD34 antibody.

#### **4.4. Primary keratinocytes culture**

Primary mouse epidermal keratinocytes were isolated from newborn (PD2) mouse skin by incubating whole skin in the Dispase (5U/ml) solution overnight. The epidermis was separated from the underlying dermis and minced in 0.1% Trypsin-EDTA to prepare a single cell suspension. Keratinocytes were cultured using low Ca<sup>+2</sup> keratinocyte E media on irradiated mouse J2 fibroblasts<sup>22</sup>.

#### **4.5. Immunofluorescence Assay (IFA)**

The immunofluorescence assay was performed on the cryosections by using anti-BrdU, Active  $\beta$ -catenin, K1, Loricrin, anti-Ki67, anti-CD34 and anti  $\alpha$ 6-integrin antibody.

### **5. Results:**

#### **5.1. Overexpression of sPLA<sub>2</sub>-IIA in mice epidermis reduces colony forming efficiency of epidermal keratinocytes**

Previously, our lab study showed a gradual depletion of the HFSCs in the K14-sPLA<sub>2</sub>-IIA mice. Further, to check the stemness potential, the ability of primary keratinocyte to form an independent colony was determined. The result showed reduction in the total numbers

of colonies in the K14-sPLA<sub>2</sub>-IIA mice keratinocytes as compared to WT keratinocytes, suggesting that the overexpression of sPLA<sub>2</sub>-IIA in mice keratinocytes affects its ability to produce an independent colony and its stemness potential.

### **5.2. Overexpression of sPLA<sub>2</sub>-IIA upregulates JNK/c-Jun signalling in vitro and in vivo**

sPLA<sub>2</sub>-IIA is known to enhance the binding of the EGF<sup>14</sup>. To understand the effect of sPLA<sub>2</sub>-IIA on EGFR and MAPK signalling, keratinocytes isolated from newborn mice (WT and K14-sPLA<sub>2</sub>-IIA mice) were serum starved for 24 hrs to remove the background effect and then stimulated with 10ng/ml EGF for 15 min, followed by lysis in RIPA buffer. Activation of EGFR, JNK1/2 and c-Jun including the phosphorylated forms were analysed by western blotting. The results showed an increased activation of EGFR, JNK1/2 and c-Jun in K14-sPLA<sub>2</sub>-IIA mice keratinocytes as compared to wild-type control. Similarly, western blotting analysis of epidermal lysate prepared from mouse skin also showed an increased activation of EGFR and c-Jun in K14-sPLA<sub>2</sub>-IIA mice skin. Together, these data suggest an enhancing effect of sPLA<sub>2</sub>-IIA on EGFR mediated JNK/c-Jun signalling.

### **5.3. Proliferation dynamics of the HFSCs in K14-sPLA<sub>2</sub>-IIA mice**

To understand the effect of altered signalling and proliferation dynamics of the hair follicle stem cells, we employed triple transgenic (H2BGFP-K5fTa-K14-sPLA<sub>2</sub>-IIA) (Tet-off) mice to analyse the proliferation dynamics of the HFSCs. The triple transgenic mice were chased with doxycycline (1gm/kg) from PD21 to PD49, and from PD36 to PD49 to check the effect of sPLA<sub>2</sub>-IIA on HFSCs proliferation during various stages of the hair cycle. Our results showed loss of bright peaks of GFP positive bulge cells (PD21-49 chase) and peaks of multiple divisions (PD36 to 49 Chase), suggesting that the sPLA<sub>2</sub>-IIA

induces HFSCs proliferation even during the Catagen and Telogen stages of the hair cycle. Together, these data suggest that the sPLA<sub>2</sub>-IIA induces HFSCs proliferation irrespective of their quiescence potential and alters an infrequent divisional characteristic of HFSCs.

#### **5.4. Inhibition of c-Jun signalling exhibited in-vivo reversion of depilation-induced faster hair growth**

To examine whether progenitors cells produced from remaining HFSCs in K14-sPLA<sub>2</sub>-IIA mice are able to differentiate in hair shaft producing cells, we performed hair depilation experiment, which removes entire hair shaft from the hair follicle. Our data showed faster and complete hair coat recovery in K14-sPLA<sub>2</sub>-IIA mice. Interestingly, in our in vivo reversion study, depilation on mice skin followed by topical treatment of JNK inhibitor significantly delayed hair growth in K14-sPLA<sub>2</sub>-IIA mice as compared to vehicle control. Thus, these data suggest that sPLA<sub>2</sub>-IIA induced c-Jun activation may be directly involved in the proliferation and differentiation of HFSCs. We further sought to understand the hair follicle cycling pattern and epidermal stratification during complete loss of HFSCs. Therefore, we used K14-sPLA<sub>2</sub>-IIA homozygous mice for further study.

#### **5.5. Characterization of the K14-sPLA<sub>2</sub>-IIA homozygous mice skin in relation to the loss of HFSCs**

To study the enhanced effect of sPLA<sub>2</sub>-IIA overexpression, we used K14-sPLA<sub>2</sub>-IIA homozygous mice to assess its effect on various components of the epidermis. To check its effect on the hair follicle cycling; Hematoxylin and eosin staining (H&E) on the dorsal skin sections were performed during various postnatal days (PD15, 19, 21, 25, 28, 35, 41 and 49). Our data demonstrate abnormal thickening of the interfollicular epidermis (IFE) and hair follicle halted at anagen like a stage in K14-sPLA<sub>2</sub>-IIA homozygous mice.

Moreover, we did not observe complete telogen at any postnatal day (PD15, PD17, PD21, PD25, PD28, PD30, PD35, PD41, PD45 and PD49). Importantly, our flow cytometry analysis of HFSCs showed drastic depletion of HFSCs at an early age (PD28). These data showed the pronounced effect of sPLA<sub>2</sub>-IIA on the hair follicle progression and epidermal stratification.

#### **5.6. Development of the cyclic alopecia and mechanism of defective hair shaft formation in the K14-sPLA<sub>2</sub>-IIA homozygous mice**

K14-sPLA<sub>2</sub>-IIA homozygous mice displayed hair loss at very early age. Therefore, we followed these mice from birth till six months of age to monitor the pattern of hair growth and hair loss. We observed that successive cycle of hair growth and loss was occurring repetitively after 18-22 days up to 6-8 months. Further, we investigated the expression pattern of various genes, which are known to be involved in the regulation of matrix cells proliferation and hair shaft differentiation. Our data showed aberrant expression of Sox21, Msx2 and Foxn1 along with BMP4, Lef1 and Shh. These data suggested deregulated signalling in matrix cells that might lead to defects in differentiation of IRS and formation of the hair shaft.

#### **5.7. Effect of loss of HFSCs on the wound healing response in K14-sPLA<sub>2</sub>-IIA homozygous mice skin**

To check the impact of sPLA<sub>2</sub>-IIA mediated depletion of the HFSCs on the process of wound healing, we created scratch wounds on the upper region at midline and full thickness wounds on the lower region of dorsal skin at PD49. We monitored the healing process to assess the macroscopic healing defects. Our data showed an impaired initial healing response in K14-sPLA<sub>2</sub>-IIA homozygous mice at day 5. However, the pace of

wound recovery accelerated after 5-6 days that fully recovered at the same time of wild-type mice. Thus, it demonstrates that overexpression of sPLA<sub>2</sub>-IIA delays initial response to wounding, which may explain the contribution of HFSCs in the early phase of wound healing.

#### **5.8. Efficiency of the tamoxifen-inducible deletion of Dab2 in conditional knockout mice**

To determine the efficiency of K14CreER mediated induction of gene knockout, 3mg Tamoxifen was injected for five consecutive days in K14CreER: ROSA-STOP-YFP mice and sacrificed at PD49. The dorsal skin tissue sections were analyzed for YFP expression by using anti-GFP antibody. Our results showed YFP positive cells in the basal layer of the IFE and ORS of the hair follicle, suggesting that the dose of tamoxifen is sufficient to induce Cre activity. Further, deletion of the Dab2 floxed allele in the K14CreER: Dab2<sup>fl/fl</sup> (Homozygous) mice was confirmed by performing real-time PCR analysis of Dab2 gene in the FACS sorted  $\alpha 6$  integrin<sup>+</sup> cells, which showed 60-70% reduction in the level of Dab2 in the K14CreER: Dab2<sup>fl/fl</sup> mice as compared to wild-type mice.

#### **5.9. Effect of Dab2 deletion on the proliferation of basal keratinocytes and HFSCs**

As the Dab2 is known to inhibit cell proliferation, we checked whether deletion of Dab2 has any effect on the epidermal as well as HFSCs proliferation by using the Ki67 antibody. Importantly, in contrast to its known inhibitory role on the cell proliferation, our preliminary data suggest that Dab2 deletion moderately reduces cell proliferation in the K14CreER: Dab2<sup>fl/fl</sup> mice skin as compared to wild-type mice skin.

#### **5.10. Flow cytometry analysis of HFSCs in Dab2 cKO mice**

Dab2 is highly expressed in the HFSCs; therefore we sought to understand the effect of Dab2 deletion on the maintenance of the HFSCs population. We have analyzed the CD34<sup>+</sup>

and  $\alpha 6$  integrin<sup>+</sup> dual positive bulge stem cells population at various postnatal days. However, we did not find any significant difference in the total no of CD34<sup>+</sup> and  $\alpha 6$  integrin<sup>+</sup> dual positive HFSCs.

### 5.11. Colony forming efficiency of HFSCs in Dab2 cKO mice

To examine whether the loss of Dab2 has any effect on proliferation of HFSC in vitro, we performed colony formation assays to investigate independent colony forming potential of FACS purified Bu-HFSCs. Equal numbers (10,000) of FACS purified Bu-HFSCs from wild-type, K14CreER: Dab2<sup>fl/+</sup> (Heterozygous) and K14CreER: Dab2<sup>fl/fl</sup> (Homozygous) mice were cultured in E-media with 10ng/ml EGF and 3T3 J2 cells for three weeks and allowed to form colonies. Interestingly, the HFSCs of the K14CreER: Dab2<sup>fl/fl</sup> mice were strongly impaired in their colony-forming ability, suggesting its reduced stemness potential as compared to HFSCs of the wild-type mice. This result suggests that Dab2 may have a functional role in regulating the stemness of HFSCs when they induced for the proliferation in vitro.

### 5.12. Effect of Dab2 deletion on the activation of $\beta$ -catenin

Dab2 protein is known to be upregulated in Bu-HFSCs during quiescence phase (Telogen) of the hair follicle. To investigate any effect of Dab2 deletion on the activity of the Wnt signalling in vivo, dorsal skin tissues of the wild-type, K14CreER: Dab2<sup>fl/+</sup> and K14CreER: Dab2<sup>fl/fl</sup> mice were analyzed for the level of activated  $\beta$ -catenin at PD68. Surprisingly, our results showed a reduced level of activated  $\beta$ -catenin in K14CreER: Dab2<sup>fl/fl</sup> mice as compared to wild-type mice. However, we did not observe nuclear localization of  $\beta$ -catenin during the telogen phase in the wild type, K14CreER: Dab2<sup>fl/+</sup> and K14CreER: Dab2<sup>fl/fl</sup> mice.

## **6. Summary and significance of the study:**

- a.** Overexpression of sPLA<sub>2</sub>-IIA in mice epidermis enhances the EGFR mediated JNK/c-Jun signalling in vitro and in vivo
- b.** Enhanced activation of JNK/c-Jun signalling leads to an increased proliferation of epidermal keratinocytes and HFSCs
- c.** sPLA<sub>2</sub>-IIA induced in-vivo proliferation was reverted by the topical application of JNK inhibitor
- d.** sPLA<sub>2</sub>-IIA induced proliferation alters HFSCs divisional dynamics
- e.** The homozygous mice overexpressing sPLA<sub>2</sub>-IIA develops cyclic alopecia mediated through aberrant expression of matrix cells differentiation regulators
- f.** Dab2 positively regulates  $\beta$ -catenin signalling in mouse hair follicle cells
- g.** Knockout of Disabled 2 (Dab2) in mice epidermis resulted in the proliferative defects of epidermal cells
- h.** Deletion of Dab2 strongly reduces colony forming ability of HFSCs

In conclusion, our study has investigated the functional involvement of two signalling molecules; sPLA<sub>2</sub>-IIA and Dab2, in the regulation of the HFSCs. The sPLA<sub>2</sub>-IIA induced proliferation mediated stem cells exhaustion provides mechanistic insights to understand the development of alopecia and epithelial cancers. Moreover, cell proliferation-promoting functions of Dab2 explain and support the tissue-specific and context-dependent differential functions of different signalling regulators. Collectively, this study expands our understanding of tissue stem cells maintenance and may be useful in the development of effective strategies against skin disorders and epithelial cancers.

## 7. References

1. Morrison SJ, Spradling AC. Stem cells and niches: mechanisms that promote stem cell maintenance throughout life. *Cell* **132**, 598-611 (2008).
2. Waghmare SK, Bansal R, Lee J, Zhang YV, McDermitt DJ, Tumbar T. Quantitative proliferation dynamics and random chromosome segregation of hair follicle stem cells. *The EMBO journal* **27**, 1309-1320 (2008).
3. Waghmare SK, Tumbar T. Adult hair follicle stem cells do not retain the older DNA strands in vivo during normal tissue homeostasis. *Chromosome Res* **21**, 203-212 (2013).
4. Kiel MJ, *et al.* Haematopoietic stem cells do not asymmetrically segregate chromosomes or retain BrdU. *Nature* **449**, 238-242 (2007).
5. Li L, Clevers H. Coexistence of quiescent and active adult stem cells in mammals. *Science (New York, NY)* **327**, 542-545 (2010).
6. Fuchs E, Chen T. A matter of life and death: self-renewal in stem cells. *EMBO reports* **14**, 39-48 (2013).
7. Lee J, Tumbar T. Hairy tale of signaling in hair follicle development and cycling. *Seminars in cell & developmental biology* **23**, 906-916 (2012).
8. Pebay A, Bonder CS, Pitson SM. Stem cell regulation by lysophospholipids. *Prostaglandins & other lipid mediators* **84**, 83-97 (2007).
9. Reya T, Morrison SJ, Clarke MF, Weissman IL. Stem cells, cancer, and cancer stem cells. *Nature* **414**, 105-111 (2001).
10. Alonso L, Fuchs E. The hair cycle. *Journal of cell science* **119**, 391-393 (2006).
11. Alonso L, Fuchs E. Stem cells of the skin epithelium. *Proceedings of the National Academy of Sciences of the United States of America* **100 Suppl 1**, 11830-11835 (2003).
12. Blanpain C, Fuchs E. Epidermal stem cells of the skin. *Annual review of cell and developmental biology* **22**, 339-373 (2006).
13. Greco V, *et al.* A two-step mechanism for stem cell activation during hair regeneration. *Cell stem cell* **4**, 155-169 (2009).
14. Mulherkar R, Deo MG. Further studies on the enhancing factor and its possible mechanism of action. *J Cell Physiol* **127**, 183-188 (1986).
15. Murakami M, Taketomi Y, Sato H, Yamamoto K. Secreted phospholipase A2 revisited. *J Biochem* **150**, 233-255 (2011).
16. Scott KF, *et al.* Emerging roles for phospholipase A2 enzymes in cancer. *Biochimie* **92**, 601-610 (2010).
17. Ganesan K, *et al.* Inhibition of gastric cancer invasion and metastasis by PLA2G2A, a novel beta-catenin/TCF target gene. *Cancer Res* **68**, 4277-4286 (2008).
18. Cormier RT, *et al.* Secretory phospholipase Pla2g2a confers resistance to intestinal tumorigenesis. *Nature genetics* **17**, 88-91 (1997).
19. Kennedy BP, *et al.* A natural disruption of the secretory group II phospholipase A2 gene in inbred mouse strains. *The Journal of biological chemistry* **270**, 22378-22385 (1995).

20. MacPhee M, Chepenik KP, Liddell RA, Nelson KK, Siracusa LD, Buchberg AM. The secretory phospholipase A2 gene is a candidate for the Mom1 locus, a major modifier of ApcMin-induced intestinal neoplasia. *Cell* **81**, 957-966 (1995).
21. Mulherkar R, Kirtane BM, Ramchandani A, Mansukhani NP, Kannan S, Naresh KN. Expression of enhancing factor/phospholipase A2 in skin results in abnormal epidermis and increased sensitivity to chemical carcinogenesis. *Oncogene* **22**, 1936-1944 (2003).
22. Sarate RM, Chovatiya GL, Ravi V, Khade B, Gupta S, Waghmare SK. sPLA2 -IIA Overexpression in Mice Epidermis Depletes Hair Follicle Stem Cells and Induce Differentiation Mediated Through Enhanced JNK/c-Jun Activation. *Stem Cells*, (2016).
23. Huelsken J, Vogel R, Erdmann B, Cotsarelis G, Birchmeier W. beta-Catenin controls hair follicle morphogenesis and stem cell differentiation in the skin. *Cell* **105**, 533-545 (2001).
24. Narhi K, Jarvinen E, Birchmeier W, Taketo MM, Mikkola ML, Thesleff I. Sustained epithelial beta-catenin activity induces precocious hair development but disrupts hair follicle down-growth and hair shaft formation. *Development* **135**, 1019-1028 (2008).
25. Nguyen H, *et al.* Tcf3 and Tcf4 are essential for long-term homeostasis of skin epithelia. *Nature genetics* **41**, 1068-1075 (2009).
26. Lim X, Tan SH, Yu KL, Lim SB, Nusse R. Axin2 marks quiescent hair follicle bulge stem cells that are maintained by autocrine Wnt/beta-catenin signaling. *Proceedings of the National Academy of Sciences of the United States of America* **113**, E1498-1505 (2016).
27. Kwack MH, Kim MK, Kim JC, Sung YK. Dickkopf 1 promotes regression of hair follicles. *J Invest Dermatol* **132**, 1554-1560 (2012).
28. Mok SC, *et al.* Molecular cloning of differentially expressed genes in human epithelial ovarian cancer. *Gynecologic oncology* **52**, 247-252 (1994).
29. Schwahn DJ, Medina D. p96, a MAPK-related protein, is consistently downregulated during mouse mammary carcinogenesis. *Oncogene* **17**, 1173-1178 (1998).
30. Tseng CP, Ely BD, Li Y, Pong RC, Hsieh JT. Regulation of rat DOC-2 gene during castration-induced rat ventral prostate degeneration and its growth inhibitory function in human prostatic carcinoma cells. *Endocrinology* **139**, 3542-3553 (1998).
31. Huang Y, *et al.* Doc-2/hDab2 expression is up-regulated in primary pancreatic cancer but reduced in metastasis. *Laboratory investigation; a journal of technical methods and pathology* **81**, 863-873 (2001).
32. Koral K, Erkan E. PKB/Akt partners with Dab2 in albumin endocytosis. *American journal of physiology Renal physiology* **302**, F1013-1024 (2012).
33. Jiang Y, Prunier C, Howe PH. The inhibitory effects of Disabled-2 (Dab2) on Wnt signaling are mediated through Axin. *Oncogene* **27**, 1865-1875 (2008).
34. Jiang Y, Luo W, Howe PH. Dab2 stabilizes Axin and attenuates Wnt/beta-catenin signaling by preventing protein phosphatase 1 (PP1)-Axin interactions. *Oncogene* **28**, 2999-3007 (2009).
35. Zhang YV, Cheong J, Ciapurin N, McDermitt DJ, Tumber T. Distinct self-renewal and differentiation phases in the niche of infrequently dividing hair follicle stem cells. *Cell stem cell* **5**, 267-278 (2009).
36. Morris RJ, *et al.* Capturing and profiling adult hair follicle stem cells. *Nature biotechnology* **22**, 411-417 (2004).

37. Tumber T, *et al.* Defining the epithelial stem cell niche in skin. *Science (New York, NY)* **303**, 359-363 (2004).
38. Diamond I, Owolabi T, Marco M, Lam C, Glick A. Conditional gene expression in the epidermis of transgenic mice using the tetracycline-regulated transactivators tTA and rTA linked to the keratin 5 promoter. *J Invest Dermatol* **115**, 788-794 (2000).

## **8. Publications in Refereed Journals:**

### **a. Published:**

1. **Chovatiya GL**, Sarate RM, Sunkara RR, Gawas NP, Kala V, Waghmare SK. Secretory phospholipase A<sub>2</sub>-IIA overexpressing mice exhibit cyclic alopecia mediated through aberrant hair shaft differentiation and impaired wound healing response. *Sci Rep* **7**, 11619 (2017). doi: 10.1038/s41598-017-11830-9.
2. Sarate RM, **Chovatiya GL**, Ravi V, Khade B, Gupta S, Waghmare SK. sPLA<sub>2</sub> -IIA Overexpression in Mice Epidermis Depletes Hair Follicle Stem Cells and Induce Differentiation Mediated Through Enhanced JNK/c-Jun Activation. *Stem Cells*, (2016). doi: 10.1002/stem.2418. Epub 2016 Jul 8.

### **b. Accepted: Nil**

### **c. Communicated: Nil**

### **d. Other Publications**

#### **I. Manuscript under preparation**

**Chovatiya GL**, Godbole S, Gawas NP, Waghmare SK. Context-dependent effect of secretory phospholipase A<sub>2</sub> - Group IIA induced proliferation in epidermal homeostasis and cancer

#### **II. Book/Book Chapter: Nil**

#### **III. Poster Presentation**

- 1) Poster presentation on the topic entitled “**Secretory phospholipase A<sub>2</sub>-IIA overexpression alters epidermal stem cells proliferation dynamics and differentiation associated with asymmetric cell division**” at Gordon Research Conference on Epithelial Differentiation and Keratinization, May 7-12, 2017 Italy.
- 2) Poster presentation on the topic entitled “**Effect of secretory phospholipase A<sub>2</sub>-IIA on epidermal proliferation and differentiation**” at International conference “A Conference of New Ideas in Cancer-Challenging Dogmas” held at Tata Memorial Centre, 2016, India.

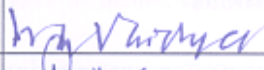
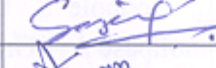
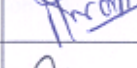
- 3) Poster presentation on the topic entitled “Effect of Secretory Phospholipase A<sub>2</sub>-IIA On Epidermal Growth and Differentiation” at International conference organized on “Tissue Homeostasis and Inflammation”, held at InStem, 2016, India
- 4) Poster presentation on the topic entitled “Synergistic effect of secretory phospholipase A<sub>2</sub> IIA controls epidermal homeostasis” at International conference organized by IACR (34<sup>th</sup> Annual Convention of Indian Association for Cancer Research), held at Jaipur, 2015, India
- 5) Poster presentation on the topic entitled “Effect of Lysophospholipids on Proliferative Dynamics of Epidermal Stem Cells” at XXVII All India Cell Biology Conference (AICBC), held at National Centre for Biological Sciences, 2013, India



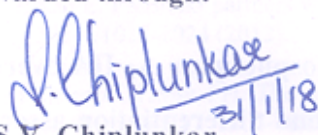
Signature of Student:

Date: 08/01/2018

**Doctoral Committee:**

| S. No. | Name                 | Designation      | Signature  | Date      |
|--------|----------------------|------------------|--|-----------|
| 1.     | Dr. Milind Vaidya    | Chairperson      |  | 10/01/18  |
| 2.     | Dr. Sanjeev Waghmare | Guide & Convener |  | 10/1/2018 |
| 3.     | Dr. Sanjay Gupta     | Member           |  | 10/01/18  |
| 4.     | Dr. Ashok Varma      | Member           |  | 10/01/18  |
| 5.     | Dr. Anjali Shiras    | Invitee          |  | 23/01/18  |

**Forwarded through:**

  
**Dr. S.V. Chiplunkar**  
 Director, ACTREC  
 Chairperson, Academic &  
 Training Programme, ACTREC  
**Dr. S. V. Chiplunkar**  
 Director  
 Advanced Centre for Treatment, Research &  
 Education in Cancer (ACTREC)  
 Tata Memorial Centre  
 Kharghar, Navi Mumbai - 410 210.

  
**Dr. K. Sharma,**  
 Director, Academics,  
 T.M.C.  
**PROF. K. S. SHARMA**  
 DIRECTOR (ACADEMICS)  
 TATA MEMORIAL CENTRE,  
 PAREL, MUMBAI

## *List of Figures*

|   |            |
|---|------------|
| <b>Figure 1.1 Isolation and differentiation of ES cells.....</b>                                | <b>26</b>  |
| <b>Figure 1.2 Tissue stem cells and their niche .....</b>                                       | <b>28</b>  |
| <b>Figure 2.1 Major components of mouse and human skin .....</b>                                | <b>31</b>  |
| <b>Figure 2.2 Development and stratification of the epidermis.....</b>                          | <b>33</b>  |
| <b>Figure 2.3 Layers of the mouse and human epidermis.....</b>                                  | <b>35</b>  |
| <b>Figure 2.4 The structure of hair follicle .....</b>  | <b>37</b>  |
| <b>Figure 2.5 Stages of the hair follicle morphogenesis.....</b>                                | <b>39</b>  |
| <b>Figure 2.6 Different phases of the hair cycle .....</b>                                      | <b>42</b>  |
| <b>Figure 2.7 Strategy for the H2BGFP (Tet Off) system.....</b>                                 | <b>45</b>  |
| <b>Figure 2.8 Serial dilution of H2BGFP during stem cells division in vivo .....</b>            | <b>46</b>  |
| <b>Figure 2.9 The structure of the sebaceous gland.....</b>                                     | <b>48</b>  |
| <b>Figure 2.10 The Wnt signaling pathway .....</b>  | <b>51</b>  |
| <b>Figure 2.11 Overview of BMP signaling pathway.....</b>                                       | <b>55</b>  |
| <b>Figure 2.12 Hedgehog signaling pathway .....</b>   | <b>57</b>  |
| <b>Figure 2.13 Notch signaling pathway .....</b>  | <b>59</b>  |
| <b>Figure 2.14 Steps of the wound healing process.....</b>                                      | <b>61</b>  |
| <b>Figure 5.1 Primary epidermal keratinocytes culture .....</b>                                 | <b>101</b> |
| <b>Figure 5.2 Colony forming efficiency of primary keratinocytes.....</b>                       | <b>102</b> |
| <b>Figure 5.3 Proliferation dynamics of HFSCs during various stages of hair cycle<br/>.....</b> | <b>104</b> |
| <b>Figure 5.4 Western blotting analysis of EGFR-JNK-c-Jun signaling pathway .</b>               | <b>106</b> |
| <b>Figure 5.5 Analysis of cell proliferation by BrdU incorporation assay .....</b>              | <b>108</b> |
| <b>Figure 5.6 Depilation induced hair growth in WT and K14-sPLA<sub>2</sub>-IIA mice ...</b>    | <b>109</b> |

|   |            |
|---|------------|
| <b>Figure 5.7 In vivo reversion of depilation induced hair growth by topical application of the JNK inhibitor .....</b> | <b>110</b> |
| <b>Figure 5.8 Histological characterization of the hair follicle cycling .....</b>                                      | <b>112</b> |
| <b>Figure 5.9 Analysis of the nutritional parameters .....</b>  | <b>113</b> |
| <b>Figure 5.10 Analysis of the cell proliferation and differentiation .....</b>   | <b>114</b> |
| <b>Figure 5.11 Analysis of the HFSCs pool in K14-sPLA<sub>2</sub>-IIA mice.....</b>                                     | <b>116</b> |
| <b>Figure 5.12 Immunohistochemical staining of Sox9 .....</b>   | <b>117</b> |
| <b>Figure 5.13 Cyclic pattern of hair loss and growth.....</b>  | <b>118</b> |
| <b>Figure 5.14 Real time PCR analysis of various genes involved in the alopecia..</b>                                   | <b>119</b> |
| <b>Figure 5.15 Time dependent comparative wound healing process.....</b>  | <b>121</b> |
| <b>Figure 5.16 Comparative hair follicle cycling and epidermal abnormalities .....</b>                                  | <b>122</b> |
| <b>Figure 6.1 Structure of the Disabled (Dab) proteins .....</b>  | <b>131</b> |
| <b>Figure 6.2 Regulation Wnt signaling by Dab2 .....</b>  | <b>133</b> |
| <b>Figure 6.3 Regulation of the BMP signaling by Dab2 .....</b>   | <b>134</b> |
| <b>Figure 6.4 Dab2 mediated regulation of MAPK signaling.....</b>   | <b>135</b> |
| <b>Figure 6.5 Real time PCR quantification of Dab2 in HFSCs.....</b>  | <b>139</b> |
| <b>Figure 6.6 Efficiency of K14CreER mediated gene knockout .....</b>   | <b>140</b> |
| <b>Figure 6.7 Histological analysis of the hair follicle cycling .....</b>  | <b>142</b> |
| <b>Figure 6.8 Nile red staining on tail wholemount tissue.....</b>  | <b>143</b> |
| <b>Figure 6.9 Comparative level of active <math>\beta</math>-catenin in the hair follicle and IFE....</b>               | <b>144</b> |
| <b>Figure 6.10 Analysis of cell proliferation by Ki67 staining.....</b>   | <b>145</b> |
| <b>Figure 6.11 Analysis of the epidermal differentiation .....</b>  | <b>146</b> |
| <b>Figure 6.12 Quantification of HFSCs by flow cytometry .....</b>  | <b>147</b> |
| <b>Figure 6.13 Colony forming efficiency of HFSCs .....</b>   | <b>149</b> |
| <b>Figure 6.14 Label retaining cells (LRCs) assay .....</b>   | <b>150</b> |

### *List of Tables*

|   |           |
|---|-----------|
| <b>Table 2.1 The role of Wnt components in epidermal homeostasis .....</b>                      | <b>54</b> |
| <b>Table 2.2 Phenotype of alopecia developing mutant mice models.....</b>                       | <b>67</b> |
| <b>Table 4.1 Composition of the tail lysis buffer .....</b>                                     | <b>75</b> |
| <b>Table 4.2 Primer sequences for mice genotyping.....</b>                                      | <b>76</b> |
| <b>Table 4.3 List of the primary and secondary antibodies .....</b>                             | <b>81</b> |
| <b>Table 4.4 Staining procedure of the HFSCs for flow cytometry .....</b>                       | <b>86</b> |
| <b>Table 4.5 Real time PCR primer sequences .....</b>   | <b>93</b> |
| <b>Table 5.1 Classification of the phospholipases .....</b>                                     | <b>96</b> |
| <b>Table 5.2 Expression of sPLA<sub>2</sub> isoforms in the mouse and human epidermis .....</b> | <b>99</b> |

## *Abbreviations*

|             |  |
|-------------|--|
| <b>AA</b>   | Arachidonic acid                       |
| <b>BCC</b>  | Basal cell carcinoma                   |
| <b>BMP</b>  | Bone morphogenetic protein             |
| <b>BrdU</b> | 5-Bromo-2-deoxyuridine                 |
| <b>Bu</b>   | Bulge                                  |
| <b>CD34</b> | Cluster of differentiation molecule 34 |
| <b>cKO</b>  | Conditional knock-out mouse            |
| <b>Cre</b>  | Cre recombinase                        |
| <b>DAB</b>  | Diaminobenzidine                       |
| <b>Dab2</b> | Disabled homolog 2                     |
| <b>DAPI</b> | 4',6-diamidino-2-phenylindole          |
| <b>DEPC</b> | Diethylpyrocarbonate                   |
| <b>Der</b>  | Dermis                                 |
| <b>DMBA</b> | 7,12-dimethylbenzanthracene            |
| <b>DMEM</b> | Dulbecco's modified eagle media        |
| <b>DMSO</b> | Dimethyl sulfoxide                     |
| <b>DNA</b>  | Deoxyribonucleic acid                  |
| <b>Doxy</b> | Doxycycline                            |
| <b>DP</b>   | Dermal papillae                        |
| <b>E</b>    | Embryonic day                          |
| <b>ECM</b>  | Extracellular matrix                   |
| <b>EDTA</b> | Ethylene Diamine Tetra Acetic acid     |
| <b>EF</b>   | Enhancing factor                       |
| <b>EGF</b>  | Epidermal growth factor                |
| <b>EGFR</b> | Epidermal growth factor receptor       |
| <b>EMT</b>  | Epithelial mesenchymal transition      |
| <b>Epi</b>  | Epidermis                              |
| <b>ER</b>   | Estrogen receptor                      |
| <b>ESCs</b> | Embryonic stem cells                   |
| <b>FACS</b> | Fluorescence activated cell sorting    |
| <b>FBS</b>  | Fetal bovine serum                     |

|                 |   |
|-----------------|---|
| <b>FGF</b>      | Fibroblast growth factor  |
| <b>FLOX</b>     | Lox Lox P flanked   |
| <b>Fz</b>       | Frizzled  |
| <b>GAPDH</b>    | Glyceraldehyde 3-phosphate dehydrogenase                        |
| <b>GFP</b>      | Green fluorescent protein                                       |
| <b>H&amp;E</b>  | Hematoxylin & eosin   |
| <b>H2B</b>      | Histone 2B  |
| <b>Hb-EGF</b>   | Heparin binding epidermal growth factor                         |
| <b>Het</b>      | Heterozygous  |
| <b>HF</b>       | Hair follicle   |
| <b>HFSCs</b>    | Hair follicle stem cells  |
| <b>HG</b>       | Hair germ   |
| <b>Hh</b>       | Hedgehog  |
| <b>HNSCC</b>    | Head and Neck Squamous Cell Carcinoma                           |
| <b>HS</b>       | Hair shaft  |
| <b>IFA</b>      | Immunofluorescence assay  |
| <b>IFE</b>      | Interfollicular epidermis                                       |
| <b>IHC</b>      | Immunohistochemistry  |
| <b>iPLA2</b>    | Intracellular phospholipase a2                                  |
| <b>IRS</b>      | Inner root sheath   |
| <b>IRS</b>      | Inner root sheath   |
| <b>JNK</b>      | C-Jun N-terminal kinase   |
| <b>JZ</b>       | Junctional zone   |
| <b>K</b>        | Keratin   |
| <b>K1</b>       | Keratin 1   |
| <b>K14</b>      | Keratin 14  |
| <b>K15</b>      | Keratin 15  |
| <b>K5</b>       | Keratin 5   |
| <b>Lef</b>      | Lymphoid enhancing factor                                       |
| <b>Lgr4/5/6</b> | Leucine-rich repeat-containing G protein-coupled receptor 4/5/6 |
| <b>Lhx</b>      | Lim-homeobox containing transcription factor                    |
| <b>LPA</b>      | Lysophosphatidic acid   |
| <b>LRCs</b>     | Label retaining cells   |

|                               |  |
|-------------------------------|--|
| <b>Lrp</b>                    | Low-density lipoprotein receptor-related protein |
| <b>Msx</b>                    | Msh homeobox containing transcription factor     |
| <b>Mx</b>                     | Matrix   |
| <b>Nfatc</b>                  | Nuclear factor of activated T-cells              |
| <b>ORS</b>                    | Outer root sheath                                |
| <b>Pc</b>                     | Placode  |
| <b>PD</b>                     | Postnatal day                                    |
| <b>PK</b>                     | Proteinase K                                     |
| <b>PLA</b>                    | Phospholipase A                                  |
| <b>PLC</b>                    | Phospholipase C                                  |
| <b>PLD</b>                    | Phospholipase D                                  |
| <b>QRT-PCR</b>                | Quantitative real time polymerase chain reaction |
| <b>R26</b>                    | Rosa26 (gene locus)                              |
| <b>RNA</b>                    | Ribonucleic acid                                 |
| <b>Runx1</b>                  | Runt related transcription factor 1              |
| <b>SDS</b>                    | Sodium dodecyl sulphate                          |
| <b>SFRP</b>                   | Secreted frizzled-related protein                |
| <b>SG</b>                     | Sebaceous gland                                  |
| <b>Shh</b>                    | Sonic hedgehog                                   |
| <b>Smo</b>                    | Smoothened                                       |
| <b>TA</b>                     | Transit-amplifying                               |
| <b>Tet</b>                    | Tetracycline                                     |
| <b>Tgf <math>\beta</math></b> | Transforming growth factor $\beta$               |
| <b>TRE</b>                    | Tetracycline response element                    |
| <b>TSC</b>                    | Tissue stem cell                                 |
| <b>tTA</b>                    | Tetracycline transactivator                      |
| <b>WT</b>                     | Wild type  |
| <b>YFP</b>                    | Yellow fluorescent protein                       |

# ***1. Introduction***



## **1.1 An introduction to stem cells**

Stem cells are classified as a specialized cells type harboring ability to self-renew and maintain themselves in an undifferentiated state. Broadly, stem cells are classified as embryonic stem cells and adult tissue stem cells. Embryonic stem cells (ESCs) are found in the inner cell mass of blastocysts, whereas adult stem cells reside in a specialized microenvironment in the adult tissues known as stem cells "niche". These cells have immense potential in organ development during embryogenesis and have substantial capacity to maintain stem cells pool in the adult tissues, which generates a diverse range of committed cell types and contributes during tissue regeneration and repair throughout the life of an organism. Because of these remarkable potentials, stem cells have tremendous promises in the clinical applications and development of new treatments for the degenerative diseases. Therefore, specific factors and conditions, which are responsible for maintenance of the stemness properties, are currently of great interest in the field of stem cells research.

## **1.2 Embryonic stem cells and pluripotency**

The fertilized oocytes or zygote undergo successive cell divisions and produce totipotent cells, which can generate embryo and the trophoblasts of the placenta. These totipotent cells further undergo specialization and form a hollow ball of cells known as a blastocyst and a cluster of cells called Inner Cell Mass (ICM). These cells of the inner cell mass are pluripotent and able to produce progeny of almost all cell types, which are derived from the three germ layers (Figure 1.1). The embryonic stem cells for the research purpose are primarily obtained from the embryos, which are developed by an *in-vitro* fertilization technique in the in vitro fertilization clinic. Importantly, the potency of the embryonic stem cells can be analyzed by injecting the ES cells into an immunosuppressed mouse, which produce a benign tumour called a

teratoma. Teratoma is a mixture of many differentiated or partially differentiated cell types, which indicate the capability of the ES cells to differentiate into multiple cell types of three germ layers. Further, ES cells can be directed towards the directed differentiation programme of a specific lineage, such as nerve cells, heart muscle cells and blood cells by manipulating their behaviour through chemical composition of the media or by inserting the regulatory genes into the ES cells.

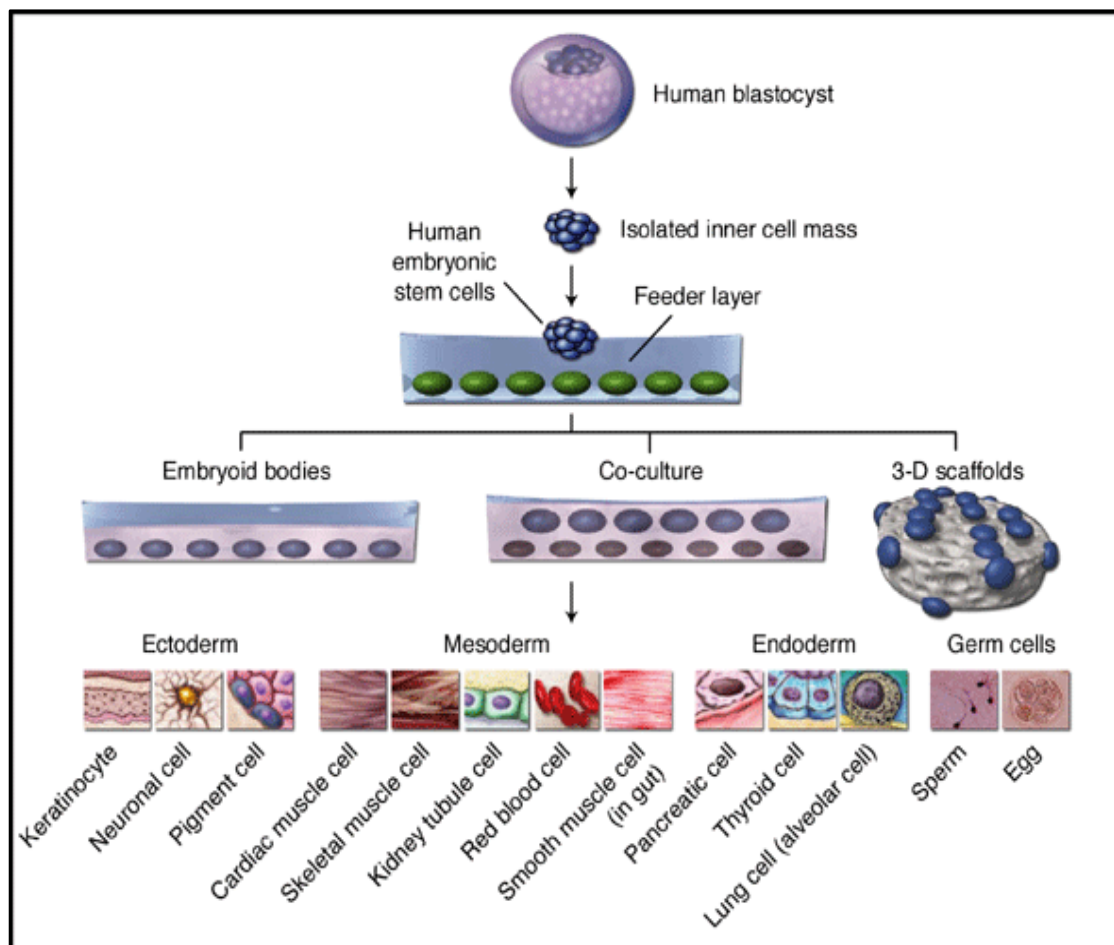


**Figure 1.1 Isolation and differentiation of ES cells**

*(Adapted from Louise A et al., 2005, Expert Reviews in Molecular Medicine) [1]*

*Graphical representation of the embryonic stem cell source, isolation, culture and differentiation into various cell types of the adult tissues*

Embryonic stem cells are at the top of hierarchical potential that are capable of generating all types of somatic cells of an adult organism. ESCs have an ability of unlimited self-renewal and therefore have massive potential for regenerative medicine and tissue regeneration after injury or disease.

### **1.3 Tissue stem cells and their potency**

Tissue stem cells are specialized cells within the adult tissue, which reside in the specific microenvironment in respective tissues known as stem cells “niche” (Figure 1.2). These cells play a functional role in the tissue regeneration upon injury and during normal adult tissue homeostasis. Unlike ES cells, tissue stem cells are relatively quiescent and have limited plasticity, which can generate the cell types of the tissue from which they originate. Based on their flexibility for production of different cell types, they can be divided into following categories.

**Multipotent:** These stem cells have the potential to produce multiple cell types of the respective tissue. As tissue stem cells are generally multipotent, many tissues exhibit heterogeneous differentiated cell population. Multipotent stem cells within the tissue maintain adult tissue homeostasis by producing progenitors cells, which further undergoes terminal differentiation throughout the life of an organism. The hematopoietic stem cells (HSC) can produce red blood cells, white blood cells, platelets etc. while the hair follicle stem cells (HFSC) can give rise to epidermal lineages such as hair follicle, sebaceous gland as well as cells of the interfollicular epidermis.

**Oligopotent:** These stem cells have limited plasticity and can produce only a few types of cells. For example, a lymphoid stem cell can generate the blood cells such as T cells, B cells, and plasma cells but not a red blood cell or a platelet. The other

example includes vascular stem cells, which can produce endothelial cells or smooth muscle cells.

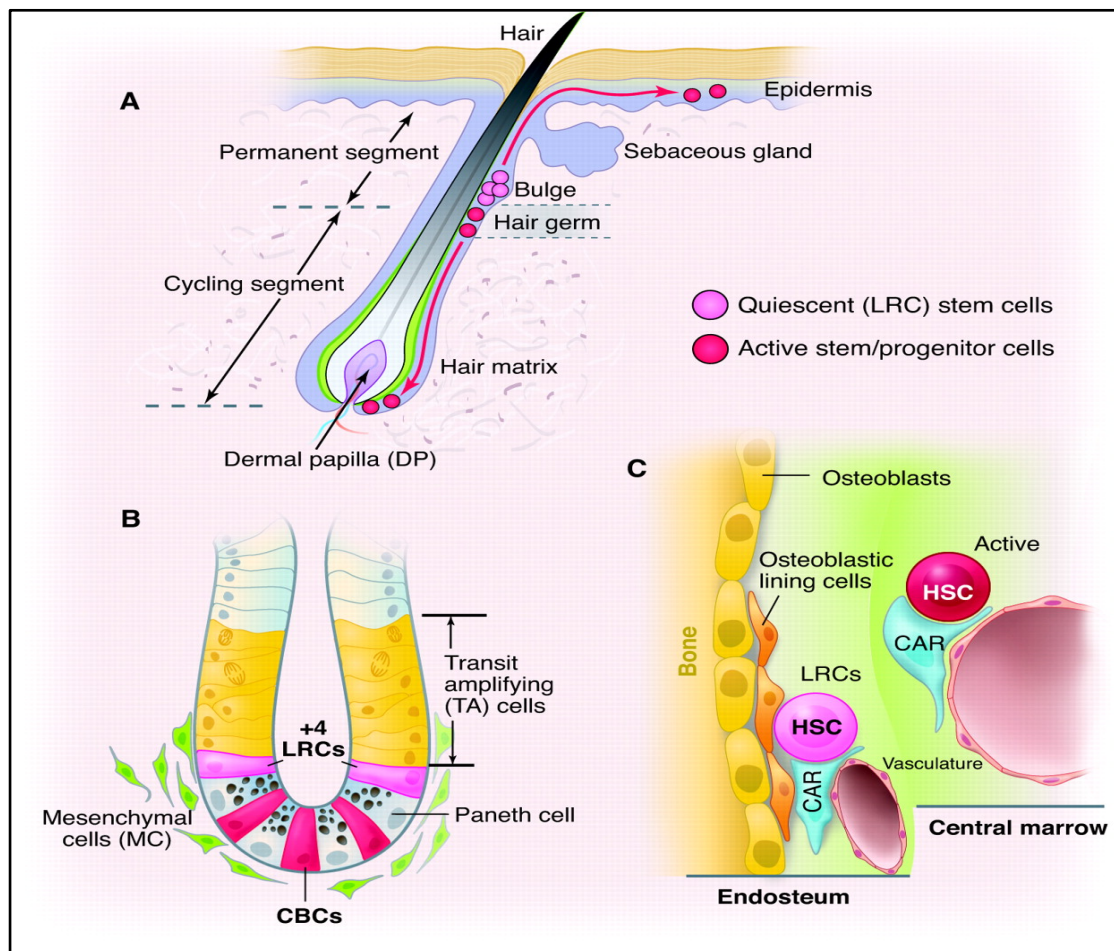


**Figure 1.2 Tissue stem cells and their niche**

*(Adapted from Li and Clevers, 2010, Science) [2]*

*Stem cell niches in the adult tissues such as (A) Hair follicle, (B) Intestine and (C) bone marrow. The stem cells “niche” also contains other cell types that contribute for maintenance of stemness by secreting signaling factors and other niche components.*

**Unipotent:** These cells have an indefinite ability to renew but have restricted plasticity that are unable to produce any other type of cells. The inter-follicular epidermal (IFE) stem cells generate epidermal cells; whereas sebaceous gland stem cells produce sebocytes that are examples of unipotent stem cells.

Recently, tissue stem cells have gained tremendous attention in regenerative application due to less concern of ethical issues and also it does not require the destruction of an embryo. Research from last two decades has strengthened our understanding of molecular mechanisms that govern quiescence of tissue stem cells. However, the role of various signaling factors, which requires for its accurate activity during regeneration and repair, is remaining poorly understood.



## ***2. Review of Literature***



## 2.1 Architecture of skin

The mammalian skin is the largest organ of the body that acts as a protective barrier between internal organs and the external environment. The entire human skin is about two square meters that consists of approximately sixteen percent of an adult human's body weight [3]. It plays a very crucial role in touch sensation, thermoregulation, immunity, insulation and forms a protective barrier against mechanical stress, pathogens and the UV radiation. The skin is a complex organ, which consists of various cell types that are derived from the differentiation of ectoderm and mesoderm cells during embryogenesis that further develops various appendages of the skin such as hair follicles, sebaceous glands, sweat glands, nerves, blood and lymph vessels.

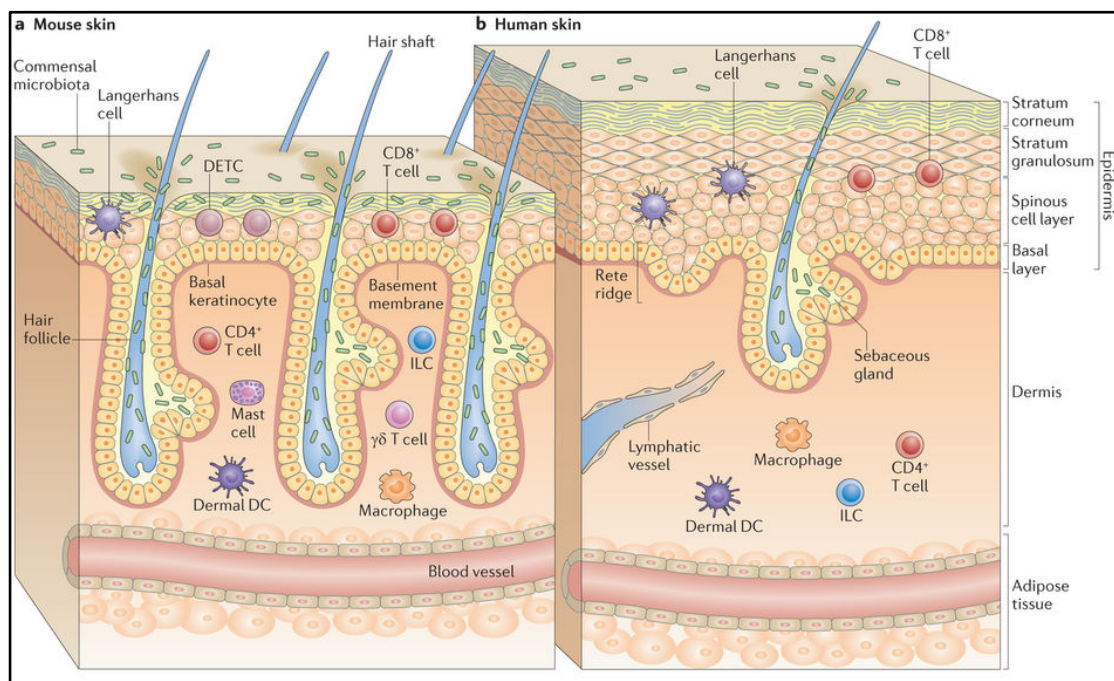


**Figure 2.1 Major components of mouse and human skin**

*(Adapted from Pasparakis M et al., 2014, Nat Rev Immunol) [4]*

*Comparative morphological structure of the human and mouse skin representing various components of the epidermis and dermis*

The entire skin can be subdivided into the epidermis, dermis and a hypodermis. Each layer contains different cellular composition and cytoskeleton organization. The outermost layer epidermis is separated from the underlying dermis by the basement membrane (Figure 2.1). The dermis majorly consists of the fibroblast and is rich in collagen and various extracellular matrix proteins. Together, the extracellular matrix generated from various secretory proteins, different cell types of the dermis and hypodermis, which provides a mechanical strength to support the outermost layer of the skin.

## **2.2 Epidermal compartments in the human and mouse skin**

The human and mouse skin epidermis contains various appendages such as hair follicles, sebaceous glands, inter follicular epidermis, sweat glands and apocrine glands (Figure 2.1). Importantly, the inter follicular epidermis, hair follicle and sebaceous glands are well studied compartments with respect to the contribution of adult tissue stem cells functions in the regulation of the tissue homeostasis [5-8]. All these compartments have their own tissue stem cells pool, which maintains their homeostatic growth and also known to migrate out of their own territory during injury-induced epithelium regeneration [9-12]. The role of the individual compartment and different stem cells pool in the regulation of the skin homeostasis is described below.

## **2.3 The Epidermis**

The outermost layer of the mammalian skin is stratified squamous epithelia, which contains keratinocytes as a major cell type along with melanocytes and various immune cells. The development and stratification of the epidermis is a complex

process that is governed by the involvement of different signaling mechanisms such as Wnt, BMP, Shh, TGFs etc. during the embryogenesis process.

### 2.3.1 Development and Stratification of the epidermis

In the vertebrate organisms, formation of the epidermis is a sequential multistage process, which includes different steps such as epidermal specification and commitment, stratification and terminal differentiation.

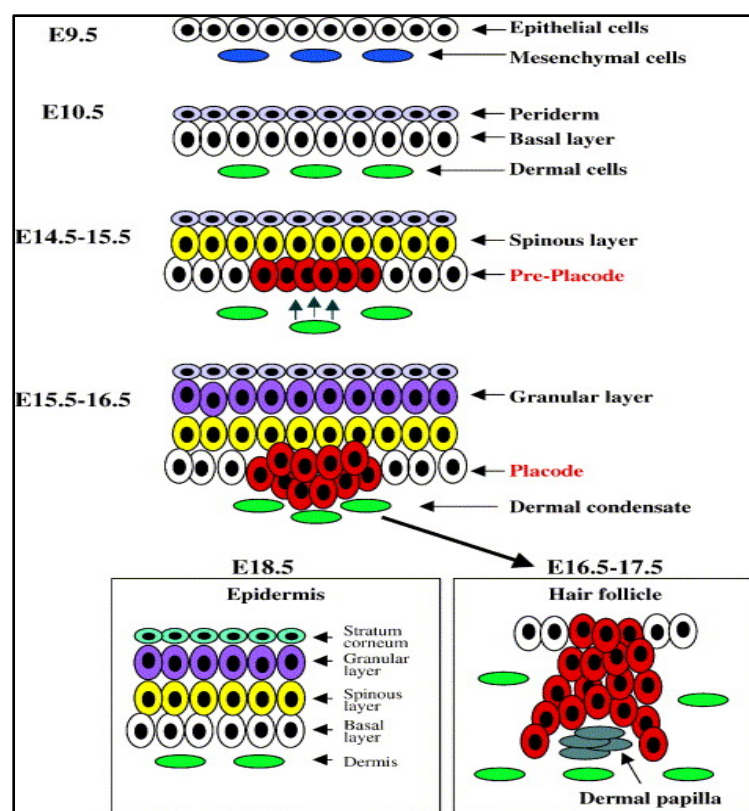


**Figure 2.2 Development and stratification of the epidermis**  
*(Adapted from Li et al., 2003, Cytokine Growth Factor Rev) [13]*

*The sequential process of the mouse embryonic epidermis development and stratification. Epidermis development and stratification starts at E9.5 and develops all the layers by E16.5.*

The process of epidermis development in the mice starts during an early stage of embryonic development at embryonic day 9.5 (E9.5) from the single cell ectodermal

layer. Importantly, Wnt, FGF and BMP signaling plays an important role in deciding the fate of the ectodermal cells between the epidermal and neural fates [14, 15]. At E9.5, the epidermal commitment is governed by the expression of Keratin 5 (K5) and Keratin 14 (K14) instead of cytokeratin K8 and K18 in the ectodermal cells [16, 17]. Further, the K5 and K14 expressing cells form the epidermal basal cell layer of the embryo. These cells further undergo rapid proliferation that produces intermediate cell type, which gives rise to K1/K10 expressing spinous layer cells (Figure 2.2). Further, cells of the spinous layer continue to differentiate, remodel their cell-to-cell junctions and move upwards to produce cells type, which expresses the Involucrin and Transglutaminase in the granular layer. These cells further rearrange their cytoskeleton networks of various intermediate filament proteins, exit the cell cycle and become flattened to form the Filaggrin and Loricrin expressing cornified cell layer [18] (Figure 2.2).

### **2.3.2 The interfollicular epidermis (IFE) and stem cells**

The epidermis between the two hair follicles is known as inter follicular epidermis (IFE). IFE is composed of the heterogeneous cell population that forms distinct layers having different molecular signatures. The lowermost layer, which is close to the dermis, contains basal undifferentiated cells that express both the K5 and K14 and remain attached to the basement membrane (BM) (Figure 2.3). These cells have a high proliferative potential that generate progeny to maintain cell density within the basal layer as well as move upwards to produce cells, which expresses K1 and K10 in the suprabasal layer, thereby regulates the thickness of the epidermis. The IFE stem cells are attached to the basement membrane and express  $\alpha 6$  and  $\beta 1$  integrin (Figure 2.3). The IFE stem cells of the human skin divide less frequently than the IFE stem cells of the mouse skin, which divide on a daily basis. The progeny of the stem cells

undergoes several rounds of the cell division before they differentiate and move upward from the basement membrane [19-21]. Importantly, in mice and human epidermis, IFE contains two types of basal cells populations; one population represents a slow-cycling stem cell, whereas the other is a rapidly proliferating transit-amplifying cells.

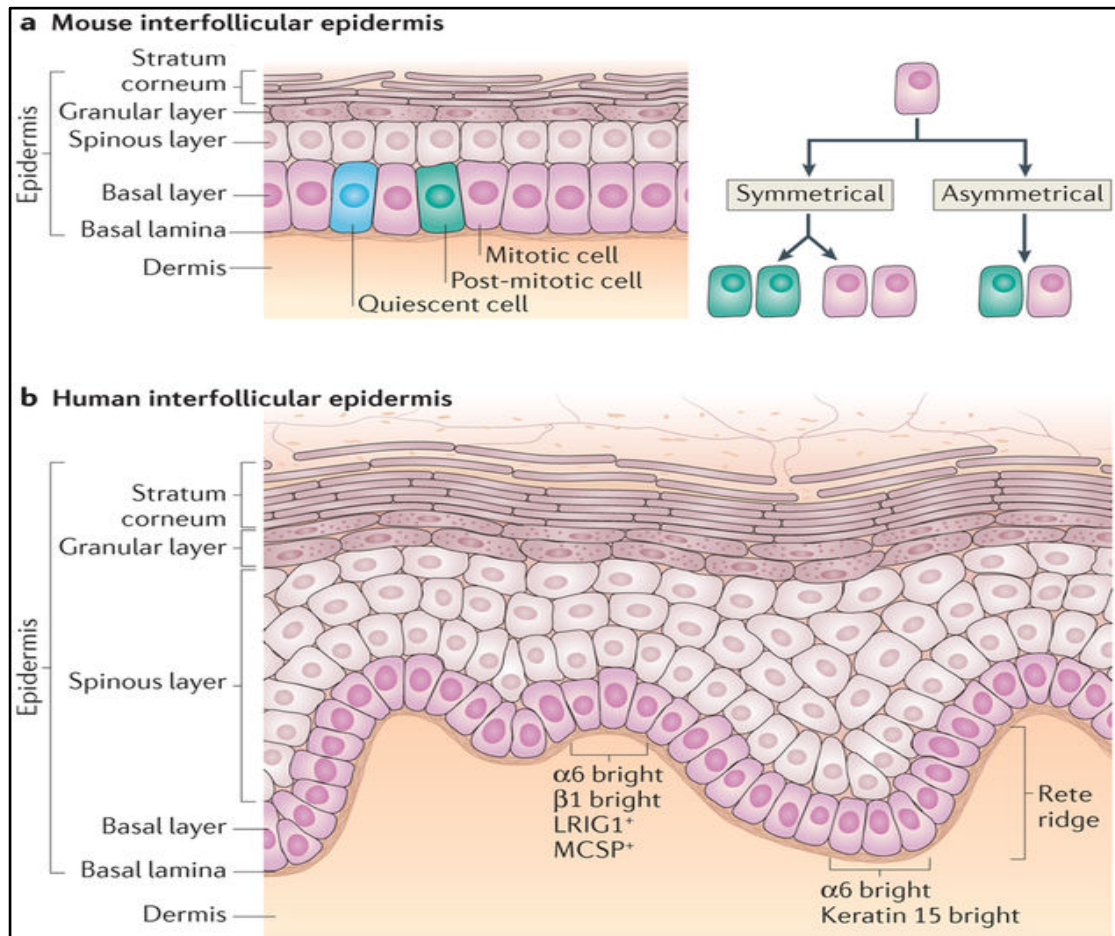


**Figure 2.3 Layers of the mouse and human epidermis**

*(Adapted from Li et al., 2003 Cytokine Growth Factor Rev) [20]*

- a) *Graphical representation of various layers of the mouse skin epidermis and mode of the cell division during the embryonic epidermis development*
- b) *Layers of the human skin epidermis that represents an increased thickness of the spinous layer*

Based on different divisional rate of the basal cells, the model of epidermal proliferative units (EPUs) was proposed to explain the role of individual population in maintaining IFE structure. According to this model, IFE can be divided into multiple EPUs with each EPU contains one stem cell, which generates progeny in the surrounding space that undergoes differentiation, move upwards and maintain the IFE structure [22, 23]. However, this model was challenged by the clonal analysis of the basal cells, which suggested that the single type of progenitor cells maintains the IFE [24, 25]. Moreover, a recent study by using H2BGFP pulse-chase experiment identified two different stem cells population. One subpopulation termed as LRCs, which divide at a slower rate and retain the GFP label, whereas rapidly dividing cells population lose their GFP label termed as non-LRCs. The LRCs comprise ~35% and non-LRCs are ~65% of the total basal layer cells [26]. The detailed molecular profiling of these subpopulations demonstrated that the LRCs and non-LRCs are molecularly distinct with independent stem cells populations. Importantly, these subpopulations reside in the specified area within the basal layer that are involved in the homeostatic process as well as contribute to epidermal regeneration during injury [26]. These studies suggest that the cross talk between different subpopulation of the stem cells within the IFE is complex. Hence, further investigations are required to point out the distinct role of different subpopulations in the specific physiological process.

#### **2.4 The hair follicle**

The hair follicles are epidermal appendages, which are derived from the embryonic epidermis. The hair follicle grows downward and extends into the dermis; however, they are constantly remains separated from the dermis by the basement membrane (BM). The hair follicle is mainly divided into two portions. The non-cyclic or

permanent portion is an upper part of the hair follicle, which does not regenerate entirely during the hair cycle. The cyclic portion of the hair follicle contains lower part of the HF, which regenerates itself during every hair cycle with varying in the length depending on the stage of the hair cycle [27]. The non-cyclic or permanent portion includes the infundibulum, which is an uppermost part of the HF and connecting point between the HF and the interfollicular epidermis (**Figure 2.4**). The outmost layer of the HF called outer root sheath (ORS), which is contiguous with the basal layer of the epidermis.

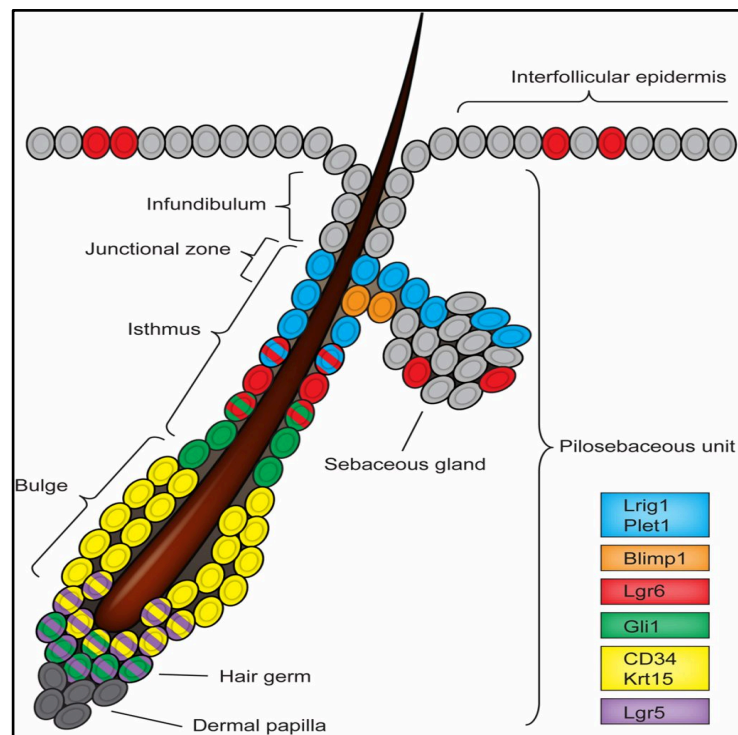


**Figure 2.4 The structure of hair follicle**

*(Adapted from Schepeler et al., 2014, Development) [28]*

*Different regions of the telogen hair follicle representing non-cyclic or permanent region above the bulge area and cycling and regenerating region below bulge area*

The permanent portion also includes the area, which is below the infundibulum and above the bulge, known as an isthmus. The different areas of the permanent portion

have distinct stem cells population. The upper portion within the isthmus is known as a junctional zone, which is recently identified as a home for the distinct type of stem cells population in the hair follicle that contribute for sebaceous gland morphogenesis and IFE maintenance [29, 30]. Importantly, the bulge region of the hair follicle is a specific niche for the multipotent stem cells of the hair follicle known as the hair follicle stem cells (HFSCs) [31, 32]. A sebaceous gland is also located at the isthmus and known to contain its own stem cell pool [15, 33] (**Figure 2.4**). The lower part of the hair follicle is densely populated with the dermal cells and enveloped by epithelial cells known as the dermal papilla [34-36]. The matrix contains rapidly proliferating transit amplifying cells, which produce various cell types for the synthesis of the inner root sheath (IRS) layers and hair shaft. The HF is a dynamic organ, which allows us to study complex signaling cues require for the tissue stem cells activation and their fate choice to maintain the integrity of the adult tissue.

#### **2.4.1 Hair follicle morphogenesis**

The hair follicle morphogenesis is the process of the new hair follicle formation. To decipher the role of different cell types and signaling mechanism, this process has been extensively studied by using various mutant mouse models. Particularly in the murine skin, the process of the hair follicle development starts during the late stage of the embryonic development at embryonic day ~14.5 (E14.5) [37]. The initial stage is known as the induction phase, which is governed by the signal from the dermis for the condensation of the epidermal progenitors to form the placode (Figure 2.5). Importantly, these initial inductive signals are known to be mediated through the Wnt/ $\beta$ -catenin signaling from the dermis [38]. Further, the formation of the placode results in the formation of the mesenchymal cells cluster below the placode known as the dermal papilla. The specification of the epidermal cells for the placode formation

leads to a rapid proliferation of these cells, which grows downwards in the dermis and forms a structure known as a hair peg (Figure 2.5). Furthermore, the cells at the base of the hair peg continue rapid proliferation and form the matrix cells that surround the dermal cells, which become mature dermal papilla. The signals from the dermal papilla majorly govern further process of the hair follicle formation. It acts as a signaling center that coordinates the process of cell proliferation and differentiation of the epidermal and dermal cells [39, 40].

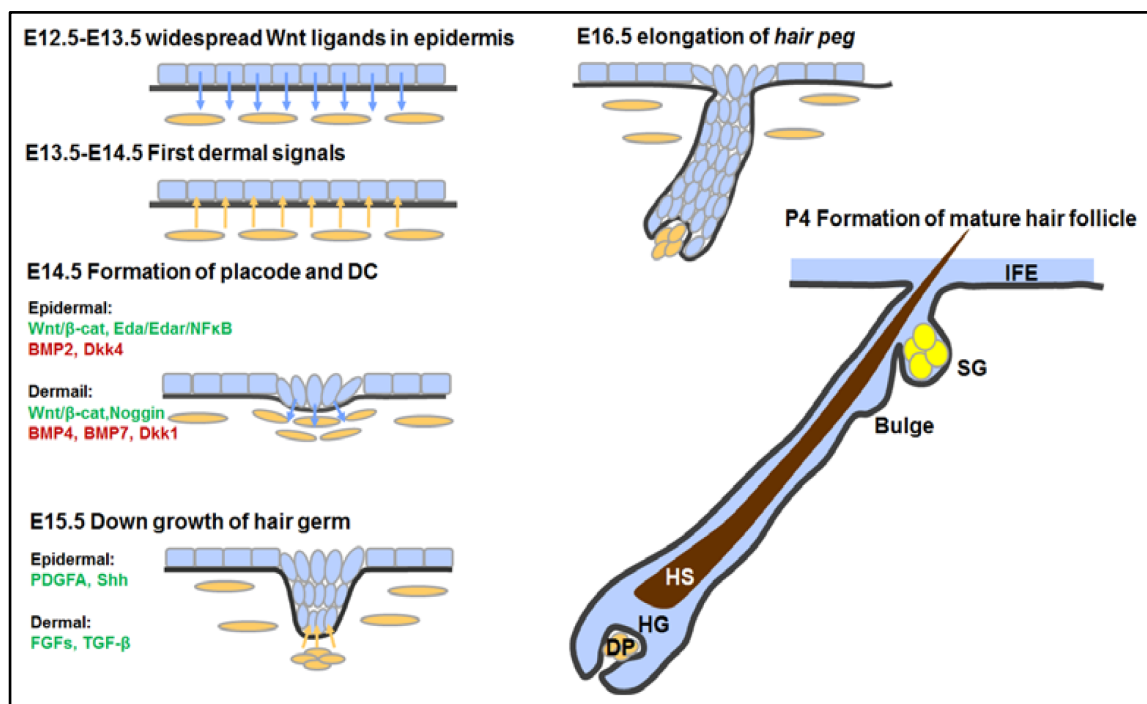


**Figure 2.5 Stages of the hair follicle morphogenesis**

*(Adapted from Liu S et al., 2013, Int J Mol Sci) [17]*

*The process of the hair follicle morphogenesis starts from the embryonic day 12.5 and continue till first postnatal week. Various stages of the hair follicle development are represented with respect to the stages of the embryonic development. E- embryonic day, P- Postnatal day, IFE- inter follicular epidermis, SG- sebaceous gland, DP- dermal papilla, Bu- bulge, HS- Hair shaft*

The epidermal and dermal cells release different signaling factors such as Wnts, FGFs, TGFs, BMP etc. and these factors mediated coordinated signaling crosstalk leads to the formation of the differentiated progeny of distinct lineages. These differentiated progenies begin to form the inner root sheath (IRS) and hair shaft of the hair follicle [41, 42]. Further developmental stages of the hair follicle include the formation of the infundibulum, sebaceous gland and elongation of the hair shaft. The morphogenesis completes with the formation of the fully differentiated layers and formation of the complete hair shaft at the end of the first week after birth.

#### **2.4.2 Hair follicle stem cells**

The bulge region of the hair follicle is the best-characterized hair follicle stem cell niche, which is located at the bottom portion of the permanent region of the hair follicle. The cell of the bulge region fully acquires their molecular signatures after completion of the hair follicle morphogenesis [43]. The bulge region as a stem cell compartment was first reported from the study of Cotsarelis and colleagues in 1990. They used [3H] tritiated thymidine to label less frequently dividing cells, which showed that the label-retaining cells are located in the bulge region of the adult hair follicle [31, 44, 45]. However, due to technical limitations in isolating the live LRCs, Tumber et al., in 2004 adapted the LRCs approach by using tetracycline-inducible, GFP-tagged Histone-2B (H2BGFP) system to isolate the live LRCs. These H2BGFP positive cells were identified to express high levels of a cell surface marker, CD34 [32, 46]. Further molecular characterization of these cells identified various bulge stem cell marker such as Keratin 15 (K15) [47, 48], Sox9 (SRY box-9) [49], Tcf3 (T-cell factor-3), Lhx2 (LIM/homeobox protein-2) [50-52], and NFATc1 (Nuclear factor of activated T-cells, cytoplasmic-1) [53]. Importantly, Oshima et al., 2001 reported the first study for the stemness characteristic and multipotency of the bulge cells.

They dissected the labelled bulge region and transplanted in the unlabeled hair follicle of the immunodeficient mice. These labeled bulge cells in the unlabeled hair follicle were able to differentiate into multiple skin lineages, suggesting its ability to produce different progeny of the hair follicle and the interfollicular epidermis [54]. Further, Morris et al., 2004 used the lineage tracing approach by using Krt15 specific promoter to drive the expression of the LacZ and shown that the bulge cells are able to produce all the epidermal lineages including the hair follicles, sebaceous glands and interfollicular epidermis [55, 56]. However, the study from the Ito et al., in 2005 showed that the hair follicle stem cells does not contribute to the normal epidermal homeostasis but migrate and contributes for the short periods during wounding [57, 58]. Further to check the potency of the individual cell, single cell (CD34<sup>+</sup>) purification was done by FACS sorting and further expanded in the culture. Transplantation of these individual culture clones revealed that individual bulge cell is capable to give rise to different epithelial lineages and the niche of the bulge stem cell [59]. These study suggested that the bulge population are heterogeneous and a mixture of different cells having different proliferative and differentiation potential.

### **2.4.3 Cyclic regeneration of the hair follicle**

The mammalian hair follicle follows a distinct cyclic pattern that progresses through various stages known as the hair cycle. Different phases of the adult hair cycle include growth (anagen), regression (catagen), resting (telogen) and shedding (exogen) phases [27, 60] (Figure 2.6). The hair cycle study is used as a classical model because the activity of the bulge stem cells correlates with the progression of different phases of the hair cycle and hair growth. In the mice, initial two hair cycle progression is mostly synchronized; however, different gender and genetic background shows some variation in the exact time and the length of different phases. Importantly, the hair

cycle of the human hair follicle is much longer and largely asynchronous. In addition, the human hair cycle does not display the wave pattern for the hair growth and some follicles last in the anagen stage up to seven to eight years [61]. The hair follicles in the mice are fully developed by the PD6 and the first growth phase of the hair follicles after birth belongs to the morphogenesis period that directly progress into the catagen phase. After completion of the morphogenesis of the hair follicle, the hair follicle enters into catagen at PD14 from the head region of the body and progresses toward the tail by PD18 [62]. The hair follicle enters in the first telogen at PD19 and lasts for two to four days depending on the genetic background [27].

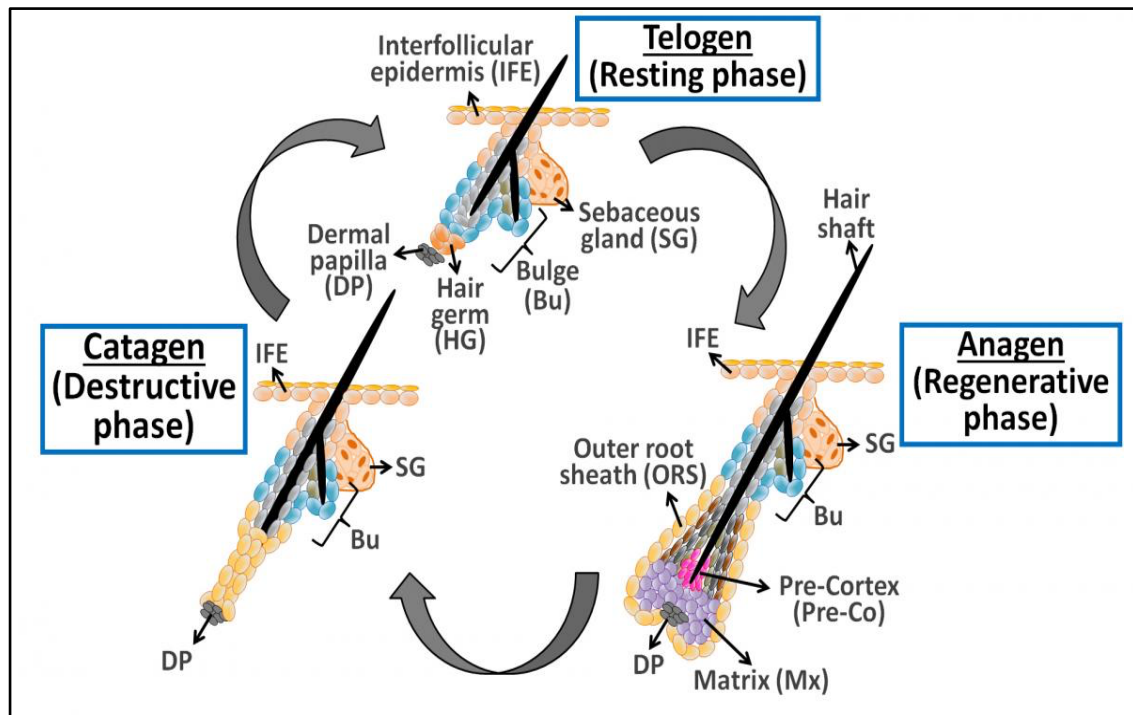


**Figure 2.6 Different phases of the hair cycle**

(Adapted from <http://easysofttech.us>)

*Hair follicle cycle progresses through different phases of the hair cycle such as Anagen, Catagen and Telogen. Each phase is represented with the major physiological processes and growth (length) of the hair follicle*

The first anagen of the adult hair cycle starts at around PD23 that can be divided into six different sub-phases [35]. During anagen-I, the hair follicle is similar to previous telogen phase but cells at the bottom of the hair follicle (hair germ) starts proliferating. In the anagen II, the DP cells along with the hair germ cells start proliferating, which display an enlarged size at the base of the follicle. The rapid proliferation of these cells further activates the hair follicle stem cells that produce progenitors, which migrates out of the bulge and contributes for the hair follicle growth. At anagen III, the progenitor cells start differentiating into various lineages such as IRS and the matrix cells undergoes specification, which further leads to the growth of the new hair shaft along with the IRS towards epidermis and growth of the hair bulb towards the dermis. The IRS and hair shaft continues to grow and reaches a level of the epidermis at the Anagen IV. At the anagen V and VI, the hair shaft emerges out of the hair follicle and attain its maximum length [62]. The anagen phase is completed at around PD35 in the mouse back skin.

The exhaustion of the proliferation potential and differentiation of all the matrix cells lead to the onset of the catagen phase. During catagen, the follicular cells within the cyclic region of the hair follicle undergo rapid apoptosis leading to a regression of the hair bulb and condensation of the dermal papilla (Figure 2.6). The dermal papilla moves upward till it reaches the base of the bulge region [63, 64]. The cells of the permanent portion of the hair follicle form the new bulge area that retains the newly synthesized hair shaft, while an old bulge maintains the previously formed hair shaft known as the club hair. The human hair follicle does not retain the old hair shaft and initiate the next phase after catagen known as the Exogen, which includes the process of the old hair shaft removal from the follicle [65-68]. The time required for the progression of the hair follicle in the anagen and catagen phase is similar for all the

hair cycles; however, the telogen phase gets extended and become longer in the subsequent hair cycles.

The last phase of the murine hair cycle is a resting phase known as the Telogen. However, the mechanistic study and molecular characterization during telogen phase demonstrated active signaling crosstalk to maintain the quiescence state of the hair follicle stem cells [69, 70]. During this phase, the growth of the hair shaft terminated and dermal papilla comes to the close contact with the bulge (Figure 2.6). The signals from the dermal papilla, which activates HFSCs through various secreted signaling factors, initiate the new hair cycle. However, recent study has identified two stages of the telogen phase. The initial phase where the induction for the new anagen onset is inhibited known as refractory telogen whereas, the later stage when hair follicle responds to the activating signals known as competent telogen [71, 72].

The hair cycle after second telogen progress asynchronously. Therefore, it becomes difficult to study the role of regulatory molecules in the progression of the hair follicle cycle after the second telogen. However, the hair follicles can be induced to synchronously enter into the anagen by wax depilation. Moreover, depilation also induces the new hair cycle in the surrounding hair follicle where hair shaft has not been removed [73]. Together, the synchronized hair cycle allows us to start the experiment at specific time point to study the effect of specific molecule in respective process.

#### **2.4.4 Proliferation dynamics of the hair follicle stem cells**

The adult tissue stem cells were thought to maintain their stemness characteristic through asymmetric cell division. The asymmetric cell division results in an unequal distribution of the cellular content to the newly formed daughter cells [74].

Specifically, the distribution of the DNA content was explained by the immortal strand hypothesis, which demonstrated a preferential and selective distribution of the older DNA strand to mother cells and newly synthesized DNA strands to the daughter cell of various tissue stem cells [75-79]. The maintenance of the older DNA strand prevents accumulation of the replication errors in the stem cells genome. In addition, different studies showed that many adult tissue stem cells divide symmetrically but minimize the introduction of the replication errors by maintaining the quiescent state within the niche [80-82]. In the same line, stem cell division generates slow cycling daughter cells and rapidly proliferating progenitor cell, which further undergoes rapid division to produce progeny for the tissue homeostasis [83, 84].

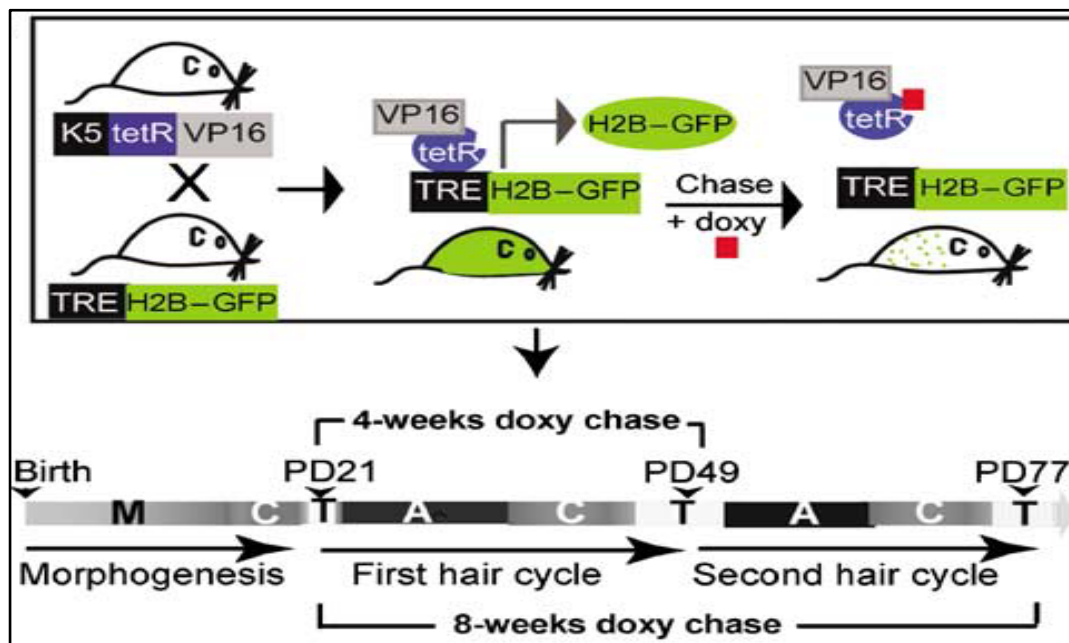


**Figure 2.7 Strategy for the H2BGFP (Tet Off) system**

*(Adapted from Waghmare et al., 2008, EMBO) [85]*

*Schematic representation of Doxycycline mediated regulation H2BGFP (Tet-Off) system. Administration of Doxy in mouse diet inhibits synthesis of the new H2B-GFP (chase) and these mice can be followed for various time points to determine the status of the cell proliferation during various stages of the hair cycle.*

However, how the tissue stem cells maintain their quiescent stem cells pool within the niche and do all stem cells divide at the same frequency during activation phase was largely remained unexplored.

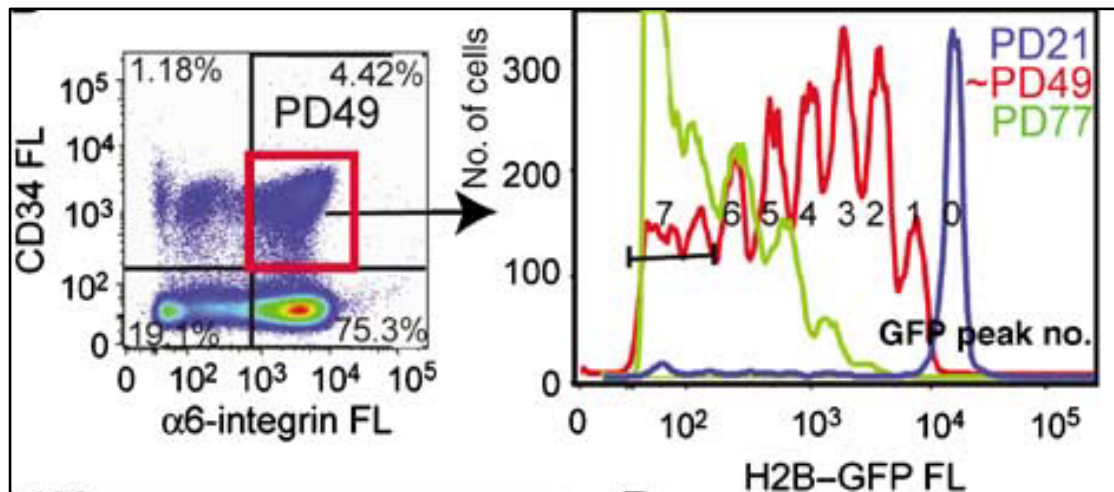


**Figure 2.8 Serial dilution of H2BGFP during stem cells division in vivo**

*(Adapted from Waghmare et al., 2008, EMBO) [85]*

The double transgenic mice were chased for different time points and the HFSCs were separated by using CD34 and  $\alpha 6$ -integrin. The HFSCs were analyzed for the GFP intensity. PD21 (no chase, blue); PD49 (4-weeks chase, red); and PD77 (8-weeks chase, green).

Waghmare et al., in 2008 used a novel strategy to count the stem cells division in unperturbed mouse skin tissue (Figure 2.7). They used pTRE-H2BGFP: K5tTa double transgenic mice (Tet-Off) system to visualize the sequential stem cell divisions mediated serial dilution of H2BGFP (Figure 2.8). The quantification of GFP intensity in subpopulations showed an exact two-fold decrease, suggesting that the each division of the stem cell results in an equal distribution of the GFP during mitosis. Based on the serial dilution of the GFP, they showed that the HFSCs divides 5 to 6 times during the first hair cycle (Chase from PD21 to PD49), whereas long-term chase (PD21 to PD77) showed multiple divisions of the HFSCs with a loss of GFP

bright cells (Peak 1-3). This study demonstrated that the stem cells within the niche divide infrequently and have different quiescence potential. Further, the non-dividing and relatively more quiescent stem cells can be activated by an external activating stimulus [85, 86]. Collectively, this study explains that the skin tissue does not utilize entire stem cell pool during normal homeostasis as well as during hair follicle regeneration and have the ability to maintain their reserve stem cells pool, thereby maintaining genome integrity in the reserved stem cells pool [85, 87, 88]. Further, different groups adopted this approach to explain the stem cell kinetics in various adult tissues [2, 89].

## **2.5 The sebaceous gland (SG) and stem cells**

The sebaceous gland (SG) is a holocrine gland, which starts developing during hair follicle morphogenesis after induction of hair germ from the  $Lrig1^+$  cells [90]. It is in continuation with the ORS layer of the hair follicle and located above the bulge region in the permanent portion of the hair follicle. It plays an important role in the formation of the epidermal barrier by producing the sebum from fatty acids, which lubricates the hair shaft and helps in the development of the epidermal barrier [91]. The mature sebaceous gland can be divided into three regions such as peripheral, the maturation and the necrotic region (Figure 2.9). The outer basal layer cells in the SG are dividing cells, which requires for the maintenance of the sebaceous gland size. The sebocytes migrate to the duct region and releases the lipid content in the hair canal [92]. The putative stem cells of the sebaceous gland remained less understood as compared to the bulge and IFE stem cells. The bulge stem cells are able to develop the entire sebaceous gland as demonstrated by the transplantation experiments [59].

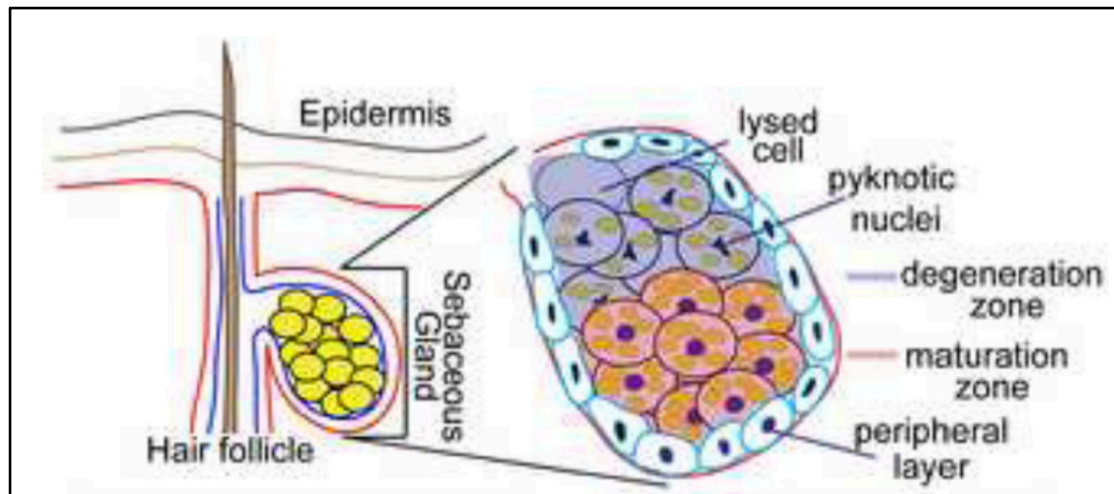


**Figure 2.9 The structure of the sebaceous gland**

*(Adapted from Niemann C et al., 2012, Semin Cell Dev Biol) [93]*

*The sebaceous gland is an epidermal appendage and located above the bulge region. Different cellular zone within the lobule of the SG is represented by different colour marking.*

In addition, various studies have shown the contribution of the putative sebaceous gland progenitors in the maintenance of the sebaceous gland, independent of the bulge cells. Recent studies have identified putative markers for the sebaceous gland progenitors such as Blimp1 [33]. However, the detailed study by using lineage-tracing techniques revealed that the Blimp1 positive cells are already differentiated sebocytes and are also located in the IFE [94]. Moreover, basal cells of the sebaceous gland express other markers such as Lrig1 and Lgr6. Further experiment by using the lineage tracing approach showed the contribution of the stem cells, which are located in different compartment of the hair follicle that is involved in the maintenance of the sebaceous gland. The MTS24<sup>+</sup> and Lgr6<sup>+</sup> cells of the isthmus and Lrig1<sup>+</sup> cells of the junctional zone reported contributing to the maintenance of the SG [29, 30, 95].

## **2.6 Signaling pathways in hair follicle morphogenesis and HFSCs activation**

In the last decade, extensive studies have been performed to elucidate the role of various signaling mechanisms in the regulation of hair follicle stem cells functions. Importantly, the Wnt signaling has been studied starting from the hair follicle morphogenesis and during adulthood to understand its role in the maintenance of stem cells quiescence, activation, proliferation and differentiation. Apart from the Wnt signaling, various other signaling mechanisms such as Bmp, Shh, TGFs and Notch have been shown to play an important role in the regulation of the HFSCs activity.

### **2.6.1 Growth factors and mitogenic signaling**

Secretory growth factors such as epidermal growth factors (EGFs) and transforming growth factors (TGFs) have been known to induce proliferation of different cell types. The EGFR family contains four members, EGFR/ErbB1/HER1, ErbB2/HER2, ErbB3/HER3 and ErbB4/HER4. Apart from the EGF, EGFR can also bind with the other growth factors such as TGF $\alpha$ , epigen (EPGN), Heparin-binding EGF-like growth factor (HBEGF), amphiregulin (AR) and epiregulin (EPR) [96]. The binding of the ligands to the receptor leads to its activation through auto and trans phosphorylation at the cytoplasmic domain of the receptor [97].

Importantly, the EGFR knockout mice displayed open eyelid at birth, impaired differentiation, hair shaft abnormalities and defects in wound healing response [97, 98]. On the other hand, overexpression of the EGF resulted in the hyperproliferation of basal layer cells and the hair follicle arrested during the development [99]. The EGFR signaling also regulates keratinocytes migration that plays an important role in the wound healing process [100]. In addition, various studies have also highlighted the role of different downstream components of the EGFR. The knockout of b-Raf in

the epidermis delayed hair follicle development and demonstrated defective wound healing response [101]. Moreover, the deletion of JNK1 and JNK2 showed the variable phenotype of the skin and hair follicle development. Deletion of the JNK1 showed defects in the eyelid closure. Importantly, the JNK signaling regulates the expression of the EGFR during epidermal development and hair follicle morphogenesis[102]. Similarly, knockout of c-Jun in the epidermis results in the defective Hb-EGF signaling that leads to the abnormal eyelid development [103].

TGF signaling is required for the hair follicle progression to the catagen phase of the hair cycle. The TGFs are expressed during the catagen phase and induce apoptosis of the follicular cells that require for the regression of the hair follicle [104, 105]. Different TGF ligands have a different role in the hair follicle development and HFSCs activation. The deletion of the TGF- $\beta$ 1 showed an early hair follicle formation, while deletion of the TGF- $\beta$ 2 demonstrates delayed hair follicle morphogenesis [106]. Specifically, the secretion of the TGF- $\beta$ 2 from the dermal papilla enhances the activation of the HFSCs. Similarly, HFSCs that are unable to respond to TGF- $\beta$ 2, showed delayed hair follicle regeneration. Importantly, the TGF- $\beta$  signaling lowers the BMP signaling mediated repressive flux and thereby activates the hair follicle stem [107].

### **2.6.2 Wnt/ $\beta$ -catenin signaling and epidermal homeostasis**

Wnts are the lipid-modified secreted glycoproteins, which operates a highly conserved downstream signaling pathway from the fruit flies to the humans. Binding of the Wnt ligands to the cell surface receptor initiates cytoplasmic signaling events that regulate diverse processes including fate specification, proliferation, differentiation and migration [108]. Wnt signaling can be classified into three

different pathways. In canonical pathway, binding of the Wnt ligands to extracellular receptor leads to the stabilization of  $\beta$ -catenin in the cytoplasm, which further translocates into the nucleus and regulates expression of various Wnt target gene (Figure 2.10).

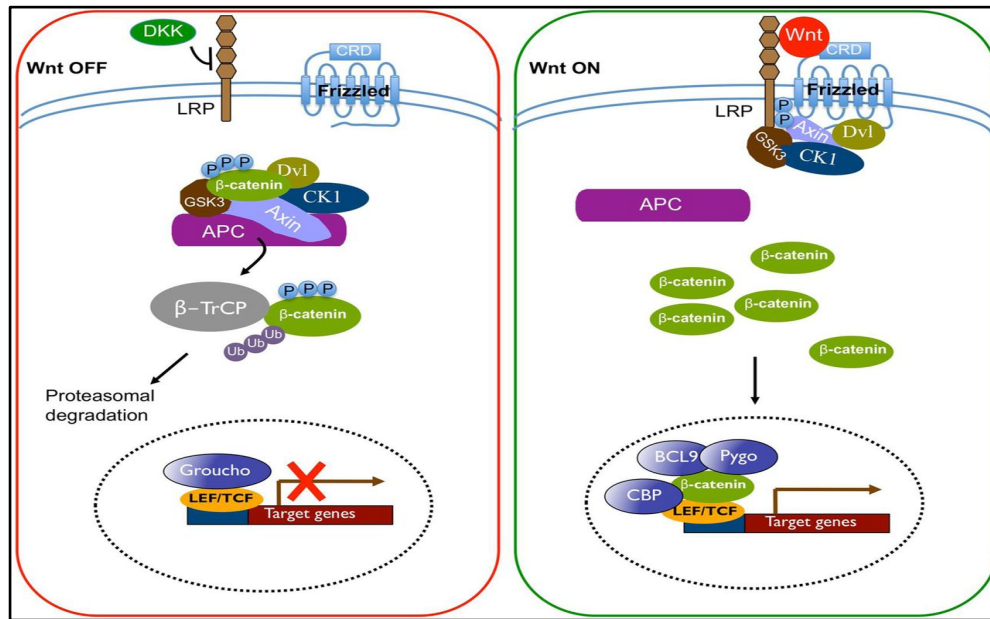


**Figure 2.10 The Wnt signaling pathway**

(Adapted from Yu et al., 2014, Biosci Rep) [109]

*Binding of the Wnt ligands to the receptor stabilizes B-catenin in the cytoplasm that further translocates to the nucleus and initiates expression of the Wnt target genes. In the absence of the Wnt ligand, B-catenin targeted for the degradation and expression of Wnt target genes suppressed.*

The other two pathways include non-canonical pathways, such as planar cell polarity (PCP) pathway and Wnt- $\text{Ca}^{+2}$  signaling pathway [110]. The non-canonical Wnt signaling functions independent of  $\beta$ -catenin that involves intracellular calcium ions and activation of the JNK signaling. It plays an important role during development and majorly regulates the processes, which involve cytoskeleton rearrangements such as cell migration, spindle orientation and apoptosis. The canonical Wnt signaling

regulates TCF/LEF mediated transcription of a wide range of different genes, which are involved in the cell cycle progression, fate determination, cytoskeleton organization, metabolism and maintaining stemness characteristics [111].

The Wnt signaling plays a fundamental role starting from the initiation of hair placode formation to maintenance of adult stem cells pool [112, 113]. Importantly, previous studies have shown that the Wnt signaling remains inhibited in the HFSCs during most of the telogen phase, while at the end of the telogen, Wnt signaling becomes active that promotes anagen progression [114]. Also, during the telogen phase,  $\beta$ -catenin predominantly localizes to the membrane of the HFSCs and nuclear  $\beta$ -catenin can be seen during the start of the anagen phase [115, 116]. The mechanism of the Wnt inhibited state during the telogen phase was further explained by the gene expression profiling on the slow-cycling stem cells, which showed upregulation of various Wnt inhibitory factors such as Sfrp1, Dab2, DKK3 and Wif1 and down-regulation of different Wnt ligands [32, 55]. Moreover, the HFSCs isolated from the human hair follicle also showed increased levels of the Wnt inhibitory factors such as Dkk3 and Wif1 [117]. Importantly, different mutant mouse studies have shown that the reduced Wnt signaling inhibit the timely emergence of the hair follicle during development, while over-activation of the Wnt signaling promotes premature hair follicle neogenesis and increased differentiation. However, recent investigations have shown the functional involvement of the Wnt signaling in the maintenance of stem cells quiescence during the telogen phase, suggesting that the differential activity of the Wnt signaling is required for the regulation of almost all aspects of the HFSCs behaviors [118]. Different components of the Wnt signaling in the regulation of various epidermal appendages have been extensively studied since last three decades.

Major phenotypic observations of the genetically mutated mouse models are summarized in the below Table 2.1

| Signals   | Mutation type                                    | Hair follicle phenotype   | Reference                       |
|-----------|--|---|---------------------------------|
| Wnt3      | <i>K14-Wnt3</i>                                  | Reduced hair follicle length, premature catagen onset                       | Millar et al., 1999 [119]       |
| Wnt7a     | <i>K14-Wnt7a</i>                                 | Increased hair follicle neogenesis upon wounding                            | Ito et al., 2007 [120]          |
| Wnt5a     | <i>Adenovirus-mediated Wnt5a expression</i>      | Inhibits the telogen-to-anagen transition                                   | Xing et al., 2013 [121, 122]    |
| Wnt10b    | <i>Adenovirus-Mediated Wnt10b Overexpression</i> | Induces Hair Follicle Regeneration  | Yu-Hong et al., 2013 [123]      |
| Dvl2      | <i>K14-Dvl2</i>                                  | Reduced hair follicle length, premature catagen onset                       | Millar et al., 1999 [119]       |
| Dkk1      | <i>K14-Dkk1</i>                                  | Lack of placode formation   | Andl et al., 2002 [124]         |
|           | <i>K5rtTA; TRE-Dkk1</i>                          | Lack of hair follicle neogenesis upon wounding                              | Ito et al., 2007 [120]          |
| APC       | <i>K14-Cre; APC<sup>fl/fl</sup></i>              | Aberrant hair follicle growth, short, curly whiskers                        | Kuraguchi et al., 2006 [125]    |
| Lef1      | <i>Lef1 -/-</i>                                  | Lack of body hair and whisker follicles                                     | van Genderen et al., 1994 [126] |
|           | <i>K14-Lef1</i>                                  | Clustered hair follicles, irregularly angled shafts                         | Zhou et al., 1995 [127]         |
|           | <i>K14-ΔN<sup>Lef1</sup></i>                     | Suppressed hair follicle differentiation, enhanced sebocyte differentiation | Merrill et al., 2001 [50]       |
|           | <i>K14-ΔN<sup>Lef1</sup></i>                     | Progressive hair loss and cyst and tumor formation                          | Niemann et al., 2002 [128]      |
| β-Catenin | <i>K14-ΔNβ-catenin (constitutively active)</i>   | De novo hair follicle induction   | Gat et al., 1998 [129]          |
|           | <i>K14-Cre; β-catenin<sup>fl/fl</sup></i>        | Lack of placode formation, loss of hair in the first hair cycle             | Huelsken et al., 2001 [130]     |
|           | <i>K5-S33Yβ-cateninER</i>                        | Anagen induction and enhanced hair follicle proliferation                   | Van Mater et al., 2003 [131]    |
|           | <i>K14-ΔNβ-cateninER</i>                         | Anagen induction and de novo hair follicle formation                        | Lo Celso et al., 2004 [132]     |
|           | <i>K14-ΔNβ-catenin (hemizygous)</i>              | Precocious bulge stem cell activation                                       | Lowry et al., 2005 [115]        |

| Signals | Mutation type  | Hair follicle phenotype  | Reference                           |
|---------|--|--|-------------------------------------|
|         | <i>K14-CreER<sup>tm</sup>; <math>\beta</math>-catenin<sup>fl/fl</sup></i>    | Loss of bulge stem cell quiescence and maintenance   | Lowry et al., 2005 [115]            |
|         | <i>K14-CreER<sup>tm</sup>; <math>\beta</math>-catenin<sup>fl/fl</sup></i>    | Lack of hair follicle neogenesis upon wounding   | Ito et al., 2007 [120]              |
|         | <i>K14-Cre; Ctnnb1<sup>(ex3)fl/+</sup> (dominant active)</i>                 | Premature hair follicle placode development, predominant differentiation toward hair shaft, defects in hair follicle development | Zhang et al., 2008 [133]            |
|         | <i>Cor-Cre (DP specific); Ctnnb1<sup>fl/fl</sup></i>                         | Reduced hair follicle length and thinning  | Enshell-Seiffers et al., 2010 [134] |
|         | <i>K15-<math>\Delta</math>N<math>\beta</math>-cateninER</i>                  | Increased bulge proliferation and expansion  | Baker et al., 2010 [135]            |
|         | <i><math>\Delta</math>K5<math>\Delta</math>N<math>\beta</math>-cateninER</i> | Ectopic hair follicle induction In sebaceous gland   | Baker et al., 2010 [135]            |
| Tcf3/4  | <i>K14-<math>\Delta</math>NTcf3</i>  | Suppressed epidermal differentiation   | Merrill et al., 2001 [50]           |
|         | <i>K14rtTA; TRE-mycTcf3</i>  | Lack of epidermal differentiation and sebaceous gland  | Nguyen et al., 2006 [51, 136]       |

**Table 2.1 The role of Wnt components in epidermal homeostasis**

(Modified from Lee et al., 2012, *Semin Cell Dev Biol*) [70]

### 2.6.3 BMP signaling and hair follicle stem cells

Bone Morphogenetic Proteins (BMPs) are class of the transforming growth factor- $\beta$  (TGF- $\beta$ ) superfamily that binds with the BMP receptor and exerts their effects in an autocrine or paracrine manner. Binding of the BMP leads to heterodimerization of type I (BMPRI-A and BMPRI-B) and type II (BMPRII) receptors. The activation of the BMP receptor leads to phosphorylation of R-Smad (Smad1/5/8) that further binds to the Smad4 and regulate target gene expression [137, 138] (

**Figure 2.11).** The BMP inhibitors such as Chordin, Noggin and Follistatin are main regulatory molecules that prevent binding of the BMP ligands to the BMP receptor that regulate BMP signaling activity [139, 140]. Importantly, in the skin, the activity

of the Wnt and BMP signaling is tightly coupled. The Wnt signaling provides activating signals that promotes proliferation of the HFSCs, while BMP signaling is inhibitory signaling that requires for the maintenance of the HFSCs quiescence [72, 141, 142]. The BMP ligands such as BMP 2, BMP 4 and its receptor BMPR-IA are known to express in the epithelial and mesenchymal cells, whereas the BMP inhibitor noggin is expressed in the dermal papilla cells.

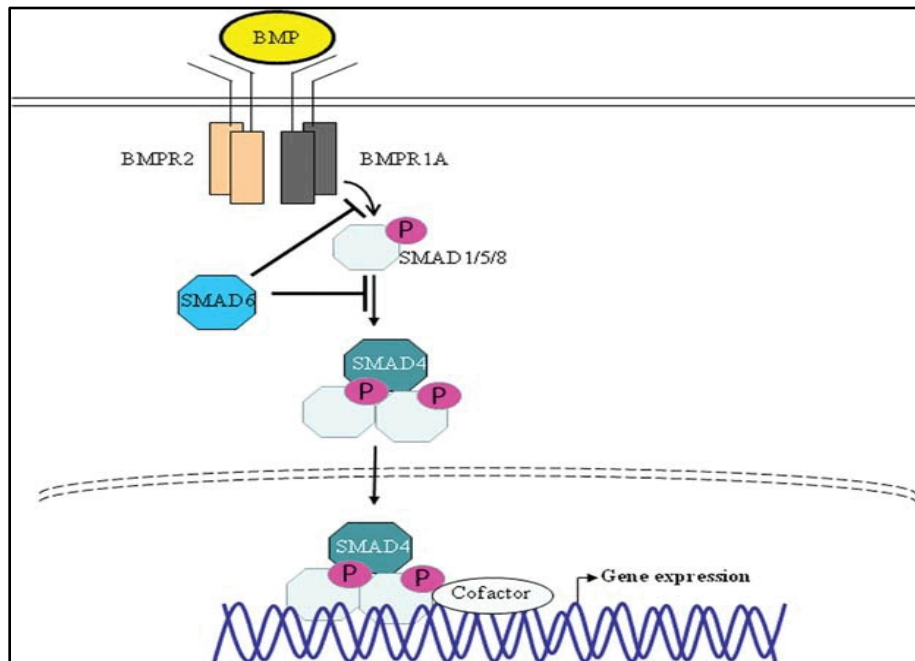


**Figure 2.11 Overview of BMP signaling pathway**

*(Adapted from Tan HL et al., 2012, Hum Mutat) [143]*

*The graphical representation of BMP signaling pathway shows the binding of BMP ligands to the type I or type II BMP receptors, which further activates SMAD1/5/8 transcription factors. The effector SMAD4 translocates to the nucleus and regulates the expression of the BMP target genes.*

The noggin knockout mice displayed reduced placode formation and impaired hair follicle development [144]. In contrast, overexpression of the noggin under MSX2 promoter in the matrix cells inhibits differentiation of the matrix cells that is required

for the hair shaft formation [145]. Further, deletion of the *Bmpr1a* by using the different Cre line showed impaired differentiation of the IRS, abnormal hair shaft formation and loss of stem cells quiescence [146, 147]. In addition, deletion of the Activin isoforms and Follistatin displayed lack of whisker follicles and mis-oriented hair follicles respectively [148].

#### **2.6.4 Other signaling pathways in HFSCs regulation**

Apart from the Wnt and BMP signaling activity in regulation of the HFSCs proliferation and quiescence, other developmental signaling pathway such as Shh, TGF and Notch have been shown to play essential roles in the epidermis development and stem cells regulation.

##### **2.6.4.1 Shh Signaling**

The Hedgehog signaling mainly governs by three different secretory ligands known as Sonic Hedgehog (Shh), Indian Hedgehog and Desert Hedgehog [149]. However, only Shh has been shown to be involved in the regulation of the epidermal regulation and regeneration [150]. The Shh ligand binds to its receptor Ptch1 and Ptch2, which results in the abrogation of the Ptch mediated inhibition of the Smoothened (Smo). The Smo further activates Gli transcription factors (Gli1, Gli2 and Gli3) that regulate expression of the Shh target genes (**Figure 2.12**). In the skin, Shh expression has been seen during the late stage of the placode formation and it is dispensable for the induction of the placode formation. However, Shh is indispensable for the further process of the hair follicle morphogenesis and hair follicle growth [151, 152]. Overexpression of the Shh in the skin resulted in massive down-growth of the hair follicle and basal cell tumor formation [153]. Deletion of the Gli2 showed hair follicle arrest during development [154].

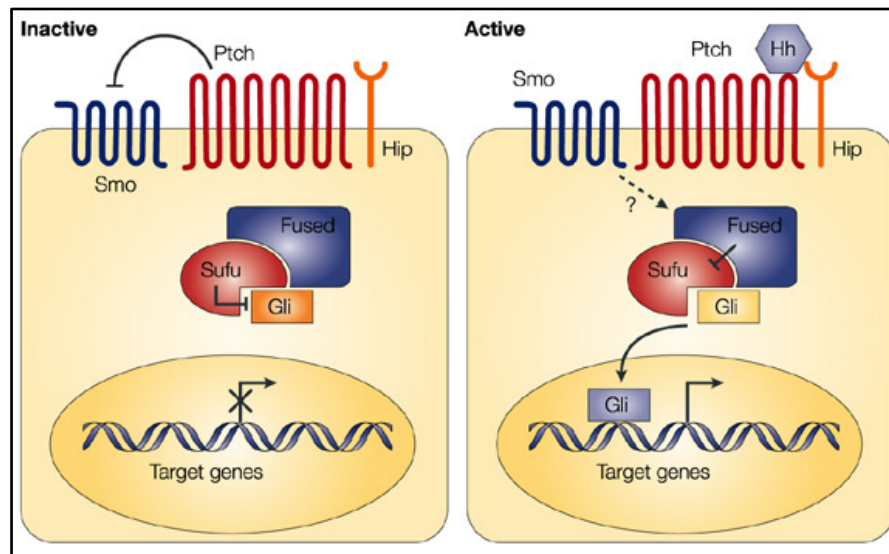


**Figure 2.12 Hedgehog signaling pathway**

*(Adapted from Magliano et al., 2003, Nat Rev Cancer) [155]*

*Binding of the Hedgehog ligands to the Ptch receptor activates the hedgehog signaling. Binding of the ligands to Ptch receptor further releases the inhibition of Ptch on Smo, which leads to the activation of Gli transcription factors.*

In addition, lineage tracing of the HFSCs with an active Shh signaling showed to generate all cell types of the hair follicle [156]. During hair follicle regeneration, the matrix cells produce Shh that further activates HFSCs and promote its proliferation [84].

#### **2.6.4.2 TGF $\beta$ signaling**

The ligands of the TGF- $\beta$  family form homodimer or heterodimer that preferentially bind to the type II receptors. The TGF- $\beta$  family includes TGF- $\beta$ s, activins and nodal [157]. These ligands activate responding Smad 2/3, which forms trimer with the common Smad-4 protein and translocates to the nucleus. TGF- $\beta$  mediated signaling plays important roles in the cell proliferation and differentiation of embryonic and

adult stem cell types. Importantly, TGF- $\beta$  signaling is required for the maintenance of the pluripotent state of the embryonic stem cells. Importantly, TGF- $\beta$  mediated signaling known to regulate Nanog expression and thereby enhances the maintenance of the pluripotent state of the human ESCs [158, 159]. The signaling through TGF- $\beta$  family ligands regulates adult stem cells behaviours by acting in the autocrine or paracrine fashion. It has been shown that various stem cells population in the epidermis responds differently to the TGF- $\beta$  signaling. In the stem cells niche of the hair follicle, the quiescent HFSCs are activated by TGF- $\beta$  ligands, which are secreted by the dermal papillae cells [107]. Further, the TGF- $\beta$  ligands that are secreted by the active HFSCs are known to regulate the quiescence of the melanocyte stem cells. Inhibition of the TGF- $\beta$  signaling promotes isthmus stem cells to epidermis and sebocyte lineages [160]. Transforming growth factor  $\beta$ 2 is required to induce Snail expression in the hair follicle bud [161]. In addition, TGF- $\beta$ 2 regulates activation of the HFSCs by suppressing the BMP mediated inhibitory signaling [107]. Apart from its regulatory functions in normal adult stem cells, TGF- $\beta$  signaling regulates an epithelial to mesenchymal transition (EMT) of breast cancer stem cells, which is a critical step in acquiring the stemness characteristics [162, 163].

#### **2.6.4.3 Notch signaling**

The Notch receptor includes various isoforms such as Notch 1, Notch 2, Notch 3 and Notch 4. It is synthesized as a single polypeptide; however, proteolytically cleavage generates two different polypeptide chains that heterodimerize and form the mature receptor [164]. The Notch signaling is mainly operated by various ligands such as Jagged-1, Jagged-2 and Delta1-4 [165, 166].

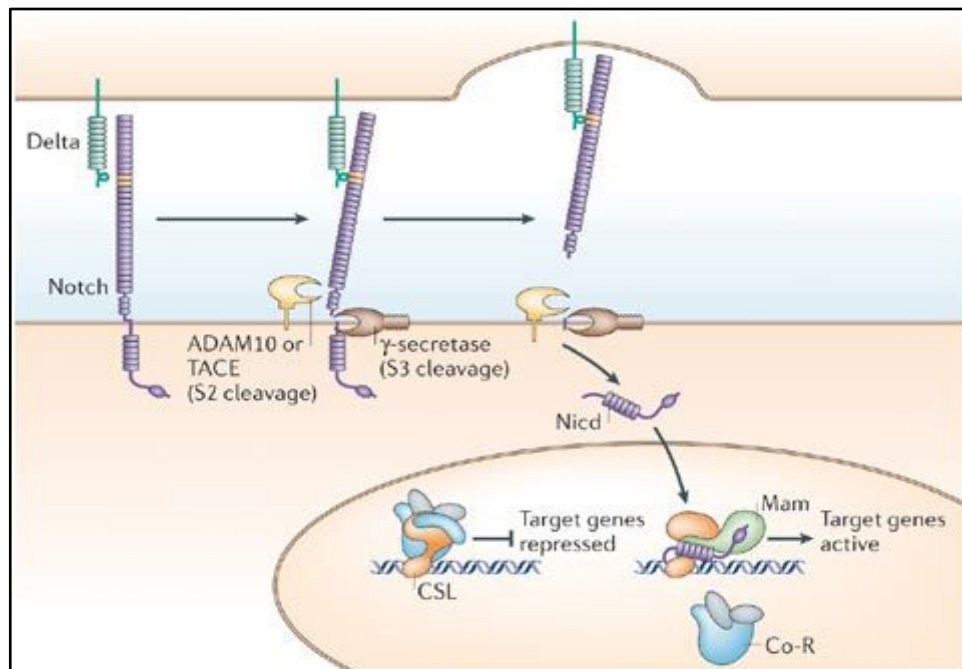


**Figure 2.13 Notch signaling pathway**

*(Adapted from Bray et al., 2006, Nat Rev Mol Cell Biol) [167]*

*The notch signaling is activated by the binding of Notch ligands to the extracellular domain of Notch receptor that leads to conformational change in the intracellular domain and releases NCID in the cytoplasm. The NICD further translocates to the nucleus and regulates expression of the Notch target genes.*

The intracellular domain of the Notch receptor further cleaved by the gamma-secretase complex and generates Notch intra-cellular domain (NICD), which translocate to the nucleus and regulate gene expression (Figure 2.13). During embryogenesis, Notch-1 as well as its ligands such as Jagged-1 and Jagged-2 expresses in the inner cells of the hair placode [168]. The Notch-1 ablation after birth resulted in the hair loss and the cyst formation [169]. In addition, expression of the constitutively active form of Notch-1 displayed an abnormal differentiation of the medulla and cuticle layers [170]. In contrast, deletion of the Notch-1 in basal layer

cells displayed epidermal hyperplasia and spontaneous skin tumours formation [171]. Bulge specific deletion of the Notch proteins showed epidermal cysts formation and stem cell fate conversion to the interfollicular epidermis [172]. Similarly, deletion of the Jagged-1 in the basal layer cells and  $\gamma$ -Secretase in the matrix cells demonstrated cyst formation, inhibition of the hair growth cycle and failure to maintain IRS cell respectively [173, 174].

## **2.7 Wound healing process**

The wound healing is a systemic multistep and multifactorial process, which involves a wide range of cell types including epithelial cells, fibroblasts and immune cells. The contribution of different cell types and its proliferation and differentiation status is closely correlated with the phases of the healing process [175]. The brief mechanism of the wound healing process and the contribution of different stem cells of the skin is described below.

### **2.7.1 Mechanisms involved in wound healing response**

The wound healing process includes various phases, which is governed by the distinct biological activities between various components of the epidermis and dermis (Figure 2.14). Immediately after skin injury, the healing process begins with the blood clotting by platelets, which is activated by the extravascular collagen [176]. Further, platelets releases secretory growth factors such as platelet-derived growth factor (PDGF) and transforming growth factor  $\beta$  (TGF- $\beta$ ) that attract inflammatory cells to the wound site and initiate inflammatory response [176]. Importantly, Martin et al., 2003 showed that the inflammatory phase is dispensable for the skin wound healing process as deletion of the PU.1 in mice, which lacks both the macrophages and neutrophils showed no effect on the wound healing rate [177].

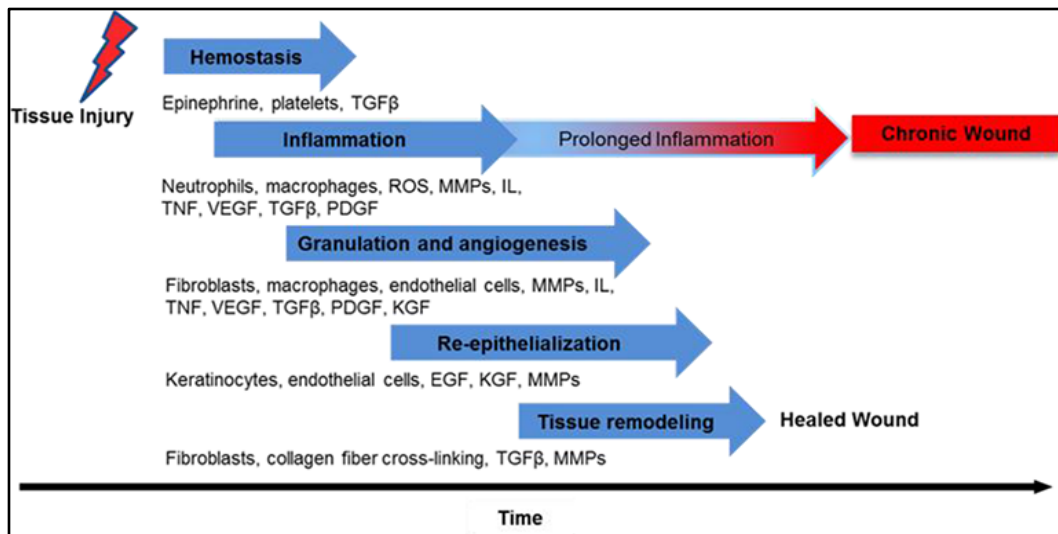


**Figure 2.14 Steps of the wound healing process**

*(Adapted from Schreml et al., 2010, Br J Dermatology) [178]*

*The phases of the wound healing process include blood clotting, inflammation, which starts immediately, proliferation of the stem cells, cell migration and angiogenesis that along with the production of the extracellular matrix components leads to re-epithelialization.*

The proliferative phase starts after two days of the injury and extended up to 2 to 3 weeks. This phase mainly includes proliferation of the epidermal basal cells and migration of its progeny along with the activation and migration of the fibroblast. This leads to the deposition of the extra cellular matrix, formation of new blood vessels and re-epithelialization of the wounded area. The newly synthesized tissue part further undergoes remodelling, which lasts until a year [179-181].

### **2.7.2 IFE stem cells in the wound healing process**

The IFE stem cells reside in the basal layer of the skin and contribute to the IFE homeostasis. Moreover, the role of the IFE stem cells in the wound-induced re-epithelialization has been explored by using lineage-tracing approach. The labeling of

the epidermal cells by using Inv-CreER and K14-CreER showed that the K14CreER targeted cells forms large clones as compared to the Inv-CreER targeted cells. In addition, the K14-CreER labelled clones generate a progeny that remains in the basal layer for a long time, whereas the progeny of the Inv-CreER labelled clones have limited contribution to the healing process [182]. Moreover, the clonal analysis demonstrated that the available progenitors during wounding divide more rapidly and leads to exhaustion of the progenitor pool, while stem cells become activated and produce new progenitors for further expansion and differentiation [183]. Importantly, a study also showed that the basal cells of the adult mice have the ability to program follicular neogenesis during wound healing process, which is dependent on the Wnt signaling as similar as the hair follicle morphogenesis during embryonic development [120]. Together, these studies showed that the IFE SCs are functionally sufficient for re-epithelization following wounding and can produce new hair follicle after re-epithelialization.

### **2.7.3 Hair follicle stem cells in the wound healing process**

The first evidence for the contribution of the follicular cells in wound healing process came in 1942. Brown and McDowell showed that the shallow wound that does not destroy the hair follicle gets completely healed at a faster rate as compared to the full thickness wound that completely destroyed hair follicles [184, 185]. Recent studies by using novel technologies revealed that within the 24 hours after wounding, the bulge cells migrates out of the niche and involves in the re-epithelialisation process [32, 56]. In contrast, diphtheria toxin-induced removal of the bulge cells does not alter healing response, suggesting that the bulge cells are dispensable for wound re-epithelialisation [186]. In addition, Ito et al., 2005 used the K15 promoter-driven LacZ expression system that showed that the repaired epithelium contains cells of the bulge origin.

However, the IFE cells derived progeny effectively replaces bulge-derived cells in a short time period after the complete healing [57]. Moreover, a recent study by using *Lgr6* promoter showed that the isthmus derived cells persist for a longer time in the neo-epidermis, suggesting that the isthmus cell have more efficiency to acquire a basal phenotype than the bulge cells [30]. The *EDA<sup>-/-</sup>* mutant strain that lacks hair in the tail showed delayed re-epithelialisation; however, hyperproliferation was observed in the distant region that may act as a compensatory mechanism for the absence of the hair follicle cells [187].

## **2.8 Development of the alopecia**

The loss of hair due to any cause is known as alopecia. There are many factors responsible for the development of the alopecia such as genetic and environmental factors. The major types of hair loss and associated symptoms are summarized below.

### **2.8.1 Types of alopecia**

There are different classification systems to classify different types of the alopecia. Here, I have briefly described the main types of the alopecia.

#### **a) Androgenetic Alopecia (AGA)**

It is known as pattern baldness, which can be a hereditary. It is characterized by time-dependent progressive hair loss

#### **b) Alopecia Areata (AA)**

This form of alopecia develops due to immune cells dysfunctions. It shows patchy hair loss on different part of the body.

#### **c) Alopecia Totalis (AT)**

It is advanced stage of the alopecia areata and can be characterized as a complete loss of hair on the scalp.

**d) Alopecia Universalis (AU)**

It is the rarest and most severe form of the alopecia areata. It can result in the total loss of the body hair and it is most challenging to treat.

**e) Scarring Alopecias**

It is also a rare disorder caused due to the permanent destruction of the hair follicle and the fibrous tissue replaces the hair follicle.

**f) Traction Alopecia**

This form of alopecia shows more aggressive phenotype over time and mainly caused due to the constant and excessive strain, which sometimes also affects the new hair shaft production and leads to the loss of hair.

**g) Anagen Effluvium**

It is characterised by hair loss during anagen phase of the hair cycle. The leading cause includes different physical and chemical treatments such as radiotherapy and chemotherapy for the cancer treatment.

**h) Telogen Effluvium**

It is a type of diffused hair loss and characterised by hair thinning and loss of more hair temporary. However, it can be completely recovered in due course of time.

**2.8.2 Molecular mechanisms involved in alopecia**

The most common factor for the development of the alopecia is deregulation of the hormonal balance, which affects both the male and female known as androgenetic alopecia. The genetic abnormalities in the hormonal metabolism resulted in the hereditary transfer of the symptoms. It is androgen-dependent, initially starts with the thinning of the hair and further follows a defined pattern of the hair loss. The main mechanism involved is a regulation of the dihydrotestosterone (DHT) and the androgen receptor (AR) activities. The affected scalp area shows high levels of DHT

and AR along with the reduced activity of androgen inactivating enzymes. The other major type of hair loss is an Alopecia Areata (AA). It is related to defects in the cycling of the hair follicle due to an attack of the inflammatory cells on anagen hair follicles. This results in the regression of the hair follicle and the hair follicle prematurely enters into catagen stage. The hair follicle is unable to retain the hair shaft and that lead to loss of the hair. However, the hair follicle is able to cycle further and have the ability to regenerate a new hair shaft. Therefore, this type of hair loss may behave in the reversible fashion. In addition, the role of various genetic factors in the development of alopecia in different mutant mice models is described in the further section.

### **2.8.3 Stem cells and alopecia**

The human hair follicle contains Keratin 15 and CD34 positive hair follicle stem cells (HFSCs). Also, these cells express embryonic stem cell factors such Oct-4 and Nanog [188]. Various studies have highlighted the functional defects of the human HFSCs in a different type of the alopecia. Interestingly, Garza et al., in 2011 have demonstrated that the K15 positive human HFSCs are not affected during the condition of the androgenetic alopecia (AGA). However, the progeny of the stem cells is markedly decreased, suggesting that the activation of the HFSCs may be abrogated in the patients with AGA [189]. Further, the stem cells niche is known to get destroyed during the chronic inflammatory disease such as Lichen planopilaris (LPP), which leads to the permanent hair loss [190]. Moreover, Yoshida et al., 2011 have shown decreased expression of the hair follicle stem cells markers in the samples of the alopecia areata [191]. However, the study on the samples of scarring and nonscarring alopecia showed that the primary target in this types of alopecia is not the bulge stem cells but the stem cells of the other parts of the ORS [192]. Interestingly, the

autologous transplantation of the HFSCs on the patients of AGA have been shown to get localised in the bulge area and increases hair density [193]. Collectively, various studies have shown that the activity of the HFSCs is altered during the condition of the hair loss, which can be rescued by the autologous transplantation of the HFSCs.

#### 2.8.4 Mutant mouse models and cyclic alopecia

The genetic alterations in different layers of the hair follicle have been reported to cause permanent or cyclic alopecia [194]. Importantly, differentiation of the matrix cells in the IRS and hair shaft producing cells is crucial for the development of mature hair. Here, the phenotype of various mutant mice models have been summarized that develop alopecia due to alterations in the functions of the specific gene that is given below in the Table 2.2.

| Gene details   | Symbol                              | Hair Phenotype   | Reference                        |
|--|-------------------------------------|--|----------------------------------|
| Overexpression of avian erythroblastosis oncogene B2         | <i>Tg(K5-erbB2)</i>                 | Alopecia and Spontaneous papillomas                                      | Kiguchi et al., 2000 [195]       |
| Over-expression Sonic hedgehog homolog                       | <i>HK1-Shh</i>                      | Pigmented lesions and regions of alopecia                                | Ellis et al., 2003 [196]         |
| Epidermal over-expression of a non-degradable mutant of IκBα | <i>K5-IκBαM</i>                     | Hair follicle degeneration and alopecia                                  | Hogerlinden et al., 1999 [197]   |
| Diacylglycerol O-acyltransferase 1                           | <i>Dgat1tm1Far</i>                  | Cyclical hair loss when retinol is abundant                              | Shih et al., 2009 [198]          |
| Prostaglandin-endoperoxide synthase 2                        | <i>Tg(K5-Ptgs2)19Kmd</i>            | Precocious catagen and development of alopecia after three months        | Muller-Decker et al., 2003 [199] |
| B-cell leukemia/lymphoma 2 (Bcl-2)                           | <i>Tg(BCL2)ITsk</i>                 | Acceleration of catagen progression Hair follicle dystrophy and Alopecia | Muller-Rover et al., 2000 [200]  |
| MutantHr gene  | <i>hr<sup>r<sup>hsl</sup></sup></i> | Hair loss or regrowth  | Zhu et al.,                      |

|  |  |   |                             |
|--|--|---|-----------------------------|
|  |  |   | 2017 [201]                  |
| $\alpha$ isoform of the PP2A catalytic subunit               | <i>Ppp2caflox/flox; Krt14-Cre</i>                    | Smaller body size and hair loss                                       | Fang et al., 2016 [202]     |
| Activin A receptor type 1b                                   | <i>Acvr1b(flox/flox); K14-Cre</i>                    | Delays in hair cycle reentry and severe hair loss                     | Qiu et al., 2011 [203]      |
| Sox21  | <i>Sox21-KO</i>                                      | Defects in the anchoring the hair shaft                               | Kiso et al., 2009 [204]     |
| Msh Homeobox 2   | <i>Msx2<sup>tm1Rilm</sup>/Msx2<sup>tm1Rilm</sup></i> | Prolongs catagen and telogen, cyclic hair loss at early age           | Liang Ma et al., 2003 [205] |
| Palmitoyl-acyl transferase                                   | <i>Zdhhc13<sup>skc4</sup></i>                        | Defects in the hair anchoring ability and premature hair loss         | MingLiu et al., 2015 [206]  |
| Dominant negative mutant of epidermal growth factor receptor | <i>K5-HERCD-533</i>                                  | mice Hair follicles fail to enter into catagen stage, Severe alopecia | Murillas et al., 1995 [207] |
| Smad4, mediator of TGF- $\beta$ signaling                    | <i>Smad4co/co; K5-Cre</i>                            | Progressive hair loss   | Yang et al., 2008 [208]     |
| BMP antagonist noggin  | <i>K14-Noggin mice</i>                               | Progressive hair loss   | Sharov et al., 2009 [209]   |

**Table 2.2 Phenotype of alopecia developing mutant mice models**



### ***3. Aims and Objectives***



### **3.1 Rational or statement of the problem**

The cell signaling mechanisms play a crucial role in regulating stemness, proliferation and differentiation potential of the embryonic as well as adult tissue stem cells. Importantly, different signaling factors are known to inhibit the induction of the cell proliferation, thereby maintain the stem cells quiescence and acts as a tumour suppressor during adult tissue maintenance. Specifically, epidermal growth factors and Wnt signaling are involved in the regulation of the proliferation, differentiation, fate determination and lineage commitment of the epidermal stem cells. Therefore, exploring the mechanistic involvement of these signaling mechanisms in the regulation of stem cells functions may enhance our horizon to utilize stem cells in therapeutic approach more effectively.

### **3.2 Hypothesis**

The sPLA<sub>2</sub>-IIA is known to promote as well as inhibit cells proliferation in different tissue types. Additionally, it is involved in the regulation of signaling pathway such as EGFR and recently reported as a  $\beta$ -catenin /TCF target (Wnt target) gene. However, the mechanism through sPLA<sub>2</sub>-IIA alters epidermal organizations, as well as HFSCs proliferation and differentiation is remaining unknown. In addition, Dab2 is a Wnt signaling inhibitor, which is involved in the endocytosis of cell surface receptors and regulates Wnt signaling negatively as well as BMP signaling positively. The Wnt signaling is inhibited and BMP signaling is activated during the HFSCs quiescence. Importantly, Dab2 is highly upregulated in the quiescent HFSCs. Therefore, Dab2 may have a crucial role in maintaining Wnt-OFF and BMP-ON status during quiescence and vice versa during induction of HFSCs proliferation. Hence, understanding the functional role of sPLA<sub>2</sub>-IIA and Dab2 in the regulation of cell signaling pathways may lend insight into the mechanisms of stem cell regulation.

### 3.3 Objectives

**Objective 1:** To decipher the role of group IIA secretory phospholipase A<sub>2</sub>/ enhancing factor in epidermal stem cell regulation

**Objective 2:** To investigate the role of disabled-2 (Dab2) in epidermal stem cell regulation

### 3.4 Outline of the study

**Objective 1: To decipher the role of group IIA secretory phospholipase A<sub>2</sub>/ enhancing factor in epidermal stem cell regulation**

**A. To determine the role of group IIA secretory phospholipase A<sub>2</sub>/ enhancing factor in regulation of molecular signaling pathways**

- a. Establishment of primary keratinocytes culture from mouse skin*
- b. Analysis of epidermal growth factor signaling in vitro*
- c. Validation of the altered signaling pathways in vivo*

**B. To determine the functional role of group IIA secretory phospholipase A<sub>2</sub>/ enhancing factor in mouse epidermal keratinocytes**

- a. Colony forming efficiency of primary keratinocytes*
- b. Analysis of cell proliferation and differentiation in vitro*
- c. Reversion of altered signaling mediated abnormal cell proliferation in vitro and in vivo*
- d. Effect of sPLA<sub>2</sub>-IIA induced proliferation on divisional dynamics of HFSCs*

**C. To characterize the K14-sPLA<sub>2</sub>-IIA homozygous mice skin in relation to the hair follicle stem cells loss**

- a. The comparative hair follicle cycling study*
- b. Analysis of epidermal proliferation and differentiation*
- c. Quantification of the HFSCs pool*
- d. Mechanism of cyclic alopecia*
- e. Effect of sPLA<sub>2</sub>-IIA on wound healing response*

**Objective 2: To investigate the role of disabled-2 (Dab2) in epidermal stem cell regulation**

**A. To characterize the effect of Dab2 deletion in hair follicle cycling and stem cells**

- a. Comparative hair follicle cycling study*
- b. Effect of Dab2 deletion on epidermal proliferation and differentiation*
- c. Analysis of sebaceous gland size in Dab2cKO mice*
- d. Role of Dab2 in the regulation of Wnt signaling in epidermis and hair follicle*

**B. Functional characterization of hair follicle stem cells in Dab2 knockout mice**

- a. Flow cytometry analysis of the HFSCs pool*
- b. Colony forming efficiency of HFSCs*
- c. Label retention cells (LRCs) analysis*

### **3.5 Work done**

The detailed description of work carried out under two different objectives is distributed into three different chapters as given below.

#### **Chapter 5: To decipher the role of group IIA secretory phospholipase A2/ enhancing factor in epidermal stem cell regulation**

- i. Introduction for Objective 1
- ii. Results of work done under Objective 1
- iii. Discussion

#### **Chapter 6: To investigate the role of disabled-2 (Dab2) in epidermal stem cell regulation**

- i. Introduction for Objective 2
- ii. Results of work done under Objective 2
- iii. Discussion

#### **Chapter 7: Summary and conclusion of both the objectives**

## ***4. Materials and Methods***



## **4.1 Mice models**

ACTREC's "Institutional Animal Ethics Committee (IAEC)" has approved all the protocols for the use of animals in different studies. All the animal studies were performed by the standard procedure. Different transgenic and knockout mice models used in these studies are mentioned below.

### **a. Mice models used in the study of Objective 1:**

The K14-sPAL<sub>2</sub>-IIA mice were a generous gift from Dr. Rita Mulherkar [210]. The hemizygous mice were crossed with the wild type FVB mice to obtain K14-sPAL<sub>2</sub>-IIA hemizygous experimental animals. The K14-sPAL<sub>2</sub>-IIA hemizygous mice were intercrossed to obtain K14-sPAL<sub>2</sub>-IIA homozygous mice [211]. The K14-sPAL<sub>2</sub>-IIA hemizygous and homozygous mice were sacrificed at various time points as mentioned in the respective experiments. The pTRE-H2B-GFP hemizygous mice [32] were crossed with the K5tTA mice [212] to obtain H2BGFP Tet-off mice [85]. The ultraviolet-based portable lamp (BLS Ltd) was used to identify GFP-expressing pups.

### **b. Mice models used in the study of Objective 2:**

The Dab2 flox mice [213], K14CRE-ER mice [214] (CD-1 background) and ROSA-STOP- YFP mice [215] were purchased from the Jackson Laboratories, USA. The K14CreER were crossed with the ROSA-STOP-YFP mice to generate K14CreER: ROSA-STOP-YFP mice for analyzing the Cre activity. The Dab2flox/flox mice were crossed with K14CRE-ER mice to obtain Dab2 conditional knockout mice (Dab2cKO). We established crossing of the K14CreER: Dab2fl/+ mice with Dab2fl/fl mice to obtain K14CreER: Dab2fl/+ mice (Heterozygous) and K14CreER: Dab2fl/fl mice (Homozygous) from the same litter. The tamoxifen was injected

intraperitoneally at a dose of 100 µg/g body-weight for five consecutive days during different postnatal day (PD).

## 4.2 Mice genotyping

The mice were weaned after postnatal day 21 (PD21) and animals were numbered as per standard procedure. The tail snips were used for genotyping purpose as the distal tail of young mice lacks bone. The tail sample collected in the lysis buffer and proceed for DNA extraction as described below.

### 4.2.1 DNA extraction from tail tissue samples

|                   | <b>Final Concentration</b> | <b>per 500ml</b> |
|-------------------|----------------------------|------------------|
| 1M Tris pH 8.0    | 10 mM                      | 5 ml             |
| 5M NaCl           | 100 mM                     | 10 ml            |
| 0.5M EDTA pH 8.0  | 10 mM                      | 10 ml            |
| 10% SDS           | 0.5 %                      | 25 ml            |
| dH <sub>2</sub> O |                            | to 500 ml        |

**Table 4.1 Composition of the tail lysis buffer**

- 1) Collect the tail sample in 1.5 ml tube containing 500 µl lysis buffer.
- 2) Add 10 µl Proteinase K (PK) per 500 µl of lysis buffer (Stock 20 mg/ml).
- 3) Invert the tube and mix it properly.
- 4) Incubate all the samples at 50-60 °C overnight.
- 5) Add 300 µl of 5 M NaCl to each tube and shake vigorously (15-20 times)
- 6) Incubate the samples at 4 °C for 10 minutes.
- 7) Centrifuge at low speed (7000 rpm) at 4°C for 10 minutes.
- 8) Collect the supernatant in a clean 1.5 ml tube.
- 9) Add 650 µl of isopropanol and immediately mix it by gently inverting the tubes and incubate at RT for 15 minutes.

- 10) Centrifuge at maximum speed for 10 minutes at RT to recover DNA.
- 11) Discard the supernatant and place tubes inverted on tissue paper to air-dry it.
- 12) Add 50  $\mu$ l of sterile water to each tube and incubate in dry-bath at 50°C for 5 min.
- 13) The DNA concentration and purity (260/280 ratio) was measured by Nanodrop quantification.
- 14) For 25  $\mu$ l PCR reaction, 1 to 2  $\mu$ l of DNA was used.

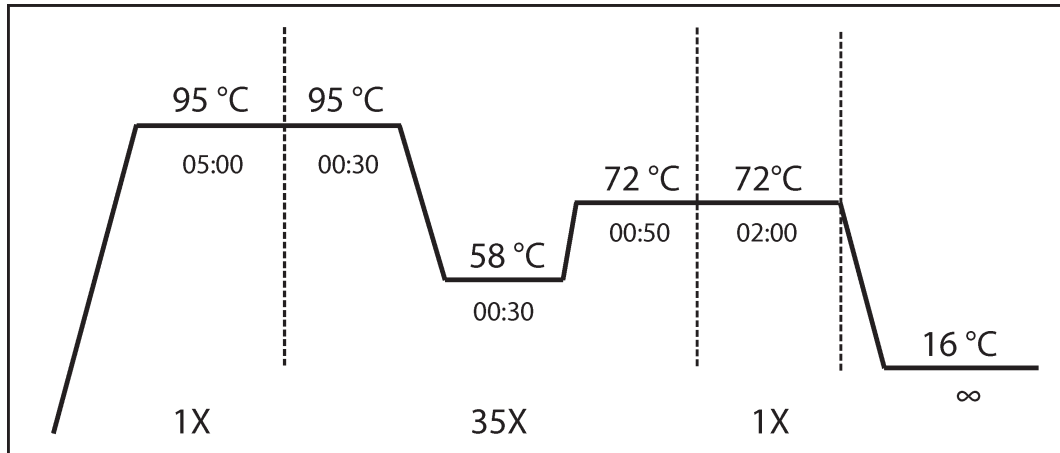
#### 4.2.2 Primer sequences for the genotyping of K14-sPAL<sub>2</sub>-IIA, K14CreER, Dab2floxed, Rosa-YFP, H2BGFP and K5tTA

| Gene Name               | Primer sequence 5'----->3'  |
|-------------------------|-----------------------------|
| P7 for EF -Forward      | GCTATGCCTTTCTATGATGCCACTGTG |
| M38 for EF -Reverse     | AATCAGCGGCGGCTTTATCG        |
| K14CreER -Forward       | GCGGTCTGGCAGTAAAACTATC      |
| K14CreER -Reverse       | GTGAAACAGCATTGCTGTCACTT     |
| K14CreER IC-Forward     | CTAGGCCACAGAATTGAAAGATCT    |
| K14CreER IC -Reverse    | GTAGGTGGAAATTCTAGCATCATCC   |
| Dab2 flox-Forward       | TTGATGATGTGCCTGATGCT        |
| Dab2 flox-Reverse       | AAGAGAACACTGGAGGCTCA        |
| Rosa YFP mutant Reverse | AAGACCGCGAAGAGTTTGTC        |
| Rosa YFP common         | AAAGTCGCTCTGAGTTGTTAT       |
| Rosa YFP WT Reverse     | GGAGCGGGAGAAATGGATATG       |
| H2BGFP0872 Forward      | AAGTTCATCTGCACCACCG         |
| H2BGFP1416 Reverse      | TCCTTGAAGAAGATGGTGCG        |
| Yo1 for K5tTA-Forward   | CTCGCCAGAAGCTAGGTGT         |
| Yo1 for K5tTA-Reverse   | CCATCGCGATGACTTAGT          |

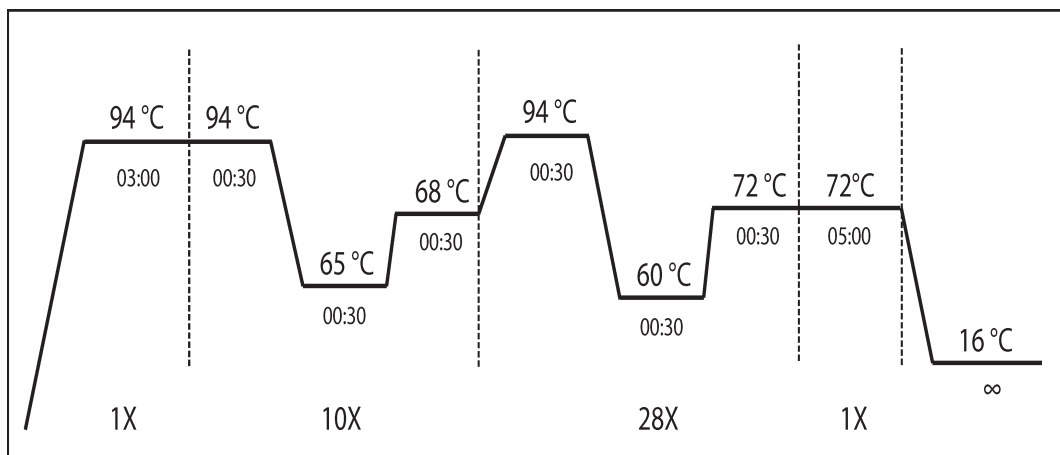
**Table 4.2 Primer sequences for mice genotyping**

### 4.2.3 PCR conditions for the genotyping

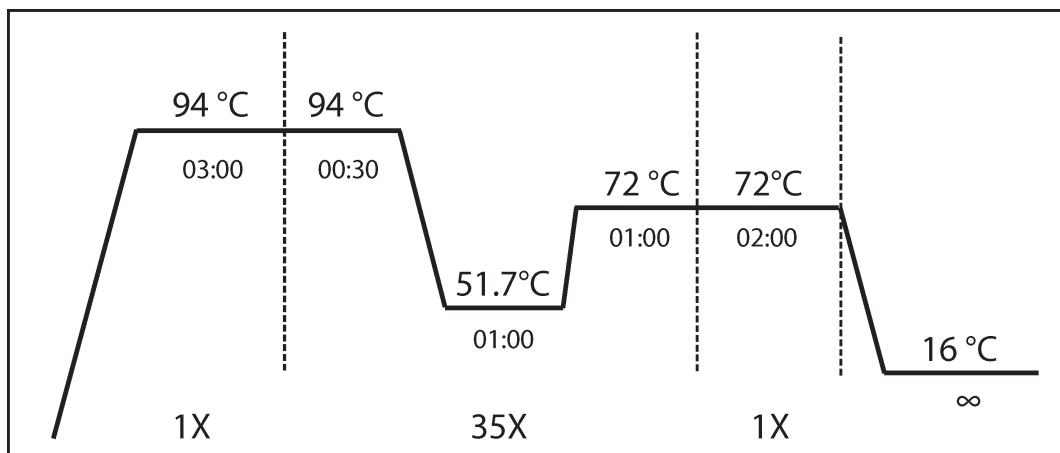
#### 1) For K14-sPAL<sub>2</sub>-IIA mice



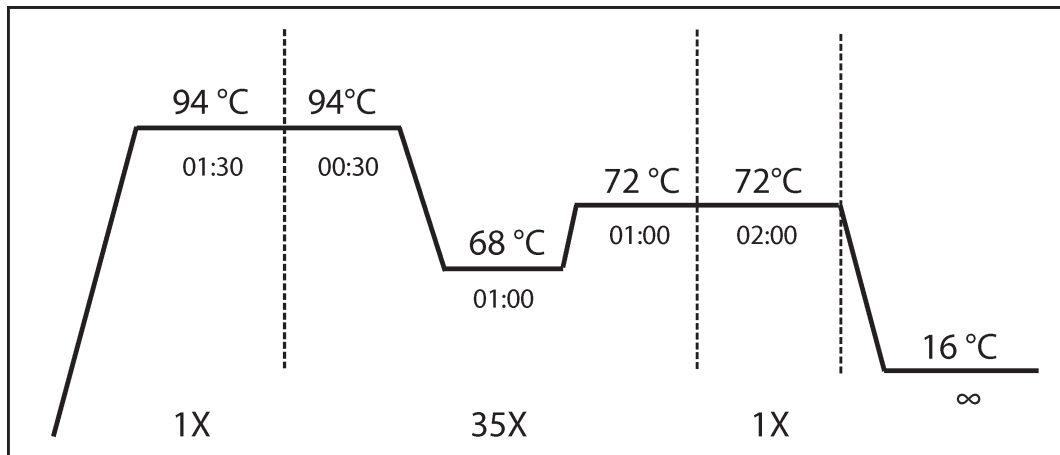
#### 2) For Dab2 flox mice



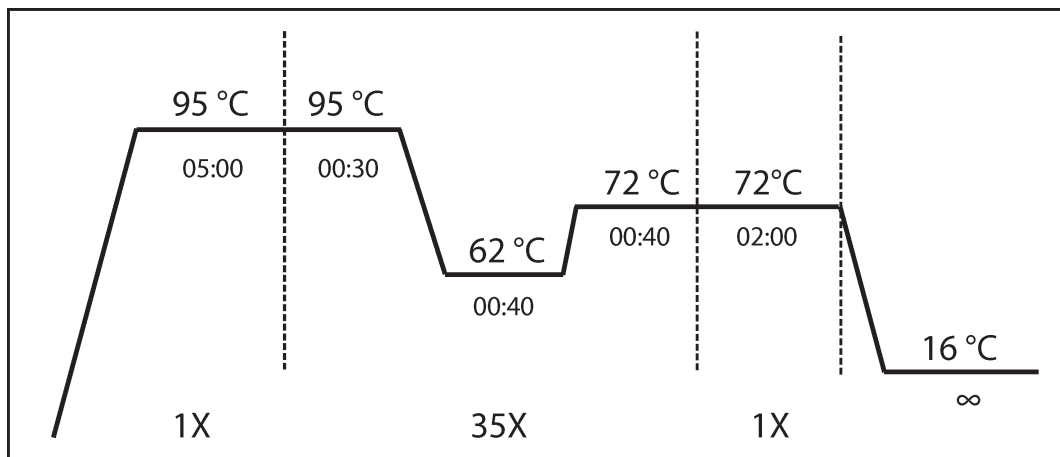
#### 3) For K14CreER mice



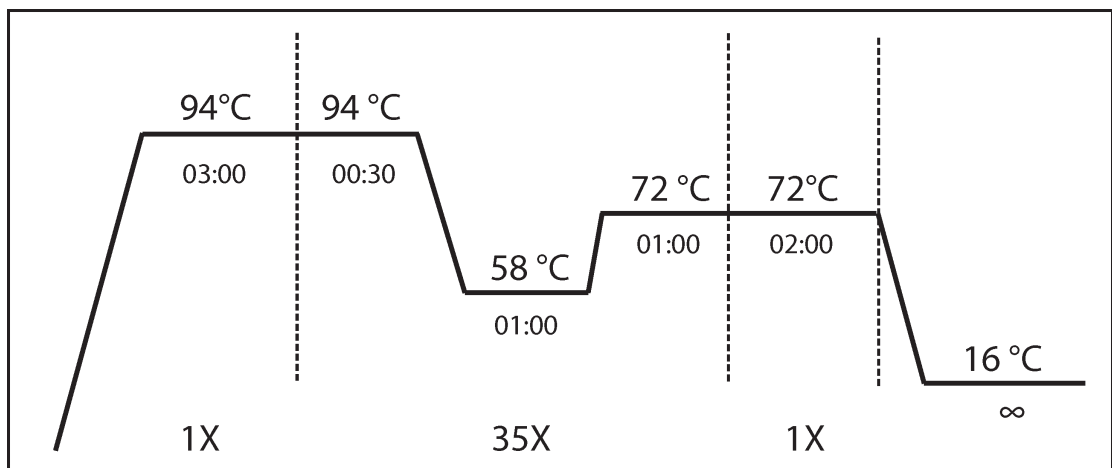
4) For H2BGFP mice



5) For K5tTa mice



6) For Rosa-STOP-YFP mice



### **4.3 Doxycycline dose for triple transgenic mice for proliferation dynamics**

We employed pTRE-H2BGFP-K5tTa (Tet-off) mice system to study the proliferation dynamics of HFSCs in the K14-sPLA<sub>2</sub>-IIA mice background. To obtain the triple transgenic mice, we crossed pTRE-H2BGFP mice with K14-sPLA<sub>2</sub>-IIA mice and the progeny of this cross (pTRE-H2BGFP:K14-sPLA<sub>2</sub>-IIA mice) were further crossed with the K5tTa mice. However, the pups, which are positive for all the three transgenes were unable to survive after one week of birth. Therefore, we supplied the Doxycycline (0.2 mg/ml) in water to mother mice for first two days after the birth of a new litter to reduce the GFP expression in the newborn pups. This dose was sufficient to reduce the GFP expression and survival of the pups. Importantly, we could achieve the complete recovery of the GFP expression by PD21. This strategy allowed us to start the Doxy chase from the start of the first hair cycle.

### **4.4 Tissue processing for Histology and paraffin blocks**

The mice were sacrificed at different time points, backskin and tail skin tissue samples were fixed in 4% NBF for two hours at RT or at 4°C overnight. For cryosectioning, the skin tissues were directly embedded in the OCT (Tissue-Teck) compound. The NBF fixed tissues were transferred to 70% alcohol for the long-term storage. Further, these tissues were dehydrated with sequential higher-grade alcohol followed by xylene and embedded in Paraffin wax.

#### **4.4.1 Hematoxylin and eosin staining procedure**

The paraffin wax embedded tissue sections were incubated at 60°C for 15 minutes to melt the paraffin wax over tissue sections. These sections further transferred into the cleaning agent xylene for 15 minutes. The rehydration of the tissue sections was done by using sequential transfer in the lower grade alcohol such as 100% alcohol, 95%

alcohol, 70% alcohol and water for 10 minutes in each. The rehydrated tissue slides were kept in the slide chamber with Hematoxylin solution for 4-5 minutes. The staining was stopped by transferring the slides in the water and washed for 2 minutes. For long-term storage, the stained sectioned were dehydrated by a higher grade of alcohol (70% alcohol, 90% alcohol, 100% alcohol for five minutes in each). Slides were cleaned by xylene: alcohol mixture and then 100% xylene for five minutes in each. The slides were air-dried and mounted by using DPX solution. The morphology of the skin tissues and stages of the hair follicle were analyzed by using the upright microscope.

#### 4.5 Antibody details

Different primary and secondary antibodies used in this study are mentioned in the below Table 4.3 with its dilution factor in particular application and its source.

| <b>Antigen/Antibody</b> | <b>Dilution /Application</b> | <b>Source</b>               |
|-------------------------|------------------------------|-----------------------------|
| EGFR                    | 1:500 WB                     | EMD Millipore               |
| p-EGFR                  | 1:500 WB                     | Cell Signaling Technologies |
| JNK                     | 1:1000 WB                    | Cell Signaling Technologies |
| p-JNK                   | 1:1000 WB                    | Cell Signaling Technologies |
| c-Jun                   | 1:1000 WB                    | Cell Signaling Technologies |
| s-63 c-Jun              | 1:1000 WB                    | Cell Signaling Technologies |
| s-73 c-Jun              | 1:1000 WB                    | Cell Signaling Technologies |
| CD34                    | 1:100 IFA                    | BD Pharmingen               |
| $\alpha$ -6 integrin    | 1:100 IFA                    | BD Pharmingen               |
| BrdU                    | 1:100 IFA                    | Abcam                       |
| Ki67                    | 1:100 IFA                    | Abcam                       |
| Keratin 1               | 1:200 IFA, 1:500 WB          | Colin Jamora lab            |
| Keratin 10              | 1:1000 IFA                   | Abcam                       |
| Filaggrin               | 1:1000 IFA                   | Abcam                       |

|                             |                      |                             |
|-----------------------------|----------------------|-----------------------------|
| Loricrin                    | 1:1000 IFA           | Abcam                       |
| Sox9                        | 1:500 IHC            | EMD Millipore               |
| Anti-GFP                    | 1:100 IFA            | Abcam                       |
| Active B-Catenin            | 1:100 IFA            | Cell Signaling Technologies |
| Anti-Rat FITC               | 1:400 IFA            | Jackson Laboratories        |
| Anti-Rabbit FITC            | 1:400 IFA            | Jackson Laboratories        |
| Anti-Rat Alexa 568          | 1:400 IFA            | Abcam                       |
| Anti-Chicken Alexa          | 1:400 IFA            | Abcam                       |
| Biotin-labelled anti-Rabbit | 1:200 IHC            | Vector Laboratories         |
| Anti-Mouse HRP              | 1:5000 WB            | Santa Cruz Biotechnology    |
| Anti-Rabbit HRP             | 1:5000 WB            | Santa Cruz Biotechnology    |
| CD34 biotin                 | 15 µl/Reaction FACS  | eBiosciences                |
| APC Streptavidin            | 7.5 µl/Reaction FACS | BD Pharmingen               |
| α-6 integrin-PE             | 20 µl/Reaction FACS  | BD Pharmingen               |

**Table 4.3 List of the primary and secondary antibodies**

#### **4.6 Immunohistochemical staining (IHC)**

Immunohistochemical staining (IHC) was preferably performed on the paraffin-embedded tissues sections as it involves a harsh method of heat mediated antigen retrieval. The general steps of IHC procedure are given below.

- a) The slides with paraffin-embedded skin sections were kept at 60°C for 10 minutes and treated with xylene for 30 minutes for complete deparaffinization.
- b) The tissue sections were treated with the xylene alcohol (1:1 mixture) for half an hour, which was followed by treatment with 100% alcohol, 90% alcohol, 70% alcohol and water for half an hour each to rehydrate the tissue sections.
- c) The antigen unmasking was performed by using the 10mM sodium citrate buffer, pH 6.0 in the microwave for 10 minutes.

- d)** Sections were allowed to cool at RT for 45 minutes and washed with water for five minutes.
- e)** The endogenous peroxidase activity was blocked by the treatment with the solution of hydrogen peroxide-methanol (3% H<sub>2</sub>O<sub>2</sub> in Methanol) for 10 minutes at RT.
- f)** Following washes with 1X PBS, combinations of different normal serum such as Normal Goat Serum (NGS), Normal Donkey Serum (NGS) and Normal Horse serum was used for the blocking (5% in PBS) and slides were incubated for 1 hour at RT.
- g)** The primary antibody was diluted in the blocking buffer and applied on the tissue sections followed by incubation at 4°C overnight.
- h)** Next day, the sections were washed with the washing buffer (PBST 0.1% Tween20) for three times 5 minutes each.
- i)** For the Avidin-Biotin complex (ABC) formation reaction, Reagent A and Reagent B were premixed for 45 minutes and then the mixture was added on the tissue sections followed by incubation for 1 hour at RT.
- j)** The solution was removed, and sections were washed with PBST three times for 5 minutes each.
- k)** The DAB (3, 3'-diaminobenzidine) was prepared in the PBS and slides were incubated in the DAB mixture for 1 to 4 minutes.
- l)** The reaction was stopped by transferring the slides in the water container.
- m)** The tissue sections were counterstained with Hematoxylin for 1 minute and washed with distilled water for 5 minutes.
- n)** The dehydration of the tissue sections was done by higher grades of the alcohol and Xylene, and the sections were mounted with DPX.

#### **4.7 Immunofluorescence staining**

- a)** The Skin tissues were embedded in the OCT and 5  $\mu\text{m}$  to 10  $\mu\text{m}$  sections were prepared using Leica cryostat machine, which was stored at  $-80^{\circ}\text{C}$ .
- b)** During the day of staining, the slides were removed from  $-80^{\circ}\text{C}$  freezer and allowed to air dry completely.
- c)** The fixation was performed by using 4% paraformaldehyde in PBS for 20 minutes at RT or in chilled Acetone for 20 minutes at the  $-20^{\circ}\text{C}$ .
- d)** The fixative was removed and sections were bordered by using hydrophobic PAP pen.
- e)** The sections were washed with PBS for three times five minutes each.
- f)** The free sites of the PFA were blocked by using 20 mM Glycine solution for three times five minutes each.
- g)** The solution of 0.2% Triton X-100 was used for the permeabilization for 10 minutes.
- h)** Sections were washed with PBS and blocked by 2.5% NDS, 2.5% NGS, 1% BSA and 2% gelatin for one hour at RT.
- i)** Primary antibody was diluted in blocking buffer and sections were incubated with the primary antibody for overnight at  $4^{\circ}\text{C}$ .
- j)** Next day, the sections were washed with the PBS containing 0.1% Tween-20 for three times five minutes each.
- k)** Secondary antibody conjugated with the fluorochrome were diluted in the PBS (1:400) and incubated with sections for one hour at RT.
- l)** Sections were washed with the PBS containing 0.1% Tween-20 for three times five minutes each and incubated with DAPI.

- m) Excess DAPI was removed by PBS wash and mounted by using Antifade, air-dried and sealed with nail polish.
- n) The images were acquired using LSM 780 Carl Zeiss Confocal system.

#### **4.8 BrdU label retaining assay**

The newborn pups (PD3-PD5) were subcutaneously injected with the 5-bromo-2'-deoxyuridine (BrdU, Sigma-Aldrich) at the dose of 50mg/kg bodyweight for every 12 hours for three days. This dose is sufficient to label almost all the cells, as the cells of newborn mice are highly proliferative. During cell division, cells distribute the label while non-dividing cells able to retain the label for long time termed as Label-retaining cells (LRCs). Mice were sacrificed at PD68 and analyzed for LRCs in the hair follicles. For proliferation assay, short-term labeling at a dose of 100 mg/kg BrdU was used and tissues were harvested two hours post intraperitoneal injection. The BrdU in the cells was exposed by treating the tissue sections with 2N HCL for 1 hour at 37°C and detected by the anti-BrdU antibody through immunofluorescence assay [32, 85, 87, 216].

#### **4.9 Fluorescence Activated Cell Sorting (FACS)**

Flow cytometry technique enables a multi-parametric analysis of single cell based on the cell size, shape and expression of the surface molecules. The population of the interest can be separated and sorted for the further experiment such as stem cell culture and expression profiling. The brief protocol of flow cytometry analysis of the HFSCs is described below.

#### **4.9.1 Isolation of total epidermal cells**

##### **Day I:**

- a) The animals were sacrificed by CO<sub>2</sub> inhalation, hair were removed and skin was cleaned with 70% alcohol.
- b) The subcutaneous fat was removed from the dermal side by scalpel blade and the skin was washed with ice-cold PBS.
- c) The skin was placed (Dermal side down) in the 100 mm plate containing 12 ml of the ice-cold 0.25% Trypsin-EDTA solution and the plates were placed in the 4°C refrigerator overnight.

##### **Day II:**

- a) The FACS tubes were coated with 50% chelated FBS for minimum three hours and then washed with ice-cold PBS and kept at 4°C.
- b) Fresh 12 ml of the 0.25% ice-cold Trypsin-EDTA solution was added in all the plates containing skin and incubated at 37°C for 30 minutes.
- c) The trypsin action was inhibited by addition of the 12 ml of ice-cold E-Media containing 15% chelated FBS.
- d) The epidermal side was scraped multiple times by scalpel blade to release the cell clumps in the solution.
- e) The solution was passed through pipette multiple times to make single cell suspension that was further strained using 70 µm and then 40 µm strainers.
- f) The filtered solution was centrifuged at 1000 rpm for five minutes at 4C.
- g) The cell pellet was washed by using ice-cold PBS and centrifuged.
- h) The cell pellet was dissolved in 750 µl of 5% chelated FBS (FACS buffer) and stained with the antibodies as described below.

- i) The cells were directly sorted in the E-media for colony forming efficiency or in the RNA lysis buffer for RNA extraction.

#### 4.9.2 Staining procedure for hair follicle stem cells

| Tube No. | Tubes details | Step-1                        | Step-2  | Step-3   | Step-4   | Step-5   |
|----------|---------------|-------------------------------|---|--|--|--|
| 1        | Only cells    | ---                           | <b>a) Mix well by gentle tapping and incubate at 4<sup>0</sup>C for 30 minutes. Do not allow cells to form pellet during incubation</b><br><br><b>b) Add double volume of ice cold PBS in the tube no 6 and 7 wash by inverting the tubes.</b><br><br><b>c) Centrifuge tube no 6 and 7 at 1000 rpm for 5 minutes at 4<sup>0</sup>C.</b><br><br><b>d) Discard the supernatant and add 100 µl FACS buffer in tube no 6 and 750 µl in tube no 7.</b> | ---  | <b>a) Mix well and incubate at 4<sup>0</sup>C for 30 minutes. Keep tapping in between.</b><br><br><b>b) Add 200 µl PBS in control tubes and 1.5 ml in test tubes. Mix by inverting the tubes.</b><br><br><b>c) Centrifuge at 1000 rpm for 5 minutes at 4<sup>0</sup>C.</b> | ---  |
| 2        | PI control    | ---                           |   | ---  |  | Add 100 µl of 2X PI, keep the tube on ice                        |
| 3        | PE Isocontrol | ---                           |   | 1.3 µl PE Iso-type control antibody            |  | Resuspend pellet in 100 µl of FACS buffer, keep the tubes on ice |
| 4        | α6 PE         | ---                           |   | 2.6 µl of α6-PE Antibody                       |  |  |
| 5        | APC control   | ---                           |   | 1 µl Streptavidin-APC Antibody                 |  | Resuspend pellet in 1X PI, keep the tubes on ice                 |
| 6        | CD34 +APC     | 2 µl of CD34 Biotin Antibody  |   | 1 µl Streptavidin-APC Antibody                 |  |  |
| 7        | Test          | 15 µl of CD34 Biotin Antibody |   | 7.5 µl Streptavidin-APC + 20 µl α6 PE Antibody |  |  |

**Table 4.4 Staining procedure of the HFSCs for flow cytometry**

#### 4.10 Colony forming efficiency of the hair follicle stem cells

The gamma irradiated (30 Gys) J2-3T3 fibroblasts were used as feeder cells for the culture of the HFSCs. The FACS-purified HFSCs (10-20K) were plated in the six-well plate containing irradiated fibroblasts and conditioned E-media. The E-media contained 15% chelated FBS and supplemented with 10 ng/ml EGF and 0.3 mM  $\text{Ca}^{+2}$ . The HFSCs were allowed to form an independent colony for three weeks with a regular supply of irradiated J2-3T3 fibroblasts. Colonies were fixed by using 1% PFA for 15 minutes and stained by 0.05% crystal violet. Total no of colonies were counted in each well and plotted with respect to the control [217].

#### 4.11 Primary keratinocytes culture

##### A. Solutions Preparation:

##### a) 5 mg/ml Insulin (minimum M.W. = 6000g, approx. $8.3 \times 10^{-4}$ M)

- Weigh out 250 mg of Insulin (Sigma I-5500)
- Add to 50 ml of 0.1N HCl and dissolve it completely
- Store in 10 ml aliquots in 15 ml tubes at 4<sup>0</sup>C in a refrigerator

##### b) 5 mg/ml Transferrin

- Weigh out 250 mg of Transferrin (Sigma T-2252)
- Add to 50 ml of sterile PBS and store frozen in 10ml aliquots

##### c) $2 \times 10^{-8}$ M T<sub>3</sub> (3,3',5-Triiodo-L-Thyronine)

- Weigh out 13.6 mg of T<sub>3</sub> (Sigma T-2752)
- Dissolve in 100 ml of 0.02N NaOH =  $2 \times 10^{-4}$  M T<sub>3</sub> (Freeze)
- Take 0.1 ml of  $2 \times 10^{-4}$  M T<sub>3</sub> and dissolve in 9.9 ml of sterile PBS =  $2 \times 10^{-6}$  M T<sub>3</sub>
- Take 0.1 ml of  $2 \times 10^{-6}$  M T<sub>3</sub> and dissolve in 9.9 ml of sterile PBS =  $2 \times 10^{-8}$  M T<sub>3</sub>

**d) 100x Cocktail**

|   |               |
|---|---------------|
| 5mg/ml Insulin  | 20 ml         |
| 5mg/ml Transferrin  | 20 ml         |
| 2 x 10 <sup>-8</sup> M T <sub>3</sub> (Tri-iodothyronine) | 20 ml         |
| <u>140ml 1xPBS (sterile)</u>                              | <u>140 ml</u> |
| <b>TOTAL</b>  | <b>200 ml</b> |

Sterilize the mixed solution and store in aliquots.

**e) Hydrocortisone**

- Calbiochem: Cat. # 386698
- Prepare stock solution 4mg/ml in 95% EtOH
- Filter-sterilize and aliquot 1ml each into a sterile 15ml Falcon tube
- Store at -20<sup>0</sup>C

**f) Cholera toxin**

- MP Biochemicals Cat. # 150005
- To prepare 10<sup>-6</sup> M stock solution: Dissolve 1mg vial of CT in 11.9 ml of glass distilled water
- Filter and make aliquot of 1 ml and store at 4<sup>0</sup>C.

**B. Media preparation**

Take 40 gms of dry Chelex X-100 resin for 100 ml FBS in a glass beaker and add 400 ml of glass-distilled H<sub>2</sub>O. Calibrate the pH meter and measure the pH continually till it become stable for at least 20 minutes. Adjust the pH to 7.5 by adding the 1N HCL multiple times, as pH fluctuates for several hours. Once the pH is stable, allow Chelex to form a compact pellet. Remove the water and repeat the procedure one more time on next day. On the third day, add serum in the beaker containing Chelex pellet and stir at low speed for one

hour at 4<sup>0</sup>C. Allow the Chelex to settle overnight and separate the FBS in a clean glass bottle next day.

Take DMEM: F12 (3:1) calcium free powder and add it in the glass beaker containing 850 ml MilliQ. Add 3.07g sodium bicarbonate and 0.475 gm/L glutamine for 1L media. Stir for 20 minutes and adjust pH to 7.2 using 1N HCl. Adjust the volume to 1L with dH<sub>2</sub>O. The compressed CO<sub>2</sub> was applied to the media for 2.5 min for 1L media. The media should have an amber colour. Take 150 ml of chelated FBS and add a cocktail and other growth factors as described previously [218]. Add 850 ml media with antibiotics and adjust final concentration of Ca<sup>+2</sup> to 0.05 mM. Filters sterilize and check for contamination test.

### **C. Preparation of the signal cell suspension and cell culture**

1. Bring the new-born mice (PD1-2) to culture hood in sterile pertiplate and sacrifice them by the decapitation.
2. Remove the skin by using sterile instruments and place the skin with dermal side up on the clean paper.
3. Gently scrape the dermal side by using a sterile scalpel blade to remove dermal fat tissues and blood vessels.
4. Transfer the skin to 70% ethanol for 1 min and immediately transfer into sterile PBS, wash the skin for two times with a sterile PBS.
5. Place the skin on the dermal side down into 35 mm plate containing 1 ml of 5 unit/ml dispase solution (Stem cell technologies).
6. Incubate it overnight at 4<sup>0</sup>C.
7. Next day, take 60 mm plate and add 4 ml of freshly prepared 0.1% Trypsin/EDTA solution.

8. Takeout the 35 mm dish from the refrigerator and bring it to the hood.
9. Carefully, separate the epidermis from the dermis by holding the skin with one forceps at one end and peeled off the epidermis by using another forcep.
10. Transfer the separated epidermis into 60 mm plate containing 0.1% Trypsin EDTA solution and mince it in small pieces by using sterile scissors.
11. Incubate at the 60 mm plate at 37<sup>0</sup>C for 5-10 mins.
12. Gently mix the trypsin solution containing cells by using a 1ml pipette for 5-6 times.
13. Add 6 ml of cold E-media into 60 mm plates and mix it with 10 ml pipette.
14. Strain the solution by using 100-micron strainer into 50 ml tubes.
15. Transfer the content in the 15 ml tube and spin at 1000 rpm for five mins.
16. Discard the supernatant and carefully resuspend the pellet in sterile PBS.
17. Spindown the cells and resuspend the pellet in 1 ml of E-media.
18. Carefully, add the cell suspension into 60 mm plate containing conditioned E-media with J2-3T3 fibroblast (prepare it one day before).
19. Allow the cells to attach and grow for two days without any disturbance.
20. Add fresh irradiated J2-3T3 fibroblast once in a week during media change.
21. First three passages are critical and care must be taken to avoid contamination and confluency induced differentiation of the primary keratinocytes.
22. Once it reaches to 70 to 80 % confluency, remove the fibroblast by differential trypsinization and add the grown keratinocytes into new 60 mm plates with already attached J2-3T3 fibroblast without any dilution.
23. The keratinocytes start growing without J2-3T3 fibroblast after passage 6 or 7 with dilution ratio 1:2 to 1:3.

#### **4.12 BrdU cell proliferation assay**

For cell proliferation assay *in vivo*, the adult mice were injected intraperitoneally with 100mg/ kg BrdU before two hours of sacrifice. The mice were sacrificed, skin was embedded in OCT and BrdU was detected by the Immunofluorescence assay. For *in-vitro* keratinocytes proliferation assay, the primary keratinocytes were serum starved for 24 hours and then BrdU was added in the complete E-media at a final concentration of 10  $\mu$ M for different time points. The cells were fixed by 4% paraformaldehyde and BrdU was exposed by 2N HCl treatment for one hour. The BrdU positive cells were labeled by anti-BrdU antibody and detected by immunofluorescence assay. The total 1000 cells were counted and plotted as % of BrdU positive cells with respective control.

#### **4.13 Western blotting**

The equal amounts of proteins were run on the Tris-Glycine SDS-PAGE gels and proteins were transferred on the nitrocellulose membrane by wet transfer procedure using Bio-Rad apparatus.

##### **4.13.1 Protein isolation from keratinocytes and skin**

The primary keratinocytes were allowed to grow till 70% confluency in 60 mm Petri plates and then subjected to serum starvation for 24 hours. Following this, the cells were stimulated with 10 ng/ml EGF for different time points and washed with ice-cold PBS. 100  $\mu$ l of ice-cold RIPA buffer (Sigma) with 1x protease phosphatase inhibitor cocktail (cell signaling technologies) was added in the plate. The cells were scraped using cell scraper and lysate was collected in the 1.5 ml tube. The tubes were kept on ice for 30 minutes with vortexing for 5 seconds at every 10 minutes. The whole cell lysate was centrifuged at maximum speed for 45 minutes at 4<sup>0</sup>C. The

supernatant was collected in the fresh tubes and stored at  $-80^{\circ}\text{C}$ . To isolate protein from the epidermis, the skin was kept in phosphate buffer containing 0.5 M ammonium thiocyanate, pH 6.8 for 20 min on ice. The epidermis was scraped in lysis buffer (1% NP-40, 0.5% deoxycholate and 0.2% SDS, 150 mM NaCl, 2 mM EDTA, 0.8 mM EGTA, 10 mM Tris-HCl, pH 7.4 with protease phosphatase inhibitor cocktail [217]). The protein lysate was prepared as described above.

#### **4.13.2 Protein estimation by modified Lowry's method**

Total protein from whole cell lysate was measured by Lowry method [219].

- a) The protein standard was prepared by using 1 ml of 5 to 25  $\mu\text{g}/\text{ml}$  of Bovine serum albumin (BSA).
- b) Four  $\mu\text{l}$  of cell extract was added in test tubes containing 996  $\mu\text{l}$  of MilliQ in triplicate.
- c) 1 ml of Copper Tartarate Carbonate (CTC) solution was added to each test tube followed by vortex for 5 sec and incubated at RT for 10 minutes.
- d) The FC reagent was diluted at 1:5 ratio and 500  $\mu\text{l}$  of diluted FC reagent was added to each tube.
- e) The combined solution was mixed and incubated at RT for 30 minutes in the dark.
- f) The absorbance was measured at 750 nm using a spectrophotometer.
- g) The protein concentration was calculated based on the standard curve.

#### 4.14 RNA extraction and Quantification

Total epidermal cells were isolated from the skin as described in the flow cytometry section. The cell pellet was dissolved in the 1 ml TRI Reagent (Sigma). The cell extract was freeze-thaw for one cycle and kept on ice for further processing. The total RNA was isolated by using isopropanol method. The RNA was washed with 70% ethanol and centrifuged at 14000 rpm for 10 minutes. Tubes were air-dried and RNA was dissolved in the nuclease-free water. The amount and quality of RNA were analysed by using the NanoDrop Spectrophotometer (Thermo Scientific, USA).

#### 4.15 Real time PCR

The cDNA was prepared as per manufacturer's protocol (Thermo Scientific, USA) by using superscript IV reverse transcriptase. Total 4 µg of total RNA was reverse transcribed and diluted to 10 ng/µl for the use in real time PCR reactions. The real time PCR was performed by using Power SYBR mastermix (Applied Biosystems, UK). The expression level of the genes was normalized to the expression of GAPDH or β-actin. The fold change was calculated by  $2^{-\Delta\Delta Ct}$  method. The sequences of the primers used are given in the below Table 4.5

| Gene    | Forward Primer 5'--->3' | Reverse Primer 5'--->3' |
|---------|-------------------------|-------------------------|
| Sox21   | CCTGGGCAGCGTGGCGGA      | CAGACTGCGGGAAGAAGACG    |
| Msx2    | AACACAAGACCAACCGGAAG    | CGCTCTGCTATGGACAGGTA    |
| Krt82   | TCTATGGGGCTGAAGACCAG    | GGTGGCTTTGAAGAAATGA     |
| Krt71   | TCAGATCCAGTCCCACATCA    | GTACAGGGCCTCAGCTTCAG    |
| Zdhhc13 | GACTGGACGCTGCATAGGTT    | TGGCACAATGATTTGACCAG    |
| Gata3   | TTATCAAGCCCAAGCGAAG     | TGGTGGTGGTCTGACAGTTC    |
| Shh     | ACCCCGACATCATATTTAAGGA  | TTAACTTGTCTTTGCACCTCTGA |
| Foxn1   | TGACGGAGCACTTCCCTTAC    | GACAGGTTATGGCGAACAGAA   |
| S100a9  | CACCCTGAGCAAGAAGGAAT    | TGTCATTTATGAGGGCTTCATTT |
| Lef1    | GCCACCGATGAGATGATCCC    | TTGATGTTCGGCTAAGTCGCC   |
| BMP4    | GCCCTGCAGTCCTTCGCTGG    | CTGACGTGCTGGCCCTGGTG    |

**Table 4.5 Real time PCR primer sequences**

#### **4.16 Hair depilation study on the dorsal skin**

The wild type and K14-sPLA<sub>2</sub>-IIA mice were anaesthetized via isoflurane inhalation at PD45. The hot wax was applied on the shaved region of the dorsal skin and pressed with the hair removing strips. The strips were detached from skin in the tail to head direction. These steps were repeated for two to three times to depilate the half area of the dorsal side completely. The depilated skin was gently wiped with the moderately warm water, and mice were housed communally in the regular cage.

#### **4.17 Topical application of JNK inhibitor on the mice skin**

For JNK inhibition study, the JNK inhibitor was dissolved in Acetone and applied on the shaved region for two days (0.8 mg/mouse/day) followed by depilation at PD45. The JNK inhibitor was applied on the depilated area for next ten days. The post depilation hair growth was captured by the photograph on every alternate day.

#### **4.18 Statistical analysis**

The data was analyzed by using two-tailed Student's t-test, one-way ANOVA, two-way ANOVA test. The statistical analyses were calculated by GraphPad Prism software. A p-value less than 0.05 were considered to be statistically significant. Error bars indicate the mean  $\pm$  SD of the mean. P values: \*, P < 0.05; \*\*, P < 0.005; \*\*\*, P < 0.0005.



## ***5. Objective-I***

***To decipher the role of group IIA secretory  
phospholipase A2/ enhancing factor in  
epidermal stem cell regulation***



## 5.1 Introduction

The phospholipase enzyme hydrolyzes phospholipids that generate free fatty acid along with lipophilic compounds. The phospholipase family mainly classified into four different classes such as Phospholipase A to Phospholipase D. The detailed description of the Phospholipase A<sub>2</sub> is given below.

### 5.1.1 Secretory phospholipases

Phospholipase A<sub>2</sub> (PLA<sub>2</sub>) superfamily can be divided into four different types, namely secreted (sPLA<sub>2</sub>), cytosolic (cPLA<sub>2</sub>), calcium-independent (iPLA<sub>2</sub>), and platelet activating factor (PAF) acetyl hydrolase or oxidized lipid lipoprotein-associated (Lp-PLA<sub>2</sub>) [220]. The entire family comprises of 15 different groups, which are classified based on their localization, genomic similarities, substrate specificity and enzymatic efficiency.

| Class                        | Group                     | Molecular weight (kDa) | Common name                 |
|------------------------------|---------------------------|------------------------|-----------------------------|
| <b>Histidine active site</b> |                           |                        |                             |
| sPLA <sub>2</sub>            | I (A–B)                   | 13–15                  | N/A                         |
|                              | II (A–F)                  | 13–17                  | N/A                         |
|                              | III                       | 15–18                  | N/A                         |
|                              | V                         | 14                     | N/A                         |
|                              | X                         | 14                     | N/A                         |
|                              | XI (A–B)                  | 12–13                  | N/A                         |
|                              | XII                       | 18–19                  | N/A                         |
|                              | XIII                      | <10 <sup>d</sup>       | N/A                         |
|                              | XIV                       | 13–19                  | N/A                         |
|                              | <b>Serine active site</b> |                        |                             |
| cPLA <sub>2</sub>            | IVA                       | 85                     | cPLA <sub>2</sub> α         |
|                              | IVB                       | 114                    | cPLA <sub>2</sub> β         |
|                              | IVC                       | 61                     | cPLA <sub>2</sub> γ         |
| iPLA <sub>2</sub>            | VIA-1                     | 84–85                  | iPLA <sub>2</sub> β (short) |
|                              | VIA-2                     | 88–90                  | iPLA <sub>2</sub> β (long)  |
|                              | VIB                       | 63–88                  | iPLA <sub>2</sub> γ         |
| PAF-AH                       | VII (A–B)                 | 40–45                  | PAF-AH (II)                 |
|                              | VIII (A–B)                | 26                     | PAF-AH (IB)                 |

**Table 5.1 Classification of the phospholipases**

(Adapted from Cummings et al., 2007, *Biochemical pharmacology*) [221]

Phospholipase A<sub>2</sub> (PLA<sub>2</sub>) specifically hydrolyzes the sn-2 position of the glycerophospholipids to yield fatty acids and lysophospholipids. The mammalian genome encodes more than 30 sPLA<sub>2</sub> or related enzymes, which are classified on the basis of their architecture and functions into major 11 sPLA<sub>2</sub> isozymes (IB, IIA, IIC, IID, IIE, IIF, III, V, X, XIIA and XIIB) [220, 222-224]. Importantly, isoforms of the group I/II/V/X are low molecular weight (14–19 kDa) secreted proteins, which are highly similar and possess conserved calcium-binding loop and a catalytic site. In the presence of mM calcium (Ca<sup>+2</sup>) concentrations, sPLA<sub>2</sub> enzyme hydrolyzes ester bond at the sn-2 position of glycerophospholipids [220, 222]. The highly conserved disulfide bonds provide exceptional stability to the structure of these isoforms.

### **5.1.2 Secretory Phospholipase A<sub>2</sub> Group IIA**

Secretory phospholipase A<sub>2</sub> Group-IIA (sPLA<sub>2</sub>-IIA) is the most widely studied isoform of the secretory phospholipase A<sub>2</sub>. This enzyme cleaves the sn-2 position bond of glycerophospholipids and hydrolyzes to liberate lysophosphatidylcholine and free fatty acids. In mouse, sPLA<sub>2</sub>-IIA is also known as enhancing factor (EF), which is a homologue of human secretory Group II phospholipase A<sub>2</sub> and acts as a growth factor modulator [225-228]. It has two independent activities, which includes catalytic activity and enhancing activity [229]. The radio-receptor assay showed that the mouse sPLA<sub>2</sub>-IIA promotes binding of the epidermal growth factor (EGF), thereby promotes cell growth and exhibit enhancing activity [226]. Importantly, the mouse sPLA<sub>2</sub>-IIA was initially isolated from the mouse small intestine and termed as enhancing factor (EF) [225, 230]. However, it has been shown that the sPLA<sub>2</sub>-IIA also expresses paneth cells of the small intestine and newborn mouse hair follicle, and in both the tissues, it is located near the niche of the stem cells [231-233]. The C57BL/6 and 129SV mouse strains have a natural disruption of the *Pla2g2a* gene due to a frame-

shift mutation in the exon 3. These sPLA<sub>2</sub>-IIA deficient mice are more susceptible to polyps formation and development of the colorectal carcinoma [234]. Different inflammatory stimulus increases sPLA<sub>2</sub>-IIA expression during various pathophysiological conditions such as rheumatoid arthritis, Crohn's disease and acute pancreatitis [223, 224]. Besides, sPLA<sub>2</sub>-IIA has been shown to enhance cell proliferation in different cell types. sPLA<sub>2</sub>-IIA promotes astrocytoma and microglial cells proliferation through EGFR signaling dependent mechanisms [235, 236]. In addition, deregulated expression of the sPLA<sub>2</sub>-IIA has been observed in the prostate, oesophageal, lung and colon cancer [237]. Recently, sPLA<sub>2</sub>-IIA has been shown to regulate stemness of the lung cancer stem cells and promotes cancer growth, while knockdown of the sPLA<sub>2</sub>-IIA reduces the sphere-forming ability of the cancer stem cells [238, 239]. However, the mechanism through sPLA<sub>2</sub>-IIA alters stem cells behaviors during tissue homeostasis and cancer remains elusive.

### **5.1.3 Secretory phospholipases in the regulation of skin homeostasis**

The classical role of sPLA<sub>2</sub> isoform in the skin was reported to maintain the permeability barrier mediated homeostatic function of the epidermis. sPLA<sub>2</sub> requires for maintaining acidic condition in the stratum corneum (SC), which is a critical step for the barrier functions of the epidermis [240]. Various isoforms of the sPLA<sub>2</sub> express differentially in different layer of the mouse and human epidermis as shown in the Table 5.2.

Grass et al., in 1996 reported the first study for the sPLA<sub>2</sub> functions in the skin, where they have overexpressed human group II PLA<sub>2</sub>. These transgenic mice displayed epidermal hyperplasia and hyperkeratosis [241]. Further, overexpression of the mouse sPLA<sub>2</sub>-IIA under keratin 14 promoter showed epidermal hyperplasia and increased

susceptibility to develop tumours when subjected to the chemical carcinogenesis process [210].

| sPLA <sub>2</sub> expression in skin (M = mouse; H = human). |  |  |
|--|--|--|
| Subtype  | Epidermal Localization   | Citation   |
| IB   | Suprabasal keratinocytes (M) SG – SC junction (H)  | Gurrieri 2003<br>Ma:ereeuw-Hautier<br>DOW<br>Haas 2005 |
| IIA  | Throughout epidermis (M) Upper SC (H)  | Gurrieri 2003<br>Haas 2005                             |
| IIC  | Throughout epidermis   | Gurrieri 2003  |
| IID  | Throughout epidermis (M)<br>Perinuclear localization basal keratinocytes (H)                         | Gurrieri 2003<br>Haas 2005                             |
| IIE  | Suprabasal keratinocytes (M)   | Gurrieri 2003<br>Sato 2009<br>Haas 2005                |
| IIF  | Suprabasal keratinocytes (M, H)  | Sato 2009<br>Gurrieri 2003                             |
| III  | Keratinocytes (M)<br>Basal keratinocytes (H)<br>Hyperproliferative epidermis (H)                     | Sato 2009<br>Haas 2004<br>Rys-Sihora 2003              |
| V  | Suprabasal keratinocytes (M)<br>Basal and spinous keratinocytes (H)                                  | Gurrieri 2003<br>Haas 2004<br>Gurrieri 2003            |
| X  | Basal and suprabasal keratinocytes (M)<br>Suprabasal layers (H)<br>Present only in hair follides (M) | Schadolo 2001<br>Haas 2005<br>Yamamoto 2010            |
| XII  | Suprabasal keratinocytes (M)   | Gurrieri 2003  |

**Table 5.2 Expression of sPLA<sub>2</sub> isoforms in the mouse and human epidermis**

*(Adapted from Dusko Ilic et al., 2014, Biochim Biophys Acta) [242]*

In addition, our previous study elucidated the effect of sPLA<sub>2</sub>-IIA overexpression and showed that the sPLA<sub>2</sub>-IIA promotes HFSCs proliferation and induces differentiation [211]. Also, other study reported that deletion of the sPLA<sub>2</sub>-IIF inhibits keratinocytes activation and differentiation during psoriasis and skin cancer [243]. Mice overexpressing *PLA2G10* exhibits distorted hair follicle, abnormal hair development and alopecia. Conversely, deletion of the *PLA2G10* showed reduced cell proliferation in the ORS of the hair follicle and downregulation of hair genes expression [244]. A

further study reported that the group IIE sPLA<sub>2</sub> preferentially expresses in the hair follicles and deletion of the sPLA<sub>2</sub>-IIE showed altered ultrastructure of the hair follicle and distinct phenotype than sPLA<sub>2</sub>-IIF knockout mice [245]. Overall, these studies demonstrated differential functions of various isoforms in the regulation of epidermal homeostasis. However, the mechanisms through sPLA<sub>2</sub> induce differentiation and deplete HFSCs is largely remains unexplored.

## 5.2 Results

### 5.2.1 Establishment of long-term keratinocytes culture

We established the long-term keratinocytes culture for evaluating the effect of the sPLA<sub>2</sub>-IIA in vitro. Mouse epidermal keratinocytes were isolated from the newborn mice and co-cultured with mitotically inactive feeder cells (J2-3T3) in E-media (calcium concentration 0.05 mM) till passage eight. After eight passages, keratinocytes were cultured without feeder cells.

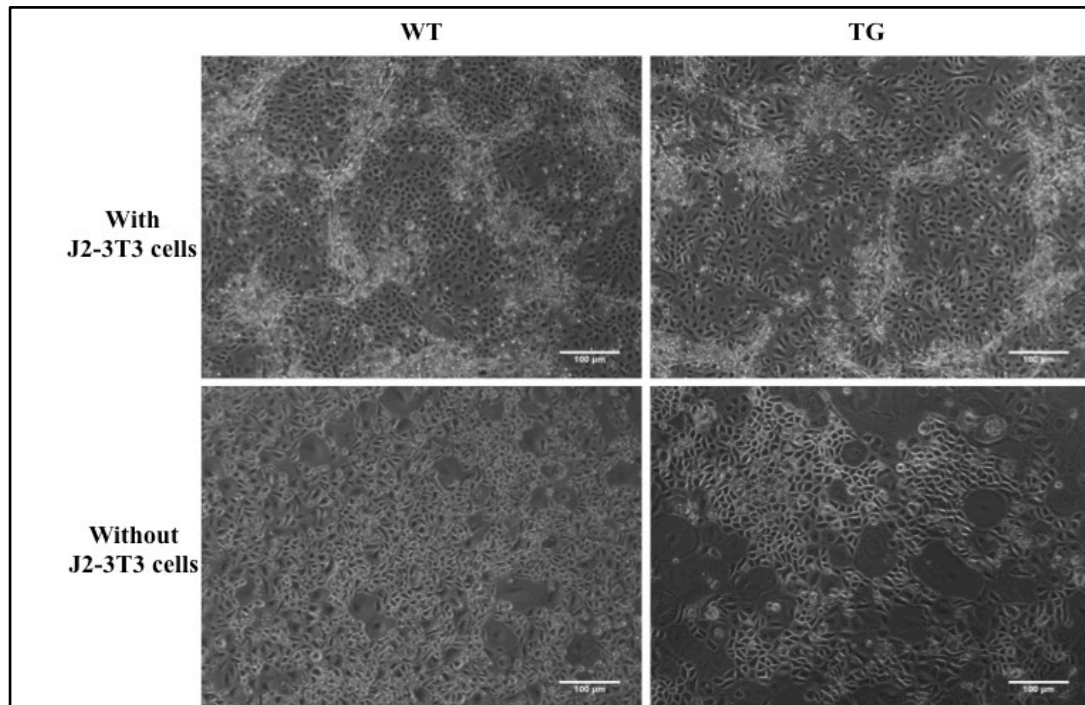


**Figure 5.1 Primary epidermal keratinocytes culture**

*Keratinocytes were co-cultured with feeder cells and feeder independent culture was established after passage 7. WT- Wild type, TG- K14-sPLA<sub>2</sub>-IIA mice. n=5 mice/genotype. Scale bar: 100 μm.*

Five independent keratinocyte lines of each genotype were established to study the effect of sPLA<sub>2</sub>-IIA overexpression on epidermal keratinocytes proliferation and differentiation (Figure 5.1).

### 5.2.2 Overexpression of sPLA<sub>2</sub>-IIA reduces colony forming efficiency of primary keratinocytes

The previous study from our laboratory demonstrated that the overexpression of the sPLA<sub>2</sub>-IIA in mice epidermis under Keratin 14 promoter leads to a loss of stem cells quiescence and stemness characteristics. To determine the efficiency of the sPLA<sub>2</sub>-IIA overexpressing keratinocytes to form an independent colony in vitro, equal number of WT and K14-sPLA<sub>2</sub>-IIA mice keratinocytes (P2) were plated in the six-well plate (5000 cells per well) and cultured for seven days in the presence of J2-3T3 fibroblast. The feeder cells were removed by differential trypsinization, colonies were stained by crystal violet, and total numbers of colonies were manually counted under an inverted microscope.

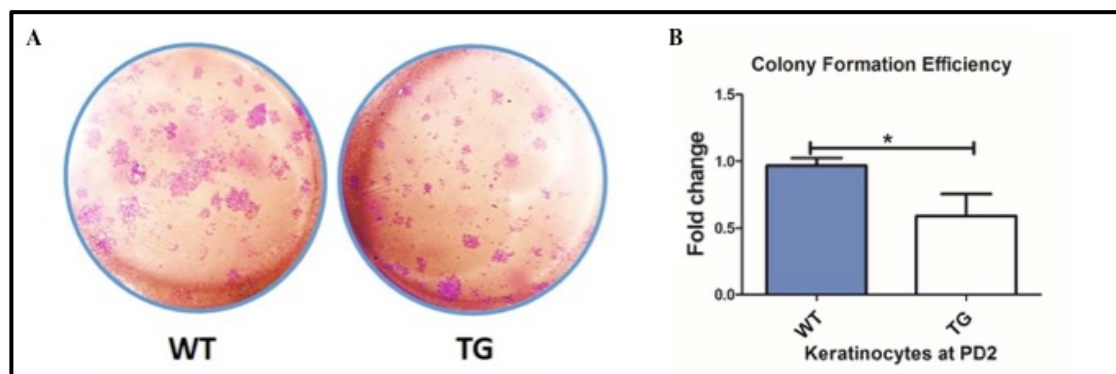


**Figure 5.2 Colony forming efficiency of primary keratinocytes**

*A) Crystal violet staining of the keratinocytes colonies B) Total numbers of colonies was counted in WT and TG mice and plotted the comparative fold change. (WT-Wild type, TG - K14-sPLA<sub>2</sub>-IIA mice, n=3 mice/genotype, \* - P ≤ 0.05)*

The result showed reduced numbers of total colonies of K14-sPLA<sub>2</sub>-IIA mice keratinocytes as compared to WT keratinocytes (Figure 5.2), suggesting that the overexpression of sPLA<sub>2</sub>-IIA in mice keratinocytes affects its ability to produce an independent colony in culture.

### 5.2.3 Overexpression of sPLA<sub>2</sub>-IIA alters proliferation dynamics of HFSCs

The HFSCs within the bulge exhibit different quiescent potential and therefore divide infrequently during hair follicle cycling. Also, we observed depletion of HFSCs pool in the K14-sPLA<sub>2</sub>-IIA mice and reduced colony forming ability of primary keratinocytes in vitro. These observations led us to examine further, whether sPLA<sub>2</sub>-IIA induced proliferation affects the characteristic of infrequent stem cell division and whether sPLA<sub>2</sub>-IIA targets the stem cells having low quiescence potential for the rapid proliferation? If so, the remaining stem cells population should possess high quiescent potential. To address this, we employed triple transgenic (H2BGFP-K5tTa-K14-sPLA<sub>2</sub>-IIA) (Tet-off) mice to understand the proliferation dynamics of HFSCs in the K14-sPLA<sub>2</sub>-IIA mice. However, as we observed the postnatal lethality of the triple transgenic mice, the GFP expression in the newborn pups was partially inhibited by supplying Doxycycline (0.2 mg/ml) in water as described in the Material and Method section. Therefore, we first confirmed the labeling efficiency of HFSCs by GFP at PD21, which is a time point from where we started the Doxycycline chase for the proliferation dynamics study. Our results showed an equal intensity of the GFP in the HFSCs of the WT and K14-sPLA<sub>2</sub>-IIA mice, which was similar to the intensity of the standard H2BGFP mice (Figure 5.3 A-C). To quantify the rate of cell proliferation during the anagen phase, we chased the mice from PD21 to PD28 (Telogen to Anagen). Our results suggest an additional division of the HFSCs in K14-sPLA<sub>2</sub>-IIA transgenic mice (Figure 5.3 D). Further, we sought to understand whether the sPLA<sub>2</sub>-IIA induced rapid proliferation is restricted to anagen phase and whether activation of repressive signaling after completion of anagen is sufficient to suppress sPLA<sub>2</sub>-IIA induced HFSCs proliferation? The triple transgenic mice were chased from PD36 to PD49 (Catagen and Telogen) and our results indicate an active proliferation of

HFSCs, even during these phases (Figure 5.3 E), suggesting that the repressive signaling during telogen phase of the hair follicle is not sufficient to inhibit sPLA<sub>2</sub>-IIA induced HFSCs proliferation. Importantly, the difference in the cell proliferation was more pronounced when we chase the mice from PD35-PD49 as compared to the Chase period of PD21-PD28.

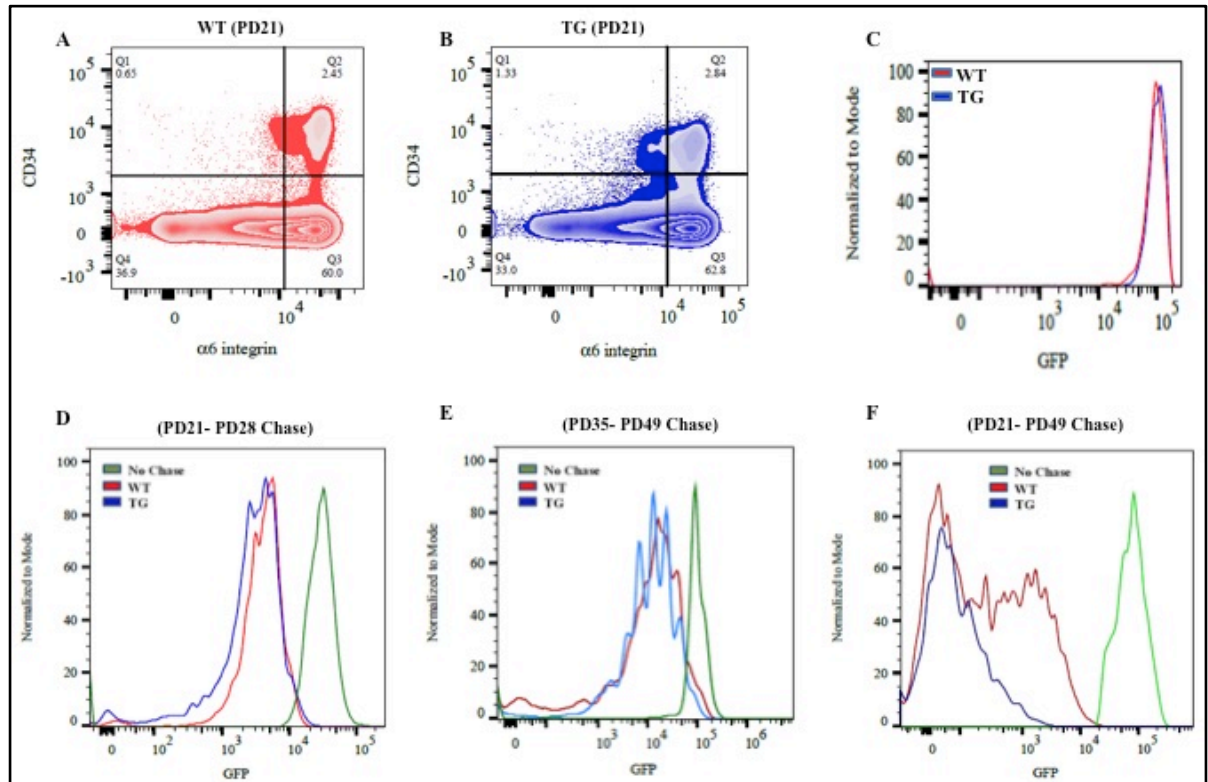


**Figure 5.3 Proliferation dynamics of HFSCs during various stages of hair cycle**

*A) And B) Separation of the HFSCs population from WT and TG mice skin by using CD34 and  $\alpha 6$  integrin markers C) Intensity of GFP signal in the HFSCs of WT and TG mice at PD21. D) The WT (H2BGFP-K5tTa, Double transgenic) and TG (K14-sPLA<sub>2</sub>-IIA-H2BGFP-K5tTa, Triple transgenic) mice were Doxycycline chased (1 g/Kg) from PD21 to PD28 and analyzed for the GFP dilution in the HFSCs. E) Doxycycline chase from PD35 to PD49 and F) Doxycycline chase from PD21 to PD49 (WT-Wild type for sPLA<sub>2</sub>-IIA and H2BGFP: K5tTa positive, TG- K14-sPLA<sub>2</sub>-IIA: H2BGFP: K5tTa positive mice, n=3 mice/genotype).*

Further, to check the maintainance of the GFP bright HFSCs after completion of the first hair cycle, the triple transgenic mice were chased with Doxycycline (1 gm/kg) from PD21 to PD49, which showed a loss of bright peaks of GFP positive bulge cells (Peak 1 to 5) (Figure 5.3 F), suggesting that the proliferation induced by the sPLA<sub>2</sub>-IIA affect all the bulge cells having different quiescence potentials. Together, these data indicate that the sPLA<sub>2</sub>-IIA induces HFSCs proliferation irrespective of their quiescence potential and alters an infrequent divisional characteristic of hair follicle stem cells.

#### **5.2.4 sPLA<sub>2</sub>-IIA alters EGFR mediates JNK c-Jun signaling**

Further, we sought to delineate the signaling mechanisms through sPLA<sub>2</sub>-IIA alters stem cells proliferation and differentiation. sPLA<sub>2</sub>-IIA is known to induce proliferation of different cell types through EGFR dependent mechanism. Moreover, it has been shown that the sPLA<sub>2</sub>-IIA enhances the binding of EGF molecules. However, the downstream signaling mechanism through sPLA<sub>2</sub>-IIA induces stem cells proliferation remains unexplored. The WT and K14-sPLA<sub>2</sub>-IIA mice keratinocytes were serum starved for 24 hours and stimulated with 10 ng/ml EGF for 15 min followed by lysis in the RIPA buffer. Activation of EGFR, JNK1/2 and c-Jun were analysed by western blotting. The results showed an increased activation of EGFR, JNK1/2 and c-Jun in K14-sPLA<sub>2</sub>-IIA mice keratinocytes as compared to wild-type control (Figure 5.4 A-C). Importantly, we did not observe significant alterations in the activation of the other downstream components such as ERK and P38 proteins. To further clarify, the JNK inhibition study was performed to confirm that the c-Jun activation is indeed mediated through JNK signaling. Inhibition of JNK before EGFR activation showed reduced c-Jun phosphorylation (Figure 5.4 B), suggesting that the EGFR mediated JNK activation is responsible for the enhanced c-Jun activation.

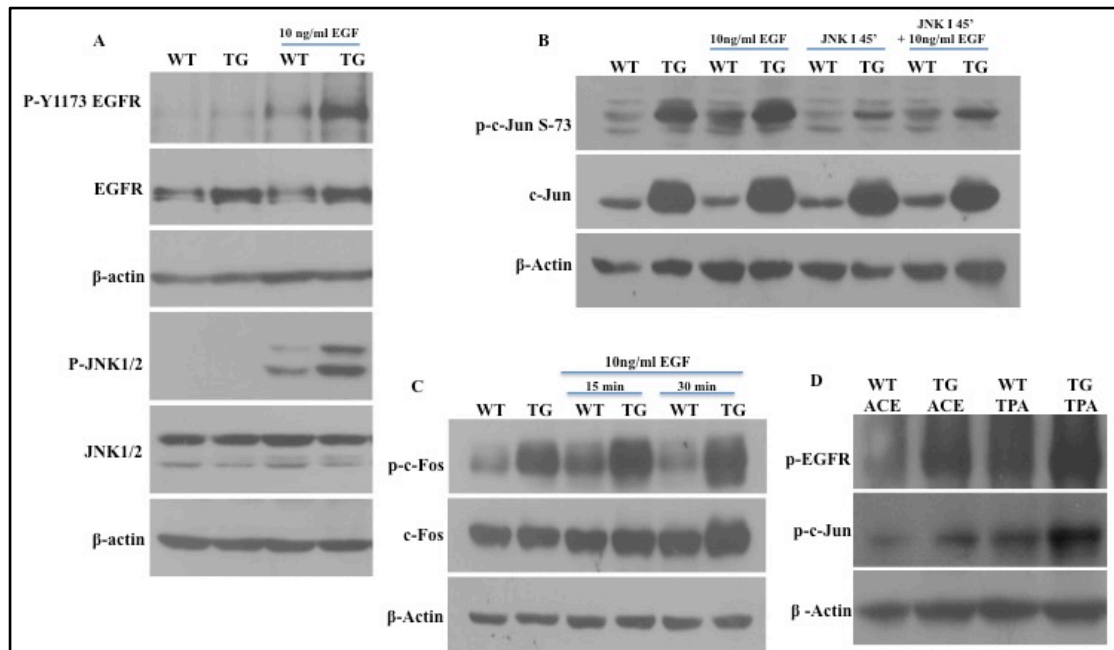


**Figure 5.4 Western blotting analysis of EGFR-JNK-c-Jun signaling pathway**

**A)** The WT and TG mouse epidermal keratinocytes were serum starved for 24 hours and stimulated with 10ng/ml EGF for indicated time periods. The activation and expression of the EGFR and JNK were analysed by western blotting. **B)** Western blotting analysis of the sPLA<sub>2</sub>-IIA induced JNK mediates c-Jun activation and expression. **C)** Western blotting of c-Fos activation upon EGF stimulation in K14-sPLA<sub>2</sub>-IIA keratinocytes. **D)** Validation of increased activation of EGFR and c-Jun in the mouse epidermis. (WT-Wild type, TG - K14-sPLA<sub>2</sub>-IIA mice, n=3 mice/genotype)

Importantly, we also observed drastic upregulation of EGFR and c-Jun expression in the K14-sPLA<sub>2</sub>-IIA mice keratinocytes, that further correlates with our microarray data on HFSCs (Data not showed). We have also checked the activation of the EGFR and c-Jun in the total lyaste, which was prepared from the mouse epidermis. Data showed increased activation of EGFR and c-Jun (Figure 5.4 D) that is similar of our in vitro data. Together, our data showed that the sPLA<sub>2</sub>-IIA induces EGFR mediated JNK/c-Jun signaling in the K14-sPLA<sub>2</sub>-IIA mice keratinocytes.

### **5.2.5 Increased c-Jun signaling enhances K14-sPLA<sub>2</sub>-IIA keratinocytes proliferation in vitro**

To determine the functional effect of enhanced EGFR-JNK-c-Jun signaling in vitro, mouse keratinocytes proliferation was evaluated by BrdU incorporation assay. Mouse primary keratinocytes were serum starved for 24 hours followed by stimulation with complete E-media containing 10  $\mu$ M BrdU for eight hours. The percentage of BrdU positive cells was calculated by counting the total number of BrdU positive cells and unstained cells. Our data demonstrated increased numbers of BrdU positive cells in the transgenic mice keratinocytes as compared to wild-type keratinocytes, suggesting a faster proliferation of K14-sPLA<sub>2</sub>-IIA mice keratinocytes (Figure 5.5 A-B).

In addition, we confirmed the differential activation of the c-Jun during the starved and unstarved condition by western blotting, which showed increased activation of c-Jun during starvation condition (Figure 5.5 D). Further, to confirm the role of enhanced c-Jun signaling in the keratinocytes proliferation, mouse primary keratinocytes were serum starved with JNK inhibitor for 24 hours followed by stimulation with complete E-media containing 10  $\mu$ M BrdU for eight hours. Our data showed that inhibition of JNK during the starvation period reduces BrdU incorporation and BrdU positive cells (Figure 5.5 C, E) keratinocytes proliferation in vitro.

Overall, these studies demonstrated that JNK signaling is further enhanced during the serum starvation, which gives proliferative advantage to primary keratinocytes when stimulated with the serum containing media, possibly through c-Jun induced EGFR expression.

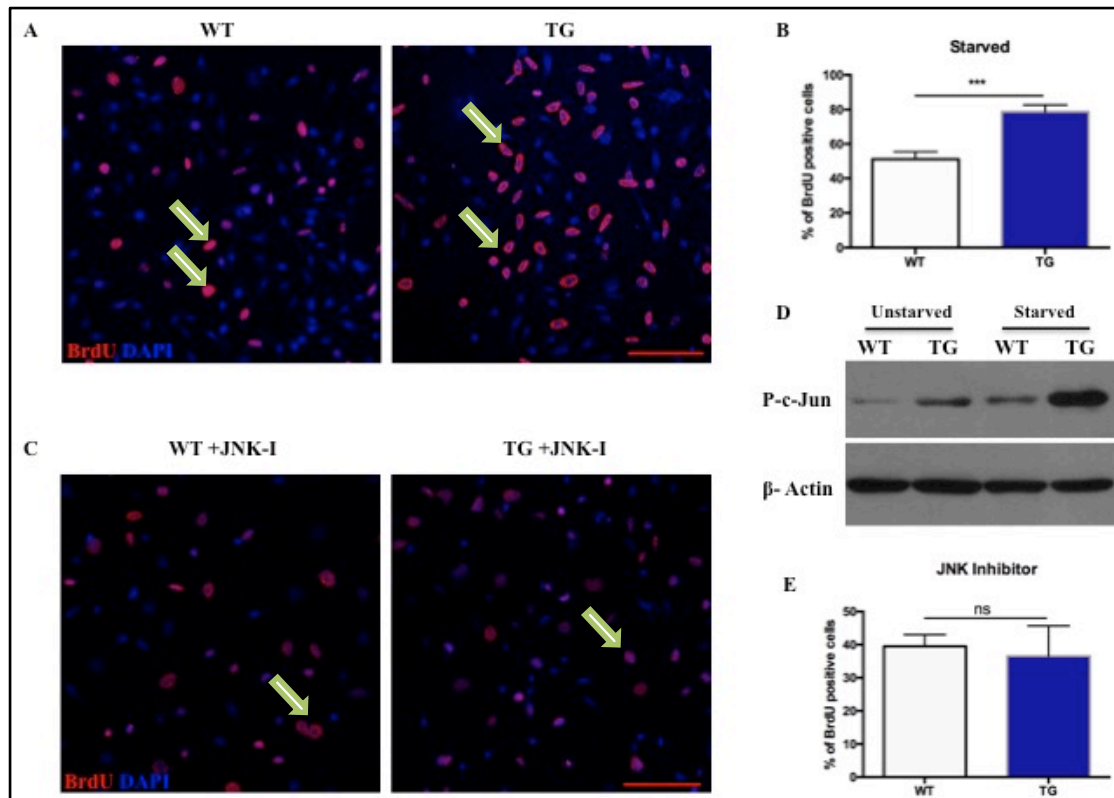


**Figure 5.5 Analysis of cell proliferation by BrdU incorporation assay**

**A)** Mouse primary keratinocytes were starved for overnight and stimulated with complete media containing  $10\mu\text{M}$  BrdU for eight hours. **B)** Quantification of BrdU<sup>+</sup> cells in wild type and K14-sPLA<sub>2</sub>-IIA mice keratinocytes. **C)** Mouse primary keratinocytes were serum starved with JNK Inhibitor for overnight and stimulated with complete media containing  $10\mu\text{M}$  BrdU for eight hours. **D)** Differential activation of the c-Jun during starved and unstarved condition in the K14-sPLA<sub>2</sub>-IIA mice keratinocytes. **E)** Quantification of BrdU<sup>+</sup> cells treated with JNK Inhibitor for overnight in wild type and K14-sPLA<sub>2</sub>-IIA mice keratinocytes. (WT-Wild type, TG - K14-sPLA<sub>2</sub>-IIA mice, n=3 mice/genotype, ns -  $P > 0.05$ , \* -  $P \leq 0.05$ , \*\* -  $P \leq 0.01$ , \*\*\* -  $P \leq 0.001$ , \*\*\*\* -  $P \leq 0.0001$ )

### 5.2.6 Functional potential of HFSCs in vivo

We observed faster proliferation and increased differentiation of HFSCs in the K14-sPLA<sub>2</sub>-IIA mice, which ultimately led to depletion of the HFSCs. Further, to examine whether remaining HFSCs are functionally able to produce progenitors that differentiate in hair shaft producing cells, we performed the hair depilation experiment. Hair depilation using hot wax removes entire hair shaft from the hair follicle and activates HFSCs that further synchronously promotes the new hair cycle.

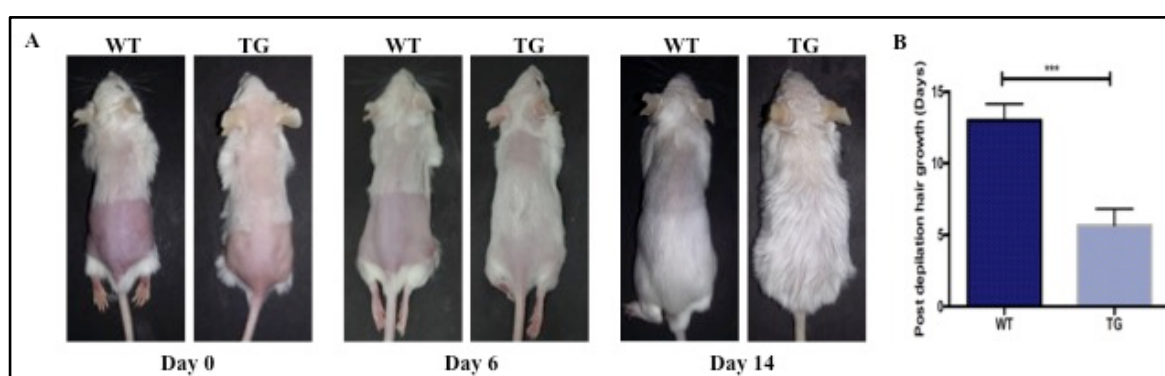


**Figure 5.6 Depilation induced hair growth in WT and K14-sPLA<sub>2</sub>-IIA mice**

*A) Comparative post depilation hair growth in WT and TG mice at different time points. B) Graphical representation of the numbers of days requires appearing hair shafts out of the epidermis.*

Our comparative post depilation study showed that the activated follicular cells in the K14-sPLA<sub>2</sub>-IIA mice are not only able to produce differentiated progeny and hair shaft but showed faster hair growth in K14-sPLA<sub>2</sub>-IIA mice as compared to wild-type mice (Figure 5.6). These data indicate that the HFSCs in the K14-sPLA<sub>2</sub>-IIA mice are in the activated state during the telogen, which requires less time for the production of cell progeny for the new hair shaft formation after depilation.

### 5.2.7 In vivo topical application of JNK inhibitor reverses depilation induced hair growth in K14-sPLA<sub>2</sub>-IIA mice

Our previous results showed upregulation of JNK/c-Jun signaling in mouse keratinocytes. Further, to explore the effect of JNK inhibition on activation of the HFSCs *in vivo*, topical pretreatment of JNK inhibitor was given for 2 days followed by application of the JNK inhibitor on the depilated area for 10 days (Figure 5.7 A).

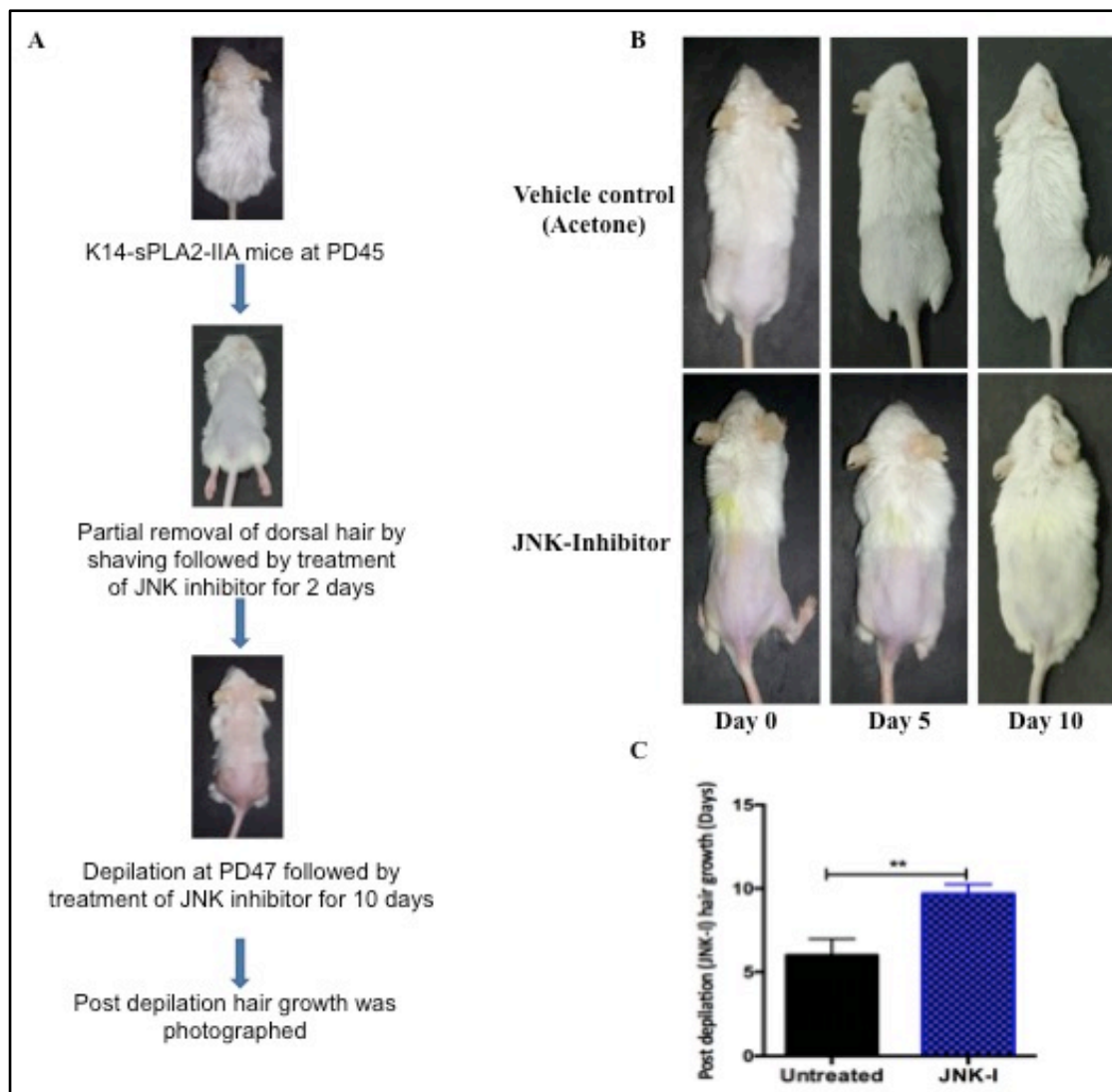


**Figure 5.7 In vivo reversal of depilation induced hair growth by topical application of the JNK inhibitor**

*A) Scheme of the JNK inhibitor treatment and in vivo reversion of the depilation induced faster hair growth analysis. B) Comparative post depilation hair growth after*

*topical application of the acetone and JNK inhibitor on TG mice. C) Graphical representation of the delay in hair growth after topical application of the JNK inhibitor. (WT - Wild type, TG - K14-sPLA<sub>2</sub>-IIA mice, n=3 mice/genotype), ns -  $P > 0.05$ , \* -  $P \leq 0.05$ , \*\* -  $P \leq 0.01$ , \*\*\* -  $P \leq 0.001$ , \*\*\*\* -  $P \leq 0.0001$ .*

Our results showed that the application of JNK inhibitor may counterbalances JNK/c-Jun induced stem cells activation as well as rapid proliferation and delays post depilation hair growth in K14-sPLA<sub>2</sub>-IIA mice as compared to untreated (Vehicle control) mice (Figure 5.7 B-C).

### **5.2.8 Characterization of K14-sPLA<sub>2</sub>-IIA homozygous mice skin**

Further, we sought to analyze the effect of enhanced overexpression of sPLA<sub>2</sub>-IIA on the epidermal development and differentiation as we observed drastic effect of sPLA<sub>2</sub>-IIA overexpression on skin architecture and hair growth starting from the birth. The K14-sPLA<sub>2</sub>-IIA homozygous mice are small in size, which displayed abnormal hair coat and whiskers as well as beaded and short tail (Figure 5.8 A). Therefore, we characterized the K14-sPLA<sub>2</sub>-IIA homozygous mice skin at various postnatal ages. First, we performed the histological examination of the dorsal skin tissue sections by using Haematoxylin and Eosin (H&E) staining at different postnatal days (PD), such as PD15, 19, 21, 25, 28, 35, 41 and 49 that includes morphogenesis and first hair cycle. Our results showed that sPLA<sub>2</sub>-IIA overexpression alters the hair cycle with hair follicle cycling being stuck at anagen like a stage. This is further supported by our observations that we have not observed complete telogen at any postnatal day (PD15, PD17, PD21, PD25, PD28, PD30, PD35, PD41, PD45 and PD49) (Figure 5.8 A-B, D). Besides, we also observed abnormal thickening of the interfollicular epidermis (IFE) starting from very early age and interfollicular

epidermal cyst formation and in the K14-sPLA<sub>2</sub>-IIA homozygous mice (Figure 5.8 C). Together, these data suggest that sPLA<sub>2</sub>-IIA alters development of the epidermal components and its homeostatic maintenance in the K14-sPLA<sub>2</sub>-IIA homozygous mice.

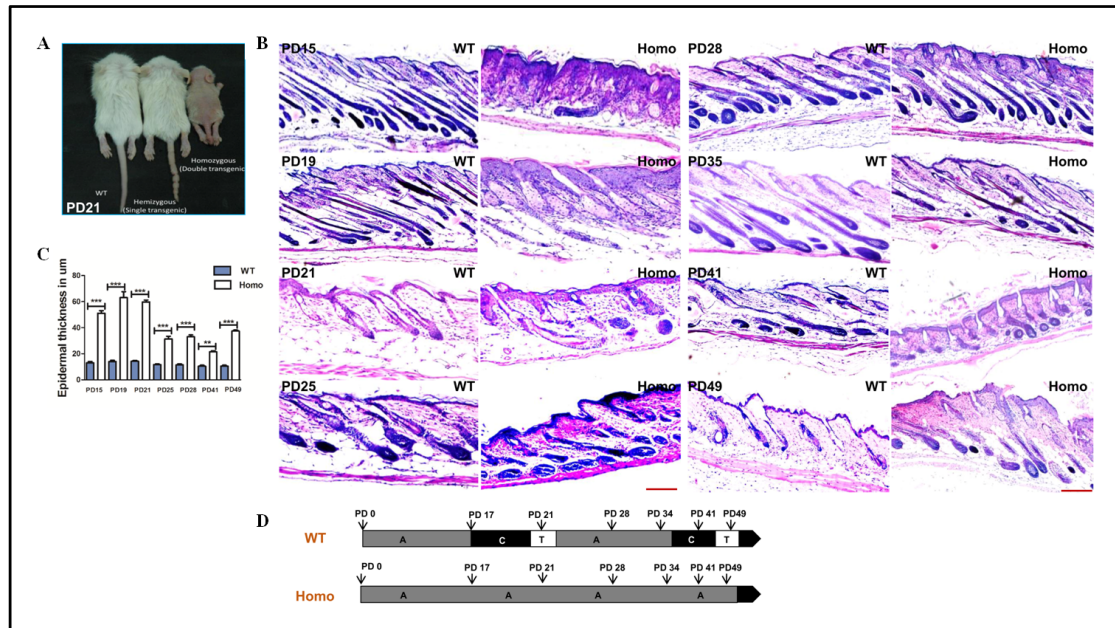


**Figure 5.8 Histological characterization of the hair follicle cycling**

**A)** The phenotypic appearance of wild-type, hemizygous and homozygous mice at postnatal day 21. **B)** Images represent hematoxylin and eosin staining of skin sections at various postnatal days of wild-type and homozygous mice to study hair follicle cycling. **C)** Graphical representation of epidermal thickness measurements in  $\mu\text{m}$ . Data are presented as mean  $\pm$  SD. \*\* $P < 0.005$ , \*\*\* $P < 0.0001$ . **D)** Comparative analysis of hair follicle progression to different stages of hair cycle (Anagen, Catagen and Telogen) at different postnatal days in wild-type and homozygous mice. WT-Wild type, Homo- K14-sPLA<sub>2</sub>-IIA homozygous mice,  $n=3$  mice/genotype. A-Anagen, C-Catagen and T-Telogen, PD-Postnatal days.

Further, to confirm whether the small size and abnormal development of the K14-sPLA<sub>2</sub>-IIA homozygous mice is due to the abnormal nutritional status or not, we

quantified major nutritional parameters from the serum of the adult K14-sPLA<sub>2</sub>-IIA homozygous mice.

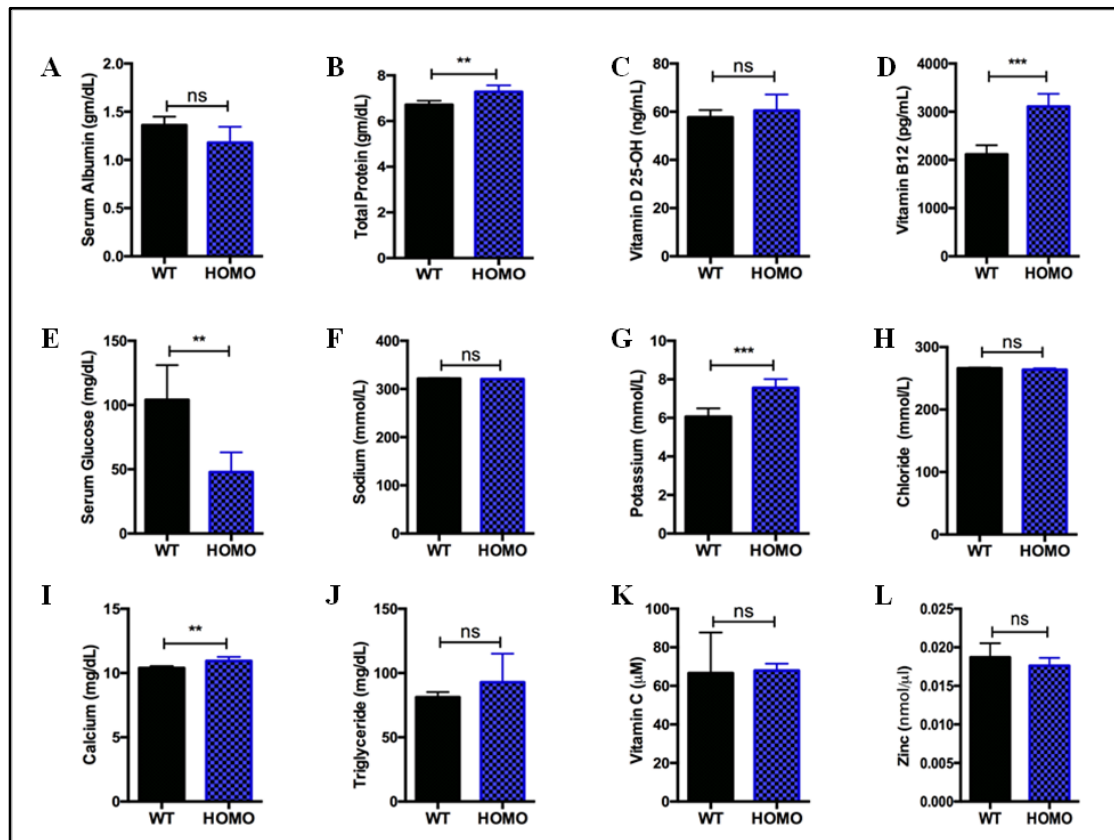


**Figure 5.9 Analysis of the nutritional parameters**

Quantification of nutritional parameters such as serum albumin, total protein, Vitamin D 25-OH, Vitamin B12, serum glucose, Sodium, Potassium, Chloride, Calcium, Triglyceride, Vitamin C and Zinc. (WT- Wild type and Homo- K14-sPLA<sub>2</sub>-IIA homozygous mice. n=4 mice/genotype. Data are presented as mean ± SD. \*\*P<0.005, \*\*\*P<0.0001)

Our data showed no significant alterations in serum components such as serum albumin, Vitamin D 25-OH, Triglyceride, Sodium, Chloride, and marginal increase was observed in the level of total protein, Vitamin B12, Calcium and Potassium (Figure 5.9 A-L). These results demonstrated that there are no significant abnormalities in the nutritional status of the K14-sPLA<sub>2</sub>-IIA homozygous mice.

### 5.2.9 Abnormal organization of epidermal components and stratification of epidermis

The hair follicle abnormalities and abnormal IFE thickness led us to investigate whether these abnormal phenotypes are supported by altered proliferation and differentiation of epidermal compartment-specific cell types.

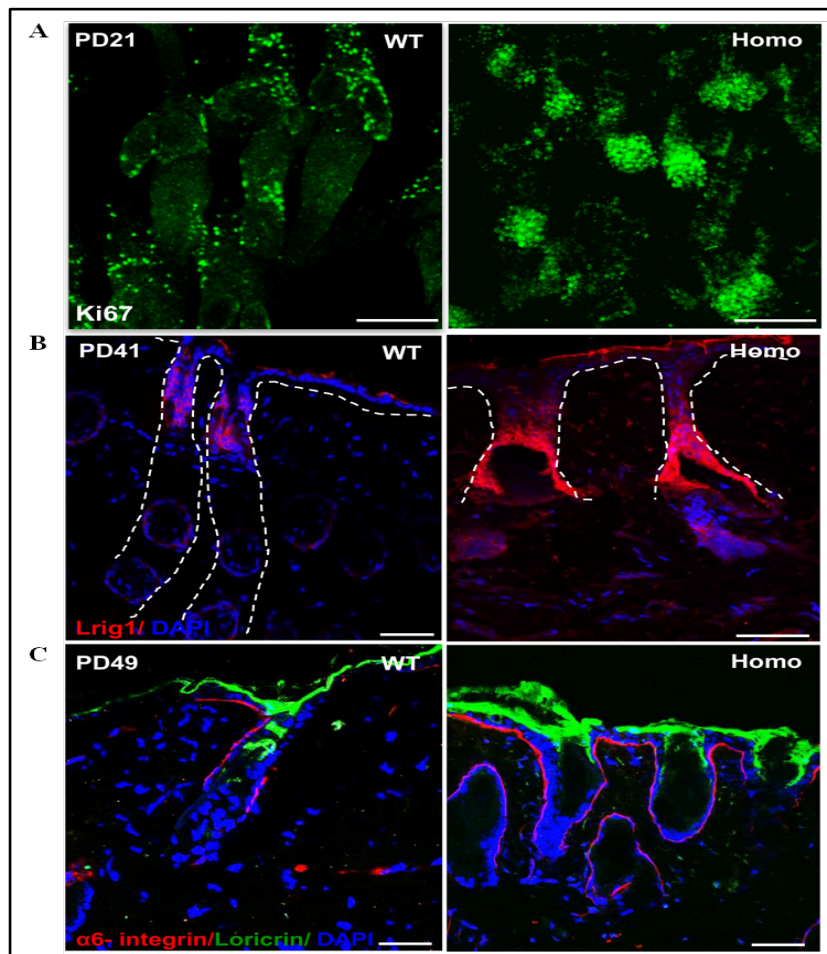


**Figure 5.10 Analysis of the cell proliferation and differentiation**

*A) Immunofluorescence staining of Ki67 to assess cell proliferation in the intact epidermal sheet of the tail skin by wholemount assay. B) Immunofluorescence labelling of Lrig1 in WT and homozygous mice skin sections. Dashed lines represent the boundary of junctional zone area. C) Immunofluorescence staining of Loricrin as a differentiation marker to label the cells of granular layers in WT and homozygous mice. (WT-Wild type, Homo- K14-sPLA<sub>2</sub>-IIA homozygous mice, n=3 mice/genotype)*

We performed the Ki67 staining on the wholemount of intact epidermal sheet to access the status of cell proliferation. Our results demonstrated increased numbers of Ki67 positive cells in the K14-sPLA<sub>2</sub>-IIA homozygous mice (Figure 5.10 A), suggesting that sPLA<sub>2</sub>-IIA enhances proliferation of the hair follicle and IFE cells in the homozygous mice. Further, to evaluate the effect of sPLA<sub>2</sub>-IIA on cells of the upper region of the hair follicle, immunofluorescence staining of the Lrig1 was performed on the skin sections that showed a significant increase in numbers of Lrig1 positive cells and expansion of the junctional zone area (Figure 5.10 B). In addition, to study whether the hyperproliferative IFE cells also generates more differentiated progeny, the later stages of terminal differentiation was evaluated. Immunofluorescence staining of Loricrin was performed that showed enhanced expression of Loricrin in the homozygous mice skin (Figure 5.10 C). This data indicates that sPLA<sub>2</sub>-IIA markedly disturb epidermal proliferation and differentiation status in different compartments that lead to an abnormal organization of these compartments in the K14-sPLA<sub>2</sub>-IIA homozygous mice.

#### **5.2.10 Drastic depletion of HFSCs in the K14-sPLA<sub>2</sub>-IIA homozygous mice**

We observed an altered hair follicle cycling and loss of hair at very early age, which suggests that the maintenance of the HFSCs within the bulge might get affected. To further profile the HFSCs pool, we performed the flow cytometry analysis of HFSCs at PD28 by using the CD34 and  $\alpha 6$  integrin markers.

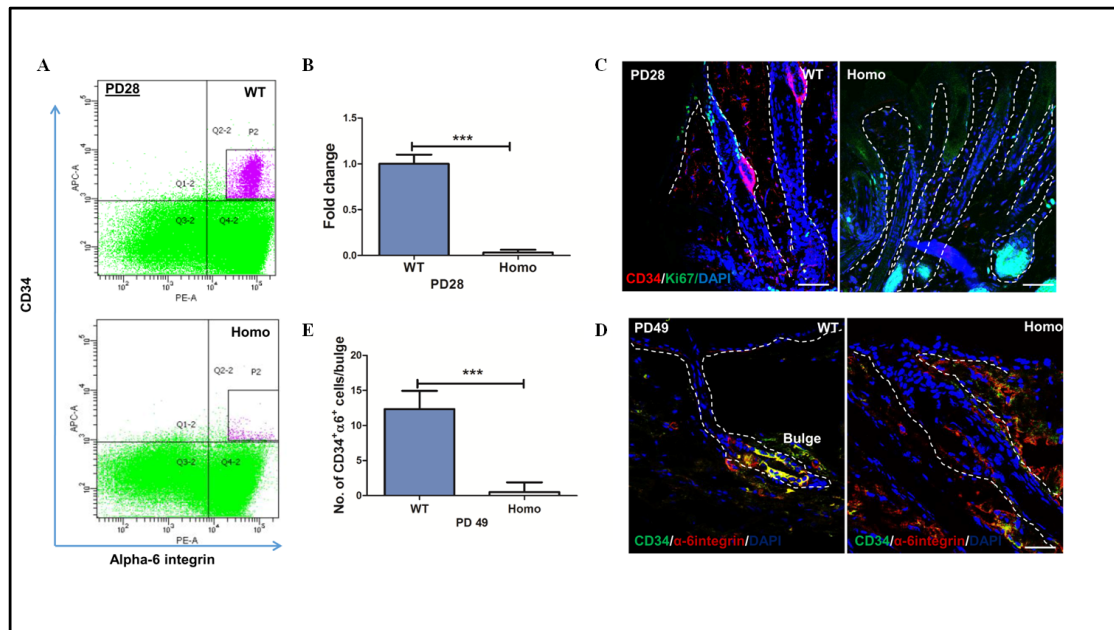


**Figure 5.11 Analysis of the HFSCs pool in K14-sPLA<sub>2</sub>-IIA mice**

**A)** Flow cytometry-based analysis of hair follicle stem cells ( $CD34^+/\alpha\text{-6 integrin}^+$ ) in wild type and homozygous mice at PD28. **B)** Quantification of FACS analysis of  $CD34^+/\alpha\text{-6 integrin}^+$  bulge HFSCs in wild type and homozygous mice at PD28. **C)** Immunofluorescence staining of  $CD34^+$  and Ki67 at PD28. Scale bar: 50  $\mu\text{m}$ . **D)** Immunofluorescence analysis of  $CD34^+/\alpha\text{-6 integrin}^+$  positive HFSCs at PD49. Scale bar: 50  $\mu\text{m}$ . **e)** Quantification of  $CD34^+/\alpha\text{-6 integrin}^+$  cells in the bulge of the dorsal skin in wild type and homozygous mice at PD49. (PD-Postnatal days, HFSC-Hair follicle stem cells. (WT-Wild type Homo- Homozygous mice,  $n=3$  mice/genotype. Data are presented as mean  $\pm$  SD. \*\*\*,  $P<0.0001$ )

Our results showed drastic depletion of  $CD34^+/\alpha\text{-6 integrin}^+$  HFSCs population in the K14-sPLA<sub>2</sub>-IIA mice (Figure 5.11 A-B). Further, these data was validated by immunofluorescence staining of CD34 on the skin tissue sections at PD28 that showed an absence of  $CD34^+$  cells in the hair follicle bulge of homozygous mice (Figure 5.11 C-D). Moreover, the counting of  $CD34/\alpha\text{-6 integrin}$  dual positive cells per hair follicle bulge indicates significant loss of HFSCs in the bulge of the hair

follicle (Figure 5.11E). In addition, we further confirmed the loss of the HFSCs compartment by immunohistochemical staining of the Sox9, which is another well-known marker for the HFSCs in the bulge of the hair follicle. Our data showed an absence of the Sox9 positive cells in the bulge region of the hair follicle of K14-sPLA<sub>2</sub>-IIA homozygous mice (Figure 5.12).

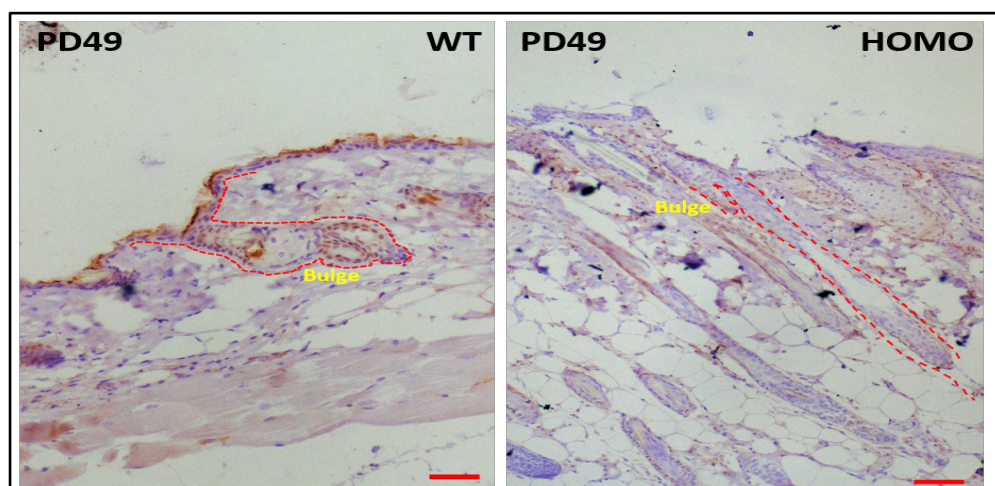


**Figure 5.12 Immunohistochemical staining of Sox9**

*Immunohistochemical staining of Sox9 at PD 49 in dorsal skin sections of WT and homozygous mice. (WT- Wild type and Homo-K14-sPLA<sub>2</sub>-IIA homozygous mice. n=3 mice/genotype. PD- postnatal day, Scale bar: 100  $\mu$ m)*

Collectively, these data suggest that sPLA<sub>2</sub>-IIA induced hyperproliferative response may leads to the subsequent depletion of the HFSCs pool and hair loss in the homozygous mice.

### **5.2.11 Development of cyclic alopecia in K14-sPLA<sub>2</sub>-IIA homozygous mice**

The newborn homozygous pups could be easily distinguished from wild-type littermates by their short and wavy whiskers as early as from day three after birth irrespective of the sex of mice. Moreover, drastic depletion of the HFSCs pool led us to investigate the detailed hair growth pattern in the homozygous mice. We followed

the homozygous mice from birth to up to six months and the hair growth patterns over time were recorded by capturing photographs at every alternate day. The hair loss was beginning from day 18 and full body hair loss was complete at PD22 (Figure 5.13). Further, the hair regrowth was started from day 27 and partially covered the body by day 33 (Figure 5.13).

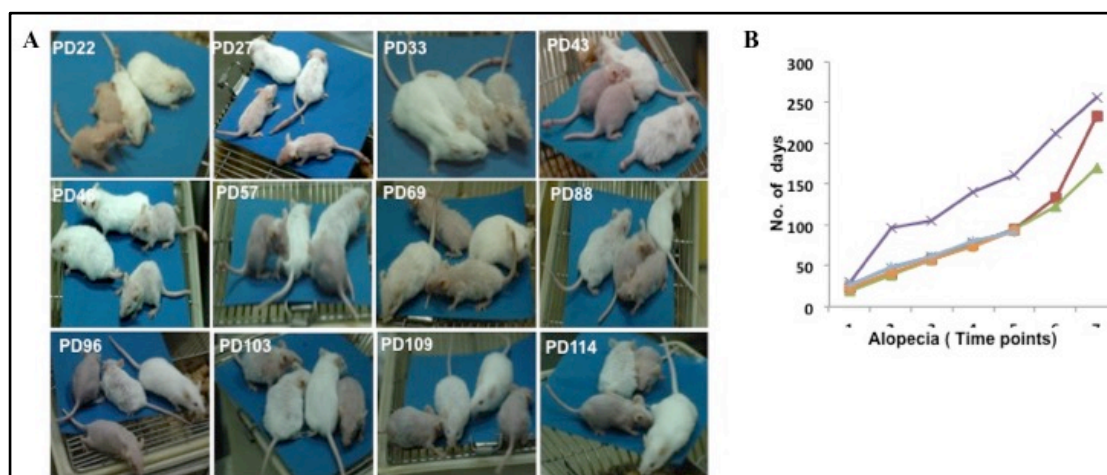


**Figure 5.13 Cyclic pattern of hair loss and growth**

*A) Phenotypic appearance of wild type and homozygous mice at different postnatal days with cyclic hair loss and growth. B) Graphical representation of alopecia time points with respect to postnatal days of the homozygous mice. (WT-Wild type Homo-K14-sPLA<sub>2</sub>-IIA homozygous mice, n=3 mice/genotype)*

However, hair of homozygous mice was short and dull as compared to a smooth and shiny hair of wild-type littermates. This successive cycle of the hair growth and loss was occurring repetitively after 18-22 days up to 6-8 months (Figure 5.13). This cyclic alopecia was observed in both the male and female mice.

### 5.2.12 Mechanism of the development of alopecia

We have further investigated whether this cyclic phenomenon relies either on the deregulation of known molecules or is an independent mechanism. We performed

real-time quantitative PCR of Sox21, Msx2, Zdhcc13 and Foxn1. Real-time PCR data showed significant downregulation of Sox21, Msx2 and Foxn1 mRNA expression as compared to wild-type control littermate (Figure 5.14 A). Importantly, Sox21 is known to regulate hair keratins expressions that are necessary for the formation of IRS (Inner root sheath) and anchoring of hair shaft.

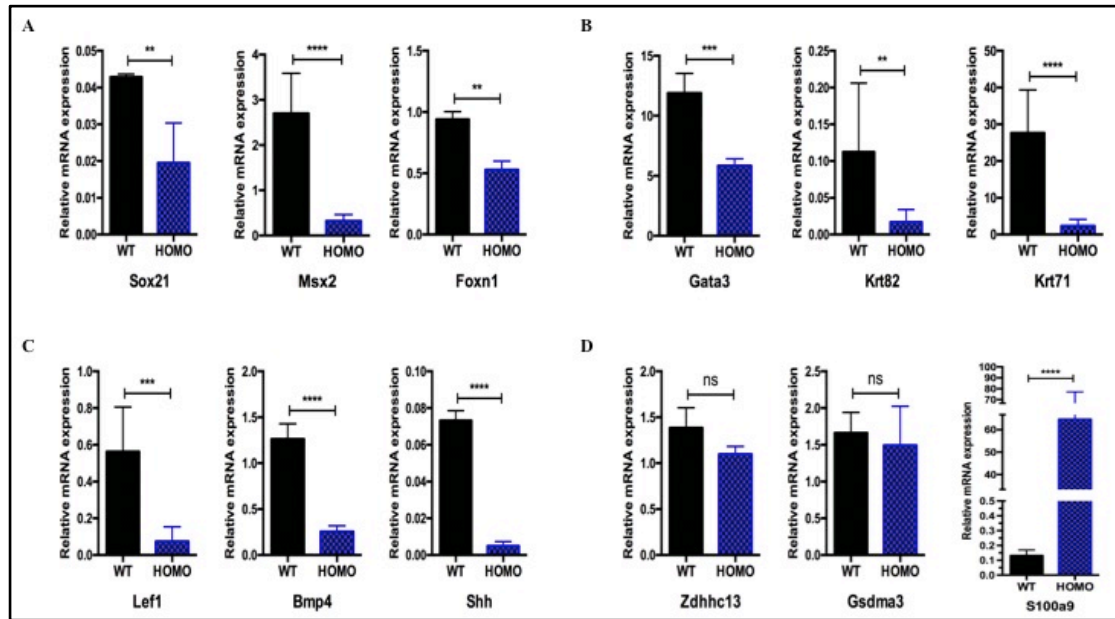


**Figure 5.14 Real time PCR analysis of various genes involved in the alopecia**

Total epidermal cells were isolated from the WT and K14-sPLA<sub>2</sub>-IIA homozygous mice and quantitative real-time PCR analysis of selected genes was performed, which are known to regulate the process of matrix cell proliferation, differentiation and hair shaft formation. (WT-Wild type, Homo- K14-sPLA<sub>2</sub>-IIA homozygous mice, n=4 mice/genotype. Data are presented as mean ± SD, ns - P > 0.05, \* - P ≤ 0.05, \*\* - P ≤ 0.01, \*\*\* - P ≤ 0.001, \*\*\*\* - P ≤ 0.0001)

Therefore, we checked the expression of Gata3, Krt82 and Krt71 by real-time PCR analysis and our results indicate down-regulation of Gata3, Krt82 and Krt71 expression that suggest an aberrant differentiation of the IRS and hair shaft precursor cells in the K14-sPLA<sub>2</sub>-IIA homozygous mice (Figure 5.14 B). Further, to investigate

the role of signaling factors that are required for the matrix cells proliferation and generation of precursors for the IRS and hair shaft formation; we analyzed levels of BMP4, Shh and Lef1. We found significant downregulation of BMP4, Lef1 and Shh in K14-sPLA<sub>2</sub>-IIA homozygous mice skin (Figure 5.14 C). However, we did not find any alterations in the *Zdhcc1* and *Gsdma3* expression, whereas terminal differentiation marker *S100a9* was highly upregulated. These data suggested that deregulated signaling in the matrix cells might lead to defects in differentiation of the IRS and formation of the hair shaft.

### **5.2.13 sPLA<sub>2</sub>-IIA alters initial wound healing response in vivo**

The process of epidermal regeneration is governed by the activity of the long-lived stem cells population within the epidermis. The regenerative capacity of epidermis after wounding slowly declines with ageing. Importantly, various studies have demonstrated the functional contribution of the HFSCs during epidermal regeneration after wounding. In our K14-sPLA<sub>2</sub>-IIA homozygous mice, we observed the drastic depletion of HFSCs, which led us to evaluate the effect of depletion of HFSCs on the wound healing response in the K14-sPLA<sub>2</sub>-IIA homozygous mice. We created scratch wounds on the upper region at midline and full-thickness wounds were created on the lower region of dorsal skin of seven-week-old animals. The areas of open wounds were monitored during the healing process to monitor macroscopic healing defects (Figure 5.15 A). Our data showed an impaired initial healing response in the K14-sPLA<sub>2</sub>-IIA homozygous mice as compared to wild-type mice as mentioned at day 5 (red circle). However, the pace of wound recovery was accelerated after 5-6 days and fully recovered at the same time of wild-type mice (green circle) (Figure 5.15 B).

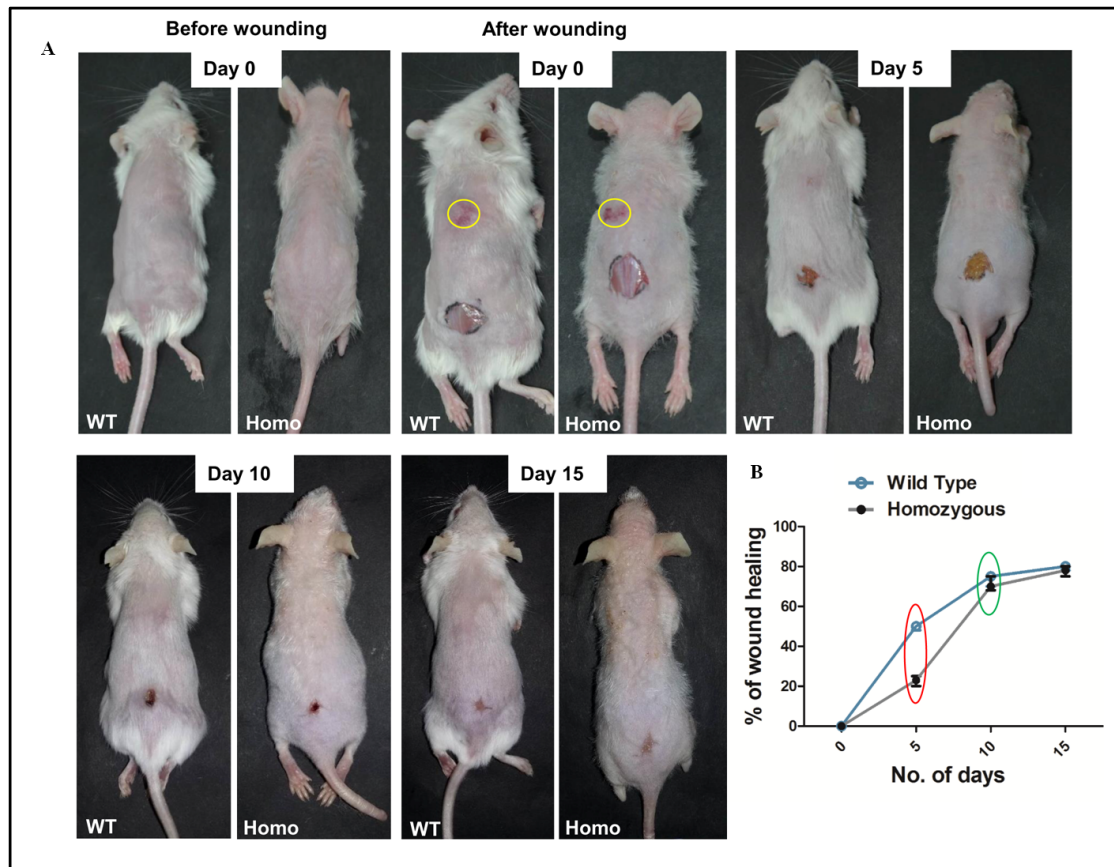


**Figure 5.15 Time dependent comparative wound healing process**

*A) Wild-type and K14-sPLA<sub>2</sub>-IIA homozygous mice at Day 0 (before wounding) and Day 0 (after wounding). The healing process was recorded by photographs at various days and representative images are presented for the Day 5, Day 10 and Day 15. B) Graphical representation of comparative wound recovery during the healing process. The red circle indicates defects in initial healing response in the K14-sPLA<sub>2</sub>-IIA homozygous mice. The green circle indicates no significant difference in time periods during the later stage. (WT-Wild type, Homo-K14-sPLA<sub>2</sub>-IIA homozygous mice, n=3 mice/genotype).*

Together, these results showed that sPLA<sub>2</sub>-IIA alters the initial wounding response but do not affects the full wound recovery in K14-sPLA<sub>2</sub>-IIA homozygous mice.

### 5.3 Graphical representation of abnormalities in the hair follicle cycling and in organization of the epidermal compartments

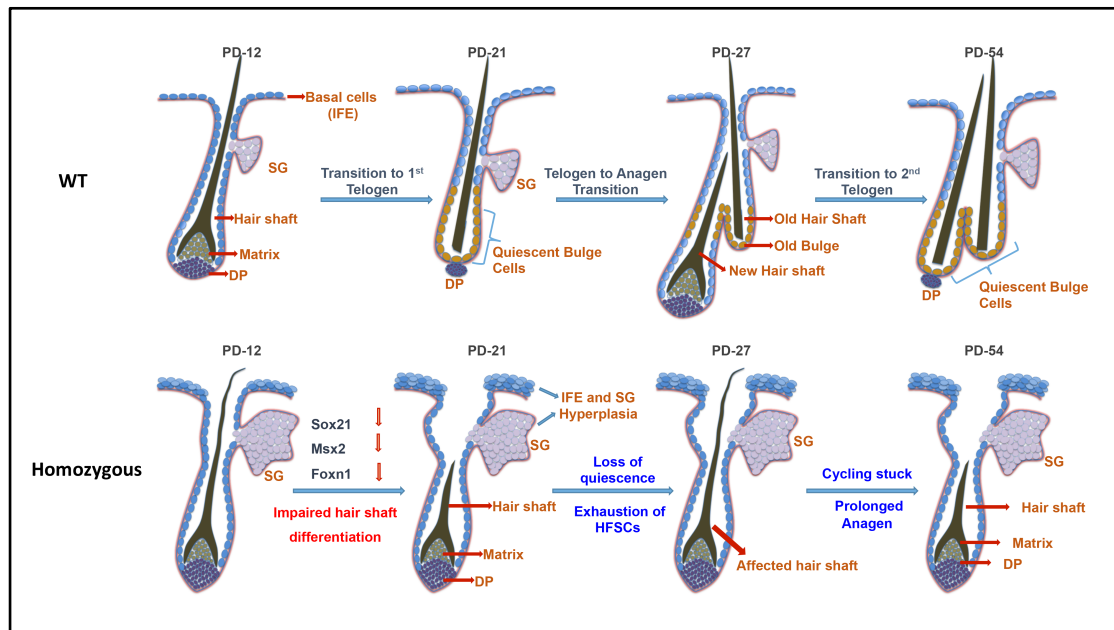


**Figure 5.16 Comparative hair follicle cycling and epidermal abnormalities**

*Proposed model of impaired hair follicle cycling in  $K14-sPLA_2-IIA$  homozygous mice.*

*WT - Graphical representation of hair follicle cycling in wild-type mice from hair follicle morphogenesis to second telogen at PD49, which is represented by the presence of club hair and subsequent progression to the next hair cycle.*

*Homozygous - Graphical representation of hair follicle cycling in  $K14-sPLA_2-IIA$  homozygous mice represented by abnormal morphology of hair follicle with the presence of affected hair shaft. (WT-Wild type, Homo-  $K14-sPLA_2-IIA$  homozygous mice, IFE: interfollicular epidermis, SG: sebaceous gland, DP: dermal papilla, PD-Postnatal days)*

## 5.4 Discussion

The phospholipase family comprises of different isoforms, which are involved in different patho-physiological processes such as arthritis, inflammation and cancer. Also, deregulated expression of secretory phospholipase family proteins, mainly sPLA<sub>2</sub>-IIA has been reported in diverse human cancers. However, the mechanism through sPLA<sub>2</sub>-IIA modulates the downstream signaling cascades and effect of these altered signaling on the behaviors of the adult tissue stem cells remaining unknown.

The adult tissue stem cells are present in different compartments of the epidermis such as IFE, sebaceous gland and bulge of the hair follicle. The HFSCs of the bulge are multipotent that are able to produce progeny, which contributes to epidermal regeneration during injury, sebaceous gland lineage and hair follicle growth. Moreover, these cells are highly dynamic in their proliferative behavior, and only a small percentage of HFSCs divide multiple times during the growth phase. Importantly, our previous study showed that the overexpression of the sPLA<sub>2</sub>-IIA in mice epidermis depletes HFSCs and induces differentiation. The effect of the sPLA<sub>2</sub>-IIA on the stemness potential was further supported by the reduced colony forming efficiency of the mouse keratinocytes in vitro. This is most likely due to the fact that sPLA<sub>2</sub>-IIA promotes rapid proliferation of these cells and induces differentiation in vitro at very low cell density, thereby affecting the development of the independent colonies. Further, we adopted the pTRE-H2BGFP system to investigate the effect of the sPLA<sub>2</sub>-IIA on proliferation dynamics. We asked whether sPLA<sub>2</sub>-IIA induces proliferation of all HFSCs at a similar rate, irrespective of their quiescence potential or it has pronounced effect on those cells, which have low quiescence potential. Our results showed that sPLA<sub>2</sub>-IIA induced proliferation targets all the cells irrespective of their quiescence potential. This data explains the mechanism through sPLA<sub>2</sub>-IIA

alters an infrequent divisional characteristic of HFSCs and loss of stem cell compartment over time during persistent mitogenic stimulation as reported by different study [208, 246, 247]. Moreover, it also suggests that the suppressive signaling during catagen and telogen is not sufficient to inhibit the proliferation of the HFSCs during resting phase. Importantly, although we observed the proliferation of the HFSCs after completion of the anagen phase in K14-sPLA<sub>2</sub>-IIA mice, we did not find any significant effect on the maintenance of telogen phase of the hair cycle at PD49 [211]. These data may explain that remaining activated stem cells population are not sufficient to independently maintain or induce anagen phase in the K14-sPLA<sub>2</sub>-IIA mice or the hair follicle may have other intrinsic compensatory mechanisms to inhibit the induction of hair follicle growth other than the status of the stem cells proliferation. These suggest that the hair follicle growth is not only dependant on the presence of the activated stem cells but some other hair cycle stage-dependent factors may have an important role in regulating the onset of the new hair cycle.

Further, sPLA<sub>2</sub>-IIA is also known as enhancing factor that promotes the binding of EGF. Our data on the cell signaling mechanism identified the crucial downstream effectors of the EGFR signaling, which plays an essential role in the regulation of cell proliferation and differentiation. In the astrocytoma and microglial cells, sPLA<sub>2</sub>-IIA has been shown to promote EGFR transactivation and cell proliferation. The mitogen-activated protein kinases (MAPK) have been reported to play an essential role in the differentiation of epidermal keratinocytes by regulating expression of the differentiation-associated genes [248]. Our study has uncovered a mechanism of sPLA<sub>2</sub>-IIA induced epidermal proliferation and differentiation through an activation of downstream MAPK signaling. We have shown that the overexpression of sPLA<sub>2</sub>-

IIA induces activation of various AP1 transcription factors including c-Jun and c-Fos in mouse epidermal keratinocytes. Further, our data showed that an increased expression of c-Jun is directly associated with increased expression of differentiation-associated Keratin 1. The K14-sPLA<sub>2</sub>-IIA primary keratinocytes showed enhanced activation of JNK1/2- c-Jun signaling that supports increased differentiation at low cell density while promotes cell proliferation through enhanced c-Jun activation. Importantly, sPLA<sub>2</sub>-IIA may provide initial trigger for JNK activation that subsequently induces differentiation because  $\Delta$ Np63 $\alpha$  induced activation of JNK signaling resulted in the onset of mouse keratinocytes differentiation. These results identified a novel function of the secretory phospholipase A<sub>2</sub> in the regulation of epidermal differentiation apart from its classical functions in the inflammation and proliferation of various cell types.

In the bulge region of the hair follicle, recent investigation has highlighted the functional involvement of the inner bulge cells in the maintenance of HFSCs quiescence. The inner bulge cells express Keratin 6 and play an important role in inhibition of outer bulge cells proliferation during telogen [73]. Importantly, we observed the proliferation of HFSCs during telogen. Therefore, we sought to investigate whether the elimination of Keratin 6 positive inner bulge cells mediated inhibition on outer bulge cells can induce faster hair growth in the K14-sPLA<sub>2</sub>-IIA mice and does remaining HFSCs population is sufficient to produce an entirely new hair shaft? Our results suggest speedier hair growth after depilation mediated removal of inner bulge cells in the K14-sPLA<sub>2</sub>-IIA mice. These data are in agreement with the previous investigations that all the bulge cells are not required to induce the new hair follicle regeneration [85, 87] and the formation of the new hair shaft. Further, it also suggests that those cells, which are rapidly proliferating and are at the point of losing

their stemness also able to induce hair follicle regeneration and are sufficient to produce an entirely new hair shaft. Notably, the depilation induced faster hair growth in the K14-sPLA<sub>2</sub>-IIA mice is mediated through an enhanced JNK/c-Jun signaling. These data are in agreement with the study of c-Jun deletion in mice epidermis, which showed reduced proliferation of basal keratinocytes and smaller papillomas in K5-SOS-F mice mediated through decreased expression of Hb-EGF and EGFR. Collectively, this data explains that balanced c-Jun activity is required to maintain epidermal homeostasis and increased or decreased level of c-Jun enhances the differentiation of basal keratinocytes.

Involvement of different growth factors including EGF, TGFs and FGFs is well studied in the regulation of epidermal stem cells proliferation and fate determination. As previously shown, deregulated release of HB-EGF in mutant mice expressing soluble proHB-EGF induced epidermal hyperproliferation and displayed hyperplasia [246]. Overexpression of TGF $\alpha$  in mice epidermis demonstrated aberrant keratins expression, hyperproliferation and development of papillomas [249]. Expression of a dominant-negative FGF receptor mutant under the control of keratin 10 (K10) promoter induced epidermal hyper thickening and showed altered keratinocyte differentiation [250]. Similarly, in our study of K14-sPLA<sub>2</sub>-IIA homozygous mice, we identified alterations in the hair follicle cycling with prolonged anagen phase of the hair follicle and epidermal hyperplasia. The increased proliferation and long anagen phase are likely due to enhanced EGFR signaling as the continuous expression of EGF prevent entry of hair follicle into the regression phase [99]. Notably, hyperproliferation induced by aberrant upstream signaling resulted in the loss of quiescence and exhaustion of stem cells pool that ultimately leads to loss of hair. Deletion of SMAD4 in the mouse epidermis inhibits programmed regression of hair

follicles and exhibits progressive alopecia with depletion of hair follicle stem cells [208, 251]. Activation of mTOR by the Wnt overexpression resulted in depletion of the HFSCs and promotes hair loss and ageing [252]. Mice expressing a dominant negative mutant of EGFR display waved severe alopecia [207]. Importantly, mice overexpressing human group II PLA<sub>2</sub> resulted in epidermal hyperplasia and complete alopecia [241] similarly as overexpression of *Pla2g2f* in mice epidermis showed psoriasis-like epidermal hyperplasia and alopecia [243]. In the agreement, our results showed hyperproliferation in various compartments of the hair follicle and complete loss of the HFSCs, which may ultimately result in the development of cyclic hair growth and hair loss pattern. Interestingly, overexpression of sPLA<sub>2</sub>-IIA may affect the establishment of the HFSCs niche as our flow cytometry analysis at PD21 where the identity of stem cells is fully established, showed significant depletion of HFSCs. Further, the contribution of the HFSCs in wound re-epithelialization following injury is well established. The bulge-derived transient amplifying cells rapidly respond to injury and contribute to wound repair but efficiently replaced by IFE derived cells over several weeks [57]. In contrast, partial ablation of the HFSCs by diphtheria toxin fails to delay healing process following wounding suggesting that bulge cells are dispensable for wound re-epithelialization [186]. Epidermal hyperproliferation induced by deficiency of Jun-B resulted in delayed wound healing response [253]. Besides, Runx1 deletion in mice showed a delay in the activation of the HFSCs, which are further activated upon skin injury [254]. Importantly, it has been shown that the HFSCs contribute to the process of wound healing and start migrating towards the wounded area within 24 hours of wounding, which suggests the involvement of the HFSCs in the initial process of wound healing [32, 56-58]. However, in the case where the HFSCs are already depleted, we observed delay in the initial response to

wounding but not in complete wound recovery in the K14-sPLA<sub>2</sub>-IIA homozygous mice, which suggest that the delay is likely due to the absence of immediate progenitor of the HFSCs, that sense the wound and migrates for healing process. However, the later stage showed no difference in the time required for complete recovery, which may be due to the effective contribution of the IFE cells, which are known to replace the progeny of the HFSCs in the epidermis after several weeks of wounding.

The development of the cyclic alopecia has been reported in various mutant mouse strains. It is well documented that genetic disruption of Sox21 resulted in the defects in anchoring hair shaft [204] and Msx2 deletion showed aberrant hair shaft differentiation [205]. However, the level of Sox21 remained unaltered in Msx2 null background, suggesting an independent mode of action of both the molecules in the development of cyclic alopecia. We observed the downregulation of Sox21 and Msx2 in the sPLA<sub>2</sub>-IIA homozygous mice, suggesting that sPLA<sub>2</sub>-IIA may function upstream of both the factors and alters their expression. Further, mutation mediated downregulation of Zdhhc13 in mice exhibits epidermal hyperproliferation, abnormal hair follicle growth and cyclic alopecia at early telogen [206, 255]. However, we did not observe any alteration in Zdhhc13 level suggesting that development of cyclic alopecia in homozygous mice is independent of cornifelin deficiency mediated cyclic alopecia in Zdhhc13 mutant mice. Importantly, the proliferation and fate determination of matrix cells to differentiate in IRS and hair shaft are governed by various signaling modulators such as BMP4, Lef1 and Shh. Specifically, BMP4 is expressed in the hair matrix cells and dermal papillae, which is known to be involved in the differentiation of hair matrix cells to precursors cells that are required for the hair shaft formation. Our results of gene expression are in agreement with the

previous study of sPLA<sub>2</sub>-X overexpressing transgenic mice that showed down-regulation of BMP4, Shh, Lef1, Foxn1 and Gata3 during the development of cyclic alopecia. Together, we found that overexpression sPLA<sub>2</sub>-IIA enhances the terminal epidermal differentiation but differentiation of matrix cells to precursors of IRS and hair shaft is severely affected. Overall, these results suggest that sPLA<sub>2</sub>-IIA may affect the lineage determination of matrix cells and subsequent differentiation of the hair follicle cells.

## ***6. Objective-II***

***To investigate the role of Disabled-2 (Dab2)  
in epidermal stem cell regulation***



## 6.1 Introduction

### 6.1.1 Disabled-2 (DAB2)

The disabled gene family mainly includes Disabled-1 (Dab1) and Disabled-2 (Dab2). They are identified as orthologs of the *Drosophila* disabled gene and encode a mammalian structural homolog of the *Drosophila* disabled (Dab) protein [256]. The expression of the Dab1 is mainly reported in the brain tissue while Dab2 expression has been identified in many adult and embryonic tissues. There are two well-known isoforms of the Dab2 protein such as p96 and p67. Both these isoforms contain phosphor-tyrosine binding domain (PTB) and a proline-rich domain (PRD) (Figure 6.1). In mammalian system, Dab2 was first isolated from the mouse macrophage cell lines as a phosphoprotein [257].

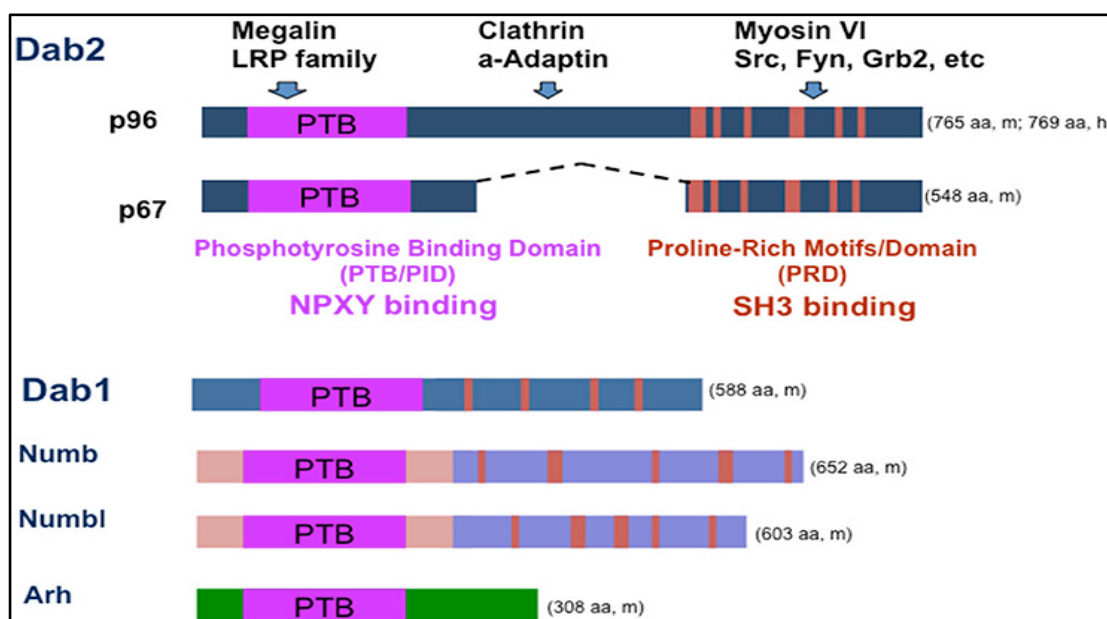


**Figure 6.1 Structure of the Disabled (Dab) proteins**

*(Adapted from Wensi et al., 2016, Front. Cell Dev. Biol) [257]*

*Dab1 and Dab2 protein contains the N-terminal phosphotyrosine-binding domain, while isoforms of the Dab2 also have a c-terminal proline-rich domain. The numbers of amino acids represents the size of the isoform.*

The Dab2 protein is involved in the regulation of many signaling cascades by regulating the process of receptor endocytosis, thereby controlling the availability of the receptors on the cell surface and downstream signaling flux. Specifically, the PTB domain of the Dab2 binds to the different signaling receptors, which are phosphorylated at Tyr residue and regulates its signaling activity through promoting endocytosis. Also, the proline-rich domain at the C-terminal region of the protein interacts with different effectors molecules such as Grb2, Fyn and Src that regulate the transcriptional activity of the target genes [258]. Importantly, studies on various tissues found no redundant functions of the Dab1 and Dab2 protein because of their distinct expression pattern in the adult tissues [257].

### **6.1.2 Role of Dab2 in regulation of Wnt signaling**

The detailed mechanistic functions of the Dab2 protein have been studied concerning the Wnt signaling activity. Dab2 negatively regulates Wnt signaling through interacting with various cytosolic components and LRP receptors. The output of the Wnt signaling is dependent on stabilization of the  $\beta$ -catenin, which is regulated by the destruction complex consisting Axin2, casein kinase 2 (CK2), protein phosphatase 1 (PP1), GSK-3 $\beta$  etc. [109]. The PP1 is known to dephosphorylates Axin that leads to its degradation, results in the stabilization of the  $\beta$ -catenin in the cytoplasm and increases the Wnt signaling. Dab2 reported to prevent the interaction between PP1 and Axin, thereby inhibits dephosphorylation and degradation of the Axin. The Axin stabilization ultimately leads to the degradation of the  $\beta$ -catenin in the cytoplasm (Figure 6.2) [259]. Moreover, the role of Dab2 as an endocytic adaptor can be best explained through the example of LRP6 endocytosis.

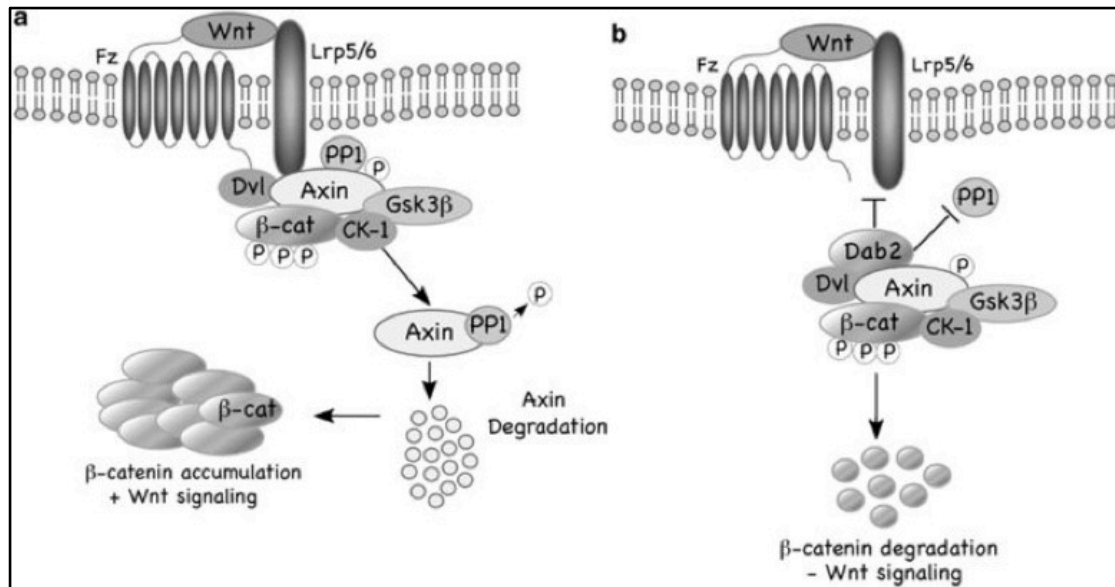


**Figure 6.2 Regulation Wnt signaling by Dab2**

*(Adapted from Jiang et al., 2009, Oncogene) [259]*

*a) In the absence of the Dab2, Axin gets phosphorylated from the PP1 that leads to Axin degradation and increased Wnt signaling. b) In the presence of Dab2, it inhibits coupling of the PP1 and Axin, thereby leads to Axin mediated stabilization of the destruction complex, which resulted in the degradation of the β-catenin and reduced Wnt signaling.*

Dab2 selectively promotes LRP6 internalization through clathrin-dependent endocytic route and bypass from the caveolin-mediated endocytosis. Further, this process is regulated by casein kinase 2 (CK2), which gets activated upon Wnt stimulation and phosphorylates LRP6 that promotes binding of the Dab2 to LRP6 [260]. In addition, Dab2 also restrict Axin stabilization through coupling with Dvl3 protein and limiting its accessibility to binding with Axin2. Therefore, Dab2 is a multifunctional protein that has an essential role in the regulation of Wnt signaling activity [261].

### 6.1.3 Regulation of TGF- $\beta$ and BMP signaling pathway by Dab2

Dab2 is an essential component that links the transforming growth factors- $\beta$  receptors to the downstream SMAD proteins by acting as an adaptor protein [262]. Dab2 also reported to regulate transforming growth factors- $\beta$  mediated signaling mechanism through limiting numbers of receptors on the cell surface [263]. Dab2 has been shown to regulate type-II transforming growth factor- $\beta$  receptor recycling through clathrin-dependent endocytosis. It has been shown that the expression of Dab2 can rescue the TGF- $\beta$  signaling in the TGF- $\beta$  mutant cells [263].

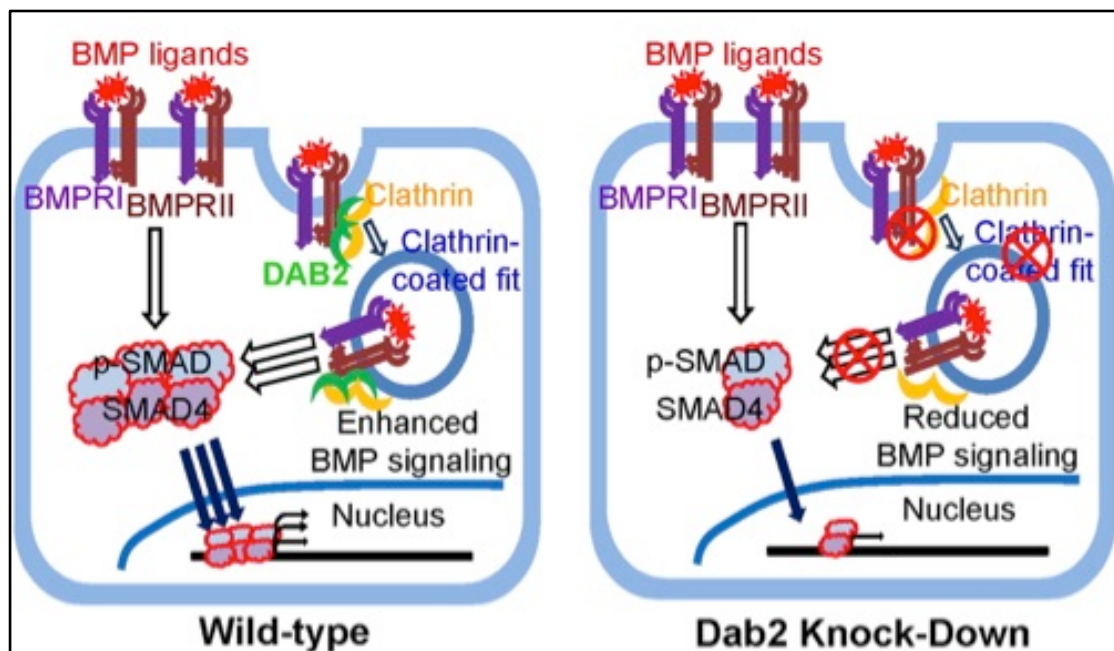


**Figure 6.3 Regulation of the BMP signaling by Dab2**

*(Adapted from Kim et al., 2012, Dev cell) [264]*

*Dab2 promotes the endocytosis of the BMP receptor-ligand complex and activates the downstream SMAD proteins. In the absence of the Dab2, activation of the SMAD protein diminished, that leads to the reduced BMP signaling. Therefore, Dab2 promotes BMP signaling outcome.*

Dab2 directly interacts with the Smad-2 and Smad-3 through its PTB domain and regulates translocation of the SMAD to the nucleus. Besides, Dab2 is also shown to directly bind to the type I and type II TGF- $\beta$  receptors in vivo. Also, Dab2 binds with the BMP type II receptor (BMPRII) and promotes internalization of the ligand-receptor complex that alters activation of the effectors SMAD proteins (Figure 6.3). Importantly, inhibition of Dab2 functions in the endothelial cells decreases SMAD-1, 5, and SMAD 8 phosphorylation and reduces BMP signaling outcome [264].

#### 6.1.4 Regulation of MAPK signaling by Dab2

The role of Dab2 as an inhibitor of cell proliferation was also suggested through its regulatory functions on the mitogenic signaling. The knockdown study of Dab2 suggests an enhanced activation of the ERK in the absence of the albumin [265].

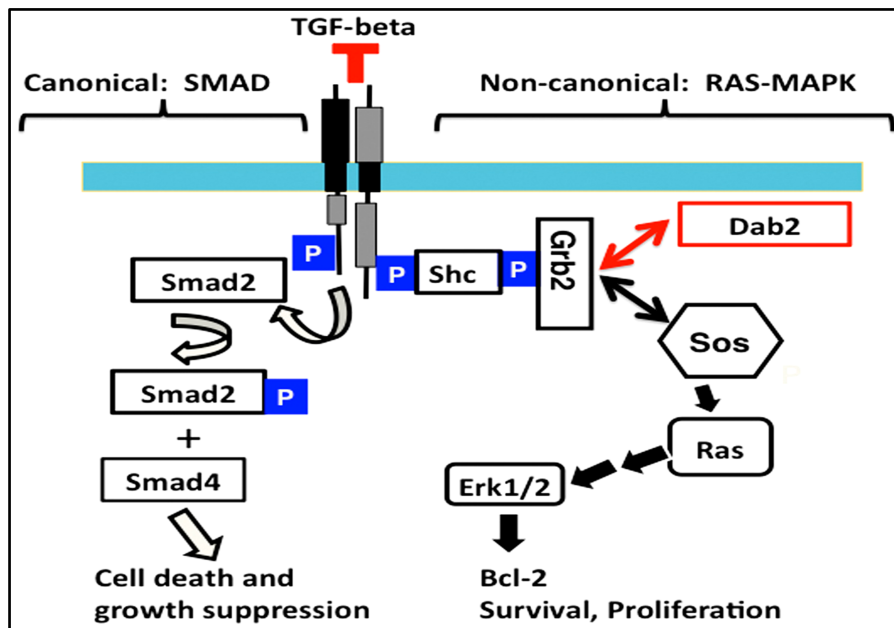


**Figure 6.4 Dab2 mediated regulation of MAPK signaling**

*(Adapted from Tao et al., 2014, Plos One) [266]*

*The Dab2 regulate MAPK signaling through limiting the accessibility of Grb2 to binds with the SOS, which leads to reduced activation of ERK1/2.*

Further, transfection induced expression of the Dab2 in the MCF-7 and SK-Br-3 cell lines showed decreased expression of c-Fos without any significant alterations in the activity of other MAPK signaling. As the expression of the c-Fos is under the control of the MAPK activity, above data suggest that Dab2 uncouples the c-Fos expression from the MAPK signaling, thereby reduces cell proliferation through inhibition of c-Fos expression [267]. Also, Dab2 known to regulate JNK activation mediated TGF- $\beta$  signaling that induces fibronectin synthesis in the NIH3T3 mouse fibroblasts and A10 rat aortic smooth muscle cells [268]. Moreover, the SOS protein regulates Ras activity by GTP exchange. The SOS binds with Grb2, which couples the tyrosine kinase receptors to the SOS protein (Figure 6.4). However, Dab2 directly competes with the SOS protein to bind with the Grb2, thereby limiting the Grb2-SOS complex formation mediated downstream signaling cascade [258]. Overall, as like Wnt signaling, Dab2 targets many proteins of the MAPK signaling pathways and reduces cell proliferation by inhibiting mitogenic signaling at multiple levels.

#### **6.1.5 Dab2 and stem cells**

Dab2 is indispensable for mouse embryonic development as conditional deletion of the Dab2 during early embryonic development leads to the embryonic lethality [213, 269]. The detailed investigation of the lethal embryonic phenotype identified its essential role in the development of the extra-embryonic endoderm. Further studies have shown that the Dab2 regulates cell polarity and cell adhesion properties [270, 271]. Therefore, deletion of the Dab2 during early embryonic development resulted in the disorganization of the ectoderm and abnormal development of the embryo. The dynamic expression pattern of the Dab2 has been identified in the hESCs as well as in the cardiomyocytes and showed that the Dab2 promotes cardiomyocytes differentiation through inhibition of WNT/ $\beta$ -catenin signaling. Importantly, Dab2 is

upregulated during mesoderm differentiation of the mouse embryonic stem cells. The shRNA mediated knockdown of Dab2 affected colony forming efficiency of the ESCs and cell-cell adhesion [272]. However, the role of Dab2 in the regulation of the adult tissue stem cell behavior remains unexplored.

#### **6.1.6 Dab2 as a tumor suppressor**

The Dab2 was initially identified as a DOC-2 (differentially expressed in ovarian carcinoma) and found to be downregulated in this cancer [273]. Further study of carcinogen-induced mammary tumours showed downregulation of Dab2 that support the role of Dab2 as a tumour suppressor [274]. Initial studies on conditional knockout mice model showed hyperproliferation in the uterine and abnormal growth of ovarian epithelium without any difference in the tumour incidence [213, 275]. However, a recent study on another Dab2 conditional mutant mouse line showed higher tumour incidence and development of pre-neoplastic lesions [270]. Also, an increased frequency of tumour incidences was observed in the colon, ovary, mammary gland and uterus with age of Dab2 null mice [270, 275]. Subsequently, reduced expression of Dab2 has been identified in the human breast cancer [276, 277], head and neck [278], colon [279], prostate [280, 281], esophageal [282], and nasopharyngeal [283]. Collectively, all these reports strongly support the role of Dab2 in the inhibition of cell proliferation and as a potent tumour suppressor protein.

#### **6.1.7 Expression of Dab2 in hair follicle stem cells**

As mentioned previously, the bulge region of the hair follicle is Wnt suppressed during the telogen phase of hair cycle. This observation is further supported by the expression profiling of the HFSCs, which are isolated from the telogen phase of hair follicle. The three different microarray screen performed by the independent groups

suggested upregulation of the Wnt inhibitory factors such as Sfrp1, Dkk1 and Dab2, while expression of the Wnt ligands and Wnt stimulatory molecules are suppressed. Importantly, during telogen phase, Dab2 is upregulated by 5-15 folds in the HFSCs as compared to non-stem cell population [32, 55, 87]. The level of Dab2 expression is closely correlates with the status of the Wnt and BMP signaling during HFSCs quiescence (Wnt low, BMP high). However, whether the Dab2 is essential for maintaining Wnt and BMP signaling flux during HFSCs quiescence remains unexplored.

## 6.2 Results

### 6.2.1 Dab2 is upregulated in quiescent hair follicle stem cells

To establish the Dab2 conditional knockout system, we first quantified the level of Dab2 expression in the HFSCs vs basal layer cells of mouse epidermis. The bulge HFSCs (CD34<sup>+</sup> and  $\alpha$ 6 integrin<sup>+</sup>) and basal keratinocytes (CD34<sup>-</sup> and  $\alpha$ 6 integrin<sup>+</sup>) were directly FACS sorted in the RNA lysis buffer at PD49 (Telogen). The Dab2 transcript was quantified by performing real-time quantitative PCR.

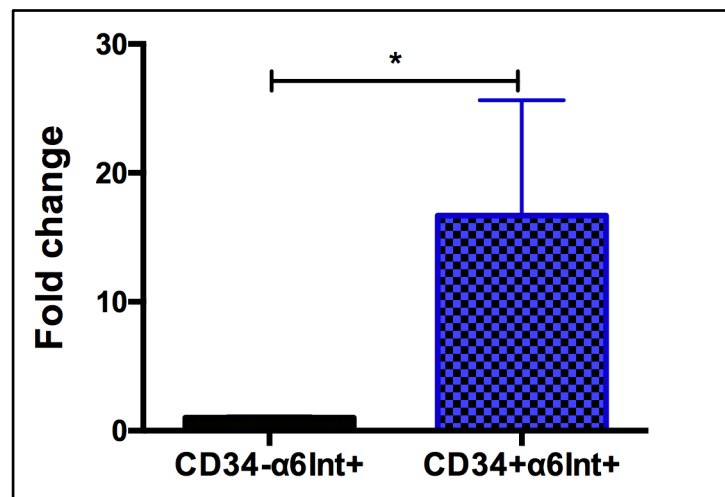


**Figure 6.5 Real time PCR quantification of Dab2 in HFSCs**

*Comparative transcript level of Dab2 in the basal keratinocytes and HFSCs at PD49.*

*The Dab2 level in the CD34<sup>-</sup>α6 integrin<sup>+</sup> cells is considered as one fold. n=2, Data are presented as mean ± SD, ns - P > 0.05, \* - P ≤ 0.05, \*\* - P ≤ 0.01, \*\*\* - P ≤ 0.001, \*\*\*\* - P ≤ 0.0001)*

Our result showed 15 to 25 folds upregulation of Dab2 transcript in the HFSCs as compared to non-stem cell population (Figure 6.5). This data confirms that the HFSCs showed an increased level of Dab2 during quiescence in the telogen phase of the hair cycle.

## 6.2.2 Efficiency of K14CreER mediated Dab2 knockout

We used K14CreER mice to conditionally ablate Dab2 in the Keratin 14 expressing mouse epidermal cells. First, to check the efficiency of the K14CreER line, we crossed K14CreER mice with the ROSA-STOP-YFP reporter mice, which express YFP protein upon deletion of the STOP codon. The K14CreER: ROSA-STOP-YFP mice were intraperitoneally injected with the tamoxifen for five consecutive days during PD20 to PD24 at the dose of 100  $\mu\text{g/g}$  body weight. The tamoxifen treated mice were sacrificed at PD49 and dorsal skin tissue sections were analysed for YFP expression by using the anti-GFP antibody.

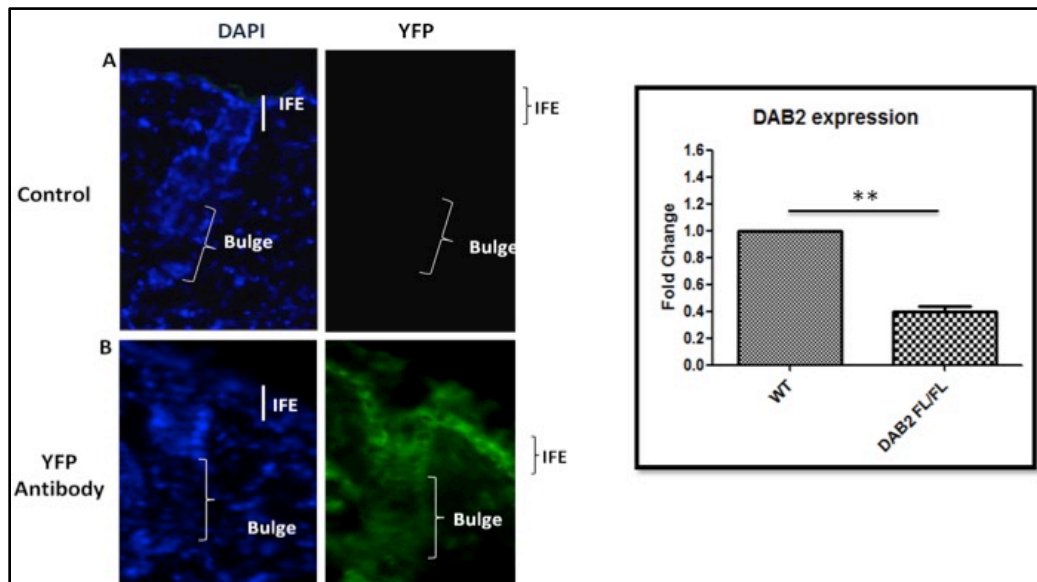


**Figure 6.6 Efficiency of K14CreER mediated gene knockout**

*A) Control tissue obtained from the K14CreER: ROSA-STOP-YFP mice. B) Tissue section treated with the anti-GFP antibody. C) The wild-type ( $Dab2^{fl/fl}$ : K14CreER<sup>-</sup>) and Dab2 cKO ( $Dab2^{fl/fl}$ : K14CreER<sup>+</sup>) mice were treated for five days with tamoxifen. The RNA was extracted from FACS sorted basal cells and analyzed for the Dab2 expression by Real Time PCR. Data are presented as mean  $\pm$  SD. (ns- non significant, \*\* $P < 0.005$ , \*\*\* $P < 0.0001$ , DAPI- Nuclear staining, YFP- Yellow fluorescent protein)*

Our results showed that the Cre induced recombination resulted in the deletion of a stop codon in basal cells of IFE and outer root sheath of the hair follicle, which are labelled by expression of YFP (Figure 6.6). This data confirmed that the tamoxifen dose is sufficient to induce Cre activity in the Keratin 14 expressing basal cells of our mouse strain. Further, the similar tamoxifen dose was used for the K14CreER: Dab2fl/fl mice and the deletion of the Dab2 floxed allele was confirmed by performing real-time PCR analysis of Dab2 gene in the FACS sorted  $\alpha 6$  integrin<sup>+</sup> cells. The data demonstrated 60-70% reduction of a Dab2 transcript in the K14CreER: Dab2fl/fl mice as compared to the wild-type mice (Figure 6.6).

### **6.2.3 Histology analysis of the hair follicle cycling in Dab2 cKO mice at various postnatal days**

To investigate the effect of Dab2 deletion on the morphological architecture of the epidermis and the hair follicle cycling, we performed the histological examination of the dorsal skin sections at various postnatal days (PD). The wild-type, K14CreER: Dab2fl/+ (Heterozygous) and K14CreER: Dab2fl/fl (Homozygous) mice were sacrificed during multiple postnatal days of the first hair cycle and followed by Hematoxylin and Eosin (H&E) staining on the dorsal skin tissue sections. Our data demonstrated a similar pattern of the hair follicle growth and hair follicle cycling in the wild type, K14CreER: Dab2fl/+ and K14CreER: Dab2fl/fl mice (Figure 6.7). In addition, we did not observe any significant histological abnormalities in the IFE structure and epidermal thickness. Importantly, the entire hair cycling pattern in this mixed background (129S4/Sv:C57BL/6:CD1) is delayed as compared to the pure background strain such as C57BL/6 or CD1 mice.

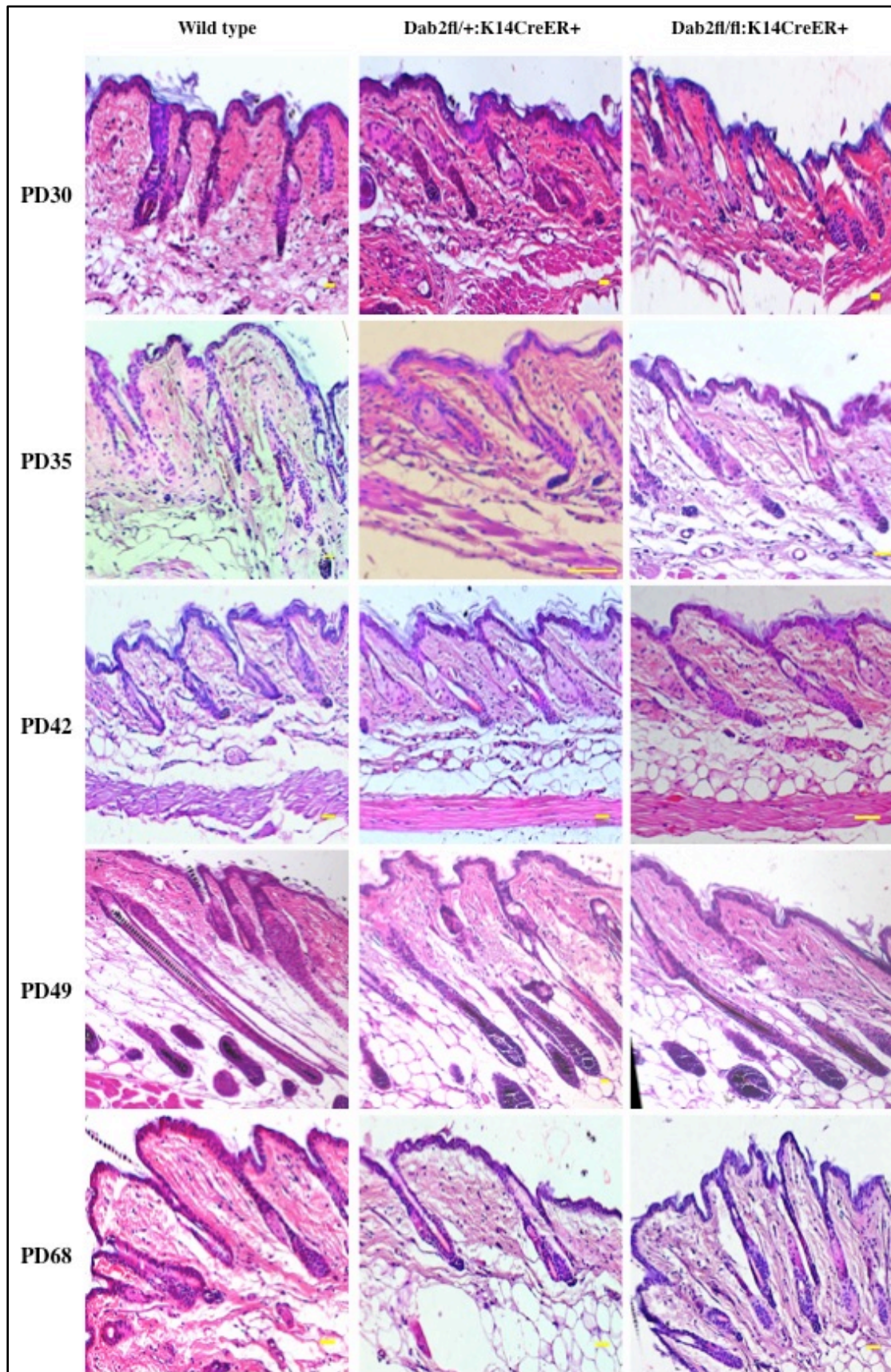


**Figure 6.7 Histological analysis of the hair follicle cycling**

*Wild type, Dab2fl/+; K14CreER<sup>+</sup> (heterozygous) and Dab2fl/fl; K14CreER<sup>+</sup> (homozygous) were sacrificed at various postnatal day ages such as PD30, PD35, PD42, PD49 and PD68. The dorsal skin tissue sections were stained by hematoxylin and eosin. PD-Postnatal Day. (n=2 mice/genotype, Scale bar: 100  $\mu$ m)*

Therefore, the study on the pure mouse line will identify whether Dab2 deletion has any effect on the hair follicle cycling and epidermal thickness. We further also evaluated the effect of Dab2 deletion on the sebaceous gland homeostasis by performing the Nile red staining on the tail skin wholemount tissues.

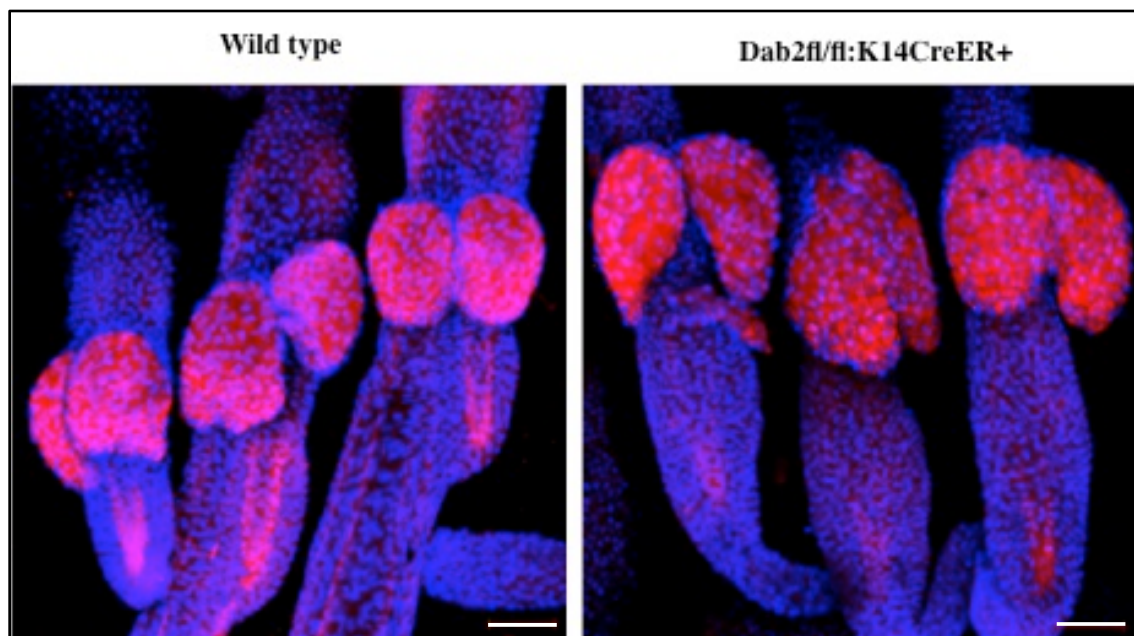


**Figure 6.8 Nile red staining on tail wholemount tissue**

*The Nile red staining was performed on the wholemount tail skin tissue at PD68. The Nile red specifically stains sebocytes and nuclei were stained with DAPI. (n=3 mice/genotype, Scale bar: 50  $\mu$ m)*

However, we did not find any significant alterations in the architecture as well as the size of the sebaceous gland (Figure 6.8). Overall, these data suggest that Dab2 may not have any significant role in maintaining the normal homeostasis of the hair cycling and sebaceous gland in vivo.

#### 6.2.4 Loss of Dab2 decreases the active $\beta$ -catenin level in hair follicle

Previous reports on the other cell type suggest a potent inhibitory activity of Dab2 on the Wnt signaling. Further, in different cell type of the epidermis and hair follicle, the Dab2 shows distinct expression pattern with the highest expression in the HFSCs. Therefore, we sought to investigate the effect of the Dab2 deletion on the active  $\beta$ -catenin level during the telogen phase of the hair cycle in the wild type, K14CreER: Dab2fl/+ and K14CreER: Dab2fl/fl mice. We injected the tamoxifen during the 1<sup>st</sup> telogen phase (PD20-24) and analyzed the level of the active  $\beta$ -catenin by immunofluorescence assay (Antibody specific for the non-phospho form of  $\beta$ -catenin, Active form) during the second telogen phase such as PD68. Surprisingly, we observed a reduced level of the active  $\beta$ -catenin, specifically in the bulge area of the telogen hair follicle of the K14CreER: Dab2fl/fl mice (Figure 6.9). However, we did not observe the nuclear localization of the  $\beta$ -catenin in any of the genotypes during telogen phase (Figure 6.9).

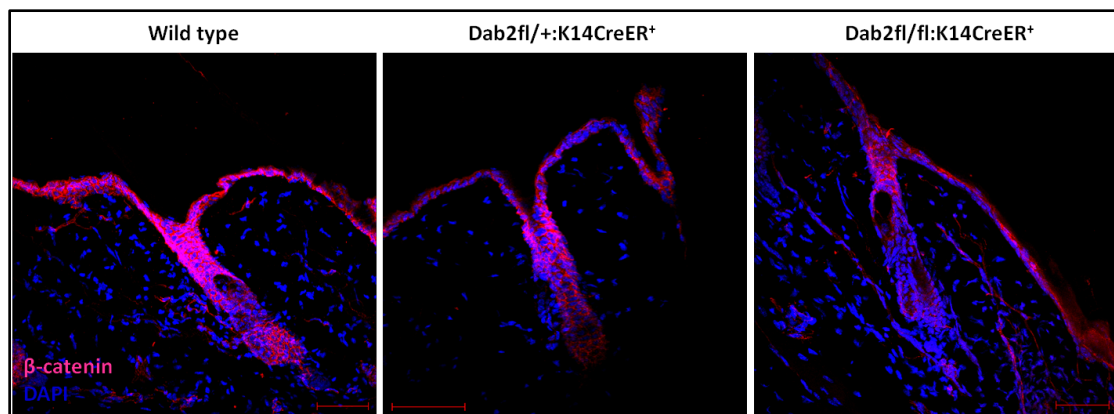


**Figure 6.9 Comparative level of active  $\beta$ -catenin in the hair follicle and IFE**

*The active and non-active form of the  $\beta$ -catenin was differentiated by using the antibody against non-phospho  $\beta$ -catenin. The level of active  $\beta$ -catenin was analysed by the Immunofluorescence analysis at PD68. (n=3 mice/genotype, Scale bar: 50  $\mu$ m)*

These data suggest that Dab2 may have a role in maintaining the level of non-phospho  $\beta$ -catenin in the cytoplasm of the cells: however, the detailed further investigation is required to decipher the role of Dab2 in the regulation of  $\beta$ -catenin expression and cytoplasmic degradation.

### 6.2.5 Decreased cell proliferation in the Dab2 cKO mice

The bulge HFSCs are in the proliferation inhibited state during the telogen phase of the hair cycle. However, the cells of the upper region of the hair follicle and epidermis undergo a cell division even during the telogen phase. To further explore the effect of the reduced level of active  $\beta$ -catenin on the cell proliferation of the hair follicle and epidermis, we performed the immunofluorescence assay by using the Ki67 antibody on the dorsal skin tissues sections.

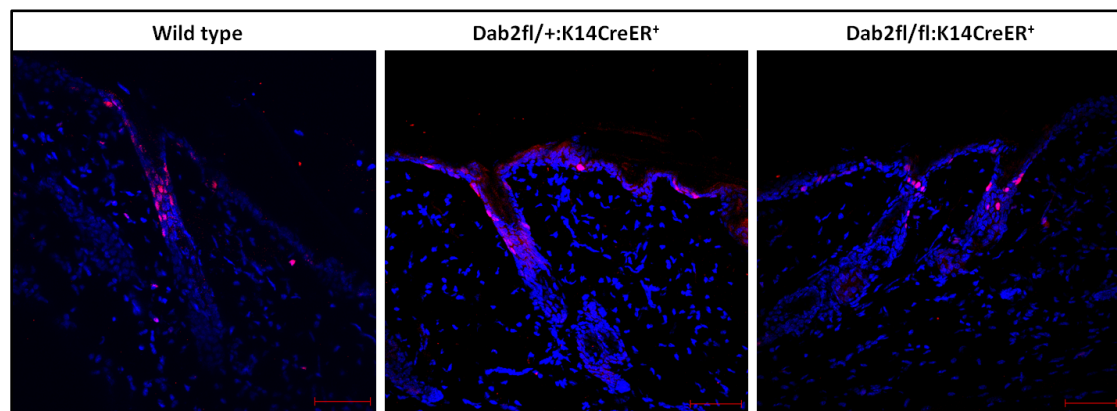


**Figure 6.10 Analysis of cell proliferation by Ki67 staining**

*The Ki67 staining measured the comparative cell proliferation during telogen phase of the hair cycle. The Ki67 positive cells were detected by the immunofluorescence analysis at PD68 in the wild-type, K14CreER: Dab2fl/+ and K14CreER: Dab2fl/fl mice. (n=3 mice/genotype, Scale bar: 50  $\mu$ m)*

Interestingly, our data showed a reduced numbers of the proliferating cells in the junctional zone area of the hair follicle (Figure 6.10). We did not observe any

abnormal cell proliferation in the other part of the hair follicle. As the Dab2 is classically reported for its tumour suppressor functions, these data suggest a divergent role of Dab2 in the regulation of the cell proliferation.

### 6.2.6 Dab2 deletion does not alter epidermal differentiation

In addition, we also evaluated the effect of Dab2 ablation on the differentiation of the keratinocytes in the interfollicular epidermis.

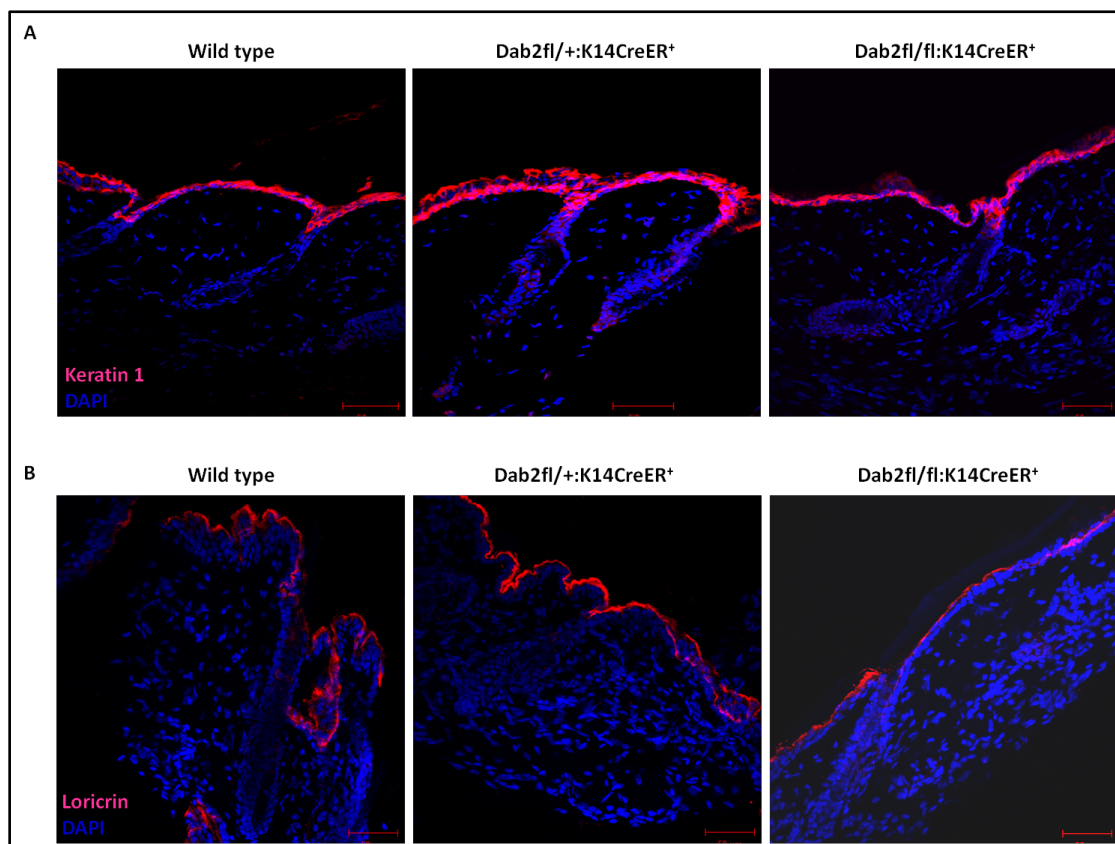


**Figure 6.11 Analysis of the epidermal differentiation**

*A) Immunofluorescence staining of Keratin 1 on the dorsal skin tissue sections of wild-type, K14CreER: Dab2fl/+ and K14CreER: Dab2fl/fl mice at PD68. B) Immunofluorescence staining of Loricrin on the dorsal skin tissue sections of wild-type, K14CreER: Dab2fl/+ and K14CreER: Dab2fl/fl mice at PD68. (n=3 mice/genotype), Scale bar: 50 $\mu$ m*

We marked the Keratin 1 expressing suprabasal keratinocytes by using anti-Keratin 1 antibody and detected by the immunofluorescence assay. Our data demonstrated no significant abnormalities in the thickness of the suprabasal cells layer and expression of the Keratin 1 in the dorsal skin tissue sections of the wild-type, K14CreER: Dab2fl/+ and K14CreER: Dab2fl/fl mice. Further, we also checked the level of the Loricrin, which is a marker of the cornified layer of the epidermis. We performed the immunofluorescence analysis on the dorsal skin tissue sections at PD68, which showed no difference of Loricrin expression in the wild-type, K14CreER: Dab2fl/+ and K14CreER: Dab2fl/fl mice tissue sections.

### 6.2.7 FACS analysis of hair follicle stem cell population

Further, the reduced level of  $\beta$ -catenin led us to investigate whether ablation of Dab2 has any effect on the overall HFSCs population during the telogen phase of the hair cycle.

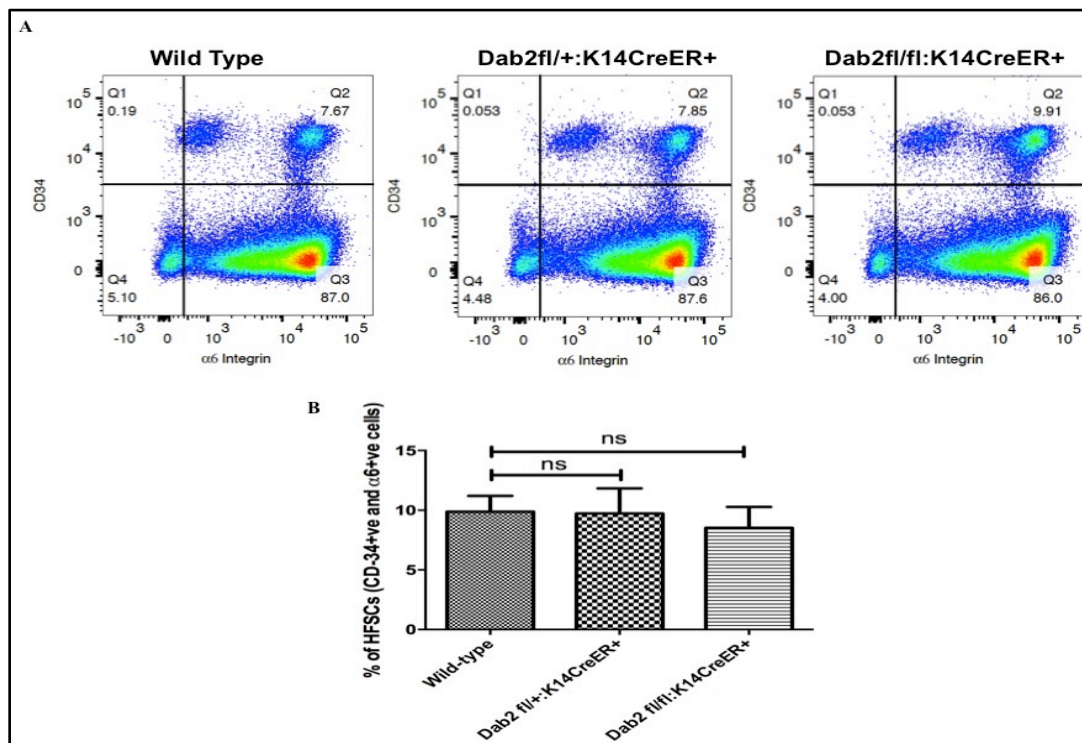


Figure 6.12 Quantification of HFSCs by flow cytometry

*A) FACS analysis of CD34+/ $\alpha$ 6-integrin+ bulge HFSCs at PD68. B) Quantification of FACS analysis of CD34+/ $\alpha$ 6-integrin+ bulge HFSCs from mouse epidermis at PD68. Data are presented as mean  $\pm$  SD. \*\* $P$ <0.005, \*\*\* $P$ <0.0001, ns- not significant*

We quantified the total numbers of the hair follicle stem cells in the wild-type, K14CreER: Dab2fl/+ and K14CreER: Dab2fl/fl mice at PD68 by performing the flow cytometry analysis. The anti-CD34 and anti- $\alpha$ 6 integrin antibodies were used for double labelling of the HFSCs. However, our data showed no significant alterations in the HFSCs pool of the wild type, K14CreER: Dab2fl/+ and K14CreER: Dab2fl/fl mice (Figure 6.12 A-B). This result suggests that the deletion of Dab2 may not affect the maintenance of the HFSCs population during the quiescent state of the hair cycle.

### **6.2.8 Dab2 ablated HFSCs showed reduced colony forming efficiency**

Our previous experiments of the HFSCs quantification by flow cytometry and cell proliferation assay by Ki67 staining showed that the deletion of the Dab2 does not affect maintenance of the stem cell pool and proliferation behaviour when they are in the quiescent state. To examine whether the loss of Dab2 has any effect on the maintenance of stemness characteristic when they are induced to proliferate in vitro, we performed the colony formation assays of FACS purified Bu-HFSCs (10,000-20,000) during the second telogen phase of the hair cycle to examine its independent colony forming potential in the wild-type, K14CreER: Dab2fl/+ and K14CreER: Dab2fl/fl mice.

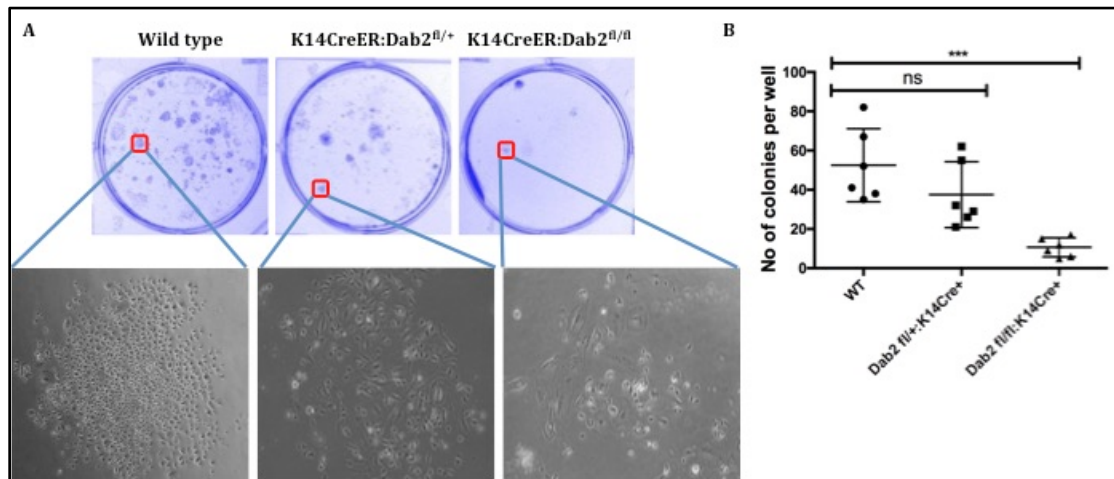


**Figure 6.13 Colony forming efficiency of HFSCs**

**A)** Hair follicle stem cells were FACS purified from wild-type, *K14CreER: Dab2fl/+* (heterozygous) and *K14CreER: Dab2fl/fl* (homozygous) and equal number HFSCs (20,000) were plated in a six-well plate. Colonies were stained by using crystal violet.

**B)** Quantification of total no of colonies per well in Wild-type, *K14CreER: Dab2fl/+* (heterozygous) and *K14CreER: Dab2fl/fl* (homozygous). Data are presented as mean  $\pm$  SD. \*\* $P < 0.005$ , \*\*\* $P < 0.0001$

The FACS sorted HFSCs were cultured in the conditioned E-media containing 3T3 J2 fibroblast with 10 ng/ml EGF for three weeks. After formation of colonies, the 3T3 J2 cells were removed by differential trypsinization; colonies were fixed with 1% PFA for 15 min and stained for one hour with 0.05% crystal violet in PBS (Figure 6.13 A). Interestingly, colonies developed from the HFSCs of the *K14CreER: Dab2fl/fl* mice showed a reduced growth as displayed from the smaller size of colonies and exhibited affected cell morphology as compared to the colonies of wild-type mice (Figure 6.13 A-B). Overall, the HFSCs from the homozygous cKO mice showed strongly decreased colony-forming ability, which suggest its reduced stemness potential when induced to proliferate in vitro. Together, *Dab2* may have an essential role in the

maintenance of the stemness potential of the HFSCs when the cells are under constant proliferative pressure.

### 6.2.9 BrdU label retaining cells (LRC) assay

To investigate the effect of the Dab2 deletion on the slow cycling characteristic of HFSCs, we performed the label retaining cells assay, which is classically used to identify the location of the slow-cycling cells in the adult tissue.

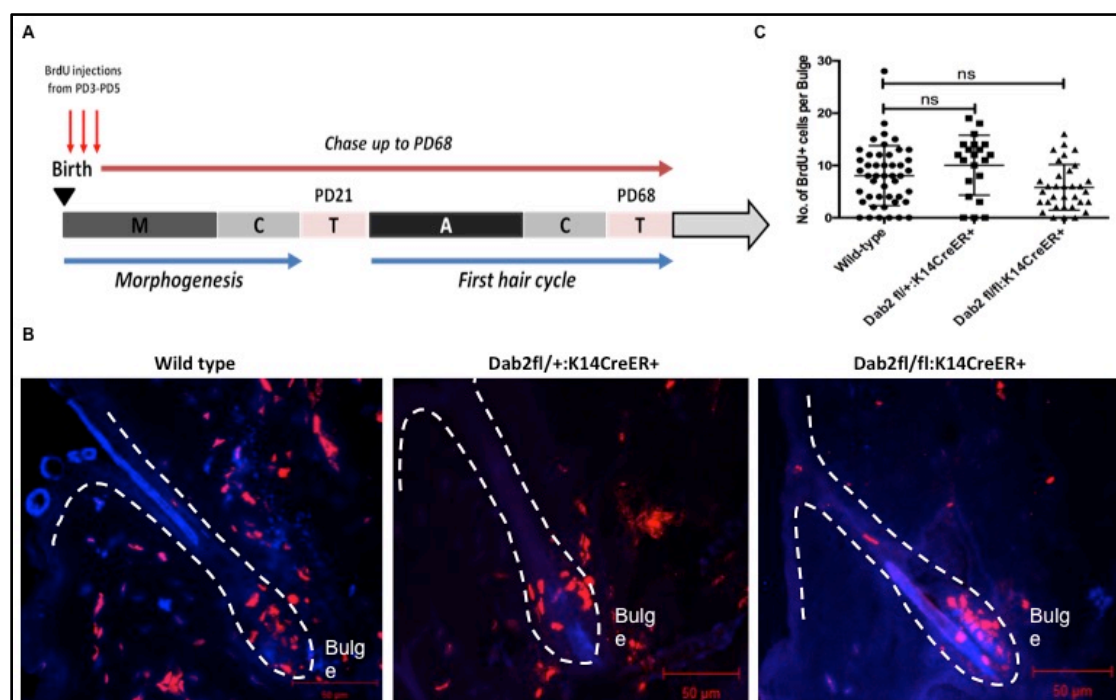


**Figure 6.14** Label retaining cells (LRCs) assay

**A)** Scheme of BrdU injection and a chase period. BrdU was injected subcutaneously at a dose of  $50\mu\text{g/g}$  body weight during PD3–PD5 at 12-h intervals and chase up to PD68. **B)** Immunofluorescence labelling of BrdU positive cells at PD68. The Label Retaining Cells per bulge were counted manually in the sections of the wild-type, *K14CreER: Dab2fl/+* (heterozygous) and *K14CreER: Dab2fl/fl* (homozygous), Scale bar:  $50\mu\text{m}$ . **C)** Quantification of BrdU positive cells in the hair follicle bulge at PD68,  $n=3$  mice/genotype. Data are presented as mean  $\pm$  SD, ns-not significant.

We subcutaneously injected BrdU at the dose of 50  $\mu\text{g/g}$  body weight during early age such as PD3-PD5 (one injection/12 hour, total six injections in three days) (Figure 6.14 A). The chances of labelling almost all the cells of the tissue are highest during this time points, as cells of the newly formed tissue are rapidly proliferating during this time window. We chased these mice till the second telogen (PD68) and then sacrificed to assess the numbers of BrdU positive cells in the bulge of the hair follicle. The BrdU positive cells were detected by performing the immunofluorescence assay on the dorsal skin tissue sections by using the anti-BrdU antibody (Figure 6.14 B). We counted the BrdU positive cells per bulge in the hair follicle of wild type, K14CreER: Dab2<sup>fl/+</sup> and K14CreER: Dab2<sup>fl/fl</sup> mice. Our data showed no statistically significant difference in the numbers of BrdU positive cells per hair follicle bulge (Figure 6.14 C). This data suggest that Dab2 deletion may not affect the slow cycling characteristic of stem cells during normal hair follicle regeneration and growth: however, it may have essential functions in the regulation of the stem cells cycling during proliferation induced by exogenous proliferative stimuli.

### 6.3 Discussion

Previous studies have characterized the role of Dab2 as an inhibitor of cell proliferation that further supported by the studies on different tumour tissues, which showed downregulation of Dab2 expression. These studies have established Dab2 as a potent tumour suppressor and regulator of cell proliferation in the normal tissue. Importantly, the slow cycling stem cells such as the HFSCs also showed increased expression of the Dab2 while they are in the resting state [32, 55, 87]. However, whether Dab2 is required for maintaining the quiescence of the adult tissue stem cells by inhibiting the cell proliferation and does the Dab2 mediated regulation of the stem cell proliferation is a mechanism through which Dab2 act as a tumour suppressor is largely remained unexplored.

The functional contribution of the Wnt signaling regulators has been well established in controlling HFSCs behavior [115, 119, 124, 134, 284-286]. It has been shown that the HFSCs expresses different Wnt inhibitors such as Dkk3, secreted frizzled-related protein 1 (Sfrp1) and disabled homolog 2 (Dab2) during quiescence. We have also validated the increased expression of the Dab2 in the quiescent HFSCs. The K14CreER mediated deletion of Dab2 showed no major abnormalities in the epidermis and sebaceous gland compartment. This is likely due to the high turnover of the epidermal cells in these compartments, where the cells undergo frequent divisions and these cells are under reduced inhibitory signaling flux. This also correlates with the comparative level of the Dab2 in the basal cells versus HFSCs. Further; we observed a reduced level of the active  $\beta$ -catenin in the Dab2 cKO mice skin. Although there is no any direct report of the Dab2 functions on the Wnt signaling regulation in skin stem cells, our observation is partly supported by the study of circadian clock regulators in the HFSCs. It has been shown that the bulge contains heterogeneous cell

population with respect to expression of the circadian clock regulators and represents an equal ratio of the Venus<sup>bright</sup> and Venus<sup>dim</sup> HFSCs. However, the microarray profiling of these cell types showed increased expression of the Dab2 in the Venus<sup>bright</sup> HFSCs as compared to Venus<sup>dim</sup> cells during the telogen phase [287]. In addition, further study of the clock regulators showed that the reduced level of the Dab2 correlated with the decreased Wnt signaling and increased TGF- $\beta$  signaling. Therefore, Dab2 may have functional involvement in controlling the level of  $\beta$ -catenin differently through regulating its degradation or expression via an unknown mechanism. Importantly, the proximal and distal promoter regions of Dab2 has been shown to contain binding sites for CLOCK regulators and as the hair cycle progress, the ratio of Venus<sup>bright</sup> and Venus<sup>dim</sup> cell reaches 90:10 during the anagen phase. However, the level of Dab2 in the Venus<sup>bright</sup> cells during this time points is unknown. Therefore, it is possible that the bulge cells population expresses Dab2 heterogeneously and the dormant cells, which are Venus<sup>dim</sup> start expressing the Dab2 during anagen onset. Therefore, Dab2 may require for the proliferation and differentiation of these cells during the anagen as shown for the other Wnt-related factors such as Sox9, which labels the HFSCs and requires for the outer root sheath differentiation [49, 288]. Also, our data of the colony forming efficiency are in agreement with the colony forming efficiency of Venus<sup>bright</sup> cells, which expresses an increased level of Dab2 and showed higher clonogenic potential than Venus<sup>dim</sup> cells. Together, all these data indicate that the Dab2 mediated regulation of the Wnt signaling and cell proliferation is context dependent and may have a positive role in the regulation of cell proliferation at least in the bulge stem cell compartment of the skin in a stage and time-dependent manner.

The downregulation of Dab2 expression has been shown in almost all epithelial tumour tissues such as breast [277, 289], head and neck [278], oesophageal and colon cancer [279, 283, 290]. The major mechanism reported for the Dab2 downregulation is promoter hypermethylation and the downregulation of the Dab2 promotes cancer cell proliferation. On the other hand, Dab2 has been shown to play an essential role in the cancer cell migration and invasion as knockdown of Dab2 resulted in reduced migration and invasion of PC3 cells along with a reduction in the tumorigenic potential. Therefore, detailed study of the Dab2 expression during different stages of the hair cycle and as well as in different processes of cancer progression and status of the cell proliferation during that time points will elucidate the Dab2 mediated mechanisms in the regulation of HFSCs and development of cancer.

## ***7. Summary and Conclusion***



## 7.1 Summary and Conclusion

The adult tissue stem cells are highly dynamic in their proliferation and differentiation potential. They divide in response to the homeostatic cues for supplying progenitors and differentiated cells against the requirement of tissue. During normal homeostatic conditions, stem cells are thought to restrict their divisions by maintaining quiescent state, which is required for the maintenance of the adult tissue stem cell pool throughout the life of an animal. Various signaling mechanisms such as developmentally conserved as well as mitogenic signaling pathways govern the regulation of this cyclic activity of stem cells. Our study highlighted the functional involvement of two different signaling regulators; Secretory phospholipase A<sub>2</sub>-IIA (sPLA<sub>2</sub>-IIA) through EGFR mediated c-Jun signaling and Dab2 through Wnt signaling in HFSCs regulation. In the first part of our study, we have investigated the effect of sPLA<sub>2</sub>-IIA overexpression on the maintenance of the HFSCs pool and discovered that sPLA<sub>2</sub>-IIA generates proliferative pressure through the enhanced expression of the mitogenic signaling regulators such as EGFR and c-Jun. The increased flux of these signaling mechanisms resulted in the rapid proliferation of HFSCs that alters their normal homeostatic proliferation dynamics. The untimely repetitive proliferative signals resulted in the exhaustion of the quiescent HFSCs pool. However, the HFSCs displayed robust regenerative potential, as when they are challenged by removing the hair shaft from the hair follicle, the remaining HFSCs population were able to produce an entire hair shaft. However, enhanced overexpression of the sPLA<sub>2</sub>-IIA in the homozygous mice resulted in the almost complete HFSCs loss and mice exhibited development of cyclic alopecia during early age. Besides, our study also confirms the limited contribution of the HFSCs in the initial phases of the wound healing process. Depletion of the HFSCs delayed only

initial recovery of the wound area, but not the complete wound closure. This is likely due to the functions of the IFE derived epidermal cells that may compensate initial delay at the later stages of wound healing. In conclusion, our work on the sPLA<sub>2</sub>-IIA demonstrated its involvement in the regulation of the adult tissue stem cells behaviour through growth factor signaling mechanisms, which was previously studied for its participation in only lipid catabolism.

In the other part of our study, we explored the involvement of the Disabled 2 (Dab2) protein in the regulation of the HFSCs. The involvement of the Wnt signaling in the regulation of the epidermal components such as the hair follicle, sebaceous gland and IFE has been extensively studied form last two decades. However, how the activity of Wnt signaling is being controlled during different stages of the hair follicle cycling is poorly understood. The Dab2 protein has been classified as a tumour suppressor and shown to get downregulated in various cancers. However, our study using conditional knockout mice model showed that Dab2 deletion reduces cell proliferation and affects the colony forming efficiency of the sorted HFSCs. In addition, deletion of Dab2 also resulted in the reduced level of active  $\beta$ -catenin. Therefore, the decreased activity of  $\beta$ -catenin likely to be a significant factor for reduced colony-forming ability of the HFSCs in vitro. However, further investigations are required for identifying the stage-dependent expression pattern of Dab2 and corresponding status of the cell proliferation for establishing role of Dab2 in the regulation of HFSCs compartment. Importantly, this is the first study to investigate the role of cytoplasmic Wnt signaling inhibitor in the context of the adult HFSCs functions.

Overall, this study has contributed in the field of tissue stem cells biology to understand how different signaling regulators affect the proliferation and

differentiation of the HFSCs and how the deregulated activity of adult tissue stem cells resulted in the abnormal tissue homeostasis and disease.

## **Salient findings**

### **Objective: 1**

1. Overexpression of sPLA<sub>2</sub>-IIA reduces colony-forming ability of the primary keratinocytes in vitro.
2. Mouse primary keratinocytes showed increased expression of the EGFR, c-Jun and enhanced activation of the JNK and c-Fos.
3. In the epidermis, we observed increased activation of the EGFR and c-Jun in the K14- sPLA<sub>2</sub>-IIA mice.
4. Increased activation of the c-Jun in the mouse primary keratinocytes is mediated through increased JNK activation.
5. Upregulated c-Jun signaling resulted in the increased keratinocytes proliferation, which was rescued by the treatment of the JNK inhibitor.
6. In our in vivo study, overexpression sPLA<sub>2</sub>-IIA resulted in the faster hair growth followed by hair depilation, which was reverted efficiently by the topical application of the JNK inhibitor.
7. The homozygous mice overexpressing sPLA<sub>2</sub>-IIA showed complete loss of HFSCs and developed cyclic alopecia at an early age. Our mechanistic study highlighted an abnormal expression of the matrix cells differentiation regulators and hair keratins in the K14- sPLA<sub>2</sub>-IIA homozygous mice.
8. In vivo wound healing experiment showed initial delay in the wound closure; however, it was completely recovered at the similar rate of wild type mice.

**Objective: 2**

1. Dab2 is highly upregulated in the HFSCs during telogen as compared to the non-stem cells population
2. Conditional ablation of Dab2 was achieved up to 70% by tamoxifen inducible K14CreER mice
3. Dab2 ablation does not affect numbers of the HFSCs in vivo as assessed by the flow cytometry and label retention cells assay
4. Deletion of Dab2 may not have any effect on the epidermal differentiation of the mouse keratinocytes
5. Deletion of Dab2 drastically impairs colony forming efficiency of the sorted HFSCs
6. Deletion of Dab2 reduces level of the active  $\beta$ -catenin in vivo
7. Loss of Dab2 partly reduces cell proliferation in vivo as assessed by Ki67

## 7.2 Future Perspectives

Our study of sPLA<sub>2</sub>-IIA was mainly focused on the regulation of the HFSCs proliferation and differentiation. However, it would be interesting to look at the other stem cells population in the epidermis such as IFE stem cells and sebaceous gland stem cells. Exploring the effect of common signaling modulator on different stem cells compartment would unravel how different stem cell populations respond differently and how they maintain stem cells pool at their best in the respective stem cell compartment. This would also highlight the level of plasticity of different stem cells in maintaining the progenitor pool, which can function as compensatory mechanisms during the absence of the specific stem cells population. In addition, the study can be performed to understand the effect of sPLA<sub>2</sub>-IIA overexpression on the dermal tissue architecture and maintenance of the melanocytes stem cells. Importantly, our study provides leads to further investigate the role of sPLA<sub>2</sub>-IIA in the conditions of an abnormal proliferation such as cancer. It has been shown that different tumours express an increased level of sPLA<sub>2</sub>-IIA. Therefore, it warrants understanding whether sPLA<sub>2</sub>-IIA has any functional role in the regulation of tumour cell proliferation and whether the enhanced proliferation is mediated through the EGFR-JNK/c-Jun mechanism? The study by using of pharmacological inhibitor will identify the specific role of sPLA<sub>2</sub>-IIA in tumour cell proliferation, metastasis and also in the regulation of cancer stem cells.

Understanding the functional role of Dab2, it is required to investigate how Dab2 level oscillates with phases of cell proliferation and quiescence during hair cycle. Immunohistochemical analysis of Dab2 expression during telogen, early anagen, mid anagen and late anagen would unravel the relationship between Dab2 and cell proliferation. It is required to investigate the role of Dab2 in the hair follicle cycling

pattern in the mouse strain having a pure genetic background as we observed a delayed initiation of the hair follicle cycle in the mixed background. Further, we think that the Dab2 deletion results in the proliferative defects only when the HFSCs are stimulated for the proliferation by exogenous cues. This can be further investigated by multiple ways such as by performing experiment of hair depilation that induces proliferation of the bulge HFSCs, topical treatment of the proliferative inducer such as TPA and scratch as well as full thickness wounding. These studies will identify if Dab2 is required for the proliferation of the HFSCs during non-homeostatic tissue maintenance and regeneration. Further, it is also required to investigate whether all bulge cells expresses Dab2 at a similar level because the previous study has shown the differential level of Dab2 in different subpopulation of the HFSCs. This can be further studied by using pTRE-H2BGFP: K5tTa system to find if the HFSCs proliferative defect is compensated by the proliferation of those cells, which expresses Dab2 differentially. Importantly, it would be interesting to investigate the role of Dab2 in skin tumour initiation, promotion and progression as the condition knockout system provide flexibility to induce gene knockout at time of interest. The DMBA/TPA induced skin carcinogenesis will also identify if Dab2 deletion has any effect on cell proliferation when they are induced for the proliferation. This study will also provide information to establish the role of Dab2 as a tumour suppressor or tumour promoter for the skin tissue.

## 8. Bibliography

1. hyslop louise a., a.l., stojkovic miodrag, lako majlinda, *human embryonic stem cells: biology and clinical implications. Expert Reviews in Molecular Medicine*. Cambridge University Press, 2005. **7**(19): p. 21.
2. Li, L. and H. Clevers, *Coexistence of quiescent and active adult stem cells in mammals*. Science, 2010. **327**(5965): p. 542-5.
3. Wickett, R.R. and M.O. Visscher, *Structure and function of the epidermal barrier*. American Journal of Infection Control. **34**(10): p. S98-S110.
4. Pasparakis, M., I. Haase, and F.O. Nestle, *Mechanisms regulating skin immunity and inflammation*. Nat Rev Immunol, 2014. **14**(5): p. 289-301.
5. Fuchs, E., *Beauty is skin deep: the fascinating biology of the epidermis and its appendages*. Harvey Lect, 1998. **94**: p. 47-77.
6. Fuchs, E. and S. Raghavan, *Getting under the skin of epidermal morphogenesis*. Nat Rev Genet, 2002. **3**(3): p. 199-209.
7. Alonso, L. and E. Fuchs, *Stem cells in the skin: waste not, Wnt not*. Genes Dev, 2003. **17**(10): p. 1189-200.
8. Alonso, L. and E. Fuchs, *Stem cells of the skin epithelium*. Proc Natl Acad Sci U S A, 2003. **100 Suppl 1**: p. 11830-5.
9. Gharzi, A., A.J. Reynolds, and C.A. Jahoda, *Plasticity of hair follicle dermal cells in wound healing and induction*. Exp Dermatol, 2003. **12**(2): p. 126-36.
10. Wang, H., B. Chen, and D. Hu, *[Role of hair follicle stem cell in wound healing and correlative signals]*. Zhongguo Xiu Fu Chong Jian Wai Ke Za Zhi, 2007. **21**(1): p. 90-3.
11. Blanpain, C. and E. Fuchs, *Stem cell plasticity. Plasticity of epithelial stem cells in tissue regeneration*. Science, 2014. **344**(6189): p. 1242281.
12. Gonzales, K.A.U. and E. Fuchs, *Skin and Its Regenerative Powers: An Alliance between Stem Cells and Their Niche*. Dev Cell, 2017. **43**(4): p. 387-401.
13. Li, A.G., M.I. Koster, and X.J. Wang, *Roles of TGFbeta signaling in epidermal/appendage development*. Cytokine Growth Factor Rev, 2003. **14**(2): p. 99-111.
14. Stern, C.D., *Neural induction: old problem, new findings, yet more questions*. Development, 2005. **132**(9): p. 2007-21.
15. Fuchs, E., *Scratching the surface of skin development*. Nature, 2007. **445**(7130): p. 834-42.
16. Byrne, C., M. Tainsky, and E. Fuchs, *Programming gene expression in developing epidermis*. Development, 1994. **120**(9): p. 2369-83.

17. Liu, S., H. Zhang, and E. Duan, *Epidermal development in mammals: key regulators, signals from beneath, and stem cells*. *Int J Mol Sci*, 2013. **14**(6): p. 10869-95.
18. Koster, M.I. and D.R. Roop, *Mechanisms regulating epithelial stratification*. *Annu Rev Cell Dev Biol*, 2007. **23**: p. 93-113.
19. Fuchs, E., *Skin stem cells: rising to the surface*. *J Cell Biol*, 2008. **180**(2): p. 273-84.
20. Solanas, G. and S.A. Benitah, *Regenerating the skin: a task for the heterogeneous stem cell pool and surrounding niche*. *Nat Rev Mol Cell Biol*, 2013. **14**(11): p. 737-48.
21. Blanpain, C. and E. Fuchs, *Epidermal homeostasis: a balancing act of stem cells in the skin*. *Nat Rev Mol Cell Biol*, 2009. **10**(3): p. 207-17.
22. Potten, C.S., *The epidermal proliferative unit: the possible role of the central basal cell*. *Cell Tissue Kinet*, 1974. **7**(1): p. 77-88.
23. Ghazizadeh, S. and L.B. Taichman, *Multiple classes of stem cells in cutaneous epithelium: a lineage analysis of adult mouse skin*. *Embo j*, 2001. **20**(6): p. 1215-22.
24. Clayton, E., et al., *A single type of progenitor cell maintains normal epidermis*. *Nature*, 2007. **446**(7132): p. 185-9.
25. Jones, P.H., B.D. Simons, and F.M. Watt, *Sic transit gloria: farewell to the epidermal transit amplifying cell?* *Cell Stem Cell*, 2007. **1**(4): p. 371-81.
26. Sada, A., et al., *Defining the cellular lineage hierarchy in the interfollicular epidermis of adult skin*. *Nat Cell Biol*, 2016. **18**(6): p. 619-31.
27. Alonso, L. and E. Fuchs, *The hair cycle*. *J Cell Sci*, 2006. **119**(Pt 3): p. 391-3.
28. Schepeler, T., M.E. Page, and K.B. Jensen, *Heterogeneity and plasticity of epidermal stem cells*. *Development*, 2014. **141**(13): p. 2559-67.
29. Jensen, K.B., et al., *Lrig1 expression defines a distinct multipotent stem cell population in mammalian epidermis*. *Cell Stem Cell*, 2009. **4**(5): p. 427-39.
30. Snippert, H.J., et al., *Lgr6 marks stem cells in the hair follicle that generate all cell lineages of the skin*. *Science*, 2010. **327**(5971): p. 1385-9.
31. Cotsarelis, G., T.T. Sun, and R.M. Lavker, *Label-retaining cells reside in the bulge area of pilosebaceous unit: implications for follicular stem cells, hair cycle, and skin carcinogenesis*. *Cell*, 1990. **61**(7): p. 1329-37.
32. Tumber, T., et al., *Defining the epithelial stem cell niche in skin*. *Science*, 2004. **303**(5656): p. 359-63.
33. Horsley, V., et al., *Blimp1 defines a progenitor population that governs cellular input to the sebaceous gland*. *Cell*, 2006. **126**(3): p. 597-609.
34. Hardy, M.H., *The secret life of the hair follicle*. *Trends Genet*, 1992. **8**(2): p. 55-61.
35. Chase, H.B., *Growth of the hair*. *Physiol Rev*, 1954. **34**(1): p. 113-26.

36. Yang, C.C. and G. Cotsarelis, *Review of hair follicle dermal cells*. J Dermatol Sci, 2010. **57**(1): p. 2-11.
37. Duverger, O. and M.I. Morasso, *Epidermal patterning and induction of different hair types during mouse embryonic development*. Birth Defects Res C Embryo Today, 2009. **87**(3): p. 263-72.
38. Millar, S.E., *Molecular mechanisms regulating hair follicle development*. J Invest Dermatol, 2002. **118**(2): p. 216-25.
39. Chi, W., E. Wu, and B.A. Morgan, *Dermal papilla cell number specifies hair size, shape and cycling and its reduction causes follicular decline*. Development, 2013. **140**(8): p. 1676-83.
40. Jahoda, C.A., K.A. Horne, and R.F. Oliver, *Induction of hair growth by implantation of cultured dermal papilla cells*. Nature, 1984. **311**(5986): p. 560-2.
41. Schneider, M.R., R. Schmidt-Ullrich, and R. Paus, *The hair follicle as a dynamic miniorgan*. Curr Biol, 2009. **19**(3): p. R132-42.
42. Legue, E. and J.F. Nicolas, *Hair follicle renewal: organization of stem cells in the matrix and the role of stereotyped lineages and behaviors*. Development, 2005. **132**(18): p. 4143-54.
43. Nowak, J.A., et al., *Hair follicle stem cells are specified and function in early skin morphogenesis*. Cell Stem Cell, 2008. **3**(1): p. 33-43.
44. Lavker, R.M., et al., *Hair follicle stem cells*. J Investig Dermatol Symp Proc, 2003. **8**(1): p. 28-38.
45. Morris, R.J. and C.S. Potten, *Highly persistent label-retaining cells in the hair follicles of mice and their fate following induction of anagen*. J Invest Dermatol, 1999. **112**(4): p. 470-5.
46. Trempus, C.S., et al., *Enrichment for living murine keratinocytes from the hair follicle bulge with the cell surface marker CD34*. J Invest Dermatol, 2003. **120**(4): p. 501-11.
47. Liu, Y., et al., *Keratin 15 promoter targets putative epithelial stem cells in the hair follicle bulge*. J Invest Dermatol, 2003. **121**(5): p. 963-8.
48. Lyle, S., et al., *The C8/144B monoclonal antibody recognizes cytokeratin 15 and defines the location of human hair follicle stem cells*. J Cell Sci, 1998. **111** ( Pt 21): p. 3179-88.
49. Vidal, V.P., et al., *Sox9 is essential for outer root sheath differentiation and the formation of the hair stem cell compartment*. Curr Biol, 2005. **15**(15): p. 1340-51.
50. Merrill, B.J., et al., *Tcf3 and Lef1 regulate lineage differentiation of multipotent stem cells in skin*. Genes Dev, 2001. **15**(13): p. 1688-705.
51. Nguyen, H., M. Rendl, and E. Fuchs, *Tcf3 governs stem cell features and represses cell fate determination in skin*. Cell, 2006. **127**(1): p. 171-83.
52. Rhee, H., L. Polak, and E. Fuchs, *Lhx2 maintains stem cell character in hair follicles*. Science, 2006. **312**(5782): p. 1946-9.

53. Horsley, V., et al., *NFATc1 balances quiescence and proliferation of skin stem cells*. Cell, 2008. **132**(2): p. 299-310.
54. Oshima, H., et al., *Morphogenesis and renewal of hair follicles from adult multipotent stem cells*. Cell, 2001. **104**(2): p. 233-45.
55. Morris, R.J., et al., *Capturing and profiling adult hair follicle stem cells*. Nat Biotechnol, 2004. **22**(4): p. 411-7.
56. Taylor, G., et al., *Involvement of follicular stem cells in forming not only the follicle but also the epidermis*. Cell, 2000. **102**(4): p. 451-61.
57. Ito, M., et al., *Stem cells in the hair follicle bulge contribute to wound repair but not to homeostasis of the epidermis*. Nat Med, 2005. **11**(12): p. 1351-4.
58. Ito, M. and G. Cotsarelis, *Is the hair follicle necessary for normal wound healing?* J Invest Dermatol, 2008. **128**(5): p. 1059-61.
59. Blanpain, C., et al., *Self-renewal, multipotency, and the existence of two cell populations within an epithelial stem cell niche*. Cell, 2004. **118**(5): p. 635-48.
60. Higgins, C.A., G.E. Westgate, and C.A. Jahoda, *From telogen to exogen: mechanisms underlying formation and subsequent loss of the hair club fiber*. J Invest Dermatol, 2009. **129**(9): p. 2100-8.
61. Stenn, K.S. and R. Paus, *Controls of hair follicle cycling*. Physiol Rev, 2001. **81**(1): p. 449-494.
62. Muller-Rover, S., et al., *A comprehensive guide for the accurate classification of murine hair follicles in distinct hair cycle stages*. J Invest Dermatol, 2001. **117**(1): p. 3-15.
63. Paus, R. and G. Cotsarelis, *The biology of hair follicles*. N Engl J Med, 1999. **341**(7): p. 491-7.
64. Straile, W.E., H.B. Chase, and C. Arsenault, *Growth and differentiation of hair follicles between periods of activity and quiescence*. J Exp Zool, 1961. **148**: p. 205-21.
65. Kligman, A.M., *The human hair cycle*. J Invest Dermatol, 1959. **33**: p. 307-16.
66. Saitoh, M., M. Uzuka, and M. Sakamoto, *Human hair cycle*. J Invest Dermatol, 1970. **54**(1): p. 65-81.
67. Van Neste, D., T. Leroy, and S. Conil, *Exogen hair characterization in human scalp*. Skin Res Technol, 2007. **13**(4): p. 436-43.
68. Stenn, K., *Exogen is an active, separately controlled phase of the hair growth cycle*. J Am Acad Dermatol, 2005. **52**(2): p. 374-5.
69. Yi, R., *Concise Review: Mechanisms of Quiescent Hair Follicle Stem Cell Regulation*. Stem Cells, 2017. **35**(12): p. 2323-2330.
70. Lee, J. and T. Tumber, *Hairy tale of signaling in hair follicle development and cycling*. Semin Cell Dev Biol, 2012. **23**(8): p. 906-16.

71. Plikus, M.V. and C.M. Chuong, *Complex hair cycle domain patterns and regenerative hair waves in living rodents*. *J Invest Dermatol*, 2008. **128**(5): p. 1071-80.
72. Plikus, M.V., et al., *Cyclic dermal BMP signaling regulates stem cell activation during hair regeneration*. *Nature*, 2008. **451**(7176): p. 340-4.
73. Hsu, Y.C., H.A. Pasolli, and E. Fuchs, *Dynamics between stem cells, niche, and progeny in the hair follicle*. *Cell*, 2011. **144**(1): p. 92-105.
74. Neumuller, R.A. and J.A. Knoblich, *Dividing cellular asymmetry: asymmetric cell division and its implications for stem cells and cancer*. *Genes Dev*, 2009. **23**(23): p. 2675-99.
75. Cairns, J., *Cancer and the immortal strand hypothesis*. *Genetics*, 2006. **174**(3): p. 1069-72.
76. Potten, C.S., et al., *The segregation of DNA in epithelial stem cells*. *Cell*, 1978. **15**(3): p. 899-906.
77. Potten, C.S., G. Owen, and D. Booth, *Intestinal stem cells protect their genome by selective segregation of template DNA strands*. *J Cell Sci*, 2002. **115**(Pt 11): p. 2381-8.
78. Smith, G.H., *Label-retaining epithelial cells in mouse mammary gland divide asymmetrically and retain their template DNA strands*. *Development*, 2005. **132**(4): p. 681-7.
79. Karpowicz, P., et al., *Support for the immortal strand hypothesis: neural stem cells partition DNA asymmetrically in vitro*. *J Cell Biol*, 2005. **170**(5): p. 721-32.
80. Rumman, M., J. Dhawan, and M. Kassem, *Concise Review: Quiescence in Adult Stem Cells: Biological Significance and Relevance to Tissue Regeneration*. *Stem Cells*, 2015. **33**(10): p. 2903-12.
81. So, W.K. and T.H. Cheung, *Molecular Regulation of Cellular Quiescence: A Perspective from Adult Stem Cells and Its Niches*. *Methods Mol Biol*, 2018. **1686**: p. 1-25.
82. Glauche, I., et al., *Stem cell proliferation and quiescence--two sides of the same coin*. *PLoS Comput Biol*, 2009. **5**(7): p. e1000447.
83. Hsu, Y.C. and E. Fuchs, *A family business: stem cell progeny join the niche to regulate homeostasis*. *Nat Rev Mol Cell Biol*, 2012. **13**(2): p. 103-14.
84. Hsu, Y.C., L. Li, and E. Fuchs, *Transit-amplifying cells orchestrate stem cell activity and tissue regeneration*. *Cell*, 2014. **157**(4): p. 935-49.
85. Waghmare, S.K., et al., *Quantitative proliferation dynamics and random chromosome segregation of hair follicle stem cells*. *EMBO J*, 2008. **27**(9): p. 1309-20.
86. Waghmare, S.K. and T. Tumbar, *Adult hair follicle stem cells do not retain the older DNA strands in vivo during normal tissue homeostasis*. *Chromosome Res*, 2013. **21**(3): p. 203-12.

87. Zhang, Y.V., et al., *Distinct self-renewal and differentiation phases in the niche of infrequently dividing hair follicle stem cells*. Cell Stem Cell, 2009. **5**(3): p. 267-78.
88. Zhang, Y.V., et al., *Stem cell dynamics in mouse hair follicles: a story from cell division counting and single cell lineage tracing*. Cell Cycle, 2010. **9**(8): p. 1504-10.
89. Kiel, M.J., et al., *Haematopoietic stem cells do not asymmetrically segregate chromosomes or retain BrdU*. Nature, 2007. **449**(7159): p. 238-42.
90. Frances, D. and C. Niemann, *Stem cell dynamics in sebaceous gland morphogenesis in mouse skin*. Dev Biol, 2012. **363**(1): p. 138-46.
91. Thody, A.J. and S. Shuster, *Control and function of sebaceous glands*. Physiol Rev, 1989. **69**(2): p. 383-416.
92. Zouboulis, C.C., et al., *Frontiers in sebaceous gland biology and pathology*. Exp Dermatol, 2008. **17**(6): p. 542-51.
93. Niemann, C. and V. Horsley, *Development and homeostasis of the sebaceous gland*. Semin Cell Dev Biol, 2012. **23**(8): p. 928-36.
94. Kretzschmar, K., et al., *BLIMP1 is required for postnatal epidermal homeostasis but does not define a sebaceous gland progenitor under steady-state conditions*. Stem Cell Reports, 2014. **3**(4): p. 620-33.
95. Nijhof, J.G., et al., *The cell-surface marker MTS24 identifies a novel population of follicular keratinocytes with characteristics of progenitor cells*. Development, 2006. **133**(15): p. 3027-37.
96. Schneider, M.R., et al., *Beyond wavy hairs: the epidermal growth factor receptor and its ligands in skin biology and pathology*. Am J Pathol, 2008. **173**(1): p. 14-24.
97. Jorissen, R.N., et al., *Epidermal growth factor receptor: mechanisms of activation and signaling*. Exp Cell Res, 2003. **284**(1): p. 31-53.
98. Hansen, L.A., et al., *Genetically null mice reveal a central role for epidermal growth factor receptor in the differentiation of the hair follicle and normal hair development*. Am J Pathol, 1997. **150**(6): p. 1959-75.
99. Mak, K.K. and S.Y. Chan, *Epidermal growth factor as a biologic switch in hair growth cycle*. J Biol Chem, 2003. **278**(28): p. 26120-6.
100. Shirakata, Y., et al., *Heparin-binding EGF-like growth factor accelerates keratinocyte migration and skin wound healing*. J Cell Sci, 2005. **118**(Pt 11): p. 2363-70.
101. Ehrenreiter, K., et al., *Raf-1 regulates Rho signaling and cell migration*. J Cell Biol, 2005. **168**(6): p. 955-64.
102. Weston, C.R., et al., *The c-Jun NH2-terminal kinase is essential for epidermal growth factor expression during epidermal morphogenesis*. Proc Natl Acad Sci U S A, 2004. **101**(39): p. 14114-9.
103. Li, G., et al., *c-Jun is essential for organization of the epidermal leading edge*. Dev Cell, 2003. **4**(6): p. 865-77.

104. Soma, T., et al., *Profile of transforming growth factor-beta responses during the murine hair cycle*. J Invest Dermatol, 2003. **121**(5): p. 969-75.
105. Foitzik, K., et al., *Control of murine hair follicle regression (catagen) by TGF-beta1 in vivo*. Faseb j, 2000. **14**(5): p. 752-60.
106. Foitzik, K., et al., *The TGF-beta2 isoform is both a required and sufficient inducer of murine hair follicle morphogenesis*. Dev Biol, 1999. **212**(2): p. 278-89.
107. Oshimori, N. and E. Fuchs, *Paracrine TGF-beta signaling counterbalances BMP-mediated repression in hair follicle stem cell activation*. Cell Stem Cell, 2012. **10**(1): p. 63-75.
108. Clevers, H., *Wnt/beta-catenin signaling in development and disease*. Cell, 2006. **127**(3): p. 469-80.
109. Yu, J. and D.M. Virshup, *Updating the Wnt pathways*. Biosci Rep, 2014. **34**(5).
110. Wodarz, A. and R. Nusse, *Mechanisms of Wnt signaling in development*. Annu Rev Cell Dev Biol, 1998. **14**: p. 59-88.
111. Logan, C.Y. and R. Nusse, *The Wnt signaling pathway in development and disease*. Annu Rev Cell Dev Biol, 2004. **20**: p. 781-810.
112. Veltri, A., C. Lang, and W.H. Lien, *Concise Review: Wnt Signaling Pathways in Skin Development and Epidermal Stem Cells*. Stem Cells, 2018. **36**(1): p. 22-35.
113. Lim, X. and R. Nusse, *Wnt signaling in skin development, homeostasis, and disease*. Cold Spring Harb Perspect Biol, 2013. **5**(2).
114. Reddy, S., et al., *Characterization of Wnt gene expression in developing and postnatal hair follicles and identification of Wnt5a as a target of Sonic hedgehog in hair follicle morphogenesis*. Mech Dev, 2001. **107**(1-2): p. 69-82.
115. Lowry, W.E., et al., *Defining the impact of beta-catenin/Tcf transactivation on epithelial stem cells*. Genes Dev, 2005. **19**(13): p. 1596-611.
116. Greco, V., et al., *A two-step mechanism for stem cell activation during hair regeneration*. Cell Stem Cell, 2009. **4**(2): p. 155-69.
117. Ohyama, M., et al., *Characterization and isolation of stem cell-enriched human hair follicle bulge cells*. J Clin Invest, 2006. **116**(1): p. 249-60.
118. Lim, X., et al., *Axin2 marks quiescent hair follicle bulge stem cells that are maintained by autocrine Wnt/beta-catenin signaling*. Proc Natl Acad Sci U S A, 2016. **113**(11): p. E1498-505.
119. Millar, S.E., et al., *WNT signaling in the control of hair growth and structure*. Dev Biol, 1999. **207**(1): p. 133-49.
120. Ito, M., et al., *Wnt-dependent de novo hair follicle regeneration in adult mouse skin after wounding*. Nature, 2007. **447**(7142): p. 316-20.
121. Xing, Y.Z., et al., *Adenovirus-mediated Wnt5a expression inhibits the telogen-to-anagen transition of hair follicles in mice*. Int J Med Sci, 2013. **10**(7): p. 908-14.

122. Xing, Y., et al., *Wnt5a Suppresses beta-catenin Signaling during Hair Follicle Regeneration*. Int J Med Sci, 2016. **13**(8): p. 603-10.
123. Li, Y.H., et al., *Adenovirus-mediated Wnt10b overexpression induces hair follicle regeneration*. J Invest Dermatol, 2013. **133**(1): p. 42-8.
124. Andl, T., et al., *WNT signals are required for the initiation of hair follicle development*. Dev Cell, 2002. **2**(5): p. 643-53.
125. Kuraguchi, M., et al., *Adenomatous polyposis coli (APC) is required for normal development of skin and thymus*. PLoS Genet, 2006. **2**(9): p. e146.
126. van Genderen, C., et al., *Development of several organs that require inductive epithelial-mesenchymal interactions is impaired in LEF-1-deficient mice*. Genes Dev, 1994. **8**(22): p. 2691-703.
127. Zhou, P., et al., *Lymphoid enhancer factor 1 directs hair follicle patterning and epithelial cell fate*. Genes Dev, 1995. **9**(6): p. 700-13.
128. Niemann, C., et al., *Expression of DeltaNLeff1 in mouse epidermis results in differentiation of hair follicles into squamous epidermal cysts and formation of skin tumours*. Development, 2002. **129**(1): p. 95-109.
129. Gat, U., et al., *De Novo hair follicle morphogenesis and hair tumors in mice expressing a truncated beta-catenin in skin*. Cell, 1998. **95**(5): p. 605-14.
130. Huelsken, J., et al., *beta-Catenin controls hair follicle morphogenesis and stem cell differentiation in the skin*. Cell, 2001. **105**(4): p. 533-45.
131. Van Mater, D., et al., *Transient activation of beta -catenin signaling in cutaneous keratinocytes is sufficient to trigger the active growth phase of the hair cycle in mice*. Genes Dev, 2003. **17**(10): p. 1219-24.
132. Lo Celso, C., D.M. Prowse, and F.M. Watt, *Transient activation of beta-catenin signaling in adult mouse epidermis is sufficient to induce new hair follicles but continuous activation is required to maintain hair follicle tumours*. Development, 2004. **131**(8): p. 1787-99.
133. Zhang, Y., et al., *Activation of beta-catenin signaling programs embryonic epidermis to hair follicle fate*. Development, 2008. **135**(12): p. 2161-72.
134. Enshell-Seijffers, D., et al., *beta-catenin activity in the dermal papilla regulates morphogenesis and regeneration of hair*. Dev Cell, 2010. **18**(4): p. 633-42.
135. Baker, C.M., et al., *Differential sensitivity of epidermal cell subpopulations to beta-catenin-induced ectopic hair follicle formation*. Dev Biol, 2010. **343**(1-2): p. 40-50.
136. Nguyen, H., et al., *Tcf3 and Tcf4 are essential for long-term homeostasis of skin epithelia*. Nat Genet, 2009. **41**(10): p. 1068-75.
137. Mishina, Y., *Function of bone morphogenetic protein signaling during mouse development*. Front Biosci, 2003. **8**: p. d855-69.
138. Hogan, B.L., *Bone morphogenetic proteins: multifunctional regulators of vertebrate development*. Genes Dev, 1996. **10**(13): p. 1580-94.

139. Zakin, L. and E.M. De Robertis, *Extracellular regulation of BMP signaling*. *Curr Biol*, 2010. **20**(3): p. R89-92.
140. Schmidt-Ullrich, R. and R. Paus, *Molecular principles of hair follicle induction and morphogenesis*. *Bioessays*, 2005. **27**(3): p. 247-61.
141. Ahn, Y., *Signaling in tooth, hair, and mammary placodes*. *Curr Top Dev Biol*, 2015. **111**: p. 421-59.
142. Plikus, M., et al., *Morpho-regulation of ectodermal organs: integument pathology and phenotypic variations in K14-Noggin engineered mice through modulation of bone morphogenetic protein pathway*. *Am J Pathol*, 2004. **164**(3): p. 1099-114.
143. Tan, H.L., et al., *Nonsynonymous variants in the SMAD6 gene predispose to congenital cardiovascular malformation*. *Hum Mutat*, 2012. **33**(4): p. 720-7.
144. Botchkarev, V.A., et al., *Noggin is a mesenchymally derived stimulator of hair-follicle induction*. *Nat Cell Biol*, 1999. **1**(3): p. 158-64.
145. Kulesa, H., G. Turk, and B.L. Hogan, *Inhibition of Bmp signaling affects growth and differentiation in the anagen hair follicle*. *Embo j*, 2000. **19**(24): p. 6664-74.
146. Kobiela, K., et al., *Loss of a quiescent niche but not follicle stem cells in the absence of bone morphogenetic protein signaling*. *Proc Natl Acad Sci U S A*, 2007. **104**(24): p. 10063-8.
147. Andl, T., et al., *Epithelial Bmpr1a regulates differentiation and proliferation in postnatal hair follicles and is essential for tooth development*. *Development*, 2004. **131**(10): p. 2257-68.
148. Matzuk, M.M., et al., *Functional analysis of activins during mammalian development*. *Nature*, 1995. **374**(6520): p. 354-6.
149. Athar, M., et al., *Hedgehog signaling in skin development and cancer*. *Exp Dermatol*, 2006. **15**(9): p. 667-77.
150. Biggs, L.C. and M.L. Mikkola, *Early inductive events in ectodermal appendage morphogenesis*. *Semin Cell Dev Biol*, 2014. **25-26**: p. 11-21.
151. St-Jacques, B., et al., *Sonic hedgehog signaling is essential for hair development*. *Curr Biol*, 1998. **8**(19): p. 1058-68.
152. Chiang, C., et al., *Essential role for Sonic hedgehog during hair follicle morphogenesis*. *Dev Biol*, 1999. **205**(1): p. 1-9.
153. Oro, A.E., et al., *Basal cell carcinomas in mice overexpressing sonic hedgehog*. *Science*, 1997. **276**(5313): p. 817-21.
154. Mill, P., et al., *Sonic hedgehog-dependent activation of Gli2 is essential for embryonic hair follicle development*. *Genes Dev*, 2003. **17**(2): p. 282-94.
155. Pasca di Magliano, M. and M. Hebrok, *Hedgehog signaling in cancer formation and maintenance*. *Nat Rev Cancer*, 2003. **3**(12): p. 903-11.
156. Xu, Z., et al., *Embryonic attenuated Wnt/beta-catenin signaling defines niche location and long-term stem cell fate in hair follicle*. *Elife*, 2015. **4**: p. e10567.

157. Sakaki-Yumoto, M., Y. Katsuno, and R. Derynck, *TGF-beta family signaling in stem cells*. Biochim Biophys Acta, 2013. **1830**(2): p. 2280-96.
158. Xu, R.H., et al., *NANOG is a direct target of TGFbeta/activin-mediated SMAD signaling in human ESCs*. Cell Stem Cell, 2008. **3**(2): p. 196-206.
159. Vallier, L., et al., *Activin/Nodal signaling maintains pluripotency by controlling Nanog expression*. Development, 2009. **136**(8): p. 1339-49.
160. Lin, H.Y. and L.T. Yang, *Differential response of epithelial stem cell populations in hair follicles to TGF-beta signaling*. Dev Biol, 2013. **373**(2): p. 394-406.
161. Jamora, C., et al., *A signaling pathway involving TGF-beta2 and snail in hair follicle morphogenesis*. PLoS Biol, 2005. **3**(1): p. e11.
162. Mani, S.A., et al., *The epithelial-mesenchymal transition generates cells with properties of stem cells*. Cell, 2008. **133**(4): p. 704-15.
163. Scheel, C., et al., *Paracrine and autocrine signals induce and maintain mesenchymal and stem cell states in the breast*. Cell, 2011. **145**(6): p. 926-40.
164. Logeat, F., et al., *The Notch1 receptor is cleaved constitutively by a furin-like convertase*. Proc Natl Acad Sci U S A, 1998. **95**(14): p. 8108-12.
165. Chillakuri, C.R., et al., *Notch receptor-ligand binding and activation: insights from molecular studies*. Semin Cell Dev Biol, 2012. **23**(4): p. 421-8.
166. Kopan, R. and M.X. Ilagan, *The canonical Notch signaling pathway: unfolding the activation mechanism*. Cell, 2009. **137**(2): p. 216-33.
167. Bray, S.J., *Notch signaling: a simple pathway becomes complex*. Nat Rev Mol Cell Biol, 2006. **7**(9): p. 678-89.
168. Favier, B., et al., *Localisation of members of the notch system and the differentiation of vibrissa hair follicles: receptors, ligands, and fringe modulators*. Dev Dyn, 2000. **218**(3): p. 426-37.
169. Vauclair, S., et al., *Notch1 is essential for postnatal hair follicle development and homeostasis*. Dev Biol, 2005. **284**(1): p. 184-93.
170. Lin, M.H., et al., *Activation of the Notch pathway in the hair cortex leads to aberrant differentiation of the adjacent hair-shaft layers*. Development, 2000. **127**(11): p. 2421-32.
171. Nicolas, M., et al., *Notch1 functions as a tumor suppressor in mouse skin*. Nat Genet, 2003. **33**(3): p. 416-21.
172. Demehri, S. and R. Kopan, *Notch signaling in bulge stem cells is not required for selection of hair follicle fate*. Development, 2009. **136**(6): p. 891-6.
173. Estrach, S., et al., *Jagged 1 is a beta-catenin target gene required for ectopic hair follicle formation in adult epidermis*. Development, 2006. **133**(22): p. 4427-38.
174. Pan, Y., et al., *gamma-secretase functions through Notch signaling to maintain skin appendages but is not required for their patterning or initial morphogenesis*. Dev Cell, 2004. **7**(5): p. 731-43.

175. Park, S., et al., *Tissue-scale coordination of cellular behaviour promotes epidermal wound repair in live mice*. Nat Cell Biol, 2017. **19**(2): p. 155-163.
176. Schultz, G.S., et al., *Principles of wound healing*, in *Mechanisms of Vascular Disease: A Reference Book for Vascular Specialists*, M. Thompson and R. Fitridge, Editors. 2011, The University of Adelaide Press. p. 423-450.
177. Martin, P., et al., *Wound healing in the PU.1 null mouse--tissue repair is not dependent on inflammatory cells*. Curr Biol, 2003. **13**(13): p. 1122-8.
178. Schreml, S., et al., *Oxygen in acute and chronic wound healing*. Br J Dermatol, 2010. **163**(2): p. 257-68.
179. Eming, S.A., P. Martin, and M. Tomic-Canic, *Wound repair and regeneration: mechanisms, signaling, and translation*. Sci Transl Med, 2014. **6**(265): p. 265sr6.
180. Shaw, T.J. and P. Martin, *Wound repair at a glance*. J Cell Sci, 2009. **122**(Pt 18): p. 3209-13.
181. Velnar, T., T. Bailey, and V. Smrkolj, *The wound healing process: an overview of the cellular and molecular mechanisms*. J Int Med Res, 2009. **37**(5): p. 1528-42.
182. Mascré, G., et al., *Distinct contribution of stem and progenitor cells to epidermal maintenance*. Nature, 2012. **489**(7415): p. 257-62.
183. Aragona, M., et al., *Defining stem cell dynamics and migration during wound healing in mouse skin epidermis*. Nat Commun, 2017. **8**: p. 14684.
184. Brown, J.B. and F. McDowell, *EPITHELIAL HEALING AND THE TRANSPLANTATION OF SKIN*. Ann Surg, 1942. **115**(6): p. 1166-81.
185. Bishop, G.H., *Regeneration after experimental removal of skin in man*. American Journal of Anatomy, 1945. **76**(2): p. 153-181.
186. Garcin, C.L., et al., *Hair Follicle Bulge Stem Cells Appear Dispensable for the Acute Phase of Wound Re-epithelialization*. Stem Cells, 2016. **34**(5): p. 1377-85.
187. Langton, A.K., S.E. Herrick, and D.J. Headon, *An extended epidermal response heals cutaneous wounds in the absence of a hair follicle stem cell contribution*. J Invest Dermatol, 2008. **128**(5): p. 1311-8.
188. Yu, H., et al., *Isolation of a novel population of multipotent adult stem cells from human hair follicles*. Am J Pathol, 2006. **168**(6): p. 1879-88.
189. Garza, L.A., et al., *Bald scalp in men with androgenetic alopecia retains hair follicle stem cells but lacks CD200-rich and CD34-positive hair follicle progenitor cells*. J Clin Invest, 2011. **121**(2): p. 613-22.
190. Harries, M.J., et al., *Lichen planopilaris is characterized by immune privilege collapse of the hair follicle's epithelial stem cell niche*. J Pathol, 2013. **231**(2): p. 236-47.
191. Yoshida, R., et al., *Involvement of the bulge region with decreased expression of hair follicle stem cell markers in senile female cases of alopecia areata*. J Eur Acad Dermatol Venereol, 2011. **25**(11): p. 1346-50.

192. Hoang, M.P., M. Keady, and M. Mahalingam, *Stem cell markers (cytokeratin 15, CD34 and nestin) in primary scarring and nonscarring alopecia*. Br J Dermatol, 2009. **160**(3): p. 609-15.
193. Gentile, P., et al., *Stem cells from human hair follicles: first mechanical isolation for immediate autologous clinical use in androgenetic alopecia and hair loss*. Stem Cell Investig, 2017. **4**: p. 58.
194. Nakamura, M., et al., *Mutant laboratory mice with abnormalities in hair follicle morphogenesis, cycling, and/or structure: an update*. J Dermatol Sci, 2013. **69**(1): p. 6-29.
195. Kiguchi, K., et al., *Constitutive expression of erbB2 in epidermis of transgenic mice results in epidermal hyperproliferation and spontaneous skin tumor development*. Oncogene, 2000. **19**(37): p. 4243-54.
196. Ellis, T., et al., *Overexpression of Sonic Hedgehog suppresses embryonic hair follicle morphogenesis*. Dev Biol, 2003. **263**(2): p. 203-15.
197. van Hogerlinden, M., et al., *Squamous cell carcinomas and increased apoptosis in skin with inhibited Rel/nuclear factor-kappaB signaling*. Cancer Res, 1999. **59**(14): p. 3299-303.
198. Shih, M.Y., et al., *Retinol Esterification by DGAT1 Is Essential for Retinoid Homeostasis in Murine Skin*. J Biol Chem, 2009. **284**(7): p. 4292-9.
199. Muller-Decker, K., et al., *Expression of cyclooxygenase isozymes during morphogenesis and cycling of pelage hair follicles in mouse skin: precocious onset of the first catagen phase and alopecia upon cyclooxygenase-2 overexpression*. J Invest Dermatol, 2003. **121**(4): p. 661-8.
200. Muller-Rover, S., et al., *Overexpression of Bcl-2 protects from ultraviolet B-induced apoptosis but promotes hair follicle regression and chemotherapy-induced alopecia*. Am J Pathol, 2000. **156**(4): p. 1395-405.
201. Zhu, K., et al., *Transgenic mice display hair loss and regrowth overexpressing mutant Hr gene*. Exp Anim, 2017. **66**(4): p. 379-386.
202. Fang, C., L. Li, and J. Li, *Conditional Knockout in Mice Reveals the Critical Roles of Ppp2ca in Epidermis Development*. Int J Mol Sci, 2016. **17**(5).
203. Qiu, W., et al., *Conditional activin receptor type 1B (Acvr1b) knockout mice reveal hair loss abnormality*. J Invest Dermatol, 2011. **131**(5): p. 1067-76.
204. Kiso, M., et al., *The disruption of Sox21-mediated hair shaft cuticle differentiation causes cyclic alopecia in mice*. Proc Natl Acad Sci U S A, 2009. **106**(23): p. 9292-7.
205. Ma, L., et al., *'Cyclic alopecia' in Msx2 mutants: defects in hair cycling and hair shaft differentiation*. Development, 2003. **130**(2): p. 379-89.
206. Liu, K.M., et al., *Cyclic Alopecia and Abnormal Epidermal Cornification in Zdhhc13-Deficient Mice Reveal the Importance of Palmitoylation in Hair and Skin Differentiation*. J Invest Dermatol, 2015. **135**(11): p. 2603-10.

207. Murillas, R., et al., *Expression of a dominant negative mutant of epidermal growth factor receptor in the epidermis of transgenic mice elicits striking alterations in hair follicle development and skin structure*. *Embo j*, 1995. **14**(21): p. 5216-23.
208. Yang, L., L. Wang, and X. Yang, *Disruption of Smad4 in mouse epidermis leads to depletion of follicle stem cells*. *Mol Biol Cell*, 2009. **20**(3): p. 882-90.
209. Sharov, A.A., et al., *Bone morphogenetic protein antagonist noggin promotes skin tumorigenesis via stimulation of the Wnt and Shh signaling pathways*. *Am J Pathol*, 2009. **175**(3): p. 1303-14.
210. Mulherkar, R., et al., *Expression of enhancing factor/phospholipase A2 in skin results in abnormal epidermis and increased sensitivity to chemical carcinogenesis*. *Oncogene*, 2003. **22**(13): p. 1936-44.
211. Sarate, R.M., et al., *sPLA2 -IIA Overexpression in Mice Epidermis Depletes Hair Follicle Stem Cells and Induce Differentiation Mediated Through Enhanced JNK/c-Jun Activation*. *Stem Cells*, 2016.
212. Diamond, I., et al., *Conditional gene expression in the epidermis of transgenic mice using the tetracycline-regulated transactivators tTA and rTA linked to the keratin 5 promoter*. *J Invest Dermatol*, 2000. **115**(5): p. 788-94.
213. Morris, S.M., et al., *Dual roles for the Dab2 adaptor protein in embryonic development and kidney transport*. *EMBO J*, 2002. **21**(7): p. 1555-64.
214. Vasioukhin, V., et al., *The magical touch: genome targeting in epidermal stem cells induced by tamoxifen application to mouse skin*. *Proc Natl Acad Sci U S A*, 1999. **96**(15): p. 8551-6.
215. Srinivas, S., et al., *Cre reporter strains produced by targeted insertion of EYFP and ECFP into the ROSA26 locus*. *BMC Dev Biol*, 2001. **1**: p. 4.
216. Osorio, K.M., K.C. Lilja, and T. Tumbar, *Runx1 modulates adult hair follicle stem cell emergence and maintenance from distinct embryonic skin compartments*. *J Cell Biol*, 2011. **193**(1): p. 235-50.
217. Niessen, M.T., et al., *aPKC $\lambda$  controls epidermal homeostasis and stem cell fate through regulation of division orientation*. *J Cell Biol*, 2013. **202**(6): p. 887-900.
218. Nowak, J.A. and E. Fuchs, *Isolation and culture of epithelial stem cells*. *Methods Mol Biol*, 2009. **482**: p. 215-32.
219. Peterson, G.L., *A simplification of the protein assay method of Lowry et al. which is more generally applicable*. *Anal Biochem*, 1977. **83**(2): p. 346-56.
220. Murakami, M., et al., *Secreted phospholipase A2 revisited*. *J Biochem*, 2011. **150**(3): p. 233-55.
221. Cummings, B.S., *Phospholipase A2 as targets for anti-cancer drugs*. *Biochem Pharmacol*, 2007. **74**(7): p. 949-59.
222. Murakami, M., et al., *Regulatory functions of phospholipase A2*. *Crit Rev Immunol*, 1997. **17**(3-4): p. 225-83.

223. Murakami, M., et al., *Recent progress in phospholipase A(2) research: from cells to animals to humans*. Prog Lipid Res, 2011. **50**(2): p. 152-92.
224. Murakami, M., et al., *Emerging roles of secreted phospholipase A2 enzymes: the 3rd edition*. Biochimie, 2014. **107 Pt A**: p. 105-13.
225. Mulherkar, R., et al., *Purification of the enhancing factor from mouse intestines*. FEBS Lett, 1986. **207**(1): p. 142-4.
226. Mulherkar, R. and M.G. Deo, *Further studies on the enhancing factor and its possible mechanism of action*. J Cell Physiol, 1986. **127**(1): p. 183-8.
227. Mulherkar, R., et al., *Enhancing factor protein from mouse small intestines belongs to the phospholipase A2 family*. FEBS Lett, 1993. **317**(3): p. 263-6.
228. Kadam, S., et al., *Sequence analysis of full length cDNA for enhancing factor/phospholipase A2*. Indian J Exp Biol, 1998. **36**(6): p. 553-8.
229. Kadam, S. and R. Mulherkar, *Enhancing activity and phospholipase A2 activity: two independent activities present in the enhancing factor molecule*. Biochem J, 1999. **340 ( Pt 1)**: p. 237-43.
230. Mulherkar, R., et al., *Expression of enhancing factor gene and its localization in mouse tissues*. Histochemistry, 1991. **96**(4): p. 367-70.
231. IDesai, S.J., et al., *Ontogeny of enhancing factor in mouse intestines and skin*. Histochemistry, 1991. **96**(4): p. 371-4.
232. Mulherkar, R., et al., *Enhancing factor, a Paneth cell specific protein from mouse small intestines: predicted amino acid sequence from RT-PCR amplified cDNA and its expression*. Biochem Biophys Res Commun, 1993. **195**(3): p. 1254-63.
233. Schewe, M., et al., *Secreted Phospholipases A2 Are Intestinal Stem Cell Niche Factors with Distinct Roles in Homeostasis, Inflammation, and Cancer*. Cell Stem Cell, 2016. **19**(1): p. 38-51.
234. Kennedy, B.P., et al., *A natural disruption of the secretory group II phospholipase A2 gene in inbred mouse strains*. J Biol Chem, 1995. **270**(38): p. 22378-85.
235. Hernandez, M., et al., *Secreted PLA2 induces proliferation in astrocytoma through the EGF receptor: another inflammation-cancer link*. Neuro Oncol, 2010. **12**(10): p. 1014-23.
236. Martin, R., C. Cordova, and M.L. Nieto, *Secreted phospholipase A2-IIA-induced a phenotype of activated microglia in BV-2 cells requires epidermal growth factor receptor transactivation and proHB-EGF shedding*. J Neuroinflammation, 2012. **9**: p. 154.
237. Scott, K.F., et al., *Emerging roles for phospholipase A2 enzymes in cancer*. Biochimie, 2010. **92**(6): p. 601-10.
238. Bennett, D.T., et al., *Cancer stem cell phenotype is supported by secretory phospholipase A2 in human lung cancer cells*. Ann Thorac Surg, 2014. **98**(2): p. 439-45; discussion 445-6.

239. Lu, S. and Z. Dong, *Overexpression of secretory phospholipase A2-IIa supports cancer stem cell phenotype via HER/ERBB-elicited signaling in lung and prostate cancer cells*. *Int J Oncol*, 2017. **50**(6): p. 2113-2122.
240. Mao-Qiang, M., et al., *Secretory phospholipase A2 activity is required for permeability barrier homeostasis*. *J Invest Dermatol*, 1996. **106**(1): p. 57-63.
241. Grass, D.S., et al., *Expression of human group II PLA2 in transgenic mice results in epidermal hyperplasia in the absence of inflammatory infiltrate*. *J Clin Invest*, 1996. **97**(10): p. 2233-41.
242. Man, M.Q., et al., *Basis for enhanced barrier function of pigmented skin*. *J Invest Dermatol*, 2014. **134**(9): p. 2399-407.
243. Yamamoto, K., et al., *The role of group IIF-secreted phospholipase A2 in epidermal homeostasis and hyperplasia*. *J Exp Med*, 2015. **212**(11): p. 1901-19.
244. Yamamoto, K., et al., *Hair follicular expression and function of group X secreted phospholipase A2 in mouse skin*. *J Biol Chem*, 2011. **286**(13): p. 11616-31.
245. Yamamoto, K., et al., *Expression and Function of Group IIE Phospholipase A2 in Mouse Skin*. *J Biol Chem*, 2016. **291**(30): p. 15602-13.
246. Yamazaki, S., et al., *Mice with defects in HB-EGF ectodomain shedding show severe developmental abnormalities*. *J Cell Biol*, 2003. **163**(3): p. 469-75.
247. Zhou, Y., et al., *Gsdma3 mutation causes bulge stem cell depletion and alopecia mediated by skin inflammation*. *Am J Pathol*, 2012. **180**(2): p. 763-74.
248. Eckert, R.L., et al., *Keratinocyte survival, differentiation, and death: many roads lead to mitogen-activated protein kinase*. *J Invest Dermatol Symp Proc*, 2002. **7**(1): p. 36-40.
249. Dominey, A.M., et al., *Targeted overexpression of transforming growth factor alpha in the epidermis of transgenic mice elicits hyperplasia, hyperkeratosis, and spontaneous, squamous papillomas*. *Cell Growth Differ*, 1993. **4**(12): p. 1071-82.
250. Werner, S., et al., *Targeted expression of a dominant-negative FGF receptor mutant in the epidermis of transgenic mice reveals a role of FGF in keratinocyte organization and differentiation*. *Embo j*, 1993. **12**(7): p. 2635-43.
251. Yang, L., et al., *Targeted disruption of Smad4 in mouse epidermis results in failure of hair follicle cycling and formation of skin tumors*. *Cancer Res*, 2005. **65**(19): p. 8671-8.
252. Castilho, R.M., et al., *mTOR mediates Wnt-induced epidermal stem cell exhaustion and aging*. *Cell Stem Cell*, 2009. **5**(3): p. 279-89.
253. Florin, L., et al., *Delayed wound healing and epidermal hyperproliferation in mice lacking JunB in the skin*. *J Invest Dermatol*, 2006. **126**(4): p. 902-11.
254. Osorio, K.M., et al., *Runx1 modulates developmental, but not injury-driven, hair follicle stem cell activation*. *Development*, 2008. **135**(6): p. 1059-68.

255. Saleem, A.N., et al., *Mice with alopecia, osteoporosis, and systemic amyloidosis due to mutation in Zdhhc13, a gene coding for palmitoyl acyltransferase*. PLoS Genet, 2010. **6**(6): p. e1000985.
256. Gertler, F.B., et al., *Drosophila abl tyrosine kinase in embryonic CNS axons: a role in axonogenesis is revealed through dosage-sensitive interactions with disabled*. Cell, 1989. **58**(1): p. 103-13.
257. Tao, W., et al., *Endocytosis and Physiology: Insights from Disabled-2 Deficient Mice*. Front Cell Dev Biol, 2016. **4**: p. 129.
258. Xu, X.X., et al., *Disabled-2 (Dab2) is an SH3 domain-binding partner of Grb2*. Oncogene, 1998. **16**(12): p. 1561-9.
259. Jiang, Y., W. Luo, and P.H. Howe, *Dab2 stabilizes Axin and attenuates Wnt/beta-catenin signaling by preventing protein phosphatase 1 (PPI)-Axin interactions*. Oncogene, 2009. **28**(33): p. 2999-3007.
260. Jiang, Y., X. He, and P.H. Howe, *Disabled-2 (Dab2) inhibits Wnt/beta-catenin signaling by binding LRP6 and promoting its internalization through clathrin*. EMBO J, 2012. **31**(10): p. 2336-49.
261. Hocevar, B.A., et al., *Regulation of the Wnt signaling pathway by disabled-2 (Dab2)*. EMBO J, 2003. **22**(12): p. 3084-94.
262. Hocevar, B.A., et al., *The adaptor molecule Disabled-2 links the transforming growth factor beta receptors to the Smad pathway*. Embo j, 2001. **20**(11): p. 2789-801.
263. Penheiter, S.G., et al., *Type II transforming growth factor-beta receptor recycling is dependent upon the clathrin adaptor protein Dab2*. Mol Biol Cell, 2010. **21**(22): p. 4009-19.
264. Kim, J.D., et al., *Context-dependent proangiogenic function of bone morphogenetic protein signaling is mediated by disabled homolog 2*. Dev Cell, 2012. **23**(2): p. 441-8.
265. Diwakar, R., et al., *Role played by disabled-2 in albumin induced MAP Kinase signaling*. Biochem Biophys Res Commun, 2008. **366**(3): p. 675-80.
266. Tao, W., et al., *Hormonal induction and roles of Disabled-2 in lactation and involution*. PLoS One, 2014. **9**(10): p. e110737.
267. He, J., E.R. Smith, and X.X. Xu, *Disabled-2 exerts its tumor suppressor activity by uncoupling c-Fos expression and MAP kinase activation*. J Biol Chem, 2001. **276**(29): p. 26814-8.
268. Hocevar, B.A., C. Prunier, and P.H. Howe, *Disabled-2 (Dab2) mediates transforming growth factor beta (TGFbeta)-stimulated fibronectin synthesis through TGFbeta-activated kinase 1 and activation of the JNK pathway*. J Biol Chem, 2005. **280**(27): p. 25920-7.
269. Morris, S.M., et al., *Myosin VI binds to and localises with Dab2, potentially linking receptor-mediated endocytosis and the actin cytoskeleton*. Traffic, 2002. **3**(5): p. 331-41.

270. Moore, R., et al., *Differential requirement for Dab2 in the development of embryonic and extra-embryonic tissues*. BMC Dev Biol, 2013. **13**: p. 39.
271. Rula, M.E., et al., *Cell autonomous sorting and surface positioning in the formation of primitive endoderm in embryoid bodies*. Genesis, 2007. **45**(6): p. 327-38.
272. Hofsteen, P., et al., *Quantitative proteomics identify DAB2 as a cardiac developmental regulator that inhibits WNT/beta-catenin signaling*. Proc Natl Acad Sci U S A, 2016. **113**(4): p. 1002-7.
273. Mok, S.C., et al., *Molecular cloning of differentially expressed genes in human epithelial ovarian cancer*. Gynecol Oncol, 1994. **52**(2): p. 247-52.
274. Schwahn, D.J. and D. Medina, *p96, a MAPK-related protein, is consistently downregulated during mouse mammary carcinogenesis*. Oncogene, 1998. **17**(9): p. 1173-8.
275. Yang, D.H., et al., *Disabled-2 heterozygous mice are predisposed to endometrial and ovarian tumorigenesis and exhibit sex-biased embryonic lethality in a p53-null background*. Am J Pathol, 2006. **169**(1): p. 258-67.
276. Sheng, Z., et al., *Restoration of positioning control following Disabled-2 expression in ovarian and breast tumor cells*. Oncogene, 2000. **19**(42): p. 4847-54.
277. Bagadi, S.A., et al., *Frequent loss of Dab2 protein and infrequent promoter hypermethylation in breast cancer*. Breast Cancer Res Treat, 2007. **104**(3): p. 277-86.
278. Hannigan, A., et al., *Epigenetic downregulation of human disabled homolog 2 switches TGF-beta from a tumor suppressor to a tumor promoter*. J Clin Invest, 2010. **120**(8): p. 2842-57.
279. Kleeff, J., et al., *Down-regulation of DOC-2 in colorectal cancer points to its role as a tumor suppressor in this malignancy*. Dis Colon Rectum, 2002. **45**(9): p. 1242-8.
280. Tseng, C.P., et al., *Regulation of rat DOC-2 gene during castration-induced rat ventral prostate degeneration and its growth inhibitory function in human prostatic carcinoma cells*. Endocrinology, 1998. **139**(8): p. 3542-53.
281. Tseng, C.P., et al., *The role of DOC-2/DAB2 protein phosphorylation in the inhibition of AP-1 activity. An underlying mechanism of its tumor-suppressive function in prostate cancer*. J Biol Chem, 1999. **274**(45): p. 31981-6.
282. Anupam, K., et al., *Loss of disabled-2 expression is an early event in esophageal squamous tumorigenesis*. World J Gastroenterol, 2006. **12**(37): p. 6041-5.
283. Tong, J.H., et al., *Putative tumour-suppressor gene DAB2 is frequently down regulated by promoter hypermethylation in nasopharyngeal carcinoma*. BMC Cancer, 2010. **10**: p. 253.
284. DasGupta, R. and E. Fuchs, *Multiple roles for activated LEF/TCF transcription complexes during hair follicle development and differentiation*. Development, 1999. **126**(20): p. 4557-68.
285. Blanpain, C., V. Horsley, and E. Fuchs, *Epithelial stem cells: turning over new leaves*. Cell, 2007. **128**(3): p. 445-58.

286. Deschene, E.R., et al., *beta-Catenin activation regulates tissue growth non-cell autonomously in the hair stem cell niche*. Science, 2014. **343**(6177): p. 1353-6.
287. Janich, P., et al., *The circadian molecular clock creates epidermal stem cell heterogeneity*. Nature, 2011. **480**(7376): p. 209-14.
288. Kadaja, M., et al., *SOX9: a stem cell transcriptional regulator of secreted niche signaling factors*. Genes Dev, 2014. **28**(4): p. 328-41.
289. Xu, S., J. Zhu, and Z. Wu, *Loss of Dab2 expression in breast cancer cells impairs their ability to deplete TGF-beta and induce Tregs development via TGF-beta*. PLoS One, 2014. **9**(3): p. e91709.
290. Wang, B., Q. Gu, and J. Li, *DOC-2/DAB2 interactive protein regulates proliferation and mobility of nasopharyngeal carcinoma cells by targeting PI3K/Akt pathway*. Oncol Rep, 2017. **38**(1): p. 317-324.

# *Publications*



# SCIENTIFIC REPORTS



OPEN

## Secretory phospholipase A<sub>2</sub>-IIA overexpressing mice exhibit cyclic alopecia mediated through aberrant hair shaft differentiation and impaired wound healing response

Gopal L. Chovatiya<sup>1,2</sup>, Rahul M. Sarate<sup>1,2</sup>, Raghava R. Sunkara<sup>1,2</sup>, Nilesh P. Gawas<sup>1</sup>, Vineet Kala<sup>1</sup> & Sanjeev K. Waghmare<sup>1,2</sup>

Secretory phospholipase A<sub>2</sub> Group-IIA (sPLA<sub>2</sub>-IIA) is involved in lipid catabolism and growth promoting activity. sPLA<sub>2</sub>-IIA is deregulated in many pathological conditions including various cancers. Here, we have studied the role of sPLA<sub>2</sub>-IIA in the development of cyclic alopecia and wound healing response in relation to complete loss of hair follicle stem cells (HFSCs). Our data showed that overexpression of sPLA<sub>2</sub>-IIA in homozygous mice results in hyperproliferation and terminal epidermal differentiation followed by hair follicle cycle being halted at anagen like stage. In addition, sPLA<sub>2</sub>-IIA induced hyperproliferation leads to compl pathological conditions including various cancers. Here ete exhaustion of hair follicle stem cell pool at PD28 (Postnatal day). Importantly, sPLA<sub>2</sub>-IIA overexpression affects the hair shaft differentiation leading to development of cyclic alopecia. Molecular investigation study showed aberrant expression of Sox21, Msx2 and signalling modulators necessary for proper differentiation of inner root sheath (IRS) and hair shaft formation. Further, full-thickness skin wounding on dorsal skin of K14-sPLA<sub>2</sub>-IIA homozygous mice displayed impaired initial healing response. Our results showed the involvement of sPLA<sub>2</sub>-IIA in regulation of matrix cells differentiation, hair shaft formation and complete loss of HFSCs mediated impaired wound healing response. These novel functions of sPLA<sub>2</sub>-IIA may have clinical implications in alopecia, cancer development and ageing.

Skin constantly renews itself throughout the adult life that acts as a protective barrier against pathogens, radiation etc.<sup>1</sup>. Adult skin is mainly composed of epidermis, dermis and hypodermis. Epidermal components mainly include interfollicular epidermis (IFE), hair follicle and sebaceous gland<sup>2</sup>. Dermis and hypodermis are mainly composed of collagen, elastic fibers and extrafibrillar matrix with various cell types including fibroblasts, adipose cells and macrophages. During embryogenesis, hair follicle is formed as an appendage of the epidermis by condensation of specialized mesenchymal cells (dermal papilla) in the dermis. The basal layer cells overlying mesenchymal cells get stimulated and subsequently form placode at E14.5 that proliferate and grow downward as a mature hair follicle at E16.5-E17.5<sup>3</sup>. The hair follicle cycle comprises of distinct stages such as telogen (resting phase), anagen (growth phase) and catagen (regression phase)<sup>4</sup>. Initially, both the pulse-chase studies carried out using tritiated thymidine (<sup>3</sup>H) and BrdU showed the presence of infrequently dividing cells in the bulge of hair follicle<sup>5</sup>. Subsequently, pTre-H2BGFP/K5tTa (Tet off) double transgenic mice study showed that the hair follicle stem cells are highly dynamic, which divide infrequently and undergo random chromosome segregation to

<sup>1</sup>Stem Cell Biology Group, Waghmare Lab, Cancer Research Institute, Advanced Centre for Treatment Research and Education in Cancer (ACTREC), Tata Memorial Centre, Kharghar, Navi Mumbai, 410210, MH, India. <sup>2</sup>Homi Bhabha National Institute, Training School Complex, Anushakti Nagar, Mumbai, 400085, India. Gopal L. Chovatiya and Rahul M. Sarate contributed equally to this work. Correspondence and requests for materials should be addressed to S.K.W. (email: [swaghmare@actrec.gov.in](mailto:swaghmare@actrec.gov.in))

maintain tissue homeostasis<sup>6–8</sup>. During follicle regeneration, the dermal papilla at the base of hair follicle provides initiatory signalling cues generated from the mesenchymal niche<sup>9</sup>. The cyclic growth of hair follicle is coordinated by the stem cells residing at the base of the bulge, which proliferate and migrate to provide progeny required for the hair-follicle regeneration and hair growth<sup>10</sup>. Further, the temporal activity of hair follicle stem cells is strictly dependent on interplay between mesenchymal niche and bulge, which is governed by secretion of various signalling modulators such as Wnt, BMP, Shh, and FGF<sup>11</sup>. In particular, Wnt signalling is necessary for the hair follicle morphogenesis and required for stem cell proliferation and differentiation during hair follicle regeneration<sup>12–14</sup>. Additionally, EGF induced EGFR signalling is indispensable for the initiation of hair growth<sup>15</sup>. The EGF signalling modulator, secretory phospholipase A<sub>2</sub> group IIA (sPLA<sub>2</sub>-IIA) is also known as enhancing factor (EF), which expressed by paneth cells in the small intestine<sup>16,17</sup>. sPLA<sub>2</sub>-IIA has two independent activities, catalytic and non-catalytic (enhancing) and both these activities rely on the two different domains of this enzyme<sup>18</sup>. Also, various studies have reported the expression of sPLA<sub>2</sub>-IIA in mouse epidermis<sup>19,20</sup>. Moreover, sPLA<sub>2</sub>-IIA has been implicated in various forms of cancer such as intestinal, colorectal, prostate<sup>21</sup> and overexpression of sPLA<sub>2</sub>-IIA in mice epidermis showed increased susceptibility towards chemical carcinogenesis<sup>22</sup>. We have recently reported that sPLA<sub>2</sub>-IIA enhances the expression of Hb-EGF, EPGN and downstream c-Jun and Fos-B<sup>23</sup>. However, the molecular insight, if sPLA<sub>2</sub>-IIA regulates the hair shaft differentiation and the development of alopecia is still unknown. Secondly, do cells of other epidermal components form hair in the complete absence of hair follicle stem cells? Thirdly, whether wound healing process is impaired in the absence of HFSCs is yet to be determined.

Notably, deregulation of various signalling modulators perturbs stem cells maintenance that may result in development and progression of cyclic alopecia. Impaired EGFR signalling by dominant negative mutant of epidermal growth factor receptor in the epidermis prevents the progression of the hair cycle to catagen stage and causes severe alopecia<sup>24</sup>. Further, knockout of Sox21 in mice alters differentiation of cuticle layer leading to development of cyclic alopecia<sup>25</sup>. Also, epidermal ablation of Smad4 resulted in hyperplasia of interfollicular epidermis (IFE) and sebaceous glands (SGs), that leads to exhaustion of the SC niche and progressive hair loss<sup>26</sup>. Expression of noggin in epidermis resulted in upregulated Wnt signalling with epidermal hyperplasia, progressive hair loss, and formation of trichofolliculoma-like tumors<sup>27</sup>. Msx2 deficiency exhibits abnormal structure of hair shafts and cycles of hair loss and regrowth<sup>28</sup>. Targeted disruption of *Orai1* gene in mouse showed sporadic hair loss while inducible deletion of *cnb1* gene in mice resulted in altered hair follicle structure and its mesenchyme adhesion, that causes cyclic alopecia<sup>29,30</sup>. However, the molecular mechanism involved in cyclic alopecia is yet to be discovered.

In this report, we studied the effect of K14-sPLA<sub>2</sub>-IIA expression in homozygous mice on alopecia and wound healing. To our knowledge, for the first time our findings on K14-sPLA<sub>2</sub>-IIA homozygous mice showed hair loss that is associated with an increased proliferation and differentiation of hair follicle stem cells, which led to exhaustion of hair follicle stem cells and development of cyclic alopecia at an early age. Additionally, K14-sPLA<sub>2</sub>-IIA homozygous mice showed impaired healing response during full thickness epidermal wounding.

## Results

**Altered hair follicle development and hair cycling in K14-sPLA<sub>2</sub>-IIA homozygous mice.** To check the expression pattern of sPLA<sub>2</sub>-IIA in mice epidermis, we performed the IHC staining of sPLA<sub>2</sub>-IIA on skin sections of wild type FVB mice at various postnatal ages. Our data showed that sPLA<sub>2</sub>-IIA expresses in basal layer, suprabasal layer and outer root sheath of hair follicle during morphogenesis, first hair cycle and one year old age (Supplementary Fig. S1). K14-sPLA<sub>2</sub>-IIA homozygous mice exhibited visible phenotypic growth abnormalities and are significantly smaller than the control littermates (Fig. 1a). Further, to confirm the nutritional status of the K14-sPLA<sub>2</sub>-IIA homozygous mice, we have quantified various nutritional parameters from the serum of the K14-sPLA<sub>2</sub>-IIA homozygous mice. Our data showed that there are no significant alterations in serum components such as serum albumin, Vitamin D 25-OH, Triglyceride, Sodium, Chloride, and marginal increase was observed in total protein, Vitamin B12, Calcium and Potassium (Supplementary Fig. S4). However, we have observed reduced serum glucose level after eight hours fasting in the K14-sPLA<sub>2</sub>-IIA homozygous mice (Supplementary Fig. S4). These results demonstrate that there are no significant alterations in the nutritional parameters of the K14-sPLA<sub>2</sub>-IIA homozygous mice. These K14-sPLA<sub>2</sub>-IIA homozygous mice showed progressive hair loss during hair follicle morphogenesis periods (PD15 and PD19). Further, haematoxylin and eosin staining (H&E) on the dorsal skin sections was performed during various postnatal days (PD15, 19, 21, 25, 28, 35, 41 and 49) (Fig. 1b). Our histological data revealed interfollicular epidermal cyst formation and abnormal thickening of the interfollicular epidermis (IFE) (Fig. 1c) as compared to wild type control littermate. Further, hair follicle cycling analysis on the dorsal skin at various postnatal days showed hair follicle is halted at anagen like stage in K14-sPLA<sub>2</sub>-IIA homozygous mice (Fig. 1d). This is due to the fact that we have not observed telogen at any postnatal day (PD15, PD17, PD21, PD25, PD28, PD30, PD35, PD41, PD45 and PD49). The change in morphology of the hair follicle is due to abnormal development of epidermal compartments. Further, we observed increased activation of  $\beta$ -catenin in K14-sPLA<sub>2</sub>-IIA homozygous mice skin as compared to hemizygous and wild type control littermate (Supplementary Fig. S2). These data indicate that the hair follicles of K14-sPLA<sub>2</sub>-IIA homozygous mice failed to progress into regression phase (Catagen) of the hair follicle cycle. Thus, epidermal overexpression of sPLA<sub>2</sub>-IIA results in morphological abnormalities of hair follicle with hair loss.

## Abnormal organization of epidermal components and stratification of epidermis.

Morphological abnormalities of the hair follicle led us to investigate if there is any effect on proliferation and differentiation in different epidermal compartments. To evaluate the effect of sPLA<sub>2</sub>-IIA on cell proliferation, we have performed immunofluorescence staining of Ki67, a proliferation marker on wholemount of intact epidermal sheets (Fig. 2a). Our results showed increased number of Ki67 positive cells in the outer root sheath and dermal papillae of the hair follicles, suggesting enhanced proliferation in K14-sPLA<sub>2</sub>-IIA homozygous mice

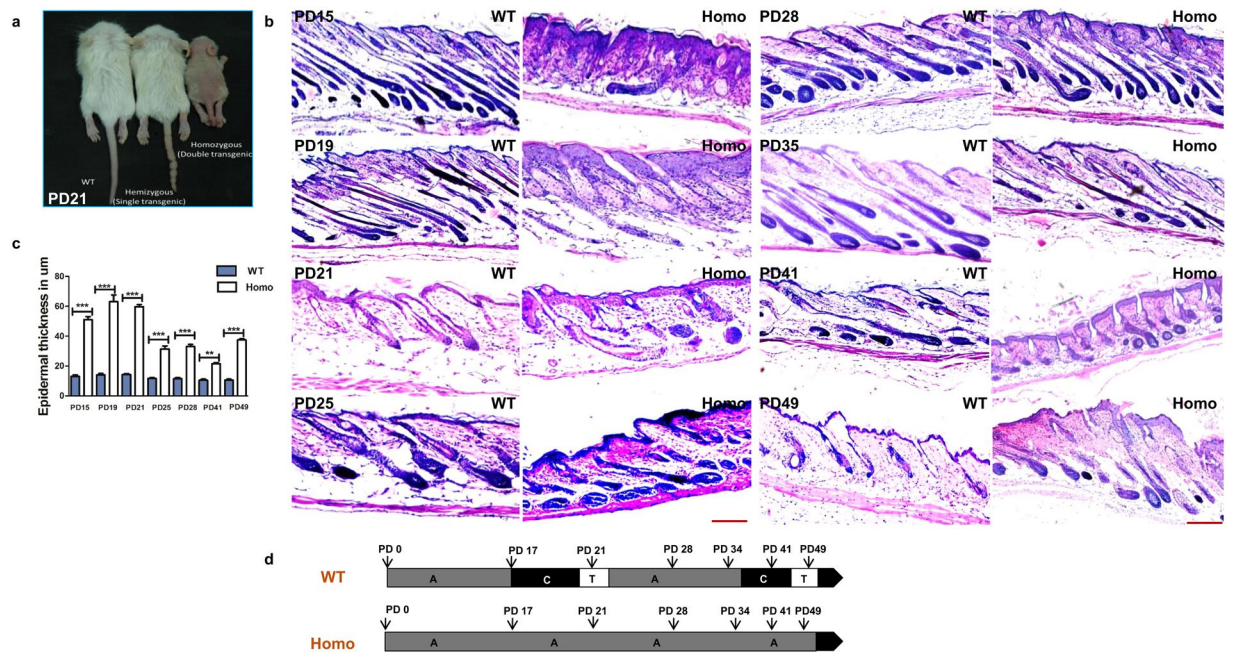


**Figure 1.** sPLA<sub>2</sub>-IIA overexpression altered the hair cycle with abnormal hair follicle morphology and hair loss. **(a)** Phenotypic appearance of WT, hemizygous and homozygous mice at PD21. **(b)** Images represent hematoxylin and eosin staining (H&E) of skin sections at various postnatal days of WT and K14-sPLA<sub>2</sub>-IIA homozygous mice to study hair follicle cycling. **(c)** Graphical representation of epidermal thickness measurements are in µm. Data are presented as mean ± SD. \*\*P < 0.005, \*\*\*P < 0.001, \*\*\*\*P < 0.0001. **(d)** Comparative analysis of hair follicle progression to different stages of hair cycle (Anagen, Catagen and Telogen) at different postnatal days in WT and K14-sPLA<sub>2</sub>-IIA homozygous mice. (WT-Wild type, Homo-K14-sPLA<sub>2</sub>-IIA homozygous mice, n = 3 mice/genotype. A-Anagen, C-Catagen and T-Telogen, PD-Postnatal days).

skin. Moreover, we observed enlarged width of infundibulum and junctional zone regions of the hair follicle in K14-sPLA<sub>2</sub>-IIA homozygous mice. Therefore, we sought to check the expression of Lrig1, the marker of junctional zone stem cells by immunofluorescence staining on skin section, which showed significant increase in the Lrig1 positive cells (Fig. 2b). Further, to study whether the hyper-proliferative cells of IFE also generate more differentiated progeny, the later stages of terminal differentiation were evaluated. Immunofluorescence staining of Loricrin showed enhanced expression of Loricrin in K14-sPLA<sub>2</sub>-IIA homozygous mice skin, which indicates that sPLA<sub>2</sub>-IIA markedly increased epidermal differentiation (Fig. 2c). This result was further confirmed by the Real time quantitative analysis of S100a9 mRNA expression that showed drastic upregulation, suggesting increased differentiation in K14-sPLA<sub>2</sub>-IIA homozygous mice (Supplementary Fig. S3).

**Complete exhaustion of hair follicle stem cells in K14-sPLA<sub>2</sub>-IIA homozygous mice.** In K14-sPLA<sub>2</sub>-IIA homozygous mice, hair follicle was halted at anagen like stage and hair loss was observed with increase in proliferation and differentiation. Therefore, we attempted to understand the profile of hair follicle stem cells. We performed FACS analysis by using the mouse hair follicle stem cell markers such as CD34 and α6 integrin. Our results showed drastic depletion of CD34<sup>+</sup>/α6 integrin<sup>+</sup> hair follicle stem cells at PD28 (Fig. 3a,b). Further, this data was validated by immunofluorescence staining (IFA) of CD34 and α6 integrin on the dorsal skin tissue sections at PD28 and PD49, which showed decrease in the number of CD34<sup>+</sup>/α6 integrin<sup>+</sup> cells in hair follicle bulge of K14-sPLA<sub>2</sub>-IIA homozygous mice (Fig. 3c,d). Moreover, the counting of CD34/α6-integrin dual positive cells per hair follicle bulge showed complete loss of hair follicle stem cells at PD49 (Fig. 3e). In addition, to further confirm the loss of the hair follicle stem cells compartment, we have checked the Sox9 positive hair follicle stem cells in bulge of the hair follicle. Our data showed an absence of Sox9 positive cells in bulge region of hair follicle in the K14-sPLA<sub>2</sub>-IIA homozygous mice as compared to the wild type control littermate (Supplementary Fig. S5). This clearly demonstrates that the hair follicle stem cell pool is depleted. These data suggest that sPLA<sub>2</sub>-IIA induced hyper-proliferative response may lead to the subsequent complete exhaustion of hair follicle stem cell pool and aging-like skin phenotype in K14-sPLA<sub>2</sub>-IIA homozygous mice.

**Development of cyclic alopecia in K14-sPLA<sub>2</sub>-IIA homozygous mice.** The new-born K14-sPLA<sub>2</sub>-IIA homozygous pups could be easily distinguished at PD3 as compared to wild type control littermate by their short and wavy whiskers. We followed the K14-sPLA<sub>2</sub>-IIA homozygous mice from birth (PD1) to up to six months (PD180) and recorded (photographed) the hair growth patterns over time at every alternate day. The hair loss began from PD18 and complete hair loss was observed at PD22 (Fig. 4a). Further, the hair regrowth was started at PD27 that partially covered the body by PD33 (Fig. 4a). However, the hair of K14-sPLA<sub>2</sub>-IIA homozygous mice was short compared to smooth and shiny hair of wild type control littermate. This successive cycle of hair growth

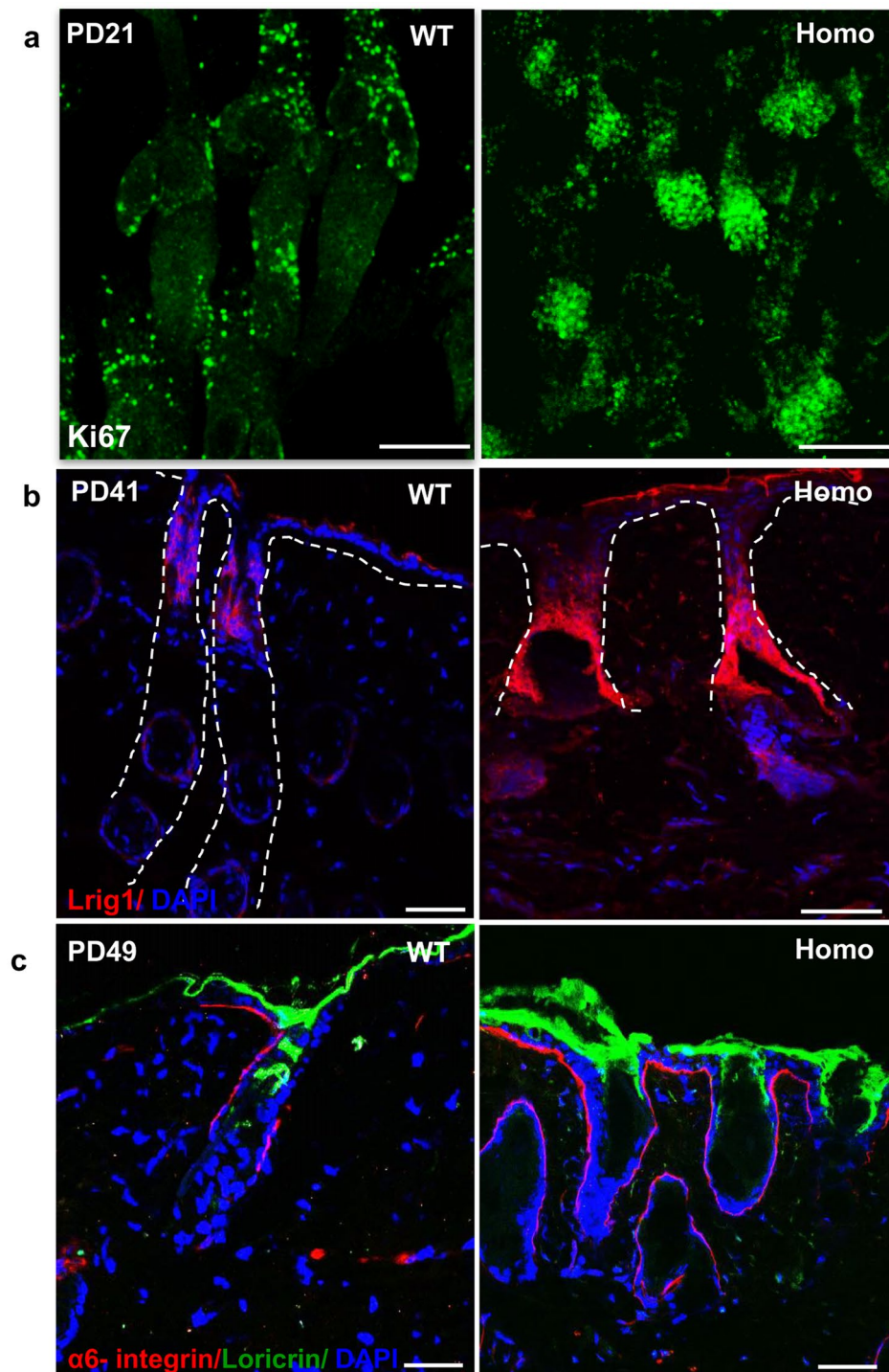


**Figure 2.** sPLA<sub>2</sub>-IIA induced proliferation affects various epidermal compartments. (a) Immunofluorescence staining of Ki67 to assess cell proliferation in intact epidermal sheet of tail skin by wholemount assay at PD21. (b) Immunofluorescence labelling of Lrig1 in WT and K14-sPLA<sub>2</sub>-IIA homozygous mice skin sections at PD41. Dashed lines represent the boundary of junctional zone area. (c) Immunofluorescence staining of loricrin as a differentiation marker to label the cells of granular layers in WT and K14-sPLA<sub>2</sub>-IIA homozygous mice at PD49.

and loss was occurring repetitively after 18–22 days up to 6–8 months (Fig. 4b). This cyclic alopecia was observed in both male and female mice. In addition, we observed permanent alopecia in K14-sPLA<sub>2</sub>-IIA homozygous mice starting at six months age till their survival (One year, Data not shown).

**Aberrant hair shaft differentiation mediated through deregulated expression of signalling modulators.** We further investigated whether this cyclic phenomenon relies on the deregulation of known

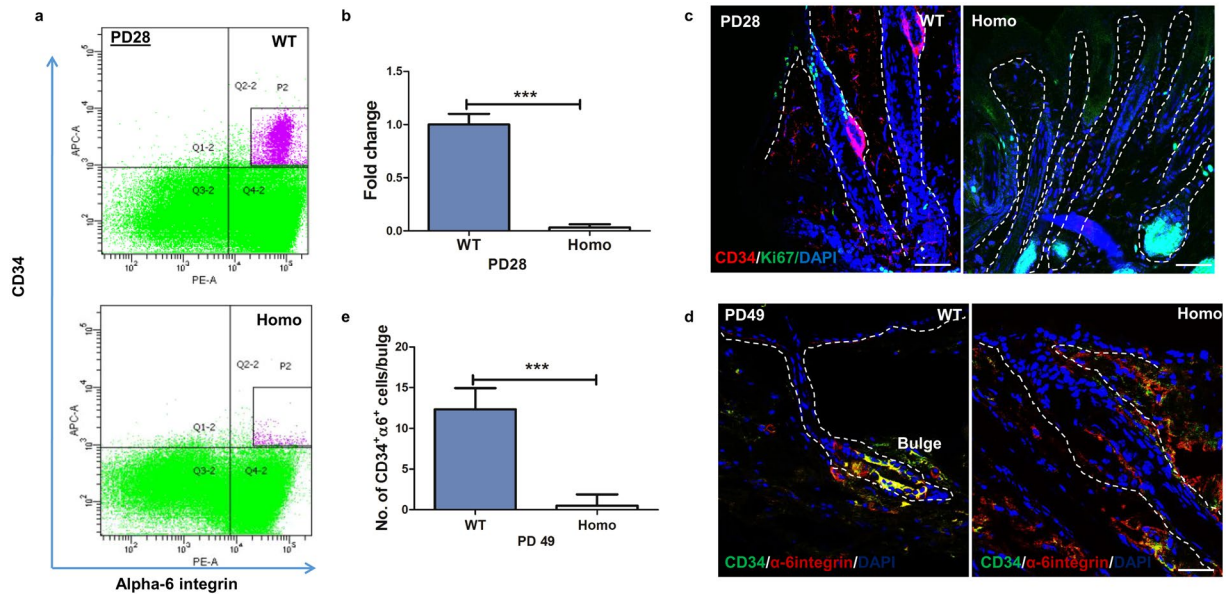


**Figure 3.** Overexpression of sPLA<sub>2</sub>-IIA leads to depletion of hair follicle stem cells. (a) Flow cytometry based analysis of hair follicle stem cells (CD34<sup>+</sup>/α-6 integrin<sup>+</sup>) in WT and K14-sPLA<sub>2</sub>-IIA homozygous mice at PD28. (b) Quantification of FACS analysis of CD34<sup>+</sup>/α6-integrin<sup>+</sup> bulge HFSCs in wild type and K14-sPLA<sub>2</sub>-IIA homozygous mice at PD28. (c) Immunofluorescence analysis of CD34 and Ki67 expression in hair follicle at PD28. Scale bar: 50 μm. (d) Immunofluorescence analysis of CD34<sup>+</sup>/α6-integrin<sup>+</sup> dual positive cells in hair follicle at PD49. Scale bar: 50 μm. (e) Quantification of CD34<sup>+</sup>/α6-integrin<sup>+</sup> cells in the bulge of the dorsal skin in wild type and K14-sPLA<sub>2</sub>-IIA homozygous mice at PD49. PD-Postnatal days, HFSCs-Hair follicle stem cells. (WT-Wild type Homo- K14-sPLA<sub>2</sub>-IIA homozygous mice, n = 3 mice/genotype, PD-Postnatal days. Data are presented as mean ± SD. \*\*P < 0.005, \*\*\*P < 0.001, \*\*\*\*P < 0.0001).

molecules or is there an unexplored novel mechanism. The expression levels of known genes such as Sox21, Msx2, Zdhc13 and Foxn1 were analysed. Real time PCR data showed significant downregulation of Sox21, Msx2 and Foxn1 mRNA expression as compared to wild type control littermate (Fig. 4c). However, we did not observe any significant difference in expression level of Zdhc13 and Gsdma3 mRNA (Supplementary Fig. S3). Importantly, Sox21 acts as a regulator of keratins expression, that is necessary for the formation of IRS (Inner root sheath) and anchoring of hair shaft. We examined the status of Gata3, Krt82 and Krt71 by real time PCR analysis. We found significant down-regulation of Gata3, Krt82 and Krt71 expression that suggest an aberrant differentiation of IRS and hair shaft precursor cells in K14-sPLA<sub>2</sub>-IIA homozygous mice (Fig. 4d). To understand the molecular mechanisms underlying impaired differentiation of the matrix cells, we checked the level of BMP4, Shh and Lef1, which are known to regulate the matrix cells proliferation and generation of precursors for IRS and hair shaft formation. We observed significant downregulation of BMP4, Lef1 and Shh in K14-sPLA<sub>2</sub>-IIA homozygous mice skin (Fig. 4e). These data suggested that deregulated signalling in matrix cells may lead to defects in differentiation of IRS and formation of hair shaft.

**Delayed wound healing response in K14-sPLA<sub>2</sub>-IIA homozygous mice.** Hair follicle stem cells contribute during epidermal regeneration after wounding. However, we observed drastic depletion of hair follicle stem cells in K14-sPLA<sub>2</sub>-IIA homozygous mice, which led us to evaluate wound healing response in K14-sPLA<sub>2</sub>-IIA homozygous mice. Scratch wounds were made on upper region at midline (yellow circle) (Fig. 5a) whereas, full thickness wounds (8 mm) were made on lower region of dorsal skin at PD49, that were monitored to assess the macroscopic healing defects (Fig. 5a). Our data showed impaired initial healing response in K14-sPLA<sub>2</sub>-IIA homozygous mice at day 5 (red circle) (Fig. 5b). However, the pace of wound recovery accelerated after 5 to 6 days and fully recovered at the same time of wild type control littermate (green circle) (Fig. 5b). To further investigate, whether the impaired wound healing response is due to the poor nutrition, we have checked the levels of serum albumin, Vitamin C, Vitamin D and Zinc from the serum. Our data showed that there is no significant difference in the levels of serum albumin, Vitamin C, Vitamin D and Zinc in the serum of the K14-sPLA<sub>2</sub>-IIA homozygous mice as compared to wild type control littermate (Supplementary Fig. S4). These results confirmed that the initial defects in the wound healing response may not be due to the poor nutrition. Thus, it demonstrates that overexpression of sPLA<sub>2</sub>-IIA delays initial response to wounding; however, the complete wound was filled at the same time point as compared to wild type control littermate.

## Discussion

The regenerative capability of adult tissue relies on activity of long-lived tissue specific stem cells. The cyclic activation of quiescent hair follicle stem cells depends on signalling cues present in the surrounding microenvironment. Involvement of different growth factors including EGF, TGFs and FGFs is well established in regulation of

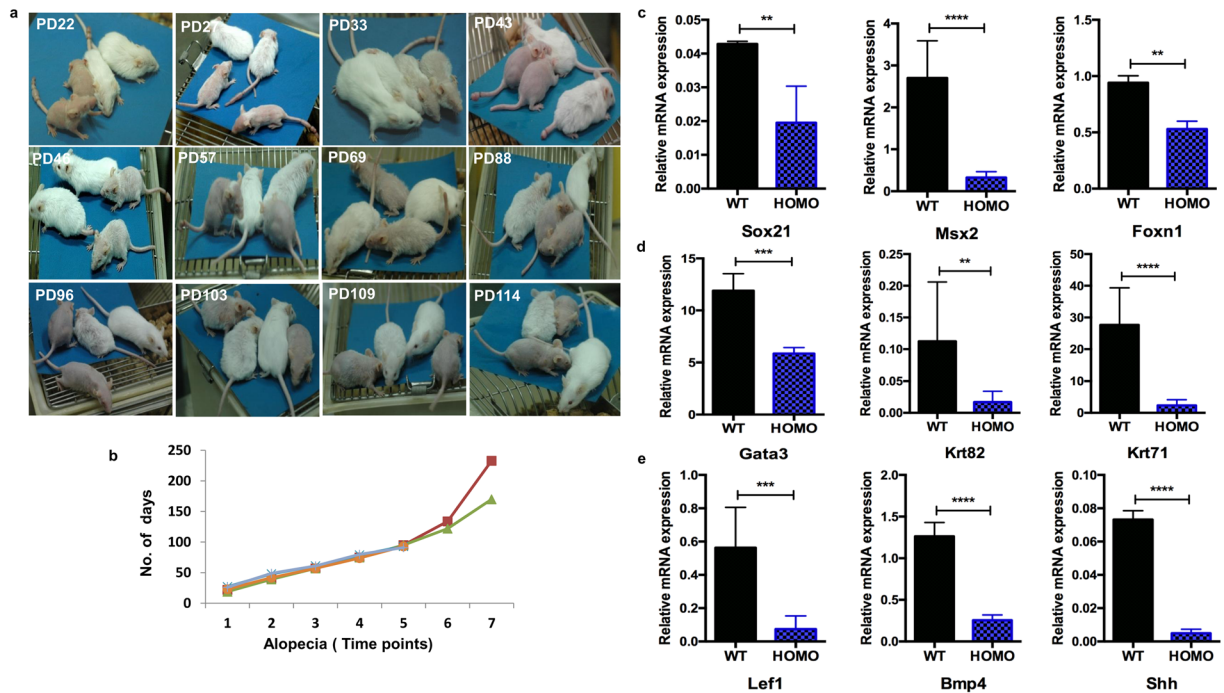


**Figure 4.** Cyclic alopecia in K14-sPLA<sub>2</sub>-IIA homozygous mice during various post-natal days. (a) Phenotypic appearance of WT and K14-sPLA<sub>2</sub>-IIA homozygous mice at different postnatal days with cyclic loss of hair and regain followed till six months. (b) Graphical representation of alopecia time points with respect to postnatal days of the K14-sPLA<sub>2</sub>-IIA homozygous mice. (c) Real time PCR gene expression analysis of Sox21, Msx2, Foxn1. (d) Gene expression analysis by Real time PCR of Gata3, Krt82 and Krt71. (e) Gene expression profiling of Lef1, BMP4, Shh. The relative quantification is with respect to expression level of  $\beta$ -actin. (WT-Wild type Homo- K14-sPLA<sub>2</sub>-IIA homozygous mice, n = 3 mice/genotype, PD-Postnatal days, Data are presented as mean  $\pm$  SD. \*\*P < 0.005, \*\*\*P < 0.001, \*\*\*\*P < 0.0001).

epidermal stem cells proliferation and fate determination<sup>11</sup>. As previously shown, deregulated release of Hb-EGF in mutant mice expressing soluble proHb-EGF induced epidermal hyperproliferation and displayed hyperplasia<sup>31</sup>. Overexpression of TGF $\alpha$  in transgenic mice epidermis demonstrates aberrant keratins expression, hyperproliferation and development of papillomas<sup>32</sup>. Further, expression of a dominant-negative FGF receptor mutant in transgenic mice under the control of Keratin 10 (K10) promoter induced epidermal hyper-thickening and altered keratinocytes differentiation<sup>33</sup>. Similarly, K14-sPLA<sub>2</sub>-IIA homozygous mice showed alterations in the hair follicle cycling, that are stuck in the anagen like phase of hair follicle and enhanced proliferation in various compartments of epidermis leading to epidermal hyperplasia. The sPLA<sub>2</sub>-IIA is known to enhance the EGF signalling in astrocytoma cells<sup>34</sup> and continuous expression of epidermal growth factor prevents entry of hair follicle into the regression phase (Catagen) of hair cycle<sup>15</sup>. In agreement, our data of increased proliferation and hair follicle stuck at anagen like phase may be due to sPLA<sub>2</sub>-IIA mediated enhanced EGF signalling. Precisely, as EGF receptors are known to be expressed in the cells of outer root sheath of the hair follicle, and the proliferative response generated by upregulated mitogens (Hb-EGF and EPGN) directly suggest the involvement of catalytic independent activity of sPLA<sub>2</sub>-IIA in modulating EGFR signalling, which is not the case for the other group of secretory phospholipases. An aberrant signalling mediated hyperproliferation of the HFSCs resulted in loss of quiescence and exhaustion of stem cell pool. Smad4 deletion in mouse epidermis inhibits programmed regression of the hair follicles and exhibits progressive alopecia with depletion of hair follicle stem cells<sup>26,35</sup>. Also, activation of mTOR by Wnt overexpression resulted in depletion of the hair follicle stem cells and accelerates hair loss and aging<sup>36</sup>. In agreement, our results showed hyperproliferation in various compartments of the hair follicle, that may lead to loss of quiescence and exhaustion of the hair follicle stem cells and development of alopecia.

Further, the contribution of the hair follicle stem cells in wound re-epithelialisation following injury is well established. Initially, the bulge-derived transient amplifying cells rapidly respond to the injury that contribute in wound repair and subsequently replaced by IFE derived cells over several weeks<sup>37</sup>. In contrast, partial ablation of the hair follicle stem cells by diphtheria toxin does not delay healing process following wounding thereby, suggesting that the bulge cells are dispensable for wound re-epithelialisation<sup>38</sup>. Epidermal hyperproliferation induced by deficiency of Jun-B resulted in delayed wound healing response<sup>39</sup>. Further, Runx1 deletion in mice showed delay in the activation of the HFSCs, which are further activated by skin injury<sup>40</sup>. Importantly, it has been shown that the bulge, hair follicle stem cells contribute to the process of wound healing and start migrating towards the wounded area within 24 hours, which suggests the involvement of the hair follicle stem cells in the initial process of wound healing<sup>6,37,41,42</sup>. Our data of K14-sPLA<sub>2</sub>-IIA homozygous mice suggested that delay in initial response to wounding is likely due to the absence of immediate progenitor of the hair follicle stem cells, that sense

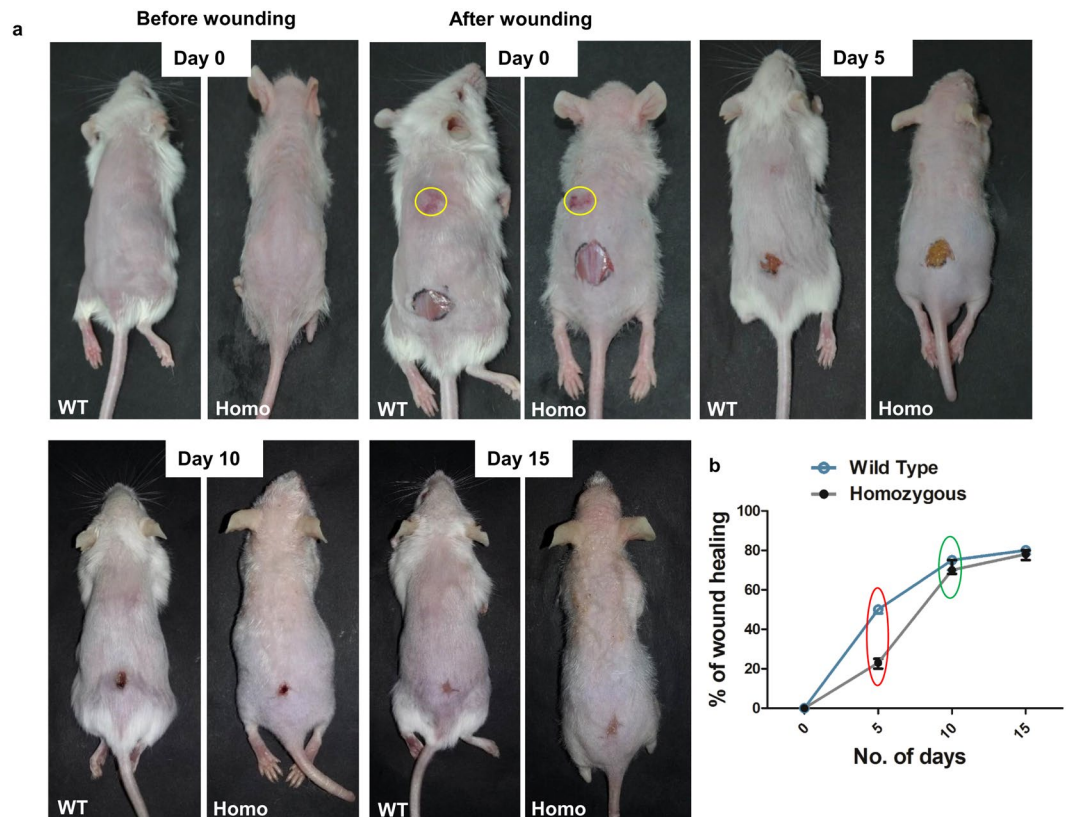


**Figure 5.** Impaired initial response to wounding in K14-sPLA<sub>2</sub>-IIA homozygous mice skin. **(a)** Photographs of WT and K14-sPLA<sub>2</sub>-IIA homozygous mice at Day 0 (before wounding) and at Day 0 (after wounding). The healing process was recorded by photographs at various days and representative images are mentioned as Day 5, Day 10 and Day 15. **(b)** Graphical representation of comparative wound recovery during healing process. Red circle indicates defects in initial healing response in K14-sPLA<sub>2</sub>-IIA homozygous mice. Green circle indicates no significant difference in time periods for complete wound recovery during later stage. (WT-Wild type Homo-K14-sPLA<sub>2</sub>-IIA homozygous mice, n = 3 mice/genotype, PD-Postnatal days).

the injury and effectively contributes towards initial healing response. Further, in agreement with the previous reports, IFE derived cells may take over the function and efficiently heal the wounded area at later time points.

Moreover, various studies have shown the phenomenon of permanent or cyclic alopecia in different genetic backgrounds of mice. The mice expressing dominant negative mutant of EGFR display severe alopecia<sup>24</sup>. Importantly, mice overexpressing human group II PLA<sub>2</sub> displayed epidermal hyperplasia and complete alopecia<sup>43</sup>. Similarly overexpression of Pla2g2f in mice epidermis showed psoriasis like epidermal hyperplasia and alopecia<sup>44</sup>. Genetic disruption of the Sox21 and Msx2 resulted in defects in anchoring of hair shaft<sup>25</sup> and aberrant hair shaft differentiation<sup>28</sup> respectively. However, the level of Sox21 remained unaltered in Msx2 null background suggesting independent mode of action of both the molecules in the development of cyclic alopecia. We observed the downregulation of Sox21 and Msx2 in the K14-sPLA<sub>2</sub>-IIA homozygous mice suggesting that sPLA<sub>2</sub>-IIA may function upstream of both the factors and altering their expression. Further, mutation mediated downregulation of Zdhhc13 in mice exhibits epidermal hyperproliferation, abnormal hair follicle growth and cyclic alopecia at early telogen<sup>45,46</sup>. However, we did not observe any alteration in Zdhhc13 level suggesting that the development of cyclic alopecia in K14-sPLA<sub>2</sub>-IIA homozygous mice is independent of cornifelin deficiency mediated cyclic alopecia as shown in Zdhhc13 mutant mice.

Importantly, the proliferation and fate determination of matrix cells to differentiate in the IRS and hair shaft is governed by various signalling modulators such as BMP4, Lef1 and Shh. Specifically, BMP4 is expressed in the hair matrix cells and dermal papillae and is known to be involved in differentiation of the hair matrix cells to precursors cells required for hair shaft formation. Our results of gene expression study are in agreement with the previous study of sPLA<sub>2</sub>-X overexpressing transgenic mice, that showed down regulation of BMP4, Shh, Lef1, Foxn1 and Gata3 during development of cyclic alopecia<sup>47</sup>. Together, we found that overexpression sPLA<sub>2</sub>-IIA enhances the terminal epidermal differentiation however, the differentiation of matrix cells to produce precursors of the IRS and hair shaft is severely affected. This is likely due to the deregulated expression of keratin gene regulators such as Sox21 and matrix cells differentiation to produce hair shaft. Overall, these results suggest that sPLA<sub>2</sub>-IIA may affect differentiation of matrix cells. With regards to our finding, we have proposed the model for comparative hair follicle cycling (Fig. 6). Altered hair follicle cycling in K14-sPLA<sub>2</sub>-IIA homozygous mice represented by abnormal morphology of hair follicle with the presence of affected hair shaft. The hair follicle cycling does not progress through the first hair cycle, as the hair follicles are being stuck in anagen like stage during the

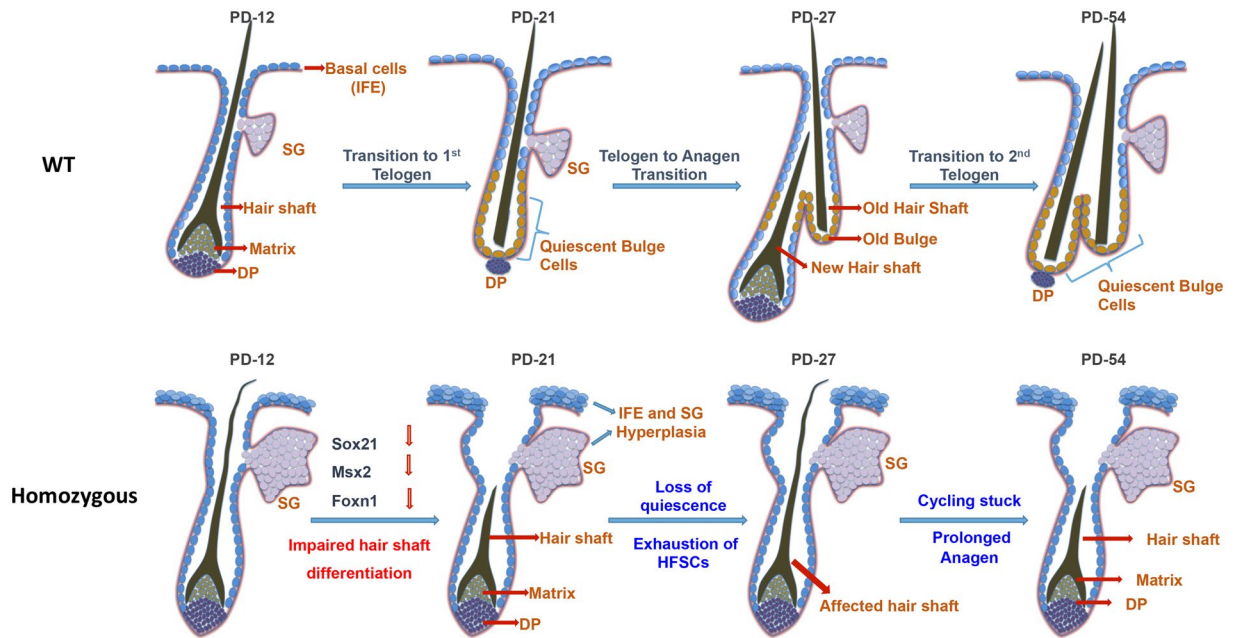


**Figure 6.** Proposed model of impaired hair follicle cycling in K14-sPLA<sub>2</sub>-IIA homozygous mice. **WT-** Graphical representation of hair follicle cycling in wild type mice from hair follicle morphogenesis to second telogen at PD49, which is represented by the presence of club hair and subsequent progression to the next hair cycle. **Homozygous-** Graphical representation of hair follicle cycling in K14-sPLA<sub>2</sub>-IIA homozygous mice represented by abnormal morphology of hair follicle with the presence of affected hair shaft. (WT-Wild type Homo- K14-sPLA<sub>2</sub>-IIA homozygous IFE: inter follicular epidermis, SG: sebaceous gland, DP: dermal papilla, PD-Postnatal days).

initiation of the first hair follicle cycling process. Further at PD28, the hair follicle is represented by the presence of an affected hair shaft due to downregulated expression of Sox21, Msx2, and Foxn1, which are known to be involved in IRS differentiation. Moreover, downregulation of signaling modulators such as Bmp4, Shh, and Lef1 is observed in K14-sPLA<sub>2</sub>-IIA homozygous mice. Together, downregulated expression of hair shaft differentiation regulators may lead to the development of alopecia in K14-sPLA<sub>2</sub>-IIA homozygous mice.

In conclusion, we showed that sPLA<sub>2</sub>-IIA mediated increased proliferation results in the complete exhaustion of the HFSCs and development of alopecia due to aberrant expression of hair shaft differentiation regulators. The cyclic growth of hair and complete re-epithelialization of the epidermis after wounding in the absence of HFSCs explains the functional involvement of stem cells from other compartments of the epidermis. This further opens a new avenue to explore the role of stem cells of other compartments of the epidermis and their ability to differentiate into hair shaft-producing cells. This study provides conceptual evidence of functional redundancy within stem cell populations that reside in various compartments of the epidermis. Further, the non-catalytic activity of sPLA<sub>2</sub>-IIA may provide information to develop potential sPLA<sub>2</sub>-IIA inhibitors for effective inhibition of sPLA<sub>2</sub>-IIA activity during various patho-physiological conditions such as arthritis, inflammation, and cancer.

## Materials and Methods

**Transgenic mice and genotyping.** K14-sPLA<sub>2</sub>-IIA mice were a gift from Dr. Rita Mulherkar<sup>22</sup>. The hemizygous K14-sPLA<sub>2</sub>-IIA was crossed to hemizygous K14-sPLA<sub>2</sub>-IIA mice to obtain the homozygous mice for the experiments. The K14-sPLA<sub>2</sub>-IIA hemizygous and homozygous transgenic mice were obtained based on phenotype and PCR genotyping as described previously<sup>22</sup>. Mice were sacrificed at various postnatal ages. Animal experimental study was approved by ACTREC's Institutional Animal Ethics Committee (IAEC), and all the experiments were performed in accordance with the approved guidelines and regulations.

**Histology, Immunostaining and tail whole mount assay.** Mice skin tissue (dorsal and tail skin) at various postnatal day ages were collected and fixed by neutral buffered formalin (NBF) or directly embedded in OCT compound (Tissue-Tek) and frozen. Immunofluorescence assays (IF) and immunohistochemical analysis (IHC-P) were performed as previously described<sup>7</sup>. Paraffin-embedded tissue blocks were sectioned and stained with Haematoxylin and Eosin (H&E) for phase analysis of the hair follicle cycle. Immunofluorescence assays (IF) and immunohistochemical analysis (IHC-P) were performed on OCT-frozen tissue and paraffin-embedded block respectively<sup>23</sup>. Tail whole mount was performed as described previously<sup>48</sup>. Briefly, tail skin was incubated in 5 mM EDTA followed by separation of the epidermal sheet from the dermis followed by fixing with 2% formaldehyde for 10 minutes. Nile red was used to stain the sebocytes of the sebaceous gland and confocal microscopy was used for image acquisition. Primary antibodies used such as: CD34 (1:100, BD Pharmingen);  $\alpha$ -6 integrin (1:100, BD Pharmingen); BrdU (1:250, Abcam); Ki67 (1:100, Novocastra); Filaggrin

(1:1000, Abcam); Loricrin (1:1000, Abcam); K10 (1:1000, Abcam); Lrig1 (1:500, R&D systems) and Sox9 (1:500, Merck Millipore).

**Fluorescence activated cell sorting analysis.** Dorsal skin of wild type control littermate and K14-sPLA<sub>2</sub>-IIA homozygous mice at PD21 and PD49 was harvested and scrapped for fat removal, followed by overnight incubation in 0.25% trypsin at 4 °C. FACS experiments were performed as described previously<sup>7</sup>. Single cell suspension was obtained by first passing through 70 µm and then 40 µm cell strainers (BD Biosciences). Cells were stained with trypan blue and the hemacytometer chamber was used to count the cells. Further cells were stained by using the hair follicle stem cells markers: CD34-Biotin (eBiosciences), Streptavidin-APC (BD Pharmingen), and anti-α6-integrin-PE (BD Pharmingen). After washing cells were subjected to FACS acquisition using a FACS Aria and data was analyzed by using FACS DiVa software (BD Biosciences).

**Real-time quantitative PCR.** Total RNA was extracted from mouse epidermis by using the Absolutely RNA Miniprep Kit (Agilent Technologies). 2 µg of total RNA was reverse transcribed using cDNA synthesis kit (Invitrogen, Carlsbad, CA) as per the manufacturer instructions. Quantitative PCR (q-PCR) was performed by using the SYBR Green (Invitrogen) as per the manufacturer's instructions. Gene expression was normalized to β-actin. The relative expression levels of mRNAs were calculated by relative quantification method with respect to β-actin. For primers sequences please refer supplementary information.

**Wound healing assay.** K14-sPLA<sub>2</sub>-IIA homozygous mice and control mice of 49 days were anaesthetized with isoflurane by inhalation for 30–60 seconds. After hair removal from the dorsal surface, single 8 mm full thickness excision skin wound on the midline was created. During the healing periods, recovery of the wounds was photographed. The wounded tissue was collected, OCT blocks and Paraffin blocks were prepared. Histological sections were stained with hematoxylin and eosin on paraffin blocks.

**Quantification of nutritional parameters from serum.** Wild type and K14-sPLA<sub>2</sub>-IIA homozygous mice were starved for eight hours before collecting the blood. Serum was separated by centrifugation at 6000 rpm for 10 mins. Further, ascorbic acid was quantified by using ascorbic acid assay kit (ab65656) and zinc was quantified by using zinc quantification kit (ab102507) as per the manufacturer's instructions. The nutritional parameters such as serum albumin, serum glucose, triglyceride, Sodium, Phosphorus, Chloride, total protein, Calcium and potassium was quantified by using Siemens's Dimension EXL with LM, automated biochem analyzer and Vitamin B12 and Vitamin D 25-OH was quantified by using Abbott's architect plus i1000SR as per the manufacturer's instructions.

**Statistical analysis.** Statistical significance was calculated to make the comparison between two groups by using the unpaired two-tailed student's t-test with GraphPad Prism 5 for the data obtained from the measurement of IFE thickness, flow cytometry, Real time PCR, counting of hair follicle stem cells in bulge and nutritional parameters. Data represented with error bar indicating the mean ± SD of the mean: \*P < 0.05, \*\*P < 0.005, \*\*\*P < 0.0001.

## References

- Fuchs, E. Skin stem cells: rising to the surface. *J Cell Biol* **180**, 273–284, doi:<https://doi.org/10.1083/jcb.200708185> (2008).
- Blanpain, C. & Fuchs, E. Epidermal stem cells of the skin. *Annual review of cell and developmental biology* **22**, 339–373, doi:<https://doi.org/10.1146/annurev.cellbio.22.010305.104357> (2006).
- Hardy, M. H. The secret life of the hair follicle. *Trends Genet* **8**, 55–61 (1992).
- Alonso, L. & Fuchs, E. The hair cycle. *Journal of cell science* **119**, 391–393, doi:<https://doi.org/10.1242/jcs.02793> (2006).
- Cotsarelis, G., Sun, T. T. & Lavker, R. M. Label-retaining cells reside in the bulge area of pilosebaceous unit: implications for follicular stem cells, hair cycle, and skin carcinogenesis. *Cell* **61**, 1329–1337 (1990).
- Tumbar, T. *et al.* Defining the epithelial stem cell niche in skin. *Science* **303**, 359–363 (2004).
- Waghmare, S. K. *et al.* Quantitative proliferation dynamics and random chromosome segregation of hair follicle stem cells. *Embo J* **27**, 1309–1320 (2008).
- Waghmare, S. K. & Tumbar, T. Adult hair follicle stem cells do not retain the older DNA strands *in vivo* during normal tissue homeostasis. *Chromosome research: an international journal on the molecular, supramolecular and evolutionary aspects of chromosome biology* **21**, 203–212, doi:<https://doi.org/10.1007/s10577-013-9355-y> (2013).
- Rompolas, P. & Greco, V. Stem cell dynamics in the hair follicle niche. *Seminars in cell & developmental biology* **25–26**, 34–42, doi:<https://doi.org/10.1016/j.semcdb.2013.12.005> (2014).
- Watt, F. M. & Jensen, K. B. Epidermal stem cell diversity and quiescence. *EMBO Mol Med* **1**, 260–267, doi:<https://doi.org/10.1002/emmm.200900033> (2009).
- Lee, J. & Tumbar, T. Hairy tale of signaling in hair follicle development and cycling. *Seminars in cell & developmental biology* **23**, 906–916, doi:<https://doi.org/10.1016/j.semcdb.2012.08.003> (2012).
- Huelsken, J., Vogel, R., Erdmann, B., Cotsarelis, G. & Birchmeier, W. beta-Catenin controls hair follicle morphogenesis and stem cell differentiation in the skin. *Cell* **105**, 533–545 (2001).
- Andl, T., Reddy, S. T., Gaddapara, T. & Millar, S. E. WNT signals are required for the initiation of hair follicle development. *Dev Cell* **2**, 643–653 (2002).
- Ito, M. *et al.* Wnt-dependent de novo hair follicle regeneration in adult mouse skin after wounding. *Nature* **447**, 316–320, doi:<https://doi.org/10.1038/nature05766> (2007).
- Mak, K. K. & Chan, S. Y. Epidermal growth factor as a biologic switch in hair growth cycle. *J Biol Chem* **278**, 26120–26126, doi:<https://doi.org/10.1074/jbc.M212082200> (2003).
- Mulherkar, R. *et al.* Enhancing factor protein from mouse small intestines belongs to the phospholipase A2 family. *FEBS Lett* **317**, 263–266 (1993).
- Schewe, M. *et al.* Secreted Phospholipases A2 Are Intestinal Stem Cell Niche Factors with Distinct Roles in Homeostasis, Inflammation, and Cancer. *Cell stem cell* **19**, 38–51, doi:<https://doi.org/10.1016/j.stem.2016.05.023> (2016).
- Kadam, S. & Mulherkar, R. Enhancing activity and phospholipase A2 activity: two independent activities present in the enhancing factor molecule. *Biochem J* **340**(Pt 1), 237–243 (1999).

19. Gurrieri, S. *et al.* Differentiation-dependent regulation of secreted phospholipases A2 in murine epidermis. *J Invest Dermatol* **121**, 156–164, doi:<https://doi.org/10.1046/j.1523-1747.2003.12315.x> (2003).
20. Ilic, D., Bollinger, J. M., Gelb, M. & Mauro, T. M. sPLA2 and the epidermal barrier. *Biochim Biophys Acta* **1841**, 416–421, doi:<https://doi.org/10.1016/j.bbali.2013.11.002> (2014).
21. Scott, K. F. *et al.* Emerging roles for phospholipase A2 enzymes in cancer. *Biochimie* **92**, 601–610, doi:<https://doi.org/10.1016/j.biochi.2010.03.019> (2010).
22. Mulherkar, R. *et al.* Expression of enhancing factor/phospholipase A2 in skin results in abnormal epidermis and increased sensitivity to chemical carcinogenesis. *Oncogene* **22**, 1936–1944, doi:<https://doi.org/10.1038/sj.onc.1206229> (2003).
23. Sarate, R. M. *et al.* sPLA2 -IIA Overexpression in Mice Epidermis Depletes Hair Follicle Stem Cells and Induce Differentiation Mediated Through Enhanced JNK/c-Jun Activation. *Stem Cells*, doi:<https://doi.org/10.1002/stem.2418> (2016).
24. Murillas, R. *et al.* Expression of a dominant negative mutant of epidermal growth factor receptor in the epidermis of transgenic mice elicits striking alterations in hair follicle development and skin structure. *Embo j* **14**, 5216–5223 (1995).
25. Kiso, M. *et al.* The disruption of Sox21-mediated hair shaft cuticle differentiation causes cyclic alopecia in mice. *Proceedings of the National Academy of Sciences of the United States of America* **106**, 9292–9297, doi:<https://doi.org/10.1073/pnas.0808324106> (2009).
26. Yang, L., Wang, L. & Yang, X. Disruption of Smad4 in mouse epidermis leads to depletion of follicle stem cells. *Molecular biology of the cell* **20**, 882–890, doi:<https://doi.org/10.1091/mbc.E08-07-0731> (2009).
27. Sharov, A. A. *et al.* Bone morphogenetic protein antagonist noggin promotes skin tumorigenesis via stimulation of the Wnt and Shh signaling pathways. *Am J Pathol* **175**, 1303–1314, doi:<https://doi.org/10.2353/ajpath.2009.090163> (2009).
28. Ma, L. *et al.* ‘Cyclic alopecia’ in Msx2 mutants: defects in hair cycling and hair shaft differentiation. *Development* **130**, 379–389 (2003).
29. Gwack, Y. *et al.* Hair loss and defective T- and B-cell function in mice lacking ORAI1. *Mol Cell Biol* **28**, 5209–5222, doi:<https://doi.org/10.1128/mcb.00360-08> (2008).
30. Mammucari, C. *et al.* Integration of Notch 1 and calcineurin/NFAT signaling pathways in keratinocyte growth and differentiation control. *Dev Cell* **8**, 665–676, doi:<https://doi.org/10.1016/j.devcel.2005.02.016> (2005).
31. Yamazaki, S. *et al.* Mice with defects in HB-EGF ectodomain shedding show severe developmental abnormalities. *J Cell Biol* **163**, 469–475, doi:<https://doi.org/10.1083/jcb.200307035> (2003).
32. Dominey, A. M. *et al.* Targeted overexpression of transforming growth factor alpha in the epidermis of transgenic mice elicits hyperplasia, hyperkeratosis, and spontaneous, squamous papillomas. *Cell growth & differentiation: the molecular biology journal of the American Association for Cancer Research* **4**, 1071–1082 (1993).
33. Werner, S. *et al.* Targeted expression of a dominant-negative FGF receptor mutant in the epidermis of transgenic mice reveals a role of FGF in keratinocyte organization and differentiation. *Embo j* **12**, 2635–2643 (1993).
34. Hernandez, M., Martin, R., Garcia-Cubillas, M. D., Maeso-Hernandez, P. & Nieto, M. L. Secreted PLA2 induces proliferation in astrocytoma through the EGF receptor: another inflammation-cancer link. *Neuro-oncology* **12**, 1014–1023, doi:<https://doi.org/10.1093/neuonc/ncq078> (2010).
35. Yang, L. *et al.* Targeted disruption of Smad4 in mouse epidermis results in failure of hair follicle cycling and formation of skin tumors. *Cancer Res* **65**, 8671–8678, doi:<https://doi.org/10.1158/0008-5472.can-05-0800> (2005).
36. Castilho, R. M., Squarize, C. H., Chodosh, L. A., Williams, B. O. & Gutkind, J. S. mTOR mediates Wnt-induced epidermal stem cell exhaustion and aging. *Cell stem cell* **5**, 279–289, doi:<https://doi.org/10.1016/j.stem.2009.06.017> (2009).
37. Ito, M. *et al.* Stem cells in the hair follicle bulge contribute to wound repair but not to homeostasis of the epidermis. *Nature medicine* **11**, 1351–1354, doi:<https://doi.org/10.1038/nm1328> (2005).
38. Garcin, C. L., Ansell, D. M., Headon, D. J., Paus, R. & Hardman, M. J. Hair Follicle Bulge Stem Cells Appear Dispensable for the Acute Phase of Wound Re-epithelialization. *Stem Cells* **34**, 1377–1385, doi:<https://doi.org/10.1002/stem.2289> (2016).
39. Florin, L. *et al.* Delayed wound healing and epidermal hyperproliferation in mice lacking JunB in the skin. *J Invest Dermatol* **126**, 902–911, doi:<https://doi.org/10.1038/sj.jid.5700123> (2006).
40. Osorio, K. M. *et al.* Runx1 modulates developmental, but not injury-driven, hair follicle stem cell activation. *Development* **135**, 1059–1068 (2008).
41. Ito, M. & Cotsarelis, G. Is the hair follicle necessary for normal wound healing? *J Invest Dermatol* **128**, 1059–1061, doi:<https://doi.org/10.1038/jid.2008.86> (2008).
42. Taylor, G., Lehrer, M. S., Jensen, P. J., Sun, T. T. & Lavker, R. M. Involvement of follicular stem cells in forming not only the follicle but also the epidermis. *Cell* **102**, 451–461 (2000).
43. Grass, D. S. *et al.* II PLA2 in transgenic mice results in epidermal hyperplasia in the absence of inflammatory infiltrate. *J Clin Invest* **97**, 2233–2241, doi:<https://doi.org/10.1172/jci118664> (1996). Expression of human group.
44. Yamamoto, K. *et al.* The role of group IIF-secreted phospholipase A2 in epidermal homeostasis and hyperplasia. *The Journal of experimental medicine* **212**, 1901–1919, doi:<https://doi.org/10.1084/jem.20141904> (2015).
45. Perez, C. J. *et al.* Increased Susceptibility to Skin Carcinogenesis Associated with a Spontaneous Mouse Mutation in the Palmitoyl Transferase Zdhhc13 Gene. *J Invest Dermatol* **135**, 3133–3143, doi:<https://doi.org/10.1038/jid.2015.314> (2015).
46. Liu, K. M. *et al.* Cyclic Alopecia and Abnormal Epidermal Cornification in Zdhhc13-Deficient Mice Reveal the Importance of Palmitoylation in Hair and Skin Differentiation. *J Invest Dermatol* **135**, 2603–2610, doi:<https://doi.org/10.1038/jid.2015.240> (2015).
47. Yamamoto, K. *et al.* Hair follicular expression and function of group X secreted phospholipase A2 in mouse skin. *J Biol Chem* **286**, 11616–11631, doi:<https://doi.org/10.1074/jbc.M110.206714> (2011).
48. Braun, K. M. *et al.* Manipulation of stem cell proliferation and lineage commitment: visualisation of label-retaining cells in whole mounts of mouse epidermis. *Development* **130**, 5241–5255, doi:<https://doi.org/10.1242/dev.00703> (2003).

## Acknowledgements

We thank Dr Rita Mulherkar for providing the K14-sPLA<sub>2</sub>-IIA mice and Dr Preeti Chavan for helping us in the quantification of nutritional parameters. We thank Vagisha Ravi, Priyanka Setia and Saloni Godbole for help in the Histology work. This work was partly supported by ACTREC ASF and ICMR Grant. We thank ACTREC Animal house, Flow cytometry and Microscopy facilities. GLC and RS supported by ACTREC fellowship, RMS supported by UGC fellowship.

## Author Contributions

S.K.W. conceived and designed the project, analyzed and interpreted the data; G.L.C. and R.M.S. performed the experiments and analyzed; R.M.S. prepared the figures; V.K. performed the cyclic alopecia follow up; R.R.S. and N.P.G. helped in the Real time P.C.R.; G.L.C., R.M.S. and S.K.W. analyzed all the data; G.L.C. and S.K.W. wrote the manuscript; S.K.W. reviewed the manuscript.

## Additional Information

**Supplementary information** accompanies this paper at doi:[10.1038/s41598-017-11830-9](https://doi.org/10.1038/s41598-017-11830-9)

**Competing Interests:** The authors declare that they have no competing interests.

**Publisher's note:** Springer Nature remains neutral with regard to jurisdictional claims in published maps and institutional affiliations.



**Open Access** This article is licensed under a Creative Commons Attribution 4.0 International License, which permits use, sharing, adaptation, distribution and reproduction in any medium or format, as long as you give appropriate credit to the original author(s) and the source, provide a link to the Creative Commons license, and indicate if changes were made. The images or other third party material in this article are included in the article's Creative Commons license, unless indicated otherwise in a credit line to the material. If material is not included in the article's Creative Commons license and your intended use is not permitted by statutory regulation or exceeds the permitted use, you will need to obtain permission directly from the copyright holder. To view a copy of this license, visit <http://creativecommons.org/licenses/by/4.0/>.

© The Author(s) 2017

## sPLA<sub>2</sub>-IIA Overexpression in Mice Epidermis Depletes Hair Follicle Stem Cells and Induces Differentiation Mediated Through Enhanced JNK/c-Jun Activation

RAHUL M. SARATE,<sup>a</sup> GOPAL L. CHOVIYA,<sup>a</sup> VAGISHA RAVI,<sup>a</sup> BHARAT KHADE,<sup>b</sup> SANJAY GUPTA,<sup>b</sup> SANJEEV K. WAGHMARE<sup>a</sup>

**Key Words.** Differentiation • Epidermis • Hair follicle stem cells • Histone • Jun

<sup>a</sup>Stem Cell Biology Group, Waghmare Lab; <sup>b</sup>Epigenetics and Chromatin Biology Group, Gupta Lab, Cancer Research Institute, Advanced Centre for Treatment Research and Education in Cancer (ACTREC), Tata Memorial Centre, Kharghar, Navi Mumbai, Maharashtra, India

Correspondence: Dr. Sanjeev K. Waghmare, PhD, Stem Cell Biology Group, Waghmare Lab, Cancer Research Institute, Advanced Centre for Treatment Research and Education in Cancer (ACTREC) Tata Memorial Centre, Kharghar, Navi Mumbai 410210, Maharashtra, India. Telephone: +91-22-27405122; Fax: +91-22-27405085; e-mail: swaghmare@actrec.gov.in

Received August 5, 2015; accepted for publication April 24, 2016; first published online in *STEM CELLS EXPRESS* June 14, 2016.

© AlphaMed Press  
1066-5099/2016/\$30.00/0

<http://dx.doi.org/10.1002/stem.2418>

### ABSTRACT

Secretory phospholipase A<sub>2</sub> Group-IIA (sPLA<sub>2</sub>-IIA) catalyzes the hydrolysis of the sn-2 position of glycerophospholipids to yield fatty acids and lysophospholipids. sPLA<sub>2</sub>-IIA is deregulated in various cancers; however, its role in hair follicle stem cell (HFSC) regulation is obscure. Here we report a transgenic mice overexpressing sPLA<sub>2</sub>-IIA (K14-sPLA<sub>2</sub>-IIA) showed depletion of HFSC pool. This was accompanied with increased differentiation, loss of ortho-parakeratotic organization and enlargement of sebaceous gland, infundibulum and junctional zone. The colony forming efficiency of keratinocytes was significantly reduced. Microarray profiling of HFSCs revealed enhanced level of epithelial mitogens and transcription factors, c-Jun and FosB that may be involved in proliferation and differentiation. Moreover, K14-sPLA<sub>2</sub>-IIA keratinocytes showed enhanced activation of EGFR and JNK1/2 that led to c-Jun activation, which co-related with enhanced differentiation. Further, depletion of stem cells in bulge is associated with high levels of chromatin silencing mark, H3K27me3 and low levels of an activator mark, H3K9ac suggestive of alteration in gene expression contributing toward stem cells differentiation. Our results, first time uncovered that overexpression of sPLA<sub>2</sub>-IIA lead to depletion of HFSCs and differentiation associated with altered histone modification. Thus involvement of sPLA<sub>2</sub>-IIA in stem cells regulation and disease pathogenesis suggest its prospective clinical implications. *STEM CELLS* 2016;34:2407–2417

### SIGNIFICANCE STATEMENT

Stem cells maintain tissue homeostasis throughout the life of an animal. Skin is highly regenerative tissue of the body that is maintained by multipotent stem cells. These tissue stem cells are regulated by various signaling pathways. Secretory phospholipase A2 (sPLA<sub>2</sub>-IIA) is involved in lipid catabolism and deregulated in various cancers. Our study provides new insights on the role of sPLA<sub>2</sub>-IIA in regulation of hair follicle stem cells and skin homeostasis. The involvement of sPLA<sub>2</sub>-IIA in stem cells regulation and various cancers suggest its prospective clinical implications. In addition, it may shed light on mechanism involved in hair loss and its prospective hair therapy.

### INTRODUCTION

Skin protects the organisms from a wide range of environmental factors, UV irradiation, viruses and other pathogens etc. Mammalian skin comprises of two tissue layers such as epidermis and dermis. Epidermis includes the hair follicle, inter-follicular epidermis, and the sebaceous gland, whereas dermis is composed largely of fibroblast. In mice, during the embryonic development, epidermis arises from ectoderm. At E14.5, stratification results in the formation of hair placode. Subsequently, it

gives rise to hair germ (E15.5) followed by hair peg (E16.5–E17.5) that further matures into hair follicle [1–3]. Hair follicle morphogenesis is followed by the first adult hair cycle that comprises of three phases such as telogen (resting phase), anagen (growing phase), and catagen (regressing phase) [4]. Hair follicle stem cells (HFSC) in the bulge are activated during telogen to anagen transition that further give rise to matrix cells. The epidermal homeostasis is maintained by multipotent stem cells which self-renew in niche and give rise to different progenitors [2, 5] and also

contribute to repair during injury. Previously, a pulse-chase study using the tritiated thymidine (<sup>3</sup>H) and BrdU demonstrated that infrequently dividing cells reside in the bulge region of the hair follicle [6–8], interfollicular epidermis (IFE) [9–11] and sebaceous gland [12]. Further, a double transgenic pTre-H2BGFP/K5tTa tetracycline off mice showed direct link between infrequently dividing cells, that is, label retaining cells (LRC) and stem cells [13]. Subsequently, a novel strategy was developed by using the pTre-H2BGFP/K5tTa mice to count the HFSC divisions over time and provided the first quantitative proliferation history of tissue stem cells HFSCs in unperturbed tissue [14, 15]. HFSC reside in the bulge region and self-renew to maintain tissue homeostasis [2, 16], which are regulated by various signalling pathways. In particular, Wnt/ $\beta$ -catenin pathway is involved in hair follicle morphogenesis, stem cell proliferation and differentiation [17–21]. Targeted overexpression of epidermal growth factor (EGF) in mice showed epidermal hyperplasia and altered hair follicle cycling [22]. Also TGF- $\alpha$  overexpression showed involvement in epidermal development and differentiation [23].

Secretory phospholipase A2 (sPLA<sub>2</sub>-IIA) plays crucial roles in vital processes within the organism including proliferation, migration, angiogenesis, inflammation etc. [24–26]. sPLA<sub>2</sub>-IIA also called as Enhancing factor, was isolated from a mouse small intestine and the expression was observed predominantly in the Paneth cells of the intestine, which are adjacent to the crypt intestinal stem cells [27]. In new born mice, sPLA<sub>2</sub>-IIA expression was seen in the outer root sheath of the active hair follicles [28]. sPLA<sub>2</sub>-IIA is a dual functioning molecule having both the catalytic and enhancing activity. A natural knockout of secretory phospholipase A2 (Pla2ga2) showed more susceptibility to colorectal tumorigenesis [29]. Moreover, transgenic mice expressing a functional sPLA<sub>2</sub>-IIA gene showed resistant to intestinal tumorigenesis [30], and in skin it showed increased sensitivity toward chemical carcinogenesis [31]. sPLA<sub>2</sub>-IIA is deregulated in various human cancers such as lung, oesophageal, prostate, and gastric cancer [32–35]. Signalling pathways such as Wnt, Notch and Sonic-hedgehog and others like EGFR etc. have been reported to be involved in the HFSC regulation [36]. Lysosphospholipids such as LPA induces EGFR signalling thereby regulating the hair follicle development [37]. Further, the role of sPLA<sub>2</sub>-IIA in regulating HFSCs is unknown. Hence, it will be important to understand the molecular mechanism that is involved in stem cell regulation and skin homeostasis.

Recently, apart from signalling pathways being involved in stem cell regulation, there are various reports that have unravelled role of histone modifications in maintaining balance between stem cell quiescence and differentiation. These modifications are different for various cell types, and the presence of histone marks varies in stem cells and differentiated cells. In epidermis, the bulge HFSCs and the IFE showed high levels of repressive mark, H3K9me3 [38]. Conversely, in active chromatin, histone H3 is acetylated at lysine 9 or trimethylated at lysine 27 [39]. The histone repressive mark H3K27me3 is catalyzed by Ezh1/Ezh2 and the loss of both Ezh1 and Ezh2 showed hyper proliferation of epidermal cells and hair loss. Further, deletion of Ezh2 showed decrease in proliferation and premature differentiation [40].

In this study, the effect of sPLA<sub>2</sub>-IIA over expression in epidermal homeostasis and stem cells regulation was investi-

gated. Our result showed depletion of HFSCs with significant decrease in the LRCs. It also showed altered proliferation and increased differentiation, loss of orthoparakeratotic organization, enlargement of sebaceous gland, junctional zone and infundibulum. In K14-sPLA<sub>2</sub>-IIA mice, HFSCs expression profiling showed enhanced activation of epithelial mitogens and also enhanced expression of c-Jun and FosB that may lead to increased proliferation and differentiation. In addition, K14-sPLA<sub>2</sub>-IIA keratinocytes showed enhanced activation of EGFR and JNK1/2 that led to enhanced c-Jun activation in coherence with differentiation. Histone modification analysis in bulge showed decrease in level of H3K9ac with increase of H3K27me3 concomitant with the loss of HFSCs quiescence.

## MATERIALS AND METHODS

### Mice

K14-sPLA<sub>2</sub>-IIA transgenic mice were a gift from Dr. Rita Mukherkar [31]. Animal work was approved by the ACTREC's Institutional Animal Ethics Committee. The hemizygous K14-sPLA<sub>2</sub>-IIA was crossed to FVB1 mice to obtain the transgenic mice for the experiments. Mice were sacrificed at various time points during morphogenesis, first and second hair cycle. PCR genotyping was performed as described [31].

### Histology and Immunofluorescence

Mice were sacrificed at various postnatal days (PD) during the hair follicle morphogenesis (PD1-PD17), first (PD21-PD49) and second hair cycle (PD49-PD77). Further, dorsal skin and tail skin was collected, then paraffin and frozen (OCT compound, Netherlands) blocks were made. Subsequently, paraffin block tissue sectioning was performed followed by Haematoxylin and Eosin staining (H&E). IHC-P (paraffin sections) and Immunofluorescence assays were performed as described [14, 41]. For further details please refer the Supporting Information.

### BrdU Proliferation Assay and Label Retention Assay

BrdU (5-bromo-3-deoxy-uridine) was injected intraperitoneally (50 mg/g of body weight in PBS buffer) at the initiation of first (PD20) and second (PD47) hair cycle followed by administration of 0.8 mg/ml BrdU in the drinking water and sacrificed after 3 days [41] followed by Immunofluorescence assay. For long term label-retaining assay, BrdU was injected subcutaneously for three days starting at PD3–PD5 (50 mg/g of body weight) at 12 hours intervals. Further the mice were chased up to PD49 and PD77 that was followed by Immunofluorescence assay as described [14].

### Tail Skin Whole Mount Assay

Tail skin whole mount was performed as mentioned in Braun et al. (2003). Intact epidermal sheet were collected at various ages and Nile Red staining was performed as described [11]. The images were captured by using confocal microscopy.

### Flow Cytometry Analysis

For each experiment, mice were euthanized and epidermis was separated by trypsinization and cells were stained with HFSC markers such as Anti- $\alpha$ 6 integrin directly coupled to PE, and Anti-CD34 biotin coupled to streptavidin-APC as described in Waghmare et al. (2008). All flow cytometry experiments

were performed on FACS Aria (BD Bioscience, San Jose, CA) and the data were analysed by using the FACS Diva software.

### Microarray Expression Profiling of HFSCs and Real Time PCR

Hair follicle stem cells (CD34+,  $\alpha$ 6integrin+) were FACS sorted by using BD FACS Aria in RNA Lysis buffer from wild type (WT) and K14-sPLA<sub>2</sub>-IIA mice. Further, RNA extraction was done by using the Absolutely RNA Miniprep Kit - Agilent Technologies, Santa Clara, CA. For further microarray details Affymetrix, Santa Clara, CA and Real Time PCR please refer to Supporting Information.

### Primary Keratinocyte Culture and Colony Forming Assays

Keratinocytes were isolated from the pups at PD2. Approximately 2–3 million cells were plated onto the culture dish having the irradiated 3T3 feeder layers and followed for two weeks. Culture media was used as mentioned [41].

Colony forming assays were performed by plating 5000 cells on irradiated 3T3 feeder layers and followed for 2 weeks. The colonies were counted and were fixed with 1% PFA for 20 minutes and stained with 0.05% crystal violet [42].

### Protein Extraction and Western Blotting

Mouse primary keratinocytes were starved for 24 hours and stimulated by 10 ng/ml EGF. Cells were washed twice with ice-cold PBS and harvested by scraping into the radioimmunoprecipitation assay buffer (Sigma, St Louis, MO) containing 1X protease phosphatase inhibitor cocktail (Cell signalling technologies, Danvers, MA). For details refer the Supporting Information.

### Statistical Analysis

Statistical analysis was performed for FACS analysis, IFE thickness, IFA stained HFSCs counting, BrdU proliferation, label-retaining study, Real Time PCR analysis and Histone analysis by using the unpaired two tailed Student's *t* test with GraphPad Prism 5. IFE thickness was measured with the Image J software. Error bar indicate the mean  $\pm$  SD of the mean values: \*,  $p < .05$ ; \*\*,  $p < .005$ ; \*\*\*,  $p < .0001$ .

## RESULTS

### Secretory Phospholipase<sub>2</sub>-IIA Overexpression Affects Skin Homeostasis

To understand the role of sPLA<sub>2</sub>-IIA in hair follicle cycling and stem cell regulation, we examined the hair cycling in dorsal skin at various postnatal days (PDs). Histology (H&E) staining of dorsal skin was performed at various PDs during morphogenesis (PD7, PD11, PD15, PD17) and first hair cycle (PD21, PD28, PD34, PD45, PD49). To confirm sPLA<sub>2</sub>-IIA expression, we performed Immunohistochemical (IHC) analysis at various postnatal ages during morphogenesis (PD8), first hair cycle (PD49) and 1 year old mice (PD365) that showed sPLA<sub>2</sub>-IIA expression (Supporting Information Fig. S1A). Histology analysis showed gradual hair loss with respect to age (Fig. 1A) and it also affects the hair follicle morphology, enlargement of sebaceous gland, junctional zone and infundibulum size as well as thickening of the IFE in dorsal skin (Fig. 1B, 1D-1F). In addition, hair follicle cycling analysis showed an acceleration of catagen phase in K14-sPLA<sub>2</sub>-

IIA that begins at PD15 and ends at PD19, whereas telogen begins early at PD19 as compared to WT (where the telogen is at PD21) (Fig. 1B, 1C). Also, in the first hair cycle, telogen begins early at PD41 in K14-sPLA<sub>2</sub>-IIA mice as compared to WT (Fig. 1B, 1C). Similarly, H&E staining was performed in the tail skin sections at various PDs and the results showed enlargement of sebaceous gland and thickening of IFE (Supporting Information Fig. S1B, S1C). In addition, the hair follicle morphology showed pronounced effect at PD49 (Fig. 1B).

### Increased Proliferation, Differentiation, Sebaceous Gland Hyperplasia and Loss of Ortho-Parakeratotic Organization

K14-sPLA<sub>2</sub>-IIA mice showed morphological abnormality in the hair follicle. Therefore, we analysed the K14 expression level in K14-sPLA<sub>2</sub>-IIA mice as compared to WT. Our analysis showed that there was no expansion of K14 basal cells (Fig. 2A) in K14-sPLA<sub>2</sub>-IIA mice. Furthermore, we sought to understand if there is any effect on the proliferation and differentiation of various epidermal lineages. To address this, we performed Immunofluorescence assay by using the proliferation marker Ki67 that showed increased proliferation in K14-sPLA<sub>2</sub>-IIA mice (Fig. 2B). Moreover, tail whole mount assay also showed increased expression of Ki67 during the onset of first hair cycle (PD21, telogen) where the stem cells are activated and divide further to progress into anagen phase of the hair cycle (Supporting Information Fig. S2A). Our data clearly indicates that there is more proliferation in K14-sPLA<sub>2</sub>-IIA mice as compared to WT mice. In addition, the size of Dermal Papillae was larger in K14-sPLA<sub>2</sub>-IIA as compared to WT (Supporting Information Fig. S2A). We also performed the Immunofluorescence assay by using Active Caspase 3 antibody that showed no difference in the number of positive cells, suggesting that there is no effect on apoptosis (Fig. 2C). Furthermore, to assess if there is any effect on the differentiation of various epidermal lineages, we performed Immunofluorescence assay by using the differentiation marker such as K10 and loricrin. Both the differentiation markers K10 and loricrin, showed increased expression in the K14-sPLA<sub>2</sub>-IIA mice indicating higher differentiation (Fig. 2D). Thus these data indicate that overexpression of sPLA<sub>2</sub>-IIA led to differentiation. Further, we performed Nile Red staining to examine the morphology of the sebaceous gland in both the dorsal skin and the tail skin. The results showed sebaceous gland hyperplasia in both the dorsal and tail skin in the K14-sPLA<sub>2</sub>-IIA mice as compared to WT (Fig. 2E, Supporting Information Fig. S2B). Therefore, we further assessed the ortho-parakeratotic organization in tail skin sections. The mice were sacrificed at various postnatal days (PDs), and the Immunofluorescence assay was performed by using the K10 and flaggrin markers, which express specifically in the orthokeratotic interscale region of the tail skin. In WT, K10 and flaggrin expression is only confined to orthokeratotic interscale region [43]; however, in K14-sPLA<sub>2</sub>-IIA mice, we observed that both the parakeratotic scale and orthokeratotic interscale expresses the K10 and flaggrin (Fig. 2F), which indicates loss of parakeratotic scale and orthokeratotic interscale organization.

### Gradual Depletion of HFSCs Pool with Increased Proliferation, Loss of LRCs and Expression Profiling of HFSCs

K14-sPLA<sub>2</sub>-IIA mice showed abnormal hair lineages and therefore we examined the overexpression of sPLA<sub>2</sub>-IIA has any

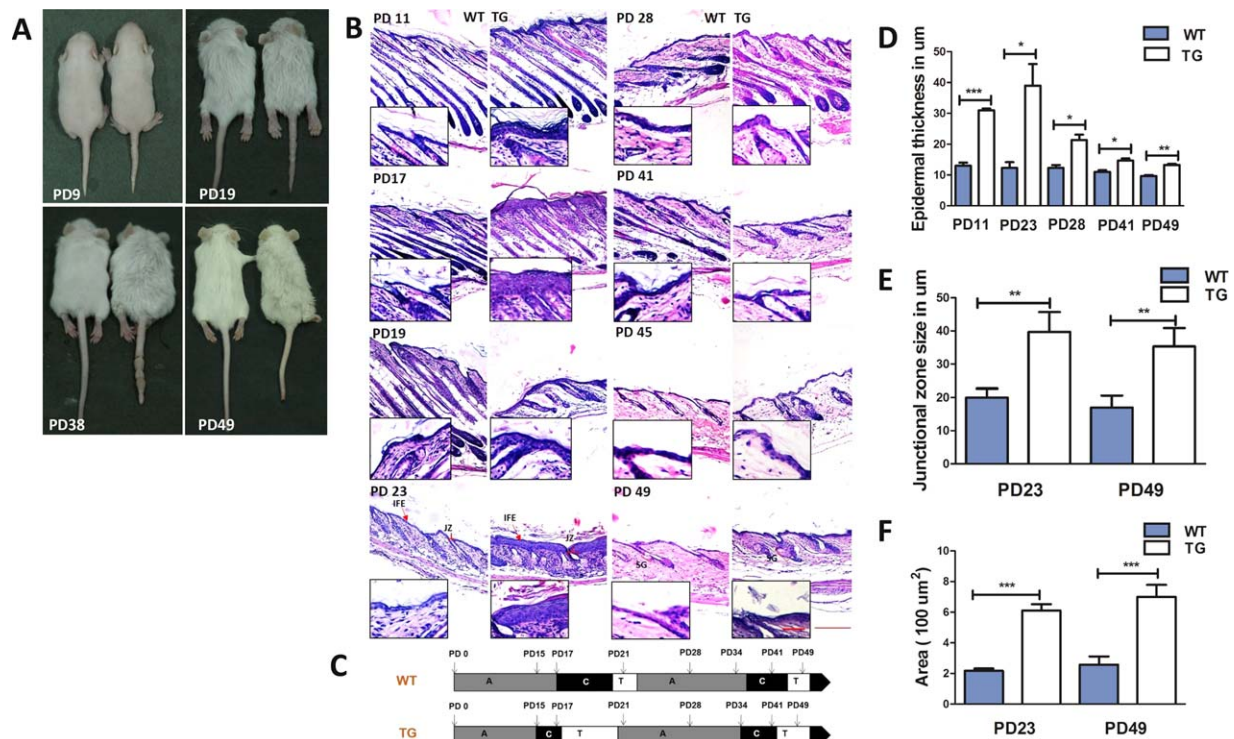


**Figure 1.** Epidermal overexpression of secretory phospholipase A<sub>2</sub> group-IIA (sPLA<sub>2</sub>-IIA) affects skin homeostasis. **(A):** Mice skin phenotype at different PDs (Phenotypic appearance of WT control littermate and K14-sPLA<sub>2</sub>-IIA mice). **(B):** Hematoxylin and eosin staining of the dorsal skin paraffin sections at various PDs. Arrow indicates the interfollicular epidermis (IFE) and bracket indicates the junctional zone size. Scale bar: 200  $\mu\text{m}$ , Inset scale bar: 50  $\mu\text{m}$ . **(C):** The schematic representation of hair cycle in WT and K14-sPLA<sub>2</sub>-IIA mice. **(D):** IFE thickness measurement at various PDs in WT control littermate and K14-sPLA<sub>2</sub>-IIA mice. **(E):** Junctional zone size measurement at PD23 and PD49 in WT control littermate and K14-sPLA<sub>2</sub>-IIA mice. **(F):** Sebaceous gland size measurement at PD23 and PD49 in WT control littermate and K14-sPLA<sub>2</sub>-IIA mice.  $n = 3$  mice/genotype. Data are presented as mean  $\pm$  SD. \*,  $p < .05$ ; \*\*,  $p < .005$ ; \*\*\*,  $p < .0001$ . Abbreviations: PDs, postnatal days; TG, K14-sPLA<sub>2</sub>-IIA mice; WT, wild type.

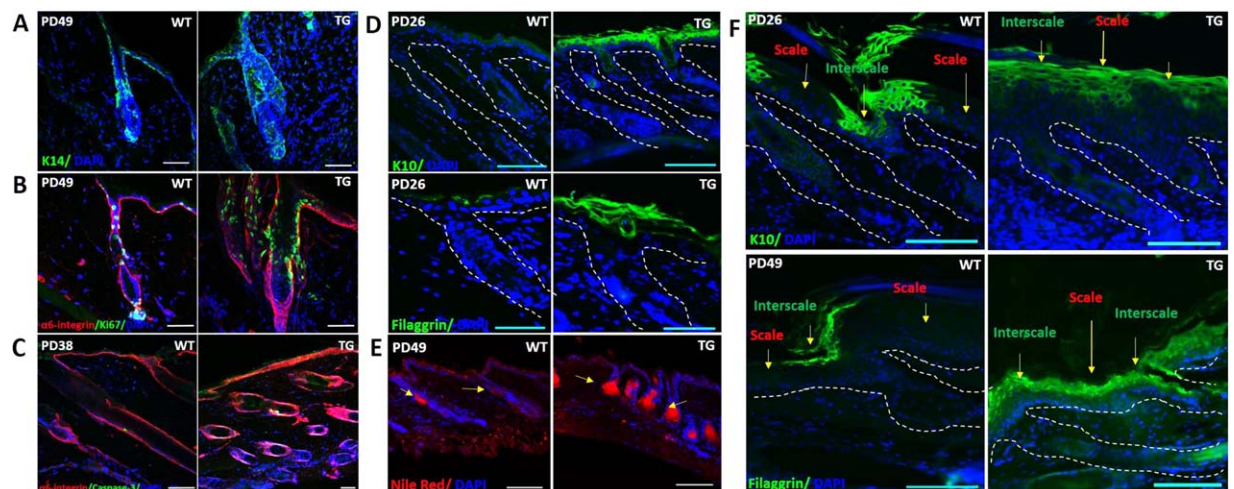


**Figure 2.** Increased proliferation, differentiation, sebaceous gland hyperplasia and loss of ortho-parakeratotic organization in K14-sPLA<sub>2</sub>-IIA mice. **(A):** Immunofluorescence staining of Keratin 14 in dorsal skin at PD49 in K14-sPLA<sub>2</sub>-IIA mice and WT control littermate. Scale bar: 50  $\mu\text{m}$ . **(B):** Immunofluorescence assay showed Ki67 expression higher in K14-sPLA<sub>2</sub>-IIA mice skin epidermis as compared to WT control littermate. Scale bar: 50  $\mu\text{m}$ . **(C):** Immunofluorescence assay showed Active caspase-3 expression was not altered in K14-sPLA<sub>2</sub>-IIA mice skin epidermis as compared to WT control littermate. Scale bar: 50  $\mu\text{m}$ . **(D):** K14-sPLA<sub>2</sub>-IIA mice showed an increased differentiation at PD26 as compared to WT control littermate. Immunofluorescence assay shows that Keratin 10 and filaggrin expression is higher in K14-sPLA<sub>2</sub>-IIA mice skin epidermis as compared to WT control littermate. Scale bar: 100  $\mu\text{m}$  for K10, Scale bar: 50  $\mu\text{m}$  for filaggrin. **(E):** Nile red staining on dorsal skin at PD49 showed enlargeeous glands, nuclei stained with DAPI Scale bar: 100  $\mu\text{m}$ . **(F):** Immunofluorescence staining of Keratin 10 and filaggrin on tail skin at PD26 and PD49 respectively.  $n = 3$  mice/genotype. Scale bar: 100  $\mu\text{m}$ . Abbreviations: PD, postnatal days; TG, K14-sPLA<sub>2</sub>-IIA mice; WT, wild type.

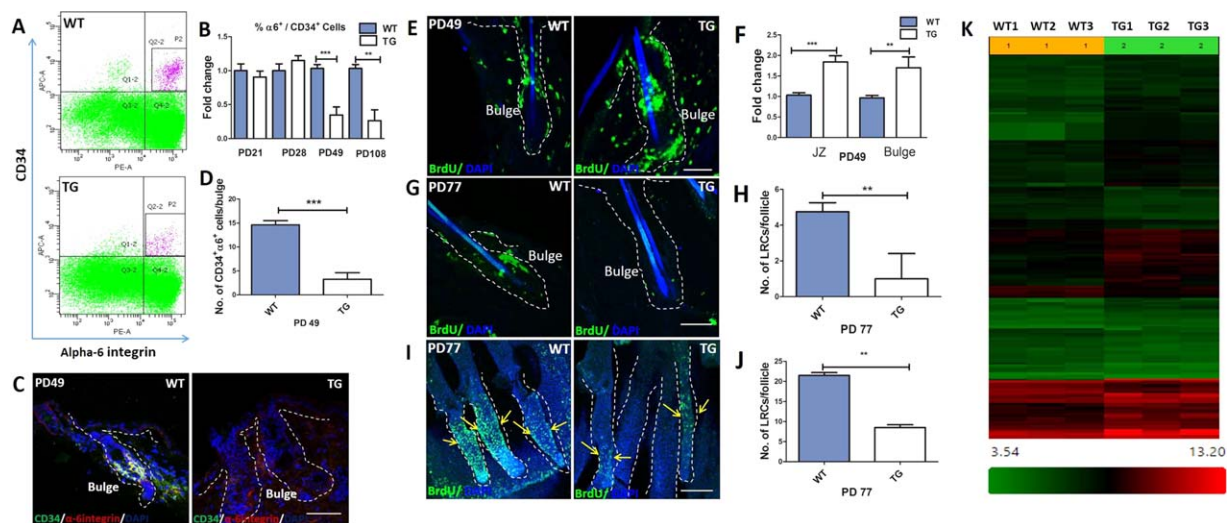


**Figure 3.** Gradual depletion of hair follicle stem cell (HFSC) with increased proliferation, loss of label retaining cells (LRC) and expression profiling. **(A):** FACS analysis of  $CD34^+/\alpha6\text{-integrin}^+$  bulge HFSCs at PD49. **(B):** Quantification of FACS analysis of  $CD34^+/\alpha6\text{-integrin}^+$  bulge HFSCs from mouse epidermis at indicated time points. Data are presented as mean  $\pm$  SD. \*\*,  $p < .005$ , \*\*\*,  $p < .0001$ . **(C):** Immunofluorescence analysis of  $CD34^+/\alpha6\text{-integrin}^+$  expression in hair follicle at PD 49. Scale bar: 50  $\mu\text{m}$ . **(D):** Quantification of  $CD34^+/\alpha6\text{-integrin}^+$  cells in the bulge of the dorsal skin in K14-sPLA<sub>2</sub>-IIA mice and WT littermate.  $n = 3$  mice/genotype. Data are presented as mean  $\pm$  SD. \*\*\*,  $p < .0001$ . **(E):** BrdU immunofluorescence assay was performed at PD49 in K14-sPLA<sub>2</sub>-IIA mice and WT control littermate. Mice were injected with BrdU during the initiation of second hair cycle (PD 46) in the intra-peritoneal cavity and followed by BrdU in drinking water (0.8 mg/ml) for 3 days. Scale bar: 50  $\mu\text{m}$ . **(F):** Quantification of BrdU positive cells in the bulge and junctional zone of the dorsal skin  $n = 3$  mice/genotype. Data are presented as mean  $\pm$  SD. \*\*,  $p < .005$ ; \*\*\*,  $p < .0001$ . **(G):** BrdU was injected subcutaneously to a final amount of 50 mg/g of body weight starting at PD3–PD5 in K14-sPLA<sub>2</sub>-IIA mice and WT control littermate. LRC were analyzed by BrdU immunofluorescence assay at PD77 in K14-sPLA<sub>2</sub>-IIA and WT control littermate. Scale bar: 50  $\mu\text{m}$ . **(H):** Quantification of BrdU positive cells in the bulge in dorsal skin. Data are presented as mean  $\pm$  SD. \*\*,  $p < .005$ . **(I):** LRCs in tail whole mount at PD77 Scale bar: 100  $\mu\text{m}$ . **(J):** Quantification of BrdU positive cells in the bulge in tail whole mount.  $n = 2$  mice/genotype. Data are presented as mean  $\pm$  SD. \*\*,  $p < .005$ . **(K):** Microarray profiling of hair follicle stem cells at PD49 in K14-sPLA<sub>2</sub>-IIA mice and WT control littermate, ( $n = 3$  mice/genotype; Log<sub>2</sub> fold change,  $p < .05$ ). Abbreviations: PD, postnatal days; TG, K14-sPLA<sub>2</sub>-IIA mice; WT, wild type.

effect on HFSC pool. Toward this end, FACS analysis was performed by using the HFSCs markers such as CD34 and  $\alpha6\text{-integrin}$  at various postnatal days (PDs) during the first hair cycle. At PD21 there was no difference in the  $CD34^+/\alpha6\text{-integrin}^+$  population; however, at PD49 there was a significant decrease in the  $CD34^+/\alpha6\text{-integrin}^+$  cells, followed by further loss at PD108 (Fig. 3A, 3B). The purity of FACS sorted population, were stained with K14 (Supporting Information Fig. S3B, S3C), and the results showed 95% K14 positive cells. To confirm the stem cell depletion, Immunofluorescence assay was performed on the dorsal skin by using the CD34 and  $\alpha6\text{-integrin}$  antibody, (Fig. 3C) that showed less number of CD34 positive cells. To quantify further, we counted the number of  $CD34^+/\alpha6\text{-integrin}^+$  cells per hair follicle bulge in WT and K14-sPLA<sub>2</sub>-IIA mice (Fig. 3D). Both the FACS and Immunofluorescence assay were in agreement that there was loss of HFSCs. Thus, the data showed that the overexpression of sPLA<sub>2</sub>-IIA results in the gradual loss of hair follicle stem pool.

Further, to investigate any effect on cell proliferation, BrdU proliferation assay was performed as described [41] followed by Immunofluorescence analysis. At PD49, BrdU positive cells were counted in the different components of the hair follicle such as bulge, junctional zone and IFE. Overall, the result showed more number of BrdU positive cells in all the epidermal components of K14-sPLA<sub>2</sub>-IIA mice as compared to WT control (Fig. 3E, 3F). Since there was increased proliferation and differentiation, we further addressed to see if there was any effect on LRCs or slow cycling property of the HFSCs. To examine the same, the mice were BrdU pulsed for 3 days

(PD3–PD5) at regular intervals of 12 hours and then chased up to PD49 and PD77. Further, Immunofluorescence analysis was performed on the dorsal and tail skin. BrdU positive cells were counted in the bulge region in dorsal and tail skin at the end of first (PD49) and second hair cycle (PD77). The result showed that number of BrdU positive cells were decreased in the bulge region at PD49 (Supporting Information Fig. S3A) and PD77 (Fig. 3G–3J) in K14-sPLA<sub>2</sub>-IIA mice as compared to WT.

To understand the molecular mechanism, we performed the genome-wide expression profiling of HFSCs in K14-sPLA<sub>2</sub>-IIA and WT mice ( $n = 3$ ). We observed 53 genes that are differentially expressed. In all the replicates of K14sPLA2IIA mice, HFSCs showed significant upregulation of sPLA2IIA expression as compared to WT confirming the reliability of the screen. The microarray data showed upregulation of epithelial mitogens such as heparin-binding EGF-like growth factor (Hb-EGF) (4.3-fold) & Epithelial mitogen (EPGN) (1.89-fold), and also upregulation of AP1 complex proteins including Jun (2.39-fold) and FosB (3.16-fold) (Fig. 3K and Fig. S4). Moreover, transcription factor such as Nr4a1 (5.3-fold) and Nr4a3 (2.0-fold) were also upregulated. To validate the microarray data, we performed Quantitative Real-time PCR. Our result showed significant upregulation of Hb-EGF, Jun, Fos and Nr4A1. (Supporting Information Fig. S4). However, the microarray data for Hb-EGF showed  $p$ -value (.06); therefore, we further confirmed by performing Quantitative Real time PCR that showed statistically significant upregulation of Hb-EGF ( $p$ -value  $< .05$ ) (Supporting Information Fig. S4). Moreover, genes involved in HFSCs regulation are not

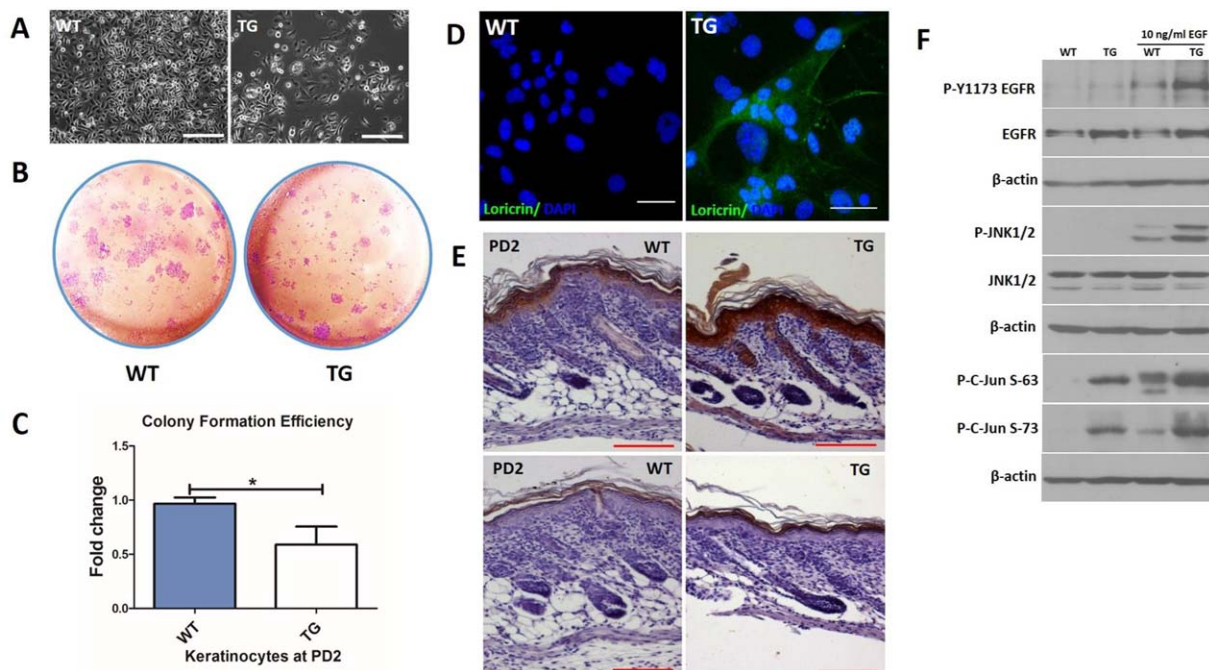


**Figure 4.** Loss of functional potential and increased differentiation associated with enhanced activation of EGFR-JNK – c-Jun signalling in keratinocytes. **(A):** Microscopic images of Keratinocytes culture in WT and K14-sPLA<sub>2</sub>-IIA mice Scale bar: 200  $\mu$ m. **(B):** Equal number (5000 cells/well) of WT and TG keratinocyte cells were plated in six well plate and cultured for 8 days. Total number of colonies were counted. Colony staining was performed by using crystal violet. **(C):** Quantitative analysis of Colony formation efficiency assay in WT and K14-sPLA<sub>2</sub>-IIA. **(D):** Immunofluorescence analysis in WT and K14-sPLA<sub>2</sub>-IIA mice keratinocytes assay by using loricrin. Scale bar: 50  $\mu$ m. **(E):** Immunohistochemical analysis of K10 and filaggrin expression in skin at PD2.  $n = 3$  mice/genotype. Scale bar: 100  $\mu$ m. Data are presented as mean  $\pm$  SD. \*,  $p < .05$ . **(F):** Keratinocytes were serum-starved for 24 hours and stimulated by 10 ng/ml EGF. Cell extracts were prepared, proteins were resolved by SDS-PAGE, and immunoblot were analysed by p-EGFR, EGFR, p-JNK1/2, JNK1/2, and p-c-Jun antibodies.  $\beta$ -actin is used as a loading control.  $n = 3$  mice/genotype. Abbreviations: PD, postnatal days; TG, K14-sPLA<sub>2</sub>-IIA mice; WT, wild type.

differentially expressed (LGR5, CD34, Sox9, Lrig1 etc.) in the microarray profile. Our data indicates that overexpression of sPLA<sub>2</sub>-IIA leads to upregulation of mitogens (Hb-EGF and EPGN) and AP1 complex proteins, which lead to enhanced proliferation and differentiation of HFSCs.

#### Loss of Functional Potential and Increased Differentiation Associated with Enhanced Activation of EGFR-JNK/c-Jun Signalling in Keratinocytes

As the data showed a gradual loss of stem cells, hence it warrants studying the functional potential of the keratinocytes. Primary keratinocytes were isolated from neo-natal mice (PD2) and grown on irradiated 3T3 feeder layers that were further subjected to assess the colony formation efficiency. K14-sPLA<sub>2</sub>-IIA keratinocytes colony displayed change in morphology as compared to WT control (Fig. 4A). The results showed reduction in colony forming efficiency in the K14-sPLA<sub>2</sub>-IIA keratinocytes as compared to WT control (Fig. 4B, 4C). To examine if reduction in colony forming led to differentiation, we performed Immunofluorescence assay by using the differentiation markers such as loricrin. The result showed increased expression of loricrin in the K14-sPLA<sub>2</sub>-IIA keratinocytes indicating higher differentiation (Fig. 4D). In addition, Immunohistochemistry (IHC) analysis on mice skin at PD2 was performed by using differentiation markers such as K10 and filaggrin (Fig. 4E) that also showed increased differentiation.

sPLA<sub>2</sub>-IIA in the presence of EGF give cells a growth advantage; however, if sPLA<sub>2</sub>-IIA directly increases the binding of EGF to the EGFR receptors is still obscure. To understand the molecular mechanism, we cultured the neo-natal primary keratinocytes from both the K14-sPLA<sub>2</sub>-IIA and WT control. To examine further, the protein extracts were prepared as mentioned and immuno-blotted by using the EGFR antibodies. The results showed enhanced activation of EGFR and increased in total EGFR expression in the K14-sPLA<sub>2</sub>-IIA as compared to WT keratinocytes (Fig. 4F).

Since there was an increase in differentiation, the downstream of EGFR signalling, that is., the level of JNK1/2 phosphorylation was checked by immunoblotting. The result showed that there was enhanced activation of JNK1/2 and c-Jun, which is a downstream target of JNK1/2 (Fig. 4F). Our result showed that the overexpression of sPLA<sub>2</sub>-IIA activates EGFR, which led to JNK1/2 activation followed by c-Jun activation that may be involved in differentiation.

#### Bulge Showed Loss of H3K9ac and Gain of H3K27me3 in K14-sPLA<sub>2</sub>-IIA Mice with Depletion of Stem Cell Pool

The overexpression of sPLA<sub>2</sub>-IIA showed depletion of HFSC pool. Further, the BrdU label retaining pulse-chase study showed pronounced loss of LRC in K14-sPLA<sub>2</sub>-IIA as compared to the WT control. To examine, if the loss of HFSCs was due to an altered histone modifications, we performed the Immunohistochemistry (IHC) analysis on serial sections by using the

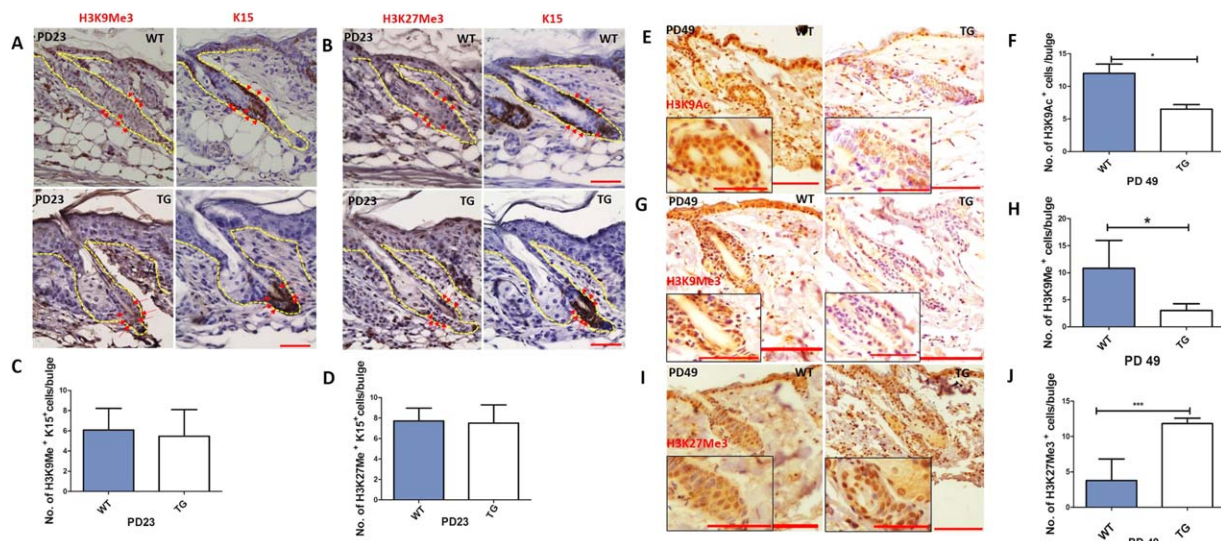


**Figure 5.** Histone modification analysis in K14-sPLA<sub>2</sub>-IIA mice. Immunohistochemical analysis of histone marks and K15 expression in bulge at PD23 dorsal skin. **(A):** H3K9me3 mark with K15 expression. **(B):** H3K27me3 mark with K15 expression. **(C):** Quantification of H3K9me3 positive and K15 positive cells in the bulge of the dorsal skin in K14-sPLA<sub>2</sub>-IIA mice and WT littermate. **(D):** Quantification of H3K27me3 positive cells and K15 positive cells in the bulge of the dorsal skin in K14-sPLA<sub>2</sub>-IIA mice and WT littermate. *n* = 3 mice/genotype. Scale bar: 50  $\mu$ m, Data are presented as mean  $\pm$  SD. \*, *p* < .05; \*\*, *p* < .005. Immunohistochemical analysis of histone marks in bulge at PD49 dorsal skin. **(E):** H3K9ac pattern. **(F):** Quantification of H3K9ac positive cells in the bulge of the dorsal skin in K14-sPLA<sub>2</sub>-IIA mice and WT littermate. *n* = 2 mice/genotype. **(G):** H3K9me3 pattern. **(H):** Quantification of H3K9me3 positive cells in the bulge of the dorsal skin in K14-sPLA<sub>2</sub>-IIA mice and WT littermate. *n* = 3 mice/genotype. **(I):** H3K27me3 pattern. **(J):** Quantification of H3K27me3 positive cells in the bulge of the dorsal skin in K14-sPLA<sub>2</sub>-IIA mice and WT littermate. *n* = 3 mice/genotype. Scale bar: 100  $\mu$ m, Inset scale bar: 50  $\mu$ m. Data are presented as mean  $\pm$  SD. \*, *p* < .05; \*\*, *p* < .005; \*\*\*, *p* < .0001. Abbreviations: PD, postnatal days; TG, K14-sPLA<sub>2</sub>-IIA mice; WT, wild type.

H3K9me3, H3K27me3 and H3K9Ac including the K15 (bulge stem cells specific marker) of K14-sPLA<sub>2</sub>-IIA mice. The IHC data showed K15 expression in the bulge region but no significant difference in H3K9me3 high and medium positive cells in K14-sPLA<sub>2</sub>-IIA mice as compared to WT at PD23 (Fig. 4A, 4C). Similarly, in IFE of the same follicles, the level of H3K9me3 remains unaltered (Supporting Information Fig. S5C, S5D). However, at PD49 there was a significant decrease in the H3K9me3 high and low positive cells in bulge as well as in IFE of K14-sPLA<sub>2</sub>-IIA mice (Fig. 5G, 5H, Supporting Information Fig. S5C, S5D). In continuation, we performed the immunohistochemistry by using the H3K27me3 at PD23 and PD49. The result showed K15 expression but no difference of H3K27me3 mark in the bulge region at PD23 (Fig. 4B, 4D). However, at PD23 the histone mark remains overall unaltered in bulge and IFE (Supporting Information Fig. S5C, S5D, S5E, S5F). Further, at PD49 the result showed that there are increased numbers of H3K27me3 positive cells in K14-sPLA<sub>2</sub>-IIA mice as compared to WT (Fig. 5I, 5J, Supporting Information Fig. S5E, S5F). Our immunohistochemistry (IHC) data showed a lower level of high and medium H3K9ac positive cells at PD49 in bulge of transgenic mice as compared to WT (Fig. 5E, 5F). The levels of histone methylation appeared to be heterogeneous in bulge cells at PD26; therefore, we further quantified in bulge, IFE and matrix, and scored each cell as high or medium stained cells (Supporting Information Fig. S5A, S5B). The data showed number of highly stained cells are more in bulge and IFE at PD26 as compared to medium stained cells in K14-sPLA<sub>2</sub>-IIA mice. Further, data showed an increased in H3K27me3 in the bulge is in coherence with the level in matrix cells. Our data showed there was an increased level of repressive histone mark, H3K27me3 thereby indicating

that could be due to decrease in the expression of genes involved in self-renewal and favoring the process of differentiation leading to depletion of stem cell pool.

### Loss of Stem Cell Pool with Ageing

There was a gradual loss of HFSC pool over time that was observed at PD49 and PD108. Therefore, we sought to understand if the hair follicle stem pool gets depleted with respect to older age of the mice. The phenotype of K14-sPLA<sub>2</sub>-IIA at 1 year was bald and the histology analysis of dorsal skin showed deformed follicle as well as formation of cyst, indicating that the hair follicle are not cycling (Fig. 6A, 6B). In addition, histology (H&E) analysis showed that hair follicles in the K14-sPLA<sub>2</sub>-IIA mice are not forming new hair shaft while the WT are forming the new shaft and have normal morphology. Further, we investigated the HFSCs profile at 1 year old K14-sPLA<sub>2</sub>-IIA mice. These data showed that there was a striking decrease in the HFSCs pool in K14-sPLA<sub>2</sub>-IIA mice as compared to the WT control (Fig. 6C, 6D). Moreover, the dorsal tissue was subjected to Immunofluorescence assay by using the CD34 and  $\alpha$ 6-integrin antibody. The staining showed that there was a decrease in the number of CD34 positive cells in K14-sPLA<sub>2</sub>-IIA mice (Fig. 6E, 6F) that corroborated with the data obtained in the FACS analysis. Overall, these data suggest that there is decrease in the stem cell pool with respect to age.

### DISCUSSION

Secretory phospholipaseA<sub>2</sub>-IIA plays an important role in catalyzing the hydrolysis of glycerophospholipids to give rise to fatty acid and lysophospholipids. sPLA<sub>2</sub>-IIA is involved in lipid

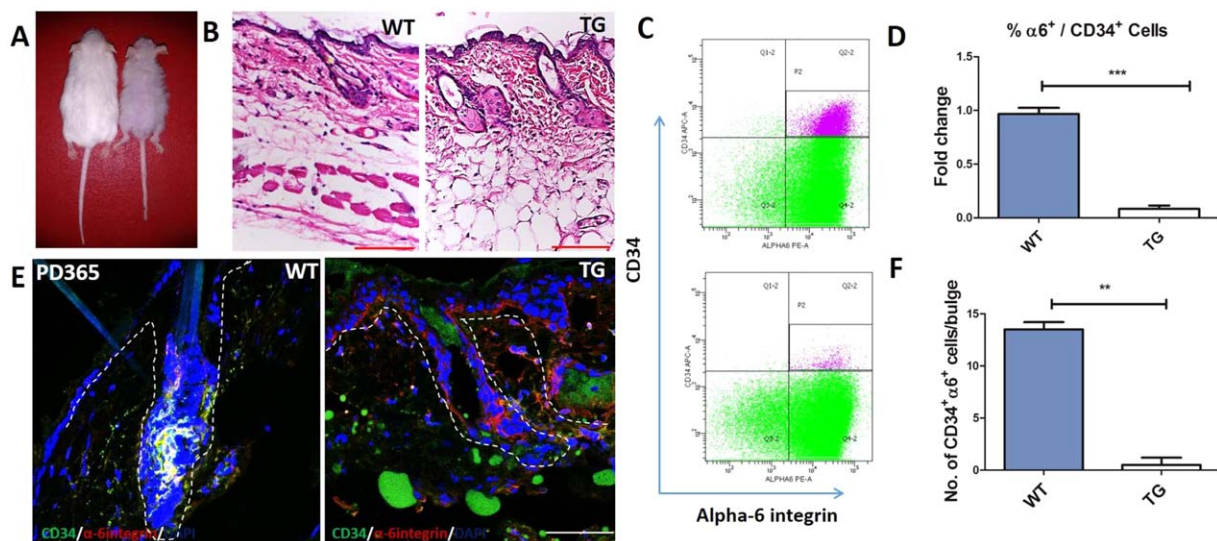


**Figure 6.** Loss of hair follicle stem cells (HFSCs) with ageing. **(A):** Phenotypic appearance of K14-sPLA<sub>2</sub>-IIA mice and WT control littermate. **(B):** Histological analysis showed deformities in hair follicle and cyst formation in K14-sPLA<sub>2</sub>-IIA mice dorsal skin as compared to WT control littermate. Scale bar: 100  $\mu$ m. **(C):** FACS analysis of CD34<sup>+</sup>/α6-integrin<sup>+</sup> bulge HFSCs in 1 year old mice. **(D):** Comparative fold change in CD34<sup>+</sup>/α6-integrin<sup>+</sup> cells. **(E):** Immunofluorescence analysis of CD34<sup>+</sup>/α6-integrin<sup>+</sup> expression in hair follicle of 1 year old mice. Scale bar: 50  $\mu$ m. **(F):** Quantification of CD34<sup>+</sup>/α6-integrin<sup>+</sup> cells in the bulge of the dorsal skin in K14-sPLA<sub>2</sub>-IIA mice and WT control littermate.  $n = 3$  mice/genotype. Data are presented as mean  $\pm$  SD. \*\*,  $p < .005$ ; \*\*\*,  $p < .0001$ . Abbreviations: PD, postnatal days; TG, K14-sPLA<sub>2</sub>-IIA mice; WT, wild type.

catabolism and deregulated in various cancers; however, its role in stem cell regulation still remains elusive.

We showed that overexpression of sPLA<sub>2</sub>-IIA in transgenic mice (K14-sPLA<sub>2</sub>-IIA) leads to gradual loss of HFSC pool with altered proliferation, differentiation and loss of orthoparakeratotic organization. We observed that there was an acceleration of catagen development and early telogen at PD19 and PD41 in TG mice. There was a decrease in the slow cycling LRC population. In addition, histone modification profile suggested loss of stem cells quiescence and higher differentiation. Together these data suggest overexpression of sPLA<sub>2</sub>-IIA alters various epidermal lineages and HFSC regulation.

While sPLA<sub>2</sub>-IIA is involved in phospholipid catabolism, it was shown that overexpression of sPLA<sub>2</sub>-IIA enhances the binding of EGF onto the membrane in A431 cells (positive control of EGFR expression) [28]. EGF overexpressing transgenic mice showed thickening of epidermis, delay in differentiation and affected morphogenesis [22]. EGFR knockout and transgenic mice either expressing dominant negative mutant of EGFR or ErbB2 in skin resulted in alopecia, sebaceous gland enlargement and affect hair follicle morphogenesis [44–47]. Similarly, in the overexpression of sPLA<sub>2</sub>-IIA mice, we observed enlargement of sebaceous gland, infundibulum and junctional zone, loss of orthoparakeratotic organization, enhanced differentiation and defects in hair follicle morphology. But how the sPLA<sub>2</sub>-IIA regulates the signalling pathway remains elusive? sPLA<sub>2</sub>-IIA is known to enhance epidermal growth factor receptor transactivation and thereby modulates proHb-EGF shedding that led to induced activation of microglia in BV-2 cells [48]. In addition, induced proliferative response in astrocytoma through secreted PLA<sub>2</sub> is mediated by increased EGF receptor activation [49]. Our gene expression profile on K14-sPLA<sub>2</sub>-IIA mice HFSCs showed upregulation of epithelial mitogens such as Hb-EGF, a member of the EGF family and EGFR ligand epigen (EPGN). A transmembrane domain-truncated form of Hb-EGF

is known to induce hyper proliferation and differentiation in epidermis that results in developmental defect such as abnormal hair follicle structure and hyperplasia [50]. In addition, over-expression of epigen during embryonic development induces sebaceous gland enlargement through EGFR signalling [51]. In agreement, K14-sPLA<sub>2</sub>-IIA showed development defects, increased proliferation and differentiation.

Further, our gene expression analysis identified up regulation of various components of AP1 transcription factors including c-Jun and FosB. A conditional ablation of c-Jun in mice epidermis results in reduced expression of Hb-EGF and EGFR signalling [52]. In addition, epidermal deletion of Fos in mice epidermis suppresses skin cancer development, which suggest involvement of Fos in epidermal cells proliferation [53]. Similarly, increased level of c-Jun and FosB in K14-sPLA<sub>2</sub>-IIA mice HFSCs co-relates with increased proliferation and differentiation. Moreover, due to upregulation of mitogens such as Hb-EGF and EPGN, which may function to increase the expression of Nr4a1 and Nr4a3 in HFSCs of K14-sPLA<sub>2</sub>-IIA mice, as other mitogen such as PDGF function have been reported to upregulate Nr4a1 [54].

Thus altogether, microarray profiling data of K14-sPLA<sub>2</sub>-IIA HFSCs indicates that over expression of sPLA<sub>2</sub>-IIA leads to increase in the proliferation and differentiation of HFSCs mediated through enhanced activation of mitogenic signalling and altered activation of c-Jun and AP1 complex proteins.

In K14-sPLA<sub>2</sub>-IIA primary keratinocytes, it showed increased activation of JNK1/2 that led to enhanced activation of c-jun that co-related with enhanced differentiation. sPLA<sub>2</sub>-IIA may provide initial trigger for JNK activation that subsequently induces differentiation. Similarly, ΔNp63α induced activation of JNK signalling cascade showed onset of mouse keratinocytes differentiation [55]. Therefore, increase in activation of JNK/c-Jun signalling may be a reason but not a result of differentiation. We also showed there was an enhanced

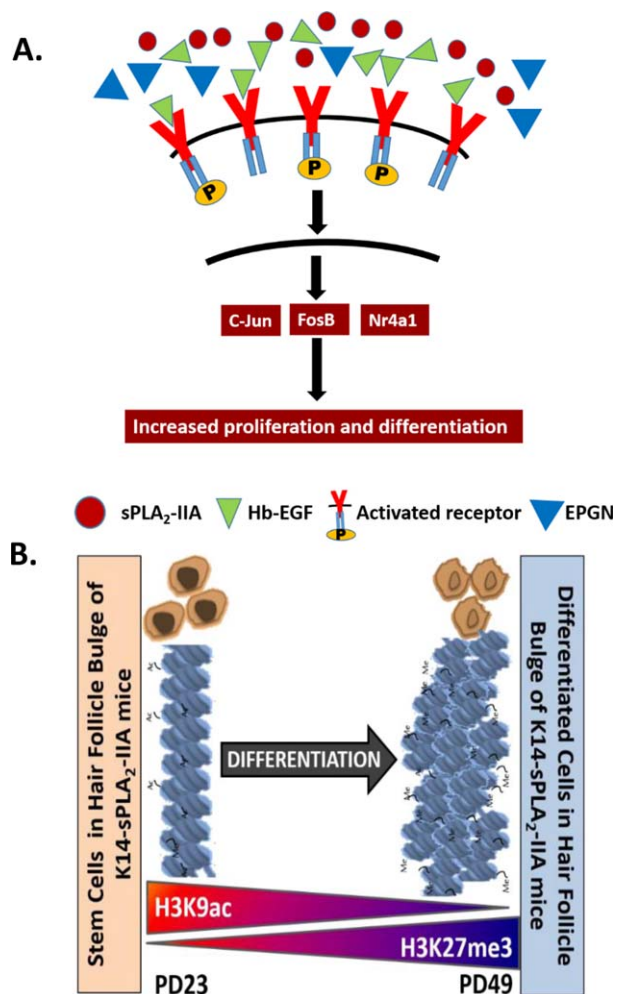


**Figure 7.** Proposed model for sPLA<sub>2</sub>-IIA mechanism. **(A):** In K14-sPLA<sub>2</sub>-IIA hair follicle stem cells (HFSC), overexpression of sPLA<sub>2</sub>-IIA leads to increase in the proliferation and differentiation of HFSCs mediated through enhanced activation of mitogenic signalling and altered activation of c-Jun and FosB. **(B):** Histone analysis in K14-sPLA<sub>2</sub>-IIA at PD23 revealed the level of activation mark, H3K9ac is inversely co-related with the level of repressive mark, H3K27me3. Also, no difference was observed for both the marks when compared to wild type at PD23. However at PD49 the levels of H3K9ac decrease with significant increase of H3K27me3. These inverse co-relationship between an active and repressive histone marks at PD23 and PD49 suggest a progressive differentiation of stem cell pool in the bulge. Together, these *in vivo* data suggest that the depletion of stem cells quiescence may be associated with higher differentiation due to change in chromatin organization. Abbreviation: sPLA<sub>2</sub>-IIA, secretory phospholipase A<sub>2</sub> Group-IIA.

differentiation at PD2 (neo-natal) and PD26 (adult) by using the differentiation markers such as K10, filaggrin and loricrin in the K14-sPLA<sub>2</sub>-IIA mice. However, further detailed study may provide more insight view on the molecular mechanism.

The overexpression of sPLA<sub>2</sub>-IIA resulted in increased proliferation that was accompanied in depletion of HFSCs. Moreover, In K14-sPLA<sub>2</sub>-IIA keratinocytes, colony forming efficiency was reduced that showed loss of functional stem cell property thereby suggesting niche independent effect of sPLA<sub>2</sub>-IIA in clonogenic potential of keratinocytes. It is well known that dermal papillae modulate HFSCs activity including its regenerative capacity, cycling characteristics and hair type specification

[56–59]. Further, tail whole mount analysis showed enlargement of dermal papillae at PD21 and it may modulate the HFSCs activity. Therefore, it may possibly have synergistic effect through niche dependent and independent mechanism on HFSCs differentiation. However, it warrants more investigation.

Recent studies have shown that histone marks varies in stem cells and differentiation. Our data on histone modification(s) profiling during the loss of stem cell quiescence and higher differentiation (PD49) in K14-sPLA<sub>2</sub>-IIA mice showed decrease in H3K9ac marks with increase in H3K27me3 mark. Earlier study has shown that in quiescent HFSC cells, the active H3K4me3 and H3K79me2 marks are present for the genes associated with stem cells fate; whereas, the genes associated with Transit amplifying cells (TA) fate have the H3K27me3 repressive mark [60]. In TA cells, exactly opposite histone profiling trend was observed where the genes associated with stem cells fate have the H3K27me3 mark; however, genes associated with TA fate have the activating H3K4me3 and H3K79me2 marks [60, 61]. Also, earlier studies in polycomb group (PcG) proteins, which mediate H3K27me3, are dispensable for maintaining pluripotency and lineage potential in ES cells, but are required for precise control of gene expression during differentiation. In adult mice, it has been shown that Ezh1/Ezh2 and Jarid2 are not required for epidermal differentiation through H3K27me3 modification [62, 63]. Further, Jarid2 have been shown to regulate epidermal stem cell differentiation in neonatal keratinocytes [63]. In coherence with our data, these studies suggest that epigenetic repression via histone modification marks, H3K27me3 and H3K9ac may be regulating stem cell fate transitions toward differentiation. These alterations in histone marks is associated with a loss of HFSC pool suggesting that cells are losing their self-renewal capacity and may be it leads to differentiation corroborating with the colony formation efficiency data that showed loss of functional properties of the stem cells. Further, matrix is known to contain differentiated cell and our data in K14-sPLA<sub>2</sub>-IIA mice showed high level of H3K27me3 mark at PD26 in matrix cells. Our data showed increased number of high and medium H3K27me3 positive cells at PD49 compared to WT control in the bulge cells. This may be associated with stage specific alteration in the down regulation of genes involved in stem cell quiescence with up-regulation of genes involved in differentiation. Interestingly, the level of another repressive mark, H3K9me3 decreased in the PD49 has also been reported to be involved in stem cell quiescence [64]. The startling findings that H3K9me3, repressive mark is also associated with transcribed region of active genes [64, 65]. These observations support our findings of decrease in H3K9me3 in PD49 of K14-sPLA<sub>2</sub>-IIA mice. Future work will help us to identify the gene-specific targets of H3K9me3 and H3K27me3 in hair follicle bulge of WT and transgenic mice, and find out the inter-relationship and genes involved in differentiation or depletion of stem cell pool in transgenic mice of sPLA<sub>2</sub>-IIA.

With respect to our findings a model has been proposed where the overexpression of sPLA<sub>2</sub>-IIA leads to an enhanced activation of mitogens such as Hb-EGF and EPGN, and transcription factor, c-Jun and FosB. Further *in vivo* histone analysis in bulge at PD23 and PD49 revealed the level of activation mark, H3K9ac is inversely co-related with the level of repressive mark, H3K27me3 (Fig. 7). Together, our *in vivo* data

suggest that the depletion of stem cells pool/quiescence may be associated with higher differentiation due to enhanced activation of c-Jun and change in chromatin organization.

## CONCLUSION

In summary, sPLA<sub>2</sub>-IIA is deregulated in various human cancers. We have unravelled for the first time, the over expression of sPLA<sub>2</sub>-IIA disrupts various epidermal lineages, loss of ortho-parakeratotic organization, stem cell depletion/quiescence and differentiation potentially associated with global differences in epigenetic status. Our study has provided significant contribution to over existing knowledge of sPLA<sub>2</sub>-IIA by showing the unexplored role of sPLA<sub>2</sub>-IIA in HFSCs and skin homeostasis mediated through signaling mechanism. This suggests that unravelling in-depth molecular role of sPLA<sub>2</sub>-IIA and its interaction with epigenetic landscape may provide information on stem cell regulation and cancer that may have clinical relevance.

## ACKNOWLEDGMENTS

We thank Dr. Rita Mulherkar for providing the sPLA<sub>2</sub>-IIA transgenic mice. We also extend thanks to Dr. Nagesh Bhat, BARC

for helping in the irradiation of feeders cells. We thank Mrs. Nirmala Mansukhani and Mr. Ganesh Bejjanki for their technical support. We thank Mr. Vineet Kala for his help in animal work. We thank Mr. Raghava Sunkara and Ms. Sweta Dash for discussion. We thank the ACTREC Animal house, flow cytometry and Microscopy facilities. RMS is supported by UGC fellowship and GLC is supported by ACTREC fellowship. This work was supported by ICMR, India.

## AUTHOR CONTRIBUTIONS

S.K.W.: conceived and designed the project, analyzed and interpreted the data. R.M.S.: performed the experiments and analyzed; G.L.C.: performed the protein and keratinocytes experiments, and analyzed; V.R.: performed the histology and analyzed, and helped in animal work; B.K.: performed the IHC of histone data, and R.M.S. analyzed the data; S.K.W.: performed RNA extraction for microarray and analyzed; R.M.S., G.L.C., S.K.W.: analyzed all the data; S.G., S.K.W.: designed, analyzed and wrote the histone data; S.K.W.: wrote the manuscript, and discussed with R.M.S., G.L.C., and S.G.

## DISCLOSURE OF POTENTIAL CONFLICTS OF INTEREST

The authors indicate no potential conflicts of interest.

## REFERENCES

- Hardy MH. The secret life of the hair follicle. *Trends Genet* 1992;8:55–61.
- Blanpain C, Fuchs E. Epidermal homeostasis: A balancing act of stem cells in the skin. *Nat Rev Mol Cell Biol* 2009;10:207–217.
- Sotiropoulou PA, Blanpain C. Development and homeostasis of the skin epidermis. *Cold Spring Harb Perspect Biol* 2012;4:a008383.
- Alonso L, Fuchs E. The hair cycle. *J Cell Sci* 2006;119(3):391–393.
- Fuchs E, Chen T. A matter of life and death: Self-renewal in stem cells. *EMBO Rep* 2013;14:39–48.
- Cotsarelis G, Sun TT, Lavker RM. Label-retaining cells reside in the bulge area of pilosebaceous unit: Implications for follicular stem cells, hair cycle, and skin carcinogenesis. *Cell* 1990;61:1329–1337.
- Taylor G, Lehrer MS, Jensen PJ et al. Involvement of follicular stem cells in forming not only the follicle but also the epidermis. *Cell* 2000;102:451–461.
- Oshima H, Rochat A, Kedzia C et al. Morphogenesis and renewal of hair follicles from adult multipotent stem cells. *Cell* 2001;104:233–245.
- Bickenbach JR. Identification and behavior of label-retaining cells in oral mucosa and skin. *J Dent Res* 1981;1611–1620.
- Lavker RM, Sun TT. Heterogeneity in epidermal basal keratinocytes: Morphological and functional correlations. *Science* 1982;215:1239–1241.
- Braun KM, Niemann C, Jensen UB et al. Manipulation of stem cell proliferation and lineage commitment: Visualisation of label-retaining cells in whole mounts of mouse epidermis. *Development* 2003;130:5241–5255.
- Horsley V, O'Carroll D, Tooze R et al. *Blimp1* defines a progenitor population that governs cellular input to the sebaceous gland. *Cell* 2006;126:597–609.
- Tumbar T, Guasch G, Greco V et al. Defining the epithelial stem cell niche in skin. *Science* 2004;303:359–363.
- Waghmare SK, Bansal R, Lee J et al. Quantitative proliferation dynamics and random chromosome segregation of hair follicle stem cells. *EMBO J* 2008;27:1309–1320.
- Waghmare SK, Tumbar T. Adult hair follicle stem cells do not retain the older DNA strands in vivo during normal tissue homeostasis. *Chromosome Res* 2013;21:203–212.
- Watt FM, Jensen KB. Epidermal stem cell diversity and quiescence. *EMBO Mol Med* 2009;1:260–267.
- Gat U, DasGupta R, Degenstein L et al. De novo hair follicle morphogenesis and hair tumors in mice expressing a truncated beta-catenin in skin. *Cell* 1998;95:605–614.
- Huelsken J, Vogel R, Erdmann B et al. beta-Catenin controls hair follicle morphogenesis and stem cell differentiation in the skin. *Cell* 2001;105:533–545.
- Andl T, Reddy ST, Gaddapara T et al. WNT signals are required for the initiation of hair follicle development. *Dev Cell* 2002;2:643–653.
- Lo Celso C, Prowse DM, Watt FM. Transient activation of beta-catenin signalling in adult mouse epidermis is sufficient to induce new hair follicles but continuous activation is required to maintain hair follicle tumours. *Development* 2004;131:1787–1799.
- Deschene ER, Myung P, Rompolas P et al. beta-Catenin activation regulates tissue growth non-cell autonomously in the hair stem cell niche. *Science* 2014;343:1353–1356.
- Mak KK, Chan SY. Epidermal growth factor as a biologic switch in hair growth cycle. *J Biol Chem* 2003;278:26120–26126.
- Vassar R, Fuchs E. Transgenic mice provide new insights into the role of TGF-alpha during epidermal development and differentiation. *Genes Dev* 1991;5:714–727.
- Murakami M, Taketomi Y, Miki Y et al. Emerging roles of secreted phospholipase A2 enzymes: The 3rd edition. *Biochimie* 2014;107Pt A:105–113.
- Ilic D, Bollinger JM, Gelb M et al. sPLA2 and the epidermal barrier. *Biochim. Biophys. Acta* 2014;1841:416–421.
- Murakami M, Taketomi Y, Miki Y et al. Recent progress in phospholipase a(2) research: From cells to animals to humans. *Prog Lipid Res* 2011;50:152–192.
- Mulherkar R, Rao R, Rao L et al. Enhancing factor protein from mouse small intestines belongs to the phospholipase A2 family. *FEBS Lett* 1993;317:263–266.
- Desai SJ, Mulherkar R, Wagle AS et al. Ontogeny of enhancing factor in mouse intestines and skin. *Histochemistry* 1991;96:371–374.
- MacPhee M, Chepenik KP, Liddell RA et al. The secretory phospholipase A2 gene is a candidate for the *Mom1* locus, a major modifier of ApcMin-induced intestinal neoplasia. *Cell* 1995;81:957–966.
- Cormier RT, Hong KH, Halberg RB et al. Secretory phospholipase Pla2g2a confers resistance to intestinal tumorigenesis. *Nat Genet* 1997;17:88–91.
- Mulherkar R, Kirtane BM, Ramchandani A et al. Expression of enhancing factor/phospholipase A2 in skin results in abnormal epidermis and increased sensitivity to chemical carcinogenesis. *Oncogene* 2003;22:1936–1944.
- Sadaria MR, Meng X, Fullerton DA et al. Secretory phospholipase A2 inhibition attenuates intercellular adhesion molecule-1 expression in human esophageal adenocarcinoma cells. *Ann Thorac Surg* 2011;91:1539–1545.

- 33** Yu JA, Mauchley D, Li H et al. Knock-down of secretory phospholipase A2 Ila reduces lung cancer growth in vitro and in vivo. *J Thorac Cardiovasc Surg* 2012;144:1185–1191.
- 34** Leung SY, Chen X, Chu KM et al. Phospholipase A2 group IIA expression in gastric adenocarcinoma is associated with prolonged survival and less frequent metastasis. *Proc Natl Acad Sci USA* 2002;99:16203–16208.
- 35** Dong Z, Liu Y, Scott KF et al. Secretory phospholipase A2-IIa is involved in prostate cancer progression and may potentially serve as a biomarker for prostate cancer. *Carcinogenesis* 2010;31:1948–1955.
- 36** Lee J, Tumber T. Hairy tale of signaling in hair follicle development and cycling. *Semin Cell Dev Biol* 2012;23:906–916.
- 37** Inoue A, Arima N, Ishiguro J et al. LPA-producing enzyme PA-PLA(1)alpha regulates hair follicle development by modulating EGFR signalling. *Embo J* 2011;30:4248–4260.
- 38** Frye M, Fisher AG, Watt FM. Epidermal stem cells are defined by global histone modifications that are altered by Myc-induced differentiation. *PLoS One* 2007;2(8):e763.
- 39** Cao R, Wang L, Wang H et al. Role of histone H3 lysine 27 methylation in Polycomb-group silencing. *Science* 2002;298:1039–1043.
- 40** Ezhkova E, Pasolli HA, Parker JS et al. Ezh2 orchestrates gene expression for the stepwise differentiation of tissue-specific stem cells. *Cell* 2009;136:1122–1135.
- 41** Osorio KM, Lee SE, McDermitt DJ et al. Runx1 modulates developmental, but not injury-driven, hair follicle stem cell activation. *Development* 2008;135:1059–1068.
- 42** Niessen MT, Scott J, Zielinski JG et al. aPKClambda controls epidermal homeostasis and stem cell fate through regulation of division orientation. *J Cell Biol* 2013;202:887–900.
- 43** Gomez C, Chua W, Miremadi A et al. The interfollicular epidermis of adult mouse tail comprises two distinct cell lineages that are differentially regulated by nt, daradd, and Lrig1. *Stem Cell Rep* 2013;1:19–27.
- 44** Xie W, Paterson AJ, Chin E et al. Targeted expression of a dominant negative epidermal growth factor receptor in the mammary gland of transgenic mice inhibits pubertal mammary duct development. *Mol Endocrinol* 1997;11:1766–1781.
- 45** Threadgill DW, Dlugosz AA, Hansen LA et al. Targeted disruption of mouse EGF receptor: Effect of genetic background on mutant phenotype. *Science* 1995;269:230–234.
- 46** Murillas R, Larcher F, Conti CJ et al. Expression of a dominant negative mutant of epidermal growth factor receptor in the epidermis of transgenic mice elicits striking alterations in hair follicle development and skin structure. *EMBO J* 1995;14:5216–5223.
- 47** Kiguchi K, Bol D, Carbajal S et al. Constitutive expression of erbB2 in epidermis of transgenic mice results in epidermal hyperproliferation and spontaneous skin tumor development. *Oncogene* 2000;19:4243–4254.
- 48** Martin R, Cordova C, Nieto ML. Secreted phospholipase A2-IIA-induced a phenotype of activated microglia in BV-2 cells requires epidermal growth factor receptor transactivation and proHB-EGF shedding. *J Neuroinflammation* 2012;9:154.
- 49** Hernandez M, Martin R, Garcia-Cubillas MD et al. Secreted PLA2 induces proliferation in astrocytoma through the EGF receptor: Another inflammation-cancer link. *Neuro Oncol* 2010;12:1014–1023.
- 50** Yamazaki S, Iwamoto R, Saeki K et al. Mice with defects in HB-EGF ectodomain shedding show severe developmental abnormalities. *J Cell Biol* 2003;163:469–475.
- 51** Dahlhoff M, Muller AK, Wolf E et al. Epigenetic transgenic mice develop enlarged sebaceous glands. *J Invest Dermatol* 2010;130:623–626.
- 52** Zenz R, Scheuch H, Martin P et al. c-un regulates eyelid closure and skin tumor development through EGFR signaling. *Dev Cell* 2003;4:879–889.
- 53** Guinea-Viniegra J, Zenz R, Scheuch H et al. Differentiation-induced skin cancer suppression by FOS, p53, and TACE/ADAM17. *J Clin Invest* 2012;122:2898–2910.
- 54** Eger G, Papadopoulos N, Lennartsson J et al. NR4A1 promotes PDGF-BB-induced cell colony formation in soft agar. *PLoS One* 2014;9:e109047.
- 55** Ogawa E, Okuyama R, Egawa T et al. p63/p51-induced onset of keratinocyte differentiation via the c-un N-terminal kinase pathway is counteracted by keratinocyte growth factor. *J Biol Chem* 2008;283:34241–34249.
- 56** Rompolas P, Mesa KR, Greco V. Spatial organization within a niche as a determinant of stem-cell fate. *Nature* 2013;502:513–518.
- 57** Rompolas P, Greco V. Stem cell dynamics in the hair follicle niche. *Semin Cell Dev Biol* 2014;25–26:34–42.
- 58** Chi W, Wu E, Morgan BA. Dermal papilla cell number specifies hair size, shape and cycling and its reduction causes follicular decline. *Development* 2013;140:1676–1683.
- 59** Mesa KR, Rompolas P, Greco V. The dynamic niche/tem cell interdependency. *Stem Cell Rep* 2015;4:961–966.
- 60** Lien WH, Guo X, Polak L et al. Genome-wide maps of histone modifications unwind in vivo chromatin states of the hair follicle lineage. *Cell Stem Cell* 2011;9:219–232.
- 61** Frye M, Benitah SA. Chromatin regulators in mammalian epidermis. *Semin Cell Dev Biol* 2012;23:897–905.
- 62** Ezhkova E, Lien WH, Stokes N et al. EZH1 and EZH2 cogovern histone H3K27 trimethylation and are essential for hair follicle homeostasis and wound repair. *Genes Dev* 2011;25:485–498.
- 63** Mejetta S, Morey L, Pascual G et al. Jarid2 regulates mouse epidermal stem cell activation and differentiation. *EMBO J* 2011;30:3635–3646.
- 64** Wiencke JK, Zheng S, Morrison Z et al. Differentially expressed genes are marked by histone 3 lysine 9 trimethylation in human cancer cells. *Oncogene* 2008;27:2412–2421.
- 65** Vakoc CR, Mandat SA, Olenchok BA et al. Histone H3 lysine 9 methylation and HP1gamma are associated with transcription elongation through mammalian chromatin. *Mol Cell* 2005;19:381–391.
- 66** Irizarry RA, Hobbs B, Collin F et al. Exploration, normalization, and summaries of high density oligonucleotide array probe level data. *Biostatistics* 2003;4:249–264.
- 67** Schmittgen TD, Livak KJ. Analyzing real-time PCR data by the comparative C(T) method. *Nat Protoc* 2008;3:1101–1108.



See [www.StemCells.com](http://www.StemCells.com) for supporting information available online.